

Middlesex University Research Repository

An open access repository of

Middlesex University research

<http://eprints.mdx.ac.uk>

Dawit, Mekibib David (2006) The biogeochemical cycling of ammonium and methylamines in intertidal sediments. PhD thesis, Middlesex University. [Thesis]

Final accepted version (with author's formatting)

This version is available at: <https://eprints.mdx.ac.uk/13583/>

Copyright:

Middlesex University Research Repository makes the University's research available electronically.

Copyright and moral rights to this work are retained by the author and/or other copyright owners unless otherwise stated. The work is supplied on the understanding that any use for commercial gain is strictly forbidden. A copy may be downloaded for personal, non-commercial, research or study without prior permission and without charge.

Works, including theses and research projects, may not be reproduced in any format or medium, or extensive quotations taken from them, or their content changed in any way, without first obtaining permission in writing from the copyright holder(s). They may not be sold or exploited commercially in any format or medium without the prior written permission of the copyright holder(s).

Full bibliographic details must be given when referring to, or quoting from full items including the author's name, the title of the work, publication details where relevant (place, publisher, date), pagination, and for theses or dissertations the awarding institution, the degree type awarded, and the date of the award.

If you believe that any material held in the repository infringes copyright law, please contact the Repository Team at Middlesex University via the following email address:

eprints@mdx.ac.uk

The item will be removed from the repository while any claim is being investigated.

See also repository copyright: re-use policy: <http://eprints.mdx.ac.uk/policies.html#copy>

Middlesex University Research Repository:

an open access repository of
Middlesex University research

<http://eprints.mdx.ac.uk>

Dawit, Mekibib David, 2006.
The biogeochemical cycling of ammonium and methylamines in inter-
tidal sediments.
Available from Middlesex University's Research Repository.

Copyright:

Middlesex University Research Repository makes the University's research available electronically.

Copyright and moral rights to this thesis/research project are retained by the author and/or other copyright owners. The work is supplied on the understanding that any use for commercial gain is strictly forbidden. A copy may be downloaded for personal, non-commercial, research or study without prior permission and without charge. Any use of the thesis/research project for private study or research must be properly acknowledged with reference to the work's full bibliographic details.

This thesis/research project may not be reproduced in any format or medium, or extensive quotations taken from it, or its content changed in any way, without first obtaining permission in writing from the copyright holder(s).

If you believe that any material held in the repository infringes copyright law, please contact the Repository Team at Middlesex University via the following email address:
eprints@mdx.ac.uk

The item will be removed from the repository while any claim is being investigated.

THE BIOGEOCHEMICAL CYCLING OF AMMONIUM AND METHYLAMINES IN INTER-TIDAL SEDIMENTS.

**A thesis submitted to Middlesex University in partial fulfilment of the degree of
Doctor of Philosophy.**

Mekibib David Dawit,

**BSc. (Chemistry), Postgraduate Diploma (Analytical Chemistry),
MSc. with Merit in 'Integrated Pollution Control'.**

School of Health and Social Sciences

Middlesex University

April, 2006

PAGE
NUMBERING
AS ORIGINAL

Abstract

The methylamines (MAs) are chemical analogues of ammonia and contain one, two or three methyl groups. This study looked at their occurrence in inter-tidal sediments and at changes in their abundance during tidal cycling, including forced and naturally occurring sediment resuspension. Two sites in the UK, Burnham Overy Staithe (BOS) and the Thames Estuary (TE), and the Ria Formosa (RF), Portugal, were chosen for the study.

The MAs were abundant in all samples collected. MA concentrations were compared to NH_4^+ at BOS and TE. A consistent trend emerged, with NH_4^+ more abundant in the pore-waters and the MAs dominating the solid phase. Most NH_4^+ and MAs were found on the solid-phase, and the general magnitude of adsorption was: $\text{TMA} > \text{DMA} > \text{MMA} > \text{NH}_4^+$. This was inconsistent with their pK_b values but could be explained by the ability of each cation to form hydrogen bonds with water.

Pore-water MA concentrations at BOS were compared with salinity but no correlation was observed. However, the clam *Ruditapes decussatus* (L.) released TMA during tidal inundation. The mechanism of release is unclear as these organisms do not osmoregulate, but the calculated TMA loss from these sediments (169 mmol m^{-2} per tide) could be increasing dissolved organic nitrogen concentrations in the Ria Formosa.

TE sediments were used in desorption experiments. Desorption of NH_4^+ was more rapid than the MAs and their mean chemical response times were 15 and 25 minutes, respectively. Increases in concentrations of dissolved NH_4^+ and MAs over a tidal cycle were coincident with remobilisation of seabed sediments. Desorption of NH_4^+ and MAs from the remobilised sediments accounted for approximately 50% and > 90% of the increase, respectively. The results are proposed as a predictor for the sorption behaviour of other ON compounds and emphasise the importance of sediment resuspension as a mechanism of ON release to the water column.

Acknowledgements

I have been lucky in having two supervisors who were rigorous and very supportive; Dr. Mark Fitzsimons and Professor Mike Revitt. I can't thank them enough for their guidance during this PhD project and their faith in me through thick and thin. I have learnt a great deal from both of them, which I have, no doubt will tap into in my future career. I am also grateful to Dr. Huw Jones for his excellent support as my mentor. I would like to thank Dr. Carlos Rocha and the University of the Algarve, Portugal for their hospitality and providing pore-water extraction equipment during my sampling trip to the Ria Formosa in September 2000. I like to say a big thank you to Professor Milward and Mr. R. Hartley of University of Plymouth the former for his help in the study of the kinetics of ammonium and methylamine release during simulated tidal experiments and the later for particle-size analysis.

It is impossible to put into words the importance of my family's unstinting support and understanding while I dedicated too much of my time and effort into this demanding research adventure. My mom Asnaku, my dad Dawit Mekibib my sister Mahader; and finally, Hewan Mekibib who is too young to understand what this means to me but in time, I hope will appreciate why I scarified too much of my time for this project. I would like also to thank my colleagues at the Urban Pollution Research Centre (UPRC) for making my work enjoyable. For all the laughs and beers we had! My thanks goes to Sam O' Hanlon, Nikolas Paterakeis, Maurice Moor and Alan Barber.

I want to express my deepest appreciation of the financial and moral support I received from different people and organisations throughout the project especially, Mrs. Hezel McLeish of 'Friends of Octavia', Mr. John Akker of CARA and the Dr. Getachew Bolodia Fund (USA). The Environment Agency and Middlesex University are acknowledged for their partial funding of my PhD work.

Acronyms and abbreviations

BOD	Biological Oxygen Demand
BOS	Burnham Overy Staithe
CPA	Cyclopropylamine
DFAA	Dissolved Free Amino Acids
DIN	Dissolved Inorganic Nitrogen
DMA	Dimethylamine
DON	Dissolved Organic Nitrogen
GC	Gas Chromatography
IS	Internal Standard
LYS	Lysine
MA	Methylamine
MMA	Monomethylamine
N	Nitrogen
NP-FID	Nitrogen Phosphorus- Flame Ionisation Detector
OLW	Overlying Water
OM	Organic Matter
ON	Organic Nitrogen
PAR	Peak Area Ratio
PC	Personal Computer
POM	Particulate Organic Matter
PON	Particulate Organic Nitrogen
PVC	Polyvinylchloride
PW	Pore-water
R.F.	Ria Formosa

RSD	Relative Standard Deviation
S.D.	Standard Deviation
SE	Southeast
SOM	Suspended Organic Matter
SP	Solid-Phase
SPM	Suspended Particulate Matter
SSW	Synthetic Seawater
STW	Sewage Treatment Work
T.E.	Thames Estuary
TMA	Trimethylamine
TMAO	Trimethylammoniumoxide
TN	Total Nitrogen
TOC	Total Organic Carbon

<u>SECTIONS</u>	Pages
ABSTRACT	i
ACKNOWLEDGEMENTS	ii
ACRONYMS AND ABBREVIATIONS	xiv
CHAPTER	
1 INTRODUCTION	1
1.1 Effect of diagenetic reactions on N cycling in marine sediments.	2
1.2 N cycling in estuarine environments.	5
1.3 N cycling in inter-tidal sediments.	6
1.3.1 Inter-tidal sediments.	6
1.3.2 Effects of tidal action on N cycling in inter-tidal sediments.	8
1.3.3 Major biogeochemical factors affecting the cycling of organic N species in inter-tidal sediments.	10
1.3.4 Methylamines.	12
1.4 Rationale for this study.	13
1.5 Objectives of this study.	17
1.6 Review of analytical methods used for the determination of methylamines.	17
1.7 Conceptual model.	18
1.8 Courses and conferences attended during the PhD study.	21
1.8.1 Courses.	21
1.8.2 Seminars.	21
1.8.3 Conferences.	21
1.8.4 Publications	22
1.9 Organisation of the thesis.	22
2 MATERIALS AND METHODS	24
2.1 Site descriptions.	24
2.1.1 Burnham Overy Staithe.	24
2.1.2 Ria Formosa.	26
2.1.3 Thames Estuary.	28
2.2 Sample collection and pre-treatment.	30
2.2.1 Burnham Overy Staithe.	30
2.2.2 Ria Formosa.	31
2.2.2.1 Sampling at Site 1.	31
	iii

2.2.2.2	Sampling at Site 2.	31
2.2.3	Thames Estuary.	32
2.2.3.1	Sample collection for determination of depth profiles of N species.	32
2.2.3.2	Determination of suspended particulate material (SPM).	34
2.3	Determination of nitrogen compounds.	34
2.3.1	Reagents and standard solutions for NH_4^+ and MA analysis.	34
2.3.2	Determination of NH_4^+ .	35
2.3.2.1	NH_4^+ extraction techniques	35
2.3.2.2	Procedure for NH_4^+ analysis	35
2.3.2.3	Calibration of the spectrophotometric technique for NH_4^+ analysis.	36
2.3.2.4	Glassware preparation.	37
2.3.3.5	Design of the micro-diffusion flask.	38
2.3.2.6	Selection of internal standard.	39
2.3.2.7	Synthetic seawater preparation.	39
2.3.3.8	Calibration of the analytical technique.	40
2.3.2.9	Calculation of analyte recovery through micro-diffusion.	44
2.3.2.10	Application of the micro-diffusion process.	46
2.3.2.11	Gas chromatography.	42
2.3.2.12	Reproducibility of environmental samples.	49
2.3.3	MA determination of Site 2 samples.	52
2.3.3.1	Mantle cavity-water.	53
2.3.3.2	Surrounding sediment and clam tissue.	53
2.3.4	Calculations of potential exchangeable MA concentrations in clam samples.	53
2.3.5	Calculation of adsorption coefficients for NH_4^+ and MAs.	54
2.4	Determination of sedimentary total organic carbon (TOC) and total nitrogen (TN) content.	55
2.5	Determination of selected physico-chemical parameters.	55
2.5.1	Measurement of pore-water content.	55
2.5.2	Porosity measurement.	56
2.5.3	Grain size analysis.	56
2.5.4	Salinity measurement.	56
2.5.5	Laboratory simulated tidal action experiment.	57
2.5.6	Extraction of sediments.	58
2.5.6.1	Calculation of extraction efficiencies.	59

3	BURNHAM OVERY STAITHE	60
3.1	Introduction.	60
3.2	Aims of the study.	61
3.3	Results.	61
3.3.1	Salinity.	61
3.3.2	Total organic carbon content, total nitrogen and C/N ratio.	62
3.3.3	Depth profiles of NH_4^+ and the MAs.	65
3.3.3.1	Pore-waters.	65
3.3.3.2	Solid-phase.	68
3.3.4	Adsorption coefficients.	72
3.4	Statistical analysis for differences in concentrations of NH_4^+ and MAs as a result of tidal action.	74
3.5	Discussion.	77
3.5.1	General observations.	77
3.5.2	Sources and controls of NH_4^+ and the MAs.	78
3.5.3	Adsorption of NH_4^+ and the MAs.	80
3.5.4	Effects of tidal fluctuations on the distributions of NH_4^+ and the MAs.	83
3.6	Summary.	86
4	RIA FORMOSA	88
4.1	Introduction.	88
4.2	Results of MA analysis of Site 1 samples.	90
4.2.1	Water content.	91
4.2.2	Particle size analysis.	91
4.2.3	Abundance of MAs.	93
4.2.3.1	Pore-water.	93
4.2.3.2	Solid-phase.	98
4.2.4	Adsorption coefficients.	101
4.3	Results of MA analysis of Site 2 samples.	103
4.3.1	Clam tissue.	103
4.3.2	Clam mantle cavity-water.	105
4.3.3	Clam bed sediments.	105
4.4	Discussion.	106
4.4.1	General observations (Site 1).	106

4.4.2	Effect of tidal cycle on MA distribution.	108
4.4.3	Influence of the clam <i>R. decussates</i> (L.) on MA cycling.	111
4.5	Summary.	116
5	THAMES ESTUARY	117
5.1	Introduction	117
5.2	Results	120
5.2.1	Seasonal NH_4^+ and MA distributions in Thames Estuary sediment samples.	120
5.2.1.1	Particle size analysis.	120
5.2.1.2	Pore-water NH_4^+ .	120
5.2.1.3	Pore-water MAs	122
5.2.1.4	Solid-phase NH_4^+	127
5.2.1.5	Solid-phase MAs	129
5.2.2	Measurement of NH_4^+ and the MAs through a tidal cycle at TE3.	134
5.2.3	Measurements of exchangeable NH_4^+ and the MAs.	135
5.2.3.1	Sequential sediment extraction with overlying water (July, 2001).	136
5.2.3.2	Sediment extraction with 2M KCl (July, 2001).	138
5.2.3.3	Sediment extraction (November, 2001).	138
5.2.3.4	Total exchangeable NH_4^+ and MA concentrations (November, 2001).	144
5.2.4	Desorption of NH_4^+ and the MAs during simulated sediment resuspension.	146
5.2.4.1	Kinetics of NH_4^+ and MA desorption during sediment resuspension.	152
5.3	Discussion of results.	156
5.3.1	Seasonal NH_4^+ and MA distributions in Thames Estuary sediment samples.	156
5.3.2	Measurement of NH_4^+ and the MAs through part of a tidal cycle at TE3.	158
5.3.3	Measurement of exchangeable NH_4^+ and MAs.	161
5.3.4	Desorption of NH_4^+ and the MAs during simulated sediment resuspension.	162
5.3.4.1	Kinetics of NH_4^+ and MA desorption during sediment resuspension.	165
5.4	Summary.	166
6.	CONCLUDING REMARKS AND RECOMMENDATIONS FOR FURTHER STUDY.	168
6.1	Conclusions.	168
6.1.1	The impact of MAs on N cycling in inter-tidal sediments.	174
6.1.2	Diagrammatic representation of the main conclusion of the study.	175
6.2	Recommendations for further work.	177

REFERENCES	179
GLOSSARY	197
APPENDIX	199
A.1 Additional data for Thames Estuary samples	199
A.1.1 Grain size analysis	199
A.1.2 Environmental data for Benfleet Sewage Treatment Plant (May – November, 2001).	201

TABLES	Pages
---------------	--------------

Chapter 1

Table 1.1 Microbial activities occurring in aerobic and anaerobic environments as a function of redox potential.	2
Table 1.2 Physical properties of NH_4^+ and the MAs.	12
Table 1.3 Some of the major analytical methods for MA determination.	18

Chapter 2

Table 2.1 Sample collection information for Cores 1-5, Burnham Overy Staithe.	30
Table 2.2 Details of sampling times at Site 1, Ria Formosa.	31
Table 2.3 Details of sampling times for sediment cores taken from the Thames Estuary transect.	33
Table 2.4 Triplicate analyses of standard NH_4^+ solutions.	36
Table 2.5 Composition of the synthetic seawater used for the determination of MAs.	39
Table 2.6 Procedure for preparation of mixed MA standards for direct-injection calibration.	41
Table 2.7 Reproducibility of MA standards (direct injection) at $2\mu\text{M}$.	41
Table 2.8 Concentration and volume of mixed MA standard solutions for calibration using micro-diffusion.	43
Table 2.9 Percentage recoveries of MA standards after micro-diffusion.	45
Table 2.10 Method detection limit of the three MAs by GC-NPD.	48
Table 2.11 GC operating conditions for the determination of MAs.	48
Table 2.12 Reproducibility of MA analysis for pore-water, sediment and clam tissue samples from Sites 1 and 2 of the Ria Formosa.	50
Table 2.13 Reproducibility of Thames Estuary MA analysis (Solid-phase, July samples).	50

Table 2.14	Reproducibility of Thames Estuary MA analysis (Pore-water, July samples).	51
Table 2.15	Reproducibility of Thames Estuary MA analysis (Solid-phase, November samples).	51
Table 2.16	Reproducibility of Thames Estuary MA analysis (Pore-water, November samples).	51
Table 2.17	Time intervals of sampling for tidal action experiment.	57

Chapter 3

Table 3.1	Mean adsorption coefficients (K^*) for the MAs and NH_4^+ in cores 1-5.	72
Table 3.2	p values for paired student's t-test on solid-phase NH_4^+ and MA concentrations.	75
Table 3.3	Correlation of mean TOC content and mean adsorption coefficients of Cores 1-5.	83

Chapter 4

Table 4.1	Depth profile of water content (%) for Ria Formosa sediment samples at Site 1.	90
Table 4.2	p values of paired t-Test of pore-water and solid-phase concentrations of Site 1.	94
Table 4.3	Adsorption coefficients (K^*) of MMA, Ria Formosa.	94
Table 4.4	Adsorption coefficients (K^*) of DMA, Ria Formosa.	102
Table 4.5	Adsorption coefficients (K^*) of TMA, Ria Formosa.	102
Table 4.6	Comparison of average MA concentrations in clam tissues for 2M KCl and OLW extraction methods.	103
Table 4.7	Concentrations of the MAs in samples of <i>R. decussates</i> (L.) and sediment taken from Site 2 before and after tidal inundation.	104

Chapter 5

Table 5.1	Depth profile of total extractable NH_4^+ and MAs in Thames Estuary sediments (November, 2001).	145
Table 5.2	Summary of physical and chemical data for surface sediments (0-5 mm depth) sampled in the Thames Estuary.	149

Table 5.3	Reaction constants for desorption experiments on Thames Estuary samples (July 2001).	150
Table 5.4	Reaction constants for desorption experiments on Thames Estuary samples (July 2001).	151
Table 5.5	Total average pore-water and solid-phase MA concentrations in Thames Estuary samples.	158

Appendix

Table A.1	Environmental data for Benfleet STW (sampled on 15/08/2001).	201
Table A.2	Environmental data for Benfleet STW (sampled on 29/08/2001).	201
Table A.3	Environmental data for Benfleet STW (sampled on 02/09/2001).	202
Table A.4	Environmental data for Benfleet STW (sampled on 17/09/2001).	202
Table A.5	Environmental data for Benfleet STW (sampled on 01/10/2001).	202
Table A.6	Environmental data for Benfleet STW (sampled on 26/10/2001).	202

FIGURES Pages

Chapter 1

Figure 1-1	A simple schematic diagram of NH_4^+ cycling in inter-tidal areas.	9
Figure 1-2	Conceptual model of the study.	20

Chapter 2

Figure 2-1	Location of Burnham Overy Staithe sampling area.	25
Figure 2-2	Maps showing the location of the Ria Formosa and positions of sampling sites.	27
Figure 2-3	Location of the sampling sites in the Thames Estuary.	29
Figure 2-4	A calibration graph for NH_4^+ standard solutions.	37
Figure 2-5	Diagrammatic representation of the micro-diffusion flask used for extraction of MAs.	38
Figure 2-6	Calibration graphs for the three MAs determined by direct injection.	42
Figure 2-7	Calibration graphs for the three MAs determined by micro-diffusion.	44
Figure 2-8	Representative chromatogram of MA standards and CPA.	47

Chapter 3

Figure 3-1	Depth profiles for salinity in Cores 1-5.	62
Figure 3-2	Depth profiles of average TOC content of Cores 1-5.	63
Figure 3-3	Depth profiles of TN in the solid-phase of Cores 1-5.	64
Figure 3-4	Depth profiles for C/N ratios (atomic) of Cores 1-5.	65
Figure 3-5	Depth profiles for NH_4^+ in the pore-water of Cores 1-5.	66
Figure 3-6	Depth profiles for pore-water MMA of Cores 1-5 (C1 = Core 1).	67
Figure 3-7	Depth profiles for DMA in the pore-water of Cores 1-5 (C1 = Core 1).	67
Figure 3-8	Depth profiles for TMA in the pore-water of Cores 1-5 (C1 = Core 1).	68
Figure 3-9	Depth profiles for solid-phase MMA in Cores 1-5.	69
Figure 3-10	Depth profiles for solid-phase DMA in Cores 1-5.	70
Figure 3-11	Depth profiles for solid-phase TMA in Core 1-5.	70
Figure 3-12	Depth profiles of the contribution of MAs (%) to TN content of solid-phase samples.	71
Figure 3-13	Plots of total solid-phase NH_4^+ and MAs versus TN.	71
Figure 3-14	Plots of total pore-water MAs and pore-water TMA versus salinity.	73
Figure 3-15	Plots of total pore-water MAs and pore-water TMA versus salinity.	79
Figure 3-16	Total pore-water MA concentration ranges of BOS samples at different stages of the tidal cycle.	84
Figure 3-17	Total solid-phase MA concentration ranges of BOS samples at different stages of the tidal cycle.	84

Chapter 4

Figure 4-1	Grain size proportions of sediment samples; RF1.	91
Figure 4-2	Grain size proportions of sediment samples; RF2.	91
Figure 4-3	Grain size proportions of sediment samples; RF3.	92
Figure 4-4	Grain size proportions of sediment samples; RF4.	92
Figure 4-5	Depth profiles of pore-water MMA concentrations, Site 1, Ria Formosa.	95
Figure 4-6	Depth profiles of pore-water DMA concentrations, Site 1, Ria Formosa.	96
Figure 4-7	Depth profiles of pore-water TMA concentrations, Site 1, Ria Formosa.	97
Figure 4-8	Depth profiles of solid-phase MMA concentrations, Site 1, Ria Formosa.	98
Figure 4-9	Depth profiles of solid-phase DMA concentrations Site 1, Ria Formosa.	99
Figure 4-10	Depth profiles of solid-phase TMA concentrations, Site 1, Ria Formosa.	100

Figure 4-11	Total pore-water MA concentration ranges of Ria Formosa Site 1 samples at different stages of a tidal cycle	109
Figure 4-12	Solid-phase MA concentration ranges of Ria Formosa Site 1 samples at different stages of a tidal cycle	109

Chapter 5

Figure 5-1	Depth profiles of Thames Estuary pore-water NH_4^+ concentrations in July 2001.	121
Figure 5-2	Depth profiles of pore-water NH_4^+ concentrations of Thames Estuary samples in November 2001.	122
Figure 5-3	Depth profiles of pore-water MA concentrations in Core TE1J.	123
Figure 5-4	Depth profiles of pore-water MA concentrations in Core TE2J.	124
Figure 5-5	Depth profiles of pore-water MA concentrations in Core TE3J.	124
Figure 5-6	Depth profiles of pore-water MA concentrations in Core TE4J.	124
Figure 5-7	Depth profiles of pore-water MA concentrations in Core TE1N.	125
Figure 5-8	Depth profiles of pore-water MA concentrations in Core TE2N.	126
Figure 5-9	Depth profiles of pore-water MA concentrations in Core TE3N.	126
Figure 5-10	Depth profiles of pore-water MA concentrations in Core TE4N.	127
Figure 5-11	Depth profiles of solid-phase NH_4^+ concentrations of Thames Estuary samples in July 2001.	128
Figure 5-12	Depth profiles of solid-phase NH_4^+ concentration of Thames Estuary samples in November 2001	128
Figure 5-13	Depth profiles of solid-phase MA concentrations in Core TE1J.	130
Figure 5-14	Depth profiles of solid-phase MA concentrations in Core TE2J.	130
Figure 5-15	Depth profiles of solid-phase MA concentrations in Core TE3J.	131
Figure 5-16	Depth profiles of solid-phase MA concentrations in Core TE4J.	131
Figure 5-17	Depth profiles of solid-phase MA concentrations in Core TE1N.	132
Figure 5-18	Depth profiles of solid-phase MA concentrations in Core TE2N.	133
Figure 5-19	Depth profiles of solid-phase MA concentrations in Core TE3N.	134
Figure 5-20	Depth profiles of solid-phase MA concentrations in Core TE4N.	135
Figure 5-21	Concentrations of SPM, dissolved NH_4^+ and total dissolved MAs over part of a tidal cycle at site TE3 in March 2002.	135
Figure 5-22	NH_4^+ concentrations in Thames Estuary sediments at 0-5 mm depth extracted with multiple volumes of OLW (July 2001).	137

Figure 5-24	MA concentrations in Thames Estuary sediments at 0-5 mm depth extracted with multiple volumes of OLW (TE1J).	137
Figure 5-24	Concentrations of NH_4^+ and MAs in Thames Estuary sediments at 0-5 mm depth using multiple volumes of 2M KCl; July.	140
Figure 5-25	NH_4^+ concentrations in Thames Estuary sediments at 0-5 mm depth	142
Figure 5-26	MA concentrations in Thames Estuary sediments at 0-5 mm depth extracted with multiple volumes of 2M KCl (2 hours, November 2001).	143
Figure 5-27	Time dependent desorption of NH_4^+ and MAs from Thames Estuary sediments collected at site TE1 in July 2001.	147
Figure 5-28	Time dependent desorption of NH_4^+ and MAs from Thames Estuary sediments collected at site TE3 in July 2001.	149

Chapter 6

Figure 6-1	Semi-quantitative conceptual map showing the impact of MAs on the cycling of N in a hypothetical inter-tidal system.	175
Figure 6-2	Conceptual model of the summary of the study.	175

Appendix

Figure A-1	Grain size proportion of sediment samples, Thames Estuary (TEJ1).	199
Figure A-2	Grain size proportion of sediment samples, Thames Estuary (TEJ2).	199
Figure A-3	Grain size proportion of sediment samples, Thames Estuary (TEJ3).	200
Figure A-4	Grain size proportion of sediment samples, Thames Estuary (TEJ4).	200

PLATES Pages

Chapter 2

Plate 2-1	The Ria Formosa site during low tide.	27
Plate 2-2	Sampling at the Thames Estuary site, TE3 (July, 2001).	33

EQUATIONS

Pages

Chapter 2

Equation 2-1	44
Equation 2-2	45
Equation 2-3	50
Equation 2-4	53
Equation 2-5	54
Equation 2-6	54
Equation 2-7	54
Equation 2-8	56
Equation 2-9	56
Equation 2-1	59

Chapter 5

Equation 5-1	141
Equation 5-2	152
Equation 5-3	153
Equation 5-4	153
Equation 5-5	153
Equation 5-6	154

1 INTRODUCTION

Nitrogen (N) occurs both in the biosphere and the geosphere in a variety of forms. Most of the fixed forms of N are important compounds, needed for the survival of plants and animals. N compounds are either inorganic or organic, and are intricately linked together in what is commonly called the N cycle. The cycling of nutrients is affected by a variety of processes in different ecosystems (Klump and Martens, 1989). N in particular, is important in coastal environments, as it exists in different forms and may be converted from one form to another under different physico-chemical conditions. N is also considered to be the nutrient limiting primary production in ecosystems such as estuaries, although there is a continuing debate about this (Glibert, 1988; Owens, 1993).

N is present in a variety of forms in estuarine sediments. The main species of interest are inorganic (NO_3^- , NO_2^- and NH_4^+) and organic (e.g., amino acids, urea and aliphatic amines), in both dissolved and particulate forms. A significant fraction of the dissolved organic nitrogen (DON) delivered to estuaries by rivers is labile and some studies have suggested that ON inputs may contribute more to estuarine and continental shelf eutrophication than was previously suspected (Seitzinger and Sanders, 1997).

1.1 Effect of diagenetic reactions on N cycling in marine sediments.

Diagenesis is defined as the overall process that brings about changes in sediments, or sedimentary rocks, subsequent to deposition (Berner, 1980). Diagenetic changes taking place in the upper few metres of sediments are driven by redox reactions resulting from the oxidation of organic matter (OM). This oxidation occurs to produce the energy needed by micro-organisms to degrade OM. The oxidising agent is dependent on the availability of different electron acceptors. When oxygen is abundant, micro-organisms preferentially use it because the energy yield is higher than for other electron acceptors. Under anaerobic conditions micro-organisms are forced to use other electron acceptors (Table 1-1).

Sedimentary diagenetic processes can be divided, on the basis of the redox potential of the sediment, into;

- 1. Oxidic diagenesis, in which dissolved oxygen is available for the oxidation process.
- 2. Suboxic diagenesis in which secondary oxidants are used in the diagenetic sequence.

Table 1-1. Microbial activities occurring in aerobic and anaerobic environments as a function of redox potential.

Process	Electron acceptor	End products	Mole of e/mole of electron acceptor	-ΔG ⁰ / mole of electrons
Aerobic	O ₂	H ₂ O, CO ₂	4	125.1
Nitrate reduction	NO ₃ ⁻	N ₂ , CO ₂	5	118.8
Manganese reduction	MnO ₂	Mn ²⁺ , CO ₂	2	94.5
Iron reduction	Fe (OH) ₃	Fe ²⁺ , CO ₂	1	24.3
Sulphate Reduction	SO ₄ ²⁻	H ₂ S, CO ₂	8	25.4
Methanogenesis	CO ₂	CH ₄	8	23.2

The main factors controlling how a diagenetic sequence operates are the magnitude of the OM flux to the sediments, and the rate at which the sediment accumulates. Sugai and Henrichs (1992) reported that amino acids adsorbed onto sediments decomposed (became altered through diagenetic processes) less rapidly than dissolved free amino acids (DFAAs) in pore-waters. Christensen and Blackburn (1980; 1982) also reported that significant fractions of alanine and acetate adsorbed irreversibly onto marine sediments during a 4-week incubation period. Therefore, the reversibility of adsorption of different organic compounds can greatly influence their decomposition rates and preservation in marine sediments.

In sediments deposited under oxic conditions, organic carbon is rapidly destroyed (with oxygen as an electron acceptor), usually at the sediment-water interface. However, in deeper sediments bioturbation by metazoans can lead to accelerated rates of OM destruction (Aller, 1982) and this greatly influences both the nature and vertical distribution of OM in the top few centimetres of the sediment column (Mayer, 1993). Montluçon and Lee (2001) conducted experiments, which showed that redox potential greatly influenced lysine (LYS) adsorption. They found that the adsorption coefficient of LYS was about six times higher in oxidised sediments than in anoxic sediments. Many studies have shown that metal oxides and other minerals commonly found in oxic mineral sediments have considerable potential to adsorb organic compounds (Sigg and Stumm, 1981; Tipping, 1981; Davis, 1982). This may explain the increased adsorption in oxic sediments. The effect of sediment redox potential on adsorption is not yet well understood; its potential influence on adsorption needs further investigation.

Decomposition of OM in marine and brackish sediments is usually dominated by oxygen consumption and sulphate reduction, with lesser utilisation of other terminal electron acceptors (Jorgensen, 1982). In the absence of physical and biological perturbation of its structure, the sediment shows a vertical gradient resulting from the thermodynamic sequence by which the redox pairs O_2/H_2O , NO_3^-/N_2 , MnO_2/Mn^{2+} , $FeOOH/Fe^{2+}$ and SO_4^{2-}/H_2S (Froelich *et al.*, 1979; Berner, 1977; 1980) are involved in OM decomposition (Stumm and Morgan, 1996). The thickness of the sediment layer, where this vertical zonation of chemical compounds is observed, narrows on a depth gradient towards shallower systems as a consequence of the richness in N and P of the sediment OM (Nixon, 1981; Blackburn and Henriksen, 1983), and the variety of abiotic stimuli to redox reactions.

The effectiveness of aerobic respiration depends on access to oxygen for which the solubility in water reaches 9 mgL^{-1} at 20°C . The consequences are that only about 8.4 mg of OM (CH_2O) can be oxidised by the oxygen contained in 1L of water. Thus, when the concentration of OM is high, the dissolved oxygen content of water can be rapidly depleted. If the aeration rate of the water body is low as is the case in stagnant water bodies, such as lacustrine or subsurface marine sediments (in the absence of resuspension by tides or winds), the biological oxygen demand (BOD) increases and the redox potential tends to fall in a stepwise direction so that nitrate reduction eventually replaces aerobic metabolism as the dominant organic carbon oxidation pathway.

1.2 N cycling in estuarine environments.

Estuaries are highly variable ecosystems featuring a salinity gradient ranging from pure freshwater at the freshwater inflow to pure seawater at the open connection to the sea. Along the salinity gradient there are typically regular patterns in water column characteristics, such as turbidity, nutrient levels and primary production (Boynton and Kemp, 1985). Like reservoirs, the primary sources of nutrients are usually the river inflows and catchments; however, estuaries may also receive significant oceanic imports of nutrients (Malcom and Sivyver, 1997).

Other sources of nutrients in estuaries include dry and wet deposition as well as anthropogenic inputs from sewage, fertiliser runoff and dredging deposits. Nutrient loadings to estuaries are, in general, much higher than in lakes (Nixon, 1988). In addition to salinity and the various sources of nutrients, estuaries are also heavily influenced by tides. These and other factors along with the structural complexity of estuaries combine to produce some of the most dynamic and productive ecosystems in the world. It is generally accepted that most estuaries tend to be N-limited, though this is not always the case (Malcolm and Sivyver, 1997). It has been reported that some of the more closed systems possessing restricted connections with the sea may behave similarly to freshwater lakes and are inclined to be phosphorus limited (Kimmerer *et al.*, 1993). The more regular situation, however, is N-limitation.

There are two main points that should be stressed when discussing the cycling of N in estuaries. The first is that estuaries typically represent major N-sinks (Seitzinger *et al.*, 1984; Carpenter and Dunham, 1985). The second relevant point is the importance of N-recycling occurring in estuaries. Indeed, as much as two thirds of the N utilised by estuarine phytoplankton has been recycled, and turnover rates are

very rapid, in the order of hours (Carpenter and Dunham, 1985; Nixon, 1988). The large daily and seasonal interconversions between inorganic and organic forms of N, as well as the relative abundance of N in its various oxidation states, are a result of the balance between the uptake of N by organisms, its release as waste, and the bacterial processes of nitrification, denitrification and N-fixation (Berounsky and Nixon, 1993).

1.3 N cycling in inter-tidal sediments.

1.3.1 Inter-tidal sediments.

Inter-tidal areas are characterised by large fluctuations in environmental conditions. Littoral plants are specially adapted to cope with variable temperatures and salinities, and to withstand periodic exposure to air. Inter-tidal systems provide very effective coastal protection (Brampton, 1992). In addition to providing a valuable coastal defence, inter-tidal sediments offer an important habitat for wildlife, food and recreation. The rich food supply in the muddy sediments makes inter-tidal areas important sanctuaries and nursery grounds for fish and invertebrates (Adam, 1990). Rocky inter-tidal regions support dense communities with a high proportion of epiflora and epifauna that may compete for limited space. The major [bio] physical disturbances that impact on inter-tidal sediments occur from tidal cycles, episodic events (and sediment movements which result from this), bioturbation, bio-irrigation and anthropogenic factors such as fishing and dredging. The disturbances occur over a wide range of time scales and influence processes on an environment that, although broadly structured, is patchy and dynamic.

The most recurrent physical process in inter-tidal areas is tidal action. Inter-tidal sediments are subject to diurnal drying (exposure) and flooding (inundation), which leads to major changes in the local transport of material to and from the

sediments. Most inter-tidal systems are prone to these changes. Clearly when the tide has ebbed there is no overlying water present and there can be no dissolved output from the sediment. This may result in increasing concentrations of dissolved substances in pore-waters that have sources within the sediment, such as NH_4^+ (Malcolm and Sivyer, 1997). This benthic pool may then be exported to the overlying water column when the sediment is flooded. In contrast, a substance whose source is in the water column, and is consumed in the sediment, may be depleted when the water is not present. This shows that inter-tidal sediments are both sinks and sources of different nutrients and that the behaviour changes with tide (Malcolm and Sivyer, 1997). Tidal cycling causes changes in the sedimentary hydraulic regime. The export and import of material from inter-tidal sediments are strongly influenced by spring/neap cycles (Vorosmarty and Loder, 1994), which are the biggest fluctuations when other weather phenomena are not taken into account.

In inter-tidal sediments, drainage and air intrusion during periods of exposure create a series of interrelated biotic and abiotic changes that are important to benthic mineralisation (Reidl and Machan, 1972). During exposure to the atmosphere, dewatering takes place. This results in a substantial amount of evaporation (especially during the summer months). Evaporation increases salinity in the pore-waters of the exposed sediments. This increases the concentration of cations that can compete for binding sites with N cations. A relationship between NH_4^+ release from sediments was observed in Texas estuaries by Gardener *et al.* (2006). In osmotically sensitive organisms, the water inside the body of the organisms diffuses into the pore-water due to osmotic pressure. The reverse process occurs during sediment flooding. This fluctuation of osmotic pressure may be controlled by uptake and release of chemical species, such as trimethylamine (TMA) (Sorenson and Glob, 1987).

1.3.2 Effects of tidal action on N cycling in inter-tidal sediments.

Tidal cycling affects both the distribution of chemical species and the habitat of benthic organisms (e.g. Neira and Hopner, 1993; Hemminga *et al.*, 1994). Indeed, tidal flushing has been implicated as an important transport mechanism for inorganic N in the Great Sippewissett Marsh (Massachusetts, USA.), causing a net export of N from the marsh (Valiela *et al.*, 1978; Valiela, 1980). In the Sado Estuary, Portugal, tidal cycling was shown to have a significant effect on the behaviour of NH_4^+ in the inter-tidal mudflat (Rocha, 1998). During sediment exposure, when the additional oxygen brought into deeper sediment by tidal action had been consumed, only oxygen diffusing downward from the air-sediment interface was available for nitrate production.

Inter-tidal sediments occupy a unique position between land and sea giving them an important role in the movement of materials from terrestrial to oceanic environments (Nowicki, 1994). Although most studies have looked in detail at the nature of the biogeochemical process of nutrient cycling (e.g. Klump and Martens, 1989), they have not made any significant quantitative analysis of these processes. Concern about the impact of nutrients on the marine environment is providing a focus for some of these studies (e.g. Nowicki and Oviatt, 1990).

Fixed N seems to have a stimulatory effect on some benthic photosynthetic communities and therefore must be limiting in some cases (Sullivan and Daiber, 1975; Darley *et al.*, 1981), while excess NH_4^+ may be inhibitory (Admiraal, 1977). The quantitative importance of benthic photosynthesis varies between localities. Benthic microalgae may be significant primary producers in shallow waters. Their activity is confined to a narrow stratum of 0.3-2 mm thickness in the sediment, but

this narrow stratum may exhibit extremely high rates of photosynthesis (Revsbech *et al.*, 1988). The micro-organisms in the uppermost sediment layers thus influence the N cycle by high rates of both incorporation and mineralisation of N compounds (Revsbech *et al.*, 1988). Figure 1-1 represents a simplified schematic diagram of NH_4^+ cycling in inter-tidal areas.

The rapid change in the hydrological status of inter-tidal sediments during tidal inundation and exposure results in different physico-chemical and biological conditions and makes understanding the relationships that exist between different N species and inter-tidal organisms extremely challenging. Furthermore, the contribution of different ON species to the nutrient status of inter-tidal areas is not clearly understood as a result of the different complex relationships involved. This is discussed in more detail below.

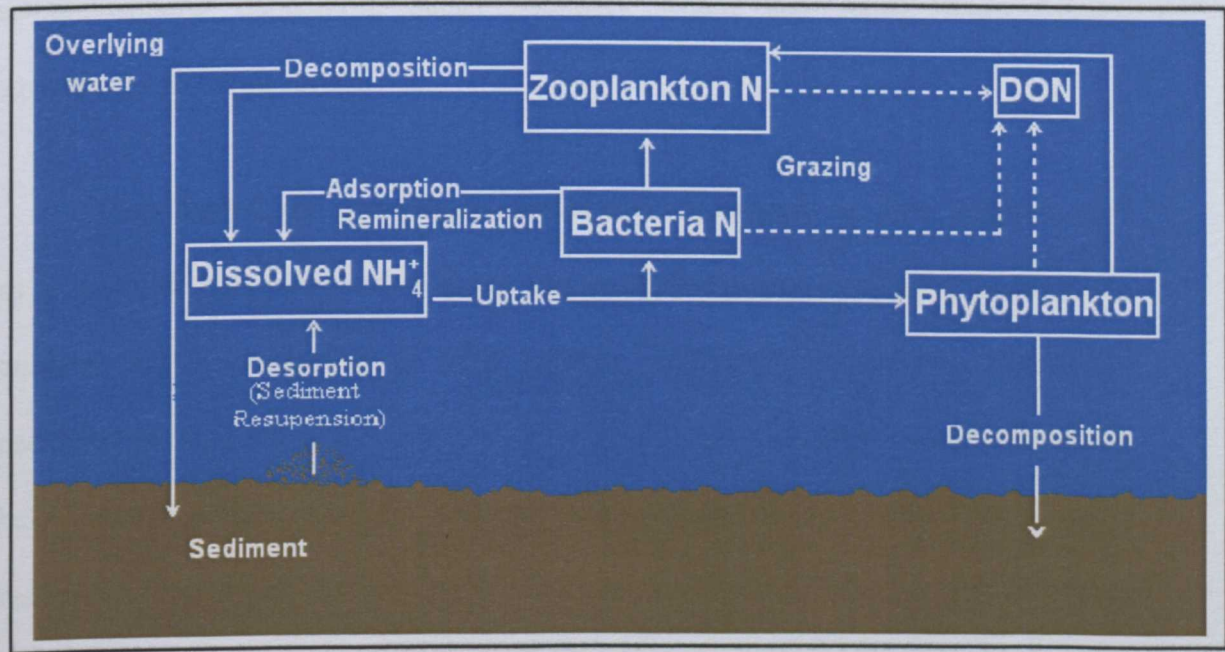


Figure 1-1. A simple schematic diagram of NH_4^+ cycling in inter-tidal areas.

1.3.3 Major biogeochemical factors affecting the cycling of organic N species in inter-tidal sediments.

ON in inter-tidal sediments is broadly divided into particulate ON (PON) and DON. Most studies of nutrient inputs to estuaries have examined the response of phytoplankton to dissolved inorganic nitrogen (DIN), as this is known to be incorporated rapidly by phytoplankton, and to contribute to eutrophication. However, DIN accounts for only a portion of total N inputs. The effect of ON, which comprises the remainder of the loading, has been largely ignored. Both the PON and DON forms of ON contribute to estuarine N loadings.

Inputs of DON can account for 20-90% of the total N loading to estuaries (Seitzinger and Sanders, 1997). A significant fraction of the DON delivered to estuaries in rainwater and polluted rivers (Delaware and Hudson) is biologically active (Seitzinger and Sanders, 1997). However, there have been very few studies on the quantity and quality of DON inputs from a wide range of non-point sources such as atmospheric deposition, ocean boundary water, and runoff from forests, agricultural and urban areas.

Very limited and non-conclusive research results exist on point sources, such as wastewater treatment plant effluent and combined sewer overflows. Data on the quantity and bioavailability of DON entering estuaries from specific sources are necessary to improve N loading and estuarine eutrophic models. These models will help identify which non-point and point sources should be targeted for nutrient reductions. These data can also be used in conjunction with land use and watershed information to develop biologically available N budgets for estuaries.

DON consists of numerous organic molecules that contain N (usually as an amino group). They range from simple organic molecules such as urea or amino sugars to much more complex macromolecules such as humic and fulvic acids (Walsh, 1989; Anita *et al.*, 1991). In sediment pore-waters, DON compounds such as dissolved amino acids can be produced as intermediates in sediment OM mineralisation (SOM) (Burdgie and Martens, 1990), whereas the refractory components of DON are produced by partial mineralisation or oxidation of SOM (Burdgie and Gardener, 1998) and abiotic condensation reactions such as polymerisation and humification (Hedges, 1988).

Concentrations of ON in marine sediment and pore-waters are generally higher than in overlying waters (Heggie *et al.*, 1987; Lomstein *et al.*, 1998; Burdige and Zheng, 1998), suggesting that sediments may be a source of ON. Since N can be a limiting nutrient in marine ecosystems (Carpenter and Capone, 1983) and DON can be used as a N source by phytoplankton (Jackson and Williams, 1985; Anita *et al.*, 1991; Bronk *et al.*, 1994), understanding the role of sediments as a source of DON to the water column is vital to have a clear understanding of N cycling in marine ecosystems.

1.3.4 Methylamines

One group of ON compounds is the methylamines (MAs). They are methylated analogues of ammonia; namely monomethylamine (MMA), dimethylamine (DMA) and trimethylamine (TMA). The main physical properties of ammonia and the MAs are shown in Table 1-2. MA cycling in marine systems has received increasing attention over the last two decades (e.g. Wang and Lee, 1990; 1993; Fitzsimons *et al.*, 1997; 2001). The MAs are a ubiquitous component of marine

sediments and, like NH_4^+ , are low molecular weight, basic and highly soluble compounds.

As N sources, the origin and distribution of MAs in marine sediments has potentially important implications for the sedimentary N budget, where uptake and release by organisms may affect their abundance. It seems that, once released, the distribution and speciation of the MAs depends on a number of chemical and biological processes. For example, TMA concentrations in coastal areas were found to be affected by seasonal changes and animal burrowing (Wang and Lee, 1994).

Table 1-2. Physical properties of NH_4^+ and the MAs.

Compound	Melting point, °C	Boiling Point, °C	Solubility (g 100g ⁻¹ , H ₂ O)	pK _b
Ammonia	-78	-33	Very Soluble	4.74
MMA	-95	-6	Very Soluble	3.36
DMA	-93	7	Very Soluble	3.27
TMA	-117	3	Very Soluble	4.19

Wang and Lee (1990) found that the MAs could become strongly adsorbed onto marine sediments, especially those with high organic matter content, but that competition with seawater cations (the MAs exist predominantly as protonated compounds at seawater pH or below) could restrict their affinity for the sedimentary exchange sites. It is thought that direct excretion by osmoregulating animals could be an important source of TMA in marine sediments (Sorensen and Glob, 1987). However, although the potential of inter-tidal benthic fauna as a source of MAs has

been demonstrated (Sorensen and Glob, 1987; Wang and Lee, 1994), there is not enough evidence to unequivocally attribute the sources of MAs in inter-tidal ecosystems.

1.4 Rationale for this study

During the past decade, studies of benthic remineralisation of OM in estuaries have underestimated the role of marsh and inter-tidal areas, in favour of subtidal areas (Malcolm and Sivyer, 1997). However, inter-tidal areas make up large fractions of *meso* and *macro* tidal estuaries all over the world and their importance as preferential areas for the deposition of OM and associated contaminants is universally recognised (Bradley and Morris, 1990). On the other hand, the location of these areas, on the border between confined aquifers and the water column, increases their potential for interaction during the transfer of drainage waters (Harvey and Odum, 1990).

This study on the impact of tidal dynamics on N cycling (especially NH_4^+ and the MAs) in inter-tidal sediments focuses on mudflats, rather than whole marsh systems. This is for the following reasons:

1. The adsorption properties of mudflat sediments have been found to be less strongly influenced by the presence of macrophyte roots and organic detritus (Wang and Lee, 1994).
2. Mudflats, though spatially varied (*e.g.* through the presence of animal burrows), represent a more homogeneous environment in which to study the biogeochemical mechanisms controlling ON cycling compared to more mature areas of salt marsh, which are less homogenous.

3. The pattern of tidal inundation is regular (i.e. diurnal). This will enable comparison of samples taken at similar times through the tidal cycle provided no drastic weather conditions have occurred.

Blooms of opportunistic green macro-algae on inter-tidal flats and shallow sublittoral areas are now widespread in European waters and are widely linked to increased nutrient concentrations. This can create ecological and amenity problems when the sediments underlying the mats become anoxic (Rafaelli and Cha, 1995). A major concern is the transfer of nutrients to the water column and subsequent effects on water quality, since this contributes to blooms of cyanobacteria (blue/green algae) (Cloern, 2001), which can thrive under such conditions and secrete toxins that can be dangerous to human health.

Incidents of these blooms have increased and it is unclear as to the degree to which these algae are sustained by nutrients from the water column as opposed to benthic nutrients produced through mineralisation and mobilisation of OM. Interestingly, a study of the algal mat-forming species *Enteromorpha* in Dublin Bay, Ireland, showed that this species could meet almost all of its nutrient requirements by intercepting the flux from underlying sediments, which is governed by the mineralisation of OM (Rafaelli and Cha, 1995).

Thus, it is clear that the question of OM retention and regeneration in the sediments, as well as in transient biomass pools, is central to the management of nutrient availability in coastal systems. The investigation of the effect of tidal dynamics (particularly the resuspension of sediments in high energy estuaries, like the Thames Estuary, England) on ON bioavailability will be crucial to an integrated

approach of tackling 'past pollution' of sediments that can release ON species to coastal waters long after the 'apparent pollution' has been dealt with. The transport of ammonia across the benthic interface has already been shown to be a potentially important source of N to the overlying waters in the Sado Estuary, Portugal (Rocha, 1998), while pore-water distributions of MAs may alter significantly through the course of a spring tidal regime in temperate estuaries (Fitzsimons *et al.*, 1997). Nonetheless, the contribution of the pool of benthic ON to the nutrient status of overlying waters in inter-tidal systems remains poorly understood.

Inter-tidal sediments are a part of the sediment system that has long helped to maintain the productivity of coastal zones via the storage and recycling of nutrients, including N imported from offshore waters (Nixon, 1986; 1992). Population growth, aquatic sewage discharges and the development of intensive agriculture have resulted in a significant change in the quantities of nutrients supplied from terrestrial sources. Sediments play an important role in estuarine ecosystems by buffering environmental nutrient concentrations in overlying waters (Morin and Morse, 1999).

The buffering capacity of inter-tidal systems is not yet fully quantified, but may be important when management measures designed to alleviate problems caused by nutrient inputs are being formulated (Malcolm and Sivy, 1997). The pore-waters of inter-tidal sediments are generally in the pH range 7-8, causing ammonia (as NH_4^+) and the MAs to exist predominantly in the protonated form. This allows them to participate in adsorption-desorption reactions and may accelerate their incorporation into the solid-phase (Rosenfeld, 1979; Fitzsimons *et al.*, 1997). This study will focus on the impact of different physico-chemical changes on the adsorption behaviour of these compounds.

Although there are some data on the effects of tidal inundation on certain inorganic N species (e.g. Rocha, 1998)), there is little comparable data on ON species, such as MAs. Fitzsimons *et al.* (1997) measured MA concentrations in a salt marsh (Oglet Bay, Mersey Estuary, UK) through a spring tidal cycle. They found that the concentrations varied significantly between the neap and spring tides, such that MAs were strongly depleted within pore-waters and sediments during tidal inundation whereas enrichments were evident soon after the neap tide. While the depletion of the MAs during tidal inundation could be attributed to pore-water flushing, their enrichment during periods of sediment exposure indicated a sedimentary source. However, interpretation of data was complicated by the fact that the three sites sampled within the marsh differed in terms of maturity and functionality. The Mersey Estuary was also receiving pulses of untreated sewage at the time, which may have provided an alternative source of MAs (Scully *et al.*, 1988).

While inorganic forms of N have been routinely determined using colorimetric methods, techniques applicable to the determination of ON species (see Chapter 2) have been more fully developed only in recent years. This partly explains why, historically, studies of the N cycle have concentrated on inorganic N. However, it is becoming increasingly obvious that ON comprises a quantitatively significant portion of the N pool in estuarine sediments (Seitzinger and Sanders, 1997; Fitzsimons *et al.*, 1997).

1.5 Objectives of this study.

In the absence of specific methods to determine the mineralisation of nitrogenous OM most investigators have used NH_4^+ production as a measure of ON mineralisation rates (Herbert, 1999). Hence, NH_4^+ biogeochemistry was chosen in this study to emulate this process. MAs (methylated analogues of NH_4^+) were chosen as proxies to represent actual ON species. In order to investigate the dynamics of MA cycling in different inter-tidal sediments; a pristine salt marsh in East Anglia, England, an urban site at Southend (Thames Estuary), South East England, and a subtropical site comparable to the English sites in terms of physical features (Ria Formosa, South West Portugal), were chosen. The influence of invertebrates on MA cycling in inter-tidal sediments was investigated using clam tissue and surrounding sediment samples from a clam-rearing site in the Ria Formosa. The role of tidal dynamics on remobilisation of adsorbed N species was investigated through laboratory resuspension and extraction experiments (using NH_4^+ and MAs to represent inorganic and ON proxies) using samples collected from four different sites along the Thames Estuary at different times of the year.

1.6 Review of analytical methods used for the determination of methylamines.

The determination of MA concentrations in both atmospheric and aqueous samples has typically involved preconcentration, followed by gas chromatography (GC) of either the concentrated free amines or the derivatised compounds. Examples of such methods are summarised in Table 1-3. Abdul-Rashid *et al.* (1991) reported a simple, cheap and reproducible method for the determination of volatile MAs preconcentrated by micro-diffusion and followed by analysis using packed column GC with nitrogen-phosphorus selective flame ionisation detection (NP-FID). This method

was applied to a variety of samples and was found to be efficient, even at very low concentrations. No derivatisation step was necessary, in contrast to the procedures of Terashi *et al.* (1990) and da Costa *et al.* (1990), where TMA could not be directly measured. The method reported by Lee and Olsen (1984) required several manipulative stages prior to GC analysis.

The method of Fitzsimons *et al.* (1997) was chosen for this study. This method compares well with previously published methods. Satisfactory resolution of the MAs was achieved by Fitzsimons *et al.* (1997) with a reasonably short analysis time (15 minutes). Although lower recoveries of MMA ($59 \pm 5\%$) and DMA ($60 \pm 3\%$) relative to TMA ($100 \pm 1\%$) were obtained, low detection limits (which are very important for environmental samples) were achieved for the three amines (MMA, 48 nM, DMA, 10 nM, TMA, 5 nM).

Table 1-3. Some of the major analytical methods for MA determination.

Reference	Method
Lee and Olsen, 1984	Several extraction steps followed by diffusion.
Terashi <i>et al.</i> , 1990	Derivatisation and extraction.
Da Costa, 1990	Derivatisation and extraction.
Kuwata <i>et al.</i> , 1983	Airborne amines collected on Cartridge.
Scully <i>et al.</i> , 1988	Preconcentration on XAD-2 resin, then purge and trap followed by extraction and derivatisation.

1.7 Conceptual model

The main framework of this research project i.e., the conceptual model of the study is summarised in Fig. 1-2. The conceptual model shows the main objectives of the study, the analytical approach and methodology employed to fulfil these objectives and the expected outcomes of the main body of the research work.

The main objective of the project

To determine the effects of selected physico-chemical parameters on the biogeochemical cycling of NH_4^+ and MAs in inter-tidal systems.

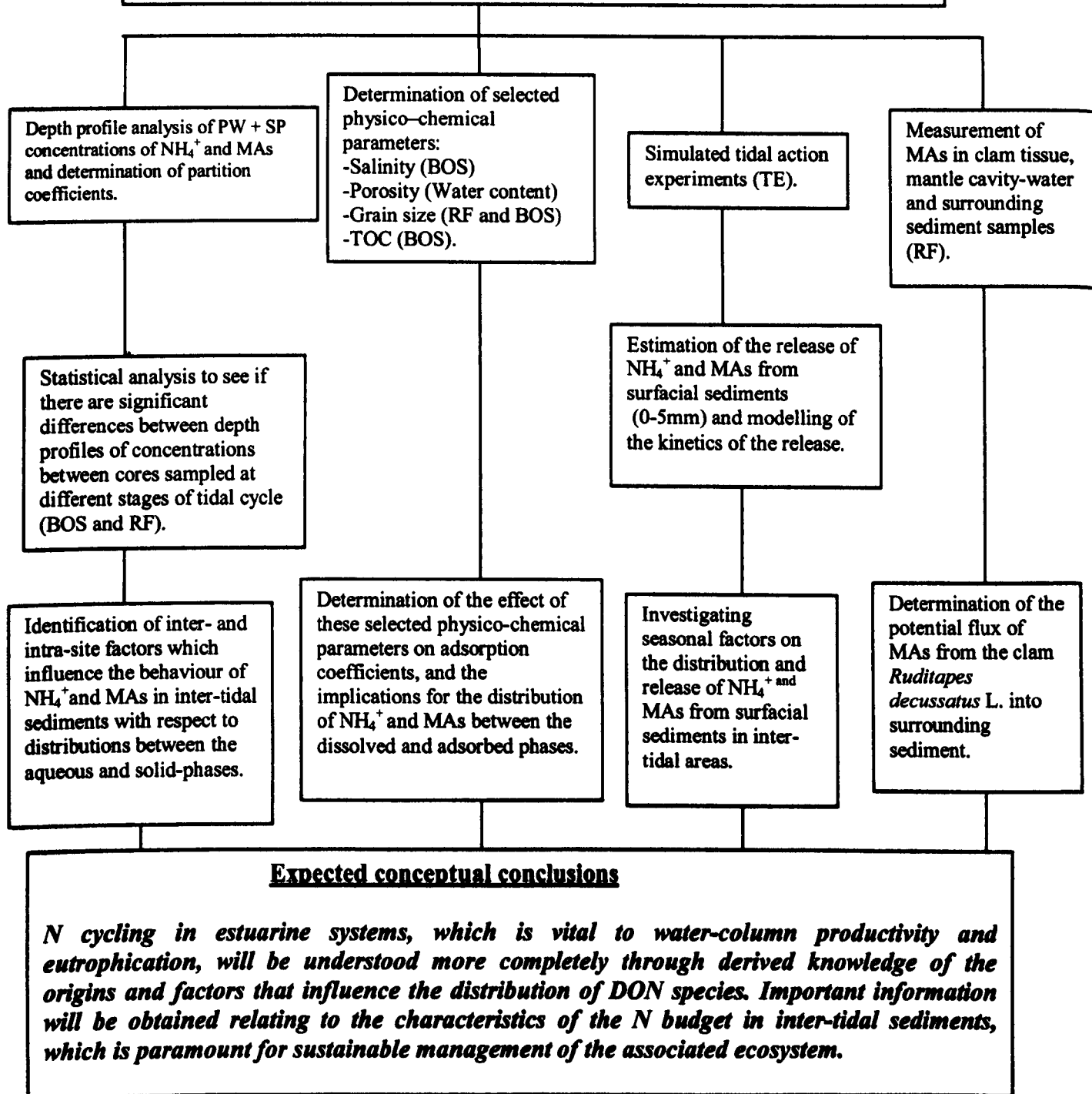


Figure 1-2. Conceptual model of the study (BOS = Burnham Overy Staithe, RF = Ria Formosa, TE = Thames Estuary), PW = pore-water, SP = solid phase, TOC = total organic carbon.

1.8 Courses and conferences attended during the PhD study.

A number of short courses, seminars and conferences have been attended that were relevant to the successful completion of this Ph.D. research project. These are listed below in chronological order.

1.8.1 Courses

- ◆ Research methodology module (ENS 4500), September 1999 (Middlesex University).
- ◆ Advanced Excel, June 2000 (Middlesex University).
- ◆ Advanced-word 97, May 2001 (Middlesex University).
- ◆ HPLC (operation), July 2001 (Biotek UK).

1.8.2 Seminars

- ◆ How to write a good Ph.D. thesis, Middlesex University, July 2002.
- ◆ Intellectual Property Rights, Middlesex University, July 2002.

1.8.3 Conferences

- ◆ British Organic Geochemistry Society (BOGS) 2000 Conference, Bristol University, July 2000 (co-author on oral presentation).
- ◆ Thames Estuary Partnership Annual Conference, University College London, October 2000.
- ◆ IWA Young Researchers 2nd Conference, Cranfield University, April 2001 (oral presentation).
- ◆ Thames Estuary Research Forum, December 2001 (workshop participant).
- ◆ BOGS 2002, Newcastle University, July 2002 (poster presentation).

1.8.4 Publications

- Fitzsimons, M.F., Millward G.E., Revitt, D.M. and Dawit, M. (2006). Desorption of ammonium and methylamines from estuarine sediments: Consequences for the cycling of nitrogen. *Mar. Chem.* **101**: (12-26).
- Fitzsimons, M.F., Dawit, M., Revitt, D.M. and Rocha, C. (2005). Effects of early tidal inundation on the cycling of methylamines in inter-tidal sediments. *Mar. Ecol. Prog. Ser.*, **294**: 51-61.
- Fitzsimons, M.F., Kamhi-Danon, B. and Dawit, M. (2001). Tidal control on distributions of the methylamines in an East-Anglian estuary: a potential role for benthic invertebrates? *Environmental and Experimental Botany*, **46**: 225-236.

1.9 Organisation of the thesis

This thesis consists of six chapters including this one. Chapter 1 deals with introductory remarks including the current state of knowledge on the cycling of NH_4^+ and the MAs in inter-tidal sediments, the outline of the thesis and the background to the research. The different analytical techniques used throughout the research are presented in Chapter 2. Explanation of the sites chosen for this research with accompanying maps and plates, methods of sample collection, pre-treatment and analyses carried out on the samples collected are given systematically in this chapter. The precision of the different analytical techniques employed and the capabilities and the limitations of the different methods used are also included in Chapter 2.

Chapter 3 describes the results obtained for the samples collected from Burnham Overy Staithe (BOS) together with their discussion. Chapter 4 is dedicated to the studies of the Ria Formosa samples as well as discussions and conclusions made from this part of the Ph.D. research. Chapter 5 is dedicated to a study on the effect of sediment resuspension on the sorption behaviour of NH_4^+ and ON,

represented by the MAs, using samples collected from the Thames Estuary, UK. The last chapter (Chapter 6) outlines the main outcomes from this research project and provides recommendations for further work. Finally, the Appendix contains additional data and material that are deemed important but not so important as to be included in the main body of the thesis. Also included are a glossary of technical terms and acronyms and abbreviations illustrating the particular context in which they were used in this thesis.

2 MATERIALS AND METHODS

2.1 Site descriptions

Three inter-tidal sites were chosen for the study; two in England (Burnham Overy Staithe, Norfolk, and the Thames Estuary, both in SE England) and one in Portugal (Ria Formosa, Algarve, Portugal). The study sites were subject to a variety of influences, both natural and anthropogenic, which are discussed below.

2.1.1 Burnham Overy Staithe.

Burnham Overy Staithe (BOS) is located in a pristine lagoonal-estuarine system with a large expanse of salt marsh and inter-tidal flats. It is part of an extensive network of salt marshes along an area known as the North Norfolk Coast. This marshland coast extends for more than 40 km and consists primarily of inter-tidal sands and muds, salt marshes, shingle banks and sand dunes. The area, much of which remains in its natural state, now constitutes one of the largest expanses of undeveloped coastal habitat of its type in Europe.

The study area was located on an exposed mud shore bordering a major tributary channel flowing from the Overy Marsh into Overy Creek (Fig. 2-1). The area represented a typical salt marsh succession, from sparsely vegetated mud at the seaward boundary of the marsh to maritime grassland on the upper marsh. The fore marsh was characterised by colonising species such as *Salicornia spp.* and *Spartina angelica*. Towards the seaward boundary was an area of mid-marsh, which was inundated at high tide. Here, *Aster tripolium* was evident along with *Limnium vulgare*.

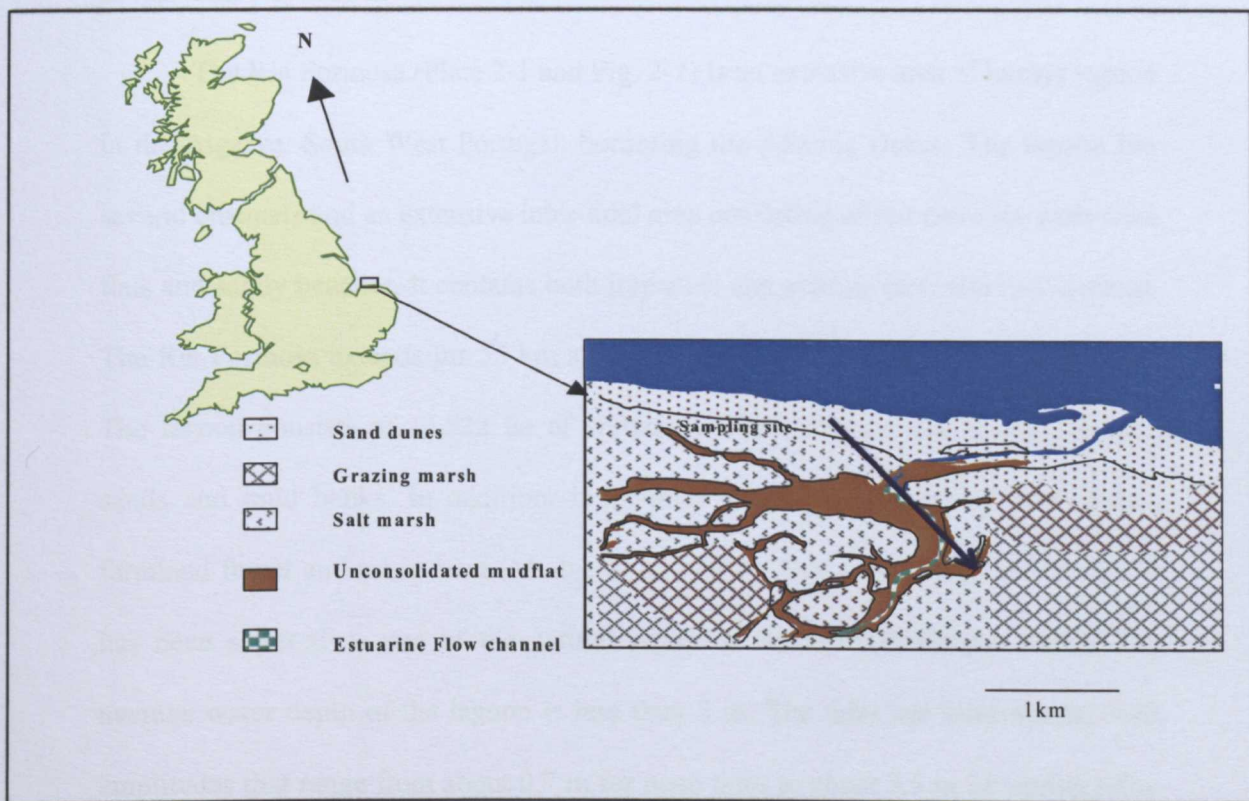


Figure 2-1. Location of Burnham Overy Staithe sampling area on the west of the North Norfolk Coast. (Lat. N 52°, 58.5', Long. E 0°, 45.3'). The location of the sampling site is indicated by the arrow within the site map.

The actual sampling site was located within the mud flat at the seaward boundary of the salt marsh, which was extensively covered by epipellic diatoms (*Naviculka Spp.* and *Nitzschia Spp.*). The sediment consisted of mainly fine silts and muds with the presence of macroinvertebrates such as polychaetes (*Nereis spp.*) and gastropods (*Hydrobia spp.*). Meiofauna comprised largely harpacticoid copepods, nematodes and ostracods. In addition, large numbers of foraminifera (presumably dead at time of sampling) were present.

2.1.2 Ria Formosa.

The Ria Formosa (Plate 2-1 and Fig. 2-2) is an extensive area of barrier lagoon in the Algarve, South West Portugal, bordering the Atlantic Ocean. The lagoon has several channels and an extensive inter-tidal area consisting of salt marshes, inter-tidal flats and sandy beaches. It contains both impacted and pristine inter-tidal ecosystems. The Ria Formosa extends for 55 km along the coast and is 6 km at its widest point. The lagoon consists of 14,522 ha of wetlands, which include salt marsh, exposed sands and mud banks. In addition, it includes a further 2478 ha of sand dunes, farmland forest and urban land (Mudge *et al.*, 1999). Due to its range of habitats, it has been selected as one of the natural parks of Portugal (Bebianno, 1995). The average water depth of the lagoon is less than 3 m. The tides are semi-diurnal with amplitudes that range from about 0.7 m for neap tides to about 3.5 m for spring tides. Bebianno (1995) estimated that there is an exchange of about 50-75% of the lagoon water with the ocean within a few tidal cycles although the inner regions are less affected by the tides than the outer ones.

There are nineteen freshwater inflows to the lagoon system, which represent a flood regime from October to April. However, most of the rivers dry out during the summer months (Austin *et al.*, 1989). As a result of this and surface evaporation, the salinity of the Ria Formosa is relatively high (32-38). In summer the population of the area increases more than three times due to tourism and this, combined with the lack of a mains sewerage system, has resulted in a large amount of sewage being released to the lagoon and increased nutrient loadings due to land runoff (Mudge and Bebianno, 1997).



Plate 2-1. The Ria Formosa site during low tide.

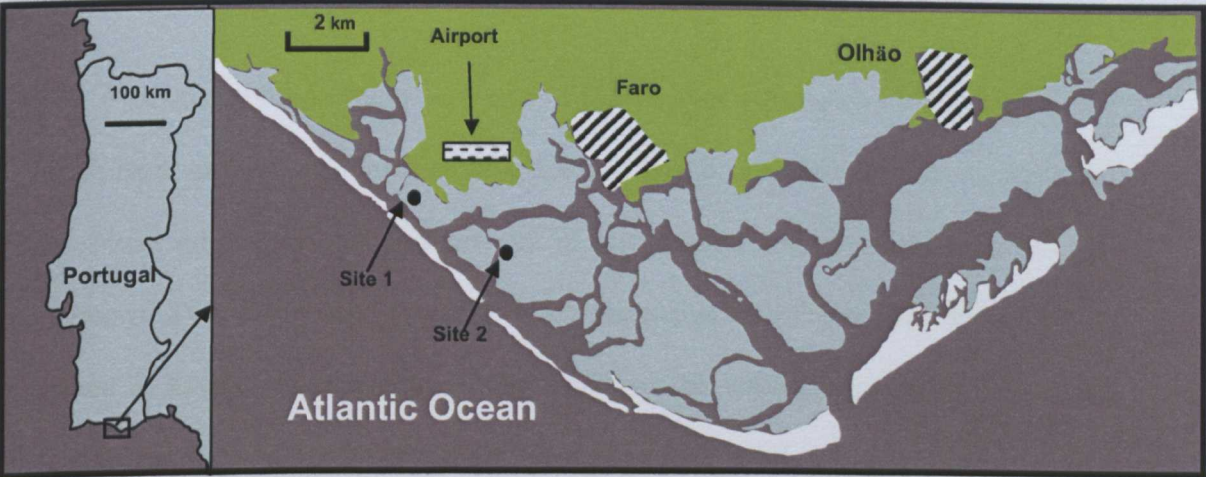


Figure 2-2. Maps showing the location of the Ria Formosa and the positions of sampling sites.

2.1.3 Thames Estuary.

The Thames Estuary is a turbid, macro-tidal estuary on the east coast of the United Kingdom (Fig. 2.3a) extending from the limit of tidal intrusion at Teddington Weir (Fig. 2.3b), through Greater London, finally discharging into the southern North Sea. The mean fluvial input is $82 \text{ m}^3 \text{ s}^{-1}$, the tidal range varies from 3 to 6 m, and the flushing time is from 20 to 40 days (Abril *et al.*, 2002). The catchment area is approximately $14,000 \text{ km}^2$ containing a population of about 11 million people. Sewage contamination of the estuary has been an issue in the past (Kinniburgh, 1998; Tinsley, 1998) and although considerable improvements in water quality have been achieved, some beaches (e.g. those near Southend; Fig. 2.3c) have achieved only mandatory compliance with the EC Bathing Water Directive. The estuary is classed as nitrate-rich (Middelburg and Nieuwenhuize, 2000) and there are indications that a fraction of the suspended particulate matter (SPM) may be sewage-derived and subject to carbon mineralisation (Abril *et al.*, 2002).

Southend marks the outer limits of the Thames Estuary and is located on the north bank of the river. The area from Canvey Island to Southend hosts a variety of inter-tidal substrata including a network of salt marshes and inter-tidal creeks in the region of Two Tree Island (see Fig. 2-3c). Extensive mudflats extend from Canvey Island to beyond the recognised outer limits of the estuary although a number of sandy beaches were constructed within the last two centuries.

2.2 Sample collection and methodology

2.2.1 Sampling Every Station

Sampling took place over a 3-day period in April 1997 when the weather

listed in Table 1-1 was typical.

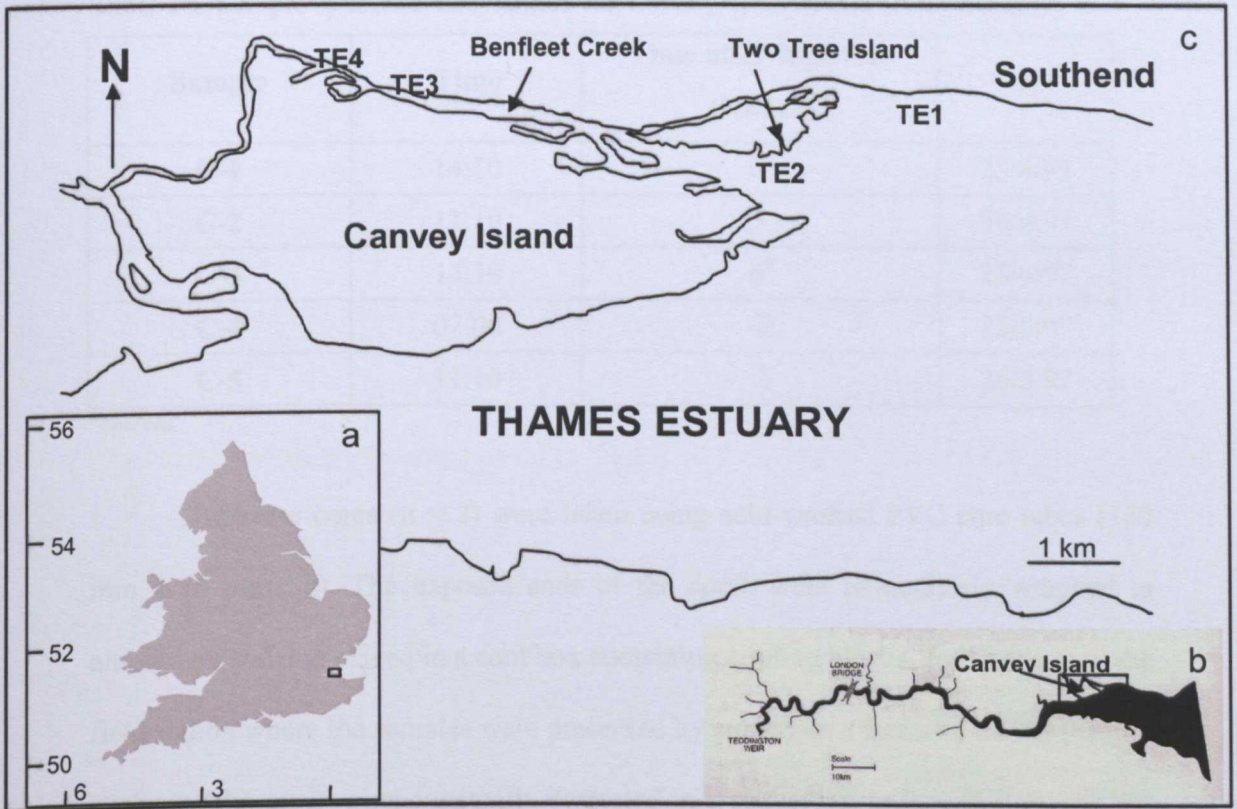


Figure 2-3. Location of the sampling sites in the Thames Estuary, United Kingdom; (a) shows the location of the Thames Estuary in SE England, (b) shows the location of the sampling area within the Estuary, while (c) shows the precise location of the sampling sites. Sampling sites are marked (e.g. TE1).

2.2 Sample collection and pre-treatment.

2.2.1 Burnham Overy Staithe.

Sampling took place over a 3-day period in April 1997 when the samples listed in Table 2-1 were collected.

Table 2-1. Sample collection information for Cores 1-5, Burnham Overy Staithe.

Sample	Time	Time after high tide (Hours)	Date
C-1	14:10	6 ^a	23/4/97
C-2	11:10	3	24/4/97
C-3	15:10	6 ^a	25/4/97
C-4	07:00	-2	25/5/97
C-5	11:10	2	26/5/97

^a Low tide.

Duplicate cores (n = 2) were taken using acid-washed PVC core tubes (150 mm x 70 mm i.d). The exposed ends of the cores were immediately wrapped in aluminium foil and placed in a cool box containing cooling blocks, for transport to the field station where the samples were preserved by storing in a freezer (-20 °C) prior to analysis. The cores were eventually defrosted in a glove box under nitrogen gas and then sectioned at 10 mm intervals over a depth range of 0-100 mm. The individual sediment core sections were transferred to nitrogen-filled plastic centrifuge tubes and the samples centrifuged at 3000 rpm for 5 minutes. The supernatant liquids from the centrifuge tubes were then filtered into acid washed glass vials, through 0.45 µm filters, using a syringe filter apparatus (Whatman). The residual sediments were freeze-dried and both the dry sediments and the supernatant liquids were kept in a freezer (-20 °C) prior to analysis.

2.2.2 Ria Formosa

2.2.2.1 Sampling at Site 1

Sampling took place in September 2000. Four sets of duplicate sediment core samples were collected using perspex core tubes (100 mm x 72 mm, see Table 2-2 for sampling times). The cores were then sectioned *in situ* at 10 mm intervals from 0-50 mm depth. Pore-water was extracted using a pressure filtration device constructed by the University of the Algarve. The filtration system was connected to a nitrogen gas cylinder for maximum efficiency and to reduce sample contact with oxygen. Following extraction, pore-water was filtered into acid-washed glass vials through 0.45 µm cellulose acetate filters (Whatman). Solid-phase and pore-water samples were then transferred to a cool-box and frozen (-20 °C) immediately on arrival in the laboratory. Samples were transported to the UK in a cool box.

Table 2-2. Details of sampling times at Site 1, Ria Formosa.

Core	Time	Stage of inundation
RF1	11:20	2 hours before inundation
RF2	12:30	1 hour before inundation
RF3	13:20	Flooding begins
RF4	13:50	0.5 hours after flooding

2.2.2.2 Sampling at Site 2

Sediment cores (50 mm depth) and individual clams (*R. decussates* L.) were collected. The first core and set of clams were collected one hour before the incoming tide had reached the site. The second sediment core and clams were collected immediately after inundation of the site. Each of the two clam sample sets contained 10 individuals. Once collected, the cores were sealed and the clams placed in plastic

sample bags. All samples were then placed in a cool box for transportation to the laboratory.

On arrival, sediment was wiped from the clam shells and their mantles opened. The entrapped water was transferred into a measuring cylinder to record the volume and then immediately transferred to an acid-washed glass vial and stored frozen for analysis. The soft tissue of the clams was then carefully removed with a knife and homogenised in a blender without addition of any solution (each sample set was blended separately). The clam tissue from each sample set was then weighed and analysed separately. Sediment cores were sectioned at 10 mm intervals and then homogenised and transferred to acid-washed Nalgene bottles. The sediment, clam mantle cavity water and clam tissue samples were frozen (-20 °C) prior to transport to the UK for analysis. Samples were analysed within 2 weeks of collection.

2.2.3 Thames Estuary.

2.2.3.1 Sample collection.

Sampling was carried out in the outer Thames Estuary in July (summer samples, Plate 2-2) and November (winter samples) 2001. Sediment cores (TE1-TE4, see Table 2-3 for sampling times) and overlying water were collected along a transect extending from Southend to upper Benfleet Creek (Fig. 2-3c). Sediment cores were collected using acid-washed PVC coring tubes (150 mm x 70 mm) and placed in a cool box for transport back to the laboratory, where a section of sediment (0-100 mm) was removed for analysis. These core sections were then sub-sampled at 10 mm intervals. The 10 mm sections were then centrifuged (3000 rpm, 5 min) and the supernatant liquid passed through a 0.45 µm Whatman filter paper into acid-washed

glass vials. Both the supernatant liquid and solid-phase samples were stored frozen (-20 °C) until analysis.

Table 2-3. Details of sampling times for sediment cores taken from the Thames Estuary transect.

Cores	Time of sampling	
	July	November
TE1	10:15	10:38
TE2	11:15	11:21
TE3	11:50	12:10
TE4	13:25	13:15
*LT(Time, height (m))	09:03, 1.1	09:28, 1.0
*HT (Time, height (m))	15:16, 5.2	15:36, 5.2

*LT = Low Tide, HT = High Tide

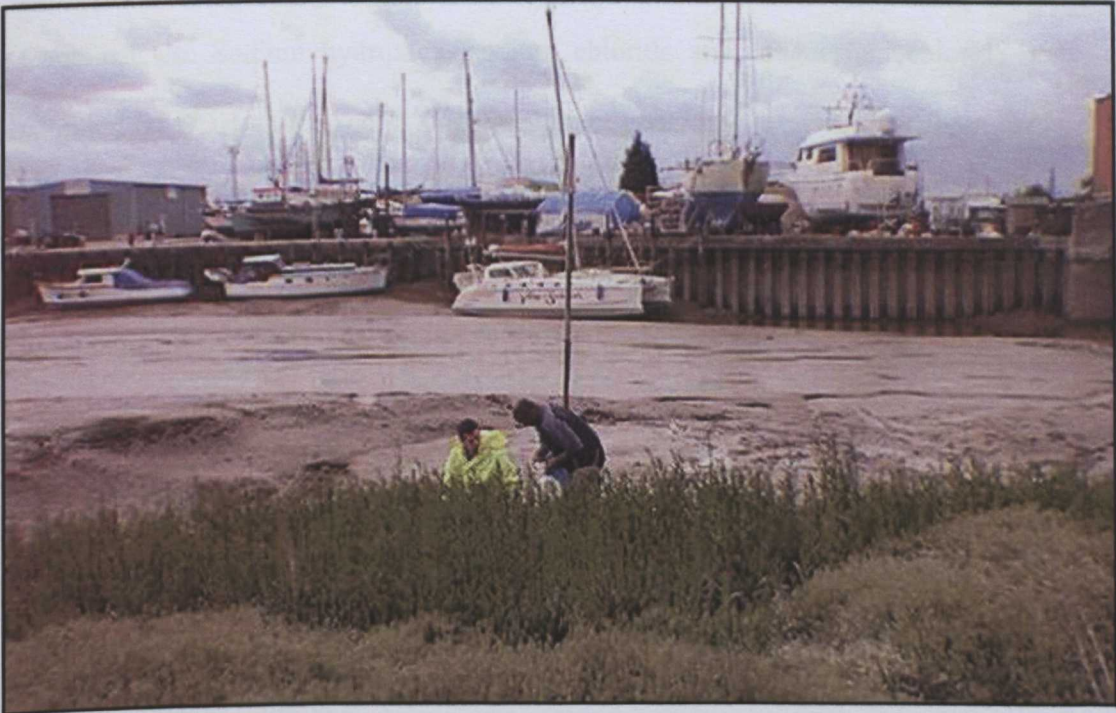


Plate 2-2. Sampling at the Thames Estuary site, TE3 (July, 2001).

2.2.3.2 Determination of suspended particulate material (SPM).

Water samples were collected, at hourly intervals for 6 h, from a bridge overlooking site TE2 during the flood period of a rising spring tide (March 22nd, 2002). Samples (0.5 L) were transferred to acid-washed Nalgene bottles and transported to the laboratory for immediate filtration through pre-weighed glass fibre filters. The filtrate was stored at 4 °C. Concentrations of suspended particulate material (SPM) were determined after drying the filters to constant weight (105 °C).

2.3 Determination of nitrogen compounds.

2.3.1 Reagents and standard solutions for NH₄⁺ and MA analysis.

Ammonium chloride, monomethylamine hydrochloride, dimethylamine hydrochloride, trimethylamine hydrochloride, cyclopropylamine, sodium citrate, phenol, sodium nitroprusside and sodium dichlorocyanurate were supplied by Aldrich Chemical Co. Sodium hydroxide, sodium chloride and magnesium chloride were supplied by BDH. All reagents were analytical grade and were used without further purification. Water for blanks and standard solutions was obtained from a SERADEST S600 system (< 0.1 µS cm⁻¹ conductivity). Stock standard solutions of ammonium (100 mM) and the MAs (1 M) were prepared by dissolution of the appropriate chloride/hydrochloride salts in water. Concentrated HCl (1 mL) was added as a preservative and the solutions made up to 100 mL in volumetric flasks. The standards were refrigerated and the MA samples were checked regularly by gas chromatography (GC) for evidence of any degradation. Working standard dilutions were prepared as required.

2.3.2 Determination of NH_4^+ .

2.3.2.1 NH_4^+ extraction techniques

Pore-water samples (0.1 mL) were analysed for NH_4^+ according to the colorimetric method of Dal Pont *et al.* (1974). Particulate NH_4^+ was determined after extraction of residual freeze-dried sediment with 2 M LiCl (1g sediment, 10 mL LiCl) as described by Wang and Lee (1994) or 2 M KCl (Morin and Morse, 1999). Samples were agitated on a mechanical shaker (2 h), and then passed through 0.45 μm filters, using a syringe filter apparatus (Whatman), and an aliquot of the filtrate (0.1 mL) then analysed.

2.3.2.2 Procedure for NH_4^+ analysis

The reagents for the NH_4^+ analysis were prepared as follows:

- 1) 'Citrate buffer': prepared by dissolving 100 g of sodium citrate in 300 mL deionised water. The mixture was boiled and sodium hydroxide (1M) was added until pH 10.2 was reached. The solution was then made up to 250 mL.
- 2) 'Phenol solution': prepared by dissolving phenol (3.5 g) and sodium nitroprusside (40 mg) in 50 mL deionised water.
- 3) 'Cyanurate': prepared by adding NaOH (2 g) and sodium dichlorocyanurate (0.2 g) to 100 mL of deionised water.

Colour development was achieved by mixing 0.1 mL of the NH_4^+ standards or samples, 0.8 mL deionised water and 0.1 mL of the citrate buffer in a glass vial. To this mixture were added 0.05 mL of 'phenol solution' and 0.05 mL of 'Cyanurate'. The solutions were covered with aluminium foil and stored in a refrigerator overnight

to minimise the risk of photo-degradation prior to determination using a PU8675 UV/Visible Spectrophotometer set to 630 nm. Standard NH_4^+ solutions were prepared by diluting 100 mM stock solutions as required (Table 2-4).

Table 2-4. Triplicate analyses of standard NH_4^+ solutions.

Standard concentration (µM)	Absorbance 1	Absorbance 2	Absorbance 3	Average	%RSD
0	0.000	0.001	0.000	0.000	N/A
50	0.042	0.043	0.043	0.043	1.4
100	0.09	0.090	0.100	0.093	2.5
200	0.177	0.179	0.178	0.178	0.6
300	0.265	0.264	0.266	0.265	0.4
500	0.44	0.450	0.470	0.453	3.4

%RSD = Percentage Relative Standard Deviation.

2.3.2.3 Calibration of the spectrophotometric technique for NH_4^+ analysis.

The spectrophotometric method was calibrated by treating standard solutions of ammonium chloride according to the procedure described in Section 2.3.2.2 and determining their absorbance at 630 nm. A typical calibration graph is shown in Fig. 2-4. Procedural blanks were determined with all calibration runs and deducted from the absorbance of standard concentrations.

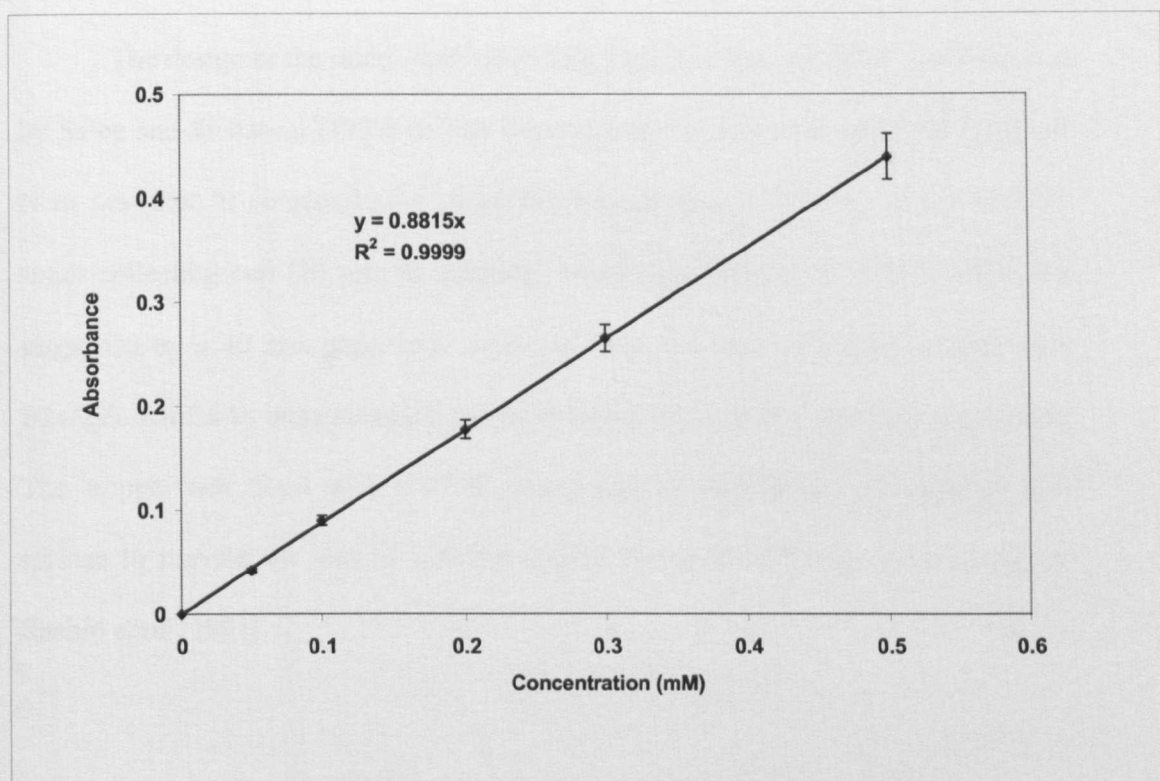


Figure 2-4. A calibration graph for NH_4^+ standard solutions.

The reproducibility of the colorimetric technique was determined by analysing triplicates of each standard solution. The reproducibility is given in Table 2-4. The percentage standard deviations were all below 5%. The detection limit was calculated as four times the standard deviation of a separate blank run ($n = 5$, mean = $0.6 \mu\text{M}$ and SD = $0.034 \mu\text{M}$). The calculated detection limit (DL) was $0.135 \mu\text{M}$.

2.3.2.4 Glassware preparation.

All glassware was acid-washed (1M HCl, 24 h) and then thoroughly rinsed with Milli-Q Water. The clean glassware was dried overnight in a fan-assisted oven (200°C) before use. The glassware was exposed to the atmosphere for only the shortest time possible to avoid contamination.

2.3.2.5 Design of the micro-diffusion flask.

The design of the micro-diffusion flask (Fig. 2-5) was similar to that described by Riley and Sinhaseni (1957) for the determination of ammonia and total inorganic N in seawater. It consisted of a pyrex Erlenmeyer flask (150 mL) within which a small collecting cup (20 mm in diameter, containing 200 μ L of 0.02 M HCl) was supported by a 40 mm glass rod suspended from the base of a glass stopper (size B24/29). All flasks were standardised by ensuring that cup and rod sizes were equal. The stopper was fitted with a PTFE sleeve and secured using two stainless steel springs to prevent the loss of volatiles during the micro-diffusion process (Abdul-Rashid *et al.*, 1991).

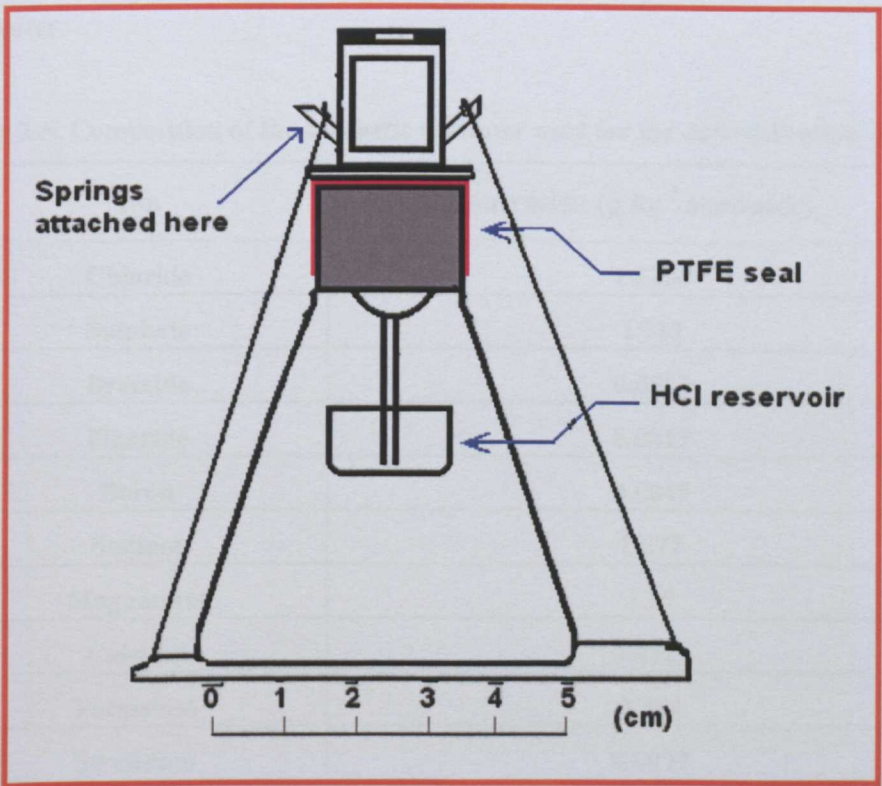


Figure 2-5. Diagrammatic representation of the micro-diffusion flask used for extraction of MAs.

2.3.2.6 Selection of internal standard.

Cyclopropylamine (CPA) was chosen as the internal standard (IS) for the micro-diffusion process. It is a volatile organic amine of low molecular weight, which has, so far, not been detected in any natural samples. The retention time during GC analysis was reasonably close to those of the MAs but with good resolution from the analytes (see Fig. 2-8), and the recovery and reproducibility of CPA had previously been found to be satisfactory (Abdul-Rashid *et al.*, 1991).

2.3.2.7 Synthetic seawater preparation.

The micro-diffusion analysis was carried out using synthetic seawater (the role of which was to match the seawater matrix prepared using the major ions whose ratio is almost constant (Wilson, 1975). Table 2-5 lists the ions and their concentrations in seawater.

Table 2-5. Composition of the synthetic seawater used for the determination of MAs.

Ion	Concentration (g kg⁻¹ seawater)
Chloride	19.354
Sulphate	2.712
Bromide	0.0673
Fluoride	0.0013
Boron	0.0045
Sodium	10.77
Magnesium	1.29
Calcium	0.4121
Potassium	0.399
Strontium	0.0079
Total	~35

Data from Wilson (1975).

2.3.2.8 Calibration of the analytical technique.

Two calibration techniques were employed. The first of these involved direct injection of standard MA solutions into a GC to determine the peak area ratio for different concentrations of MAs relative to CPA (peak area of MA/peak area of CPA). The second calibration was performed after subjecting standard MA solutions (with equivalent concentrations to those used for direct injection) to the micro-diffusion process. This enabled determination of the recovery of MAs through micro-diffusion.

a) Direct injection

Mixed standard solutions of MAs were prepared by diluting a stock solution (100 mM) of MAs (see Table 2-6 for concentrations and volumes) in synthetic seawater to which NaOH (6 M, 2 mL) and CPA (0.125 mM, 2 mL) had been added. A small aliquot (5 μ L) of the solution was injected directly into the GC (for conditions see Table 2-11). A calibration graph for the internal standard method was obtained by drawing a line of best fit through peak area ratios (peak area of MA standard/ peak area of CPA). Figure 2-6 shows a typical calibration graph for the direct injection method. The reproducibility of the GC analysis was determined using standard MA solutions (2 μ M; n = 6) and Table 2-7 shows the derived reproducibility. The tested concentrations of 2 μ M were chosen as being realistically representative of the MA levels found in a wide range of marine environmental samples.

Table 2-6. Procedure for preparation of mixed MA standards for direct-injection calibration.

Mixed standards Final Concentration (μM)	Volume of 100 μM Mixed Standard Solution (mL)	Volume of Synthetic Seawater (mL)
0.1	0.05	45.95
0.5	0.25	45.75
1	0.5	45.5
2	1	45
5	2.5	43.5
10	5	41

Table 2-7. Reproducibility of MA standards (direct injection) at 2 μM (n = 6).

MA	Mean Peak Area Ratio	Standard deviation ($\times 10^{-6}$)	Reproducibility (% Difference)
MMA	0.02	38	0.19
DMA	0.06	67	0.11
TMA	0.11	67	0.06

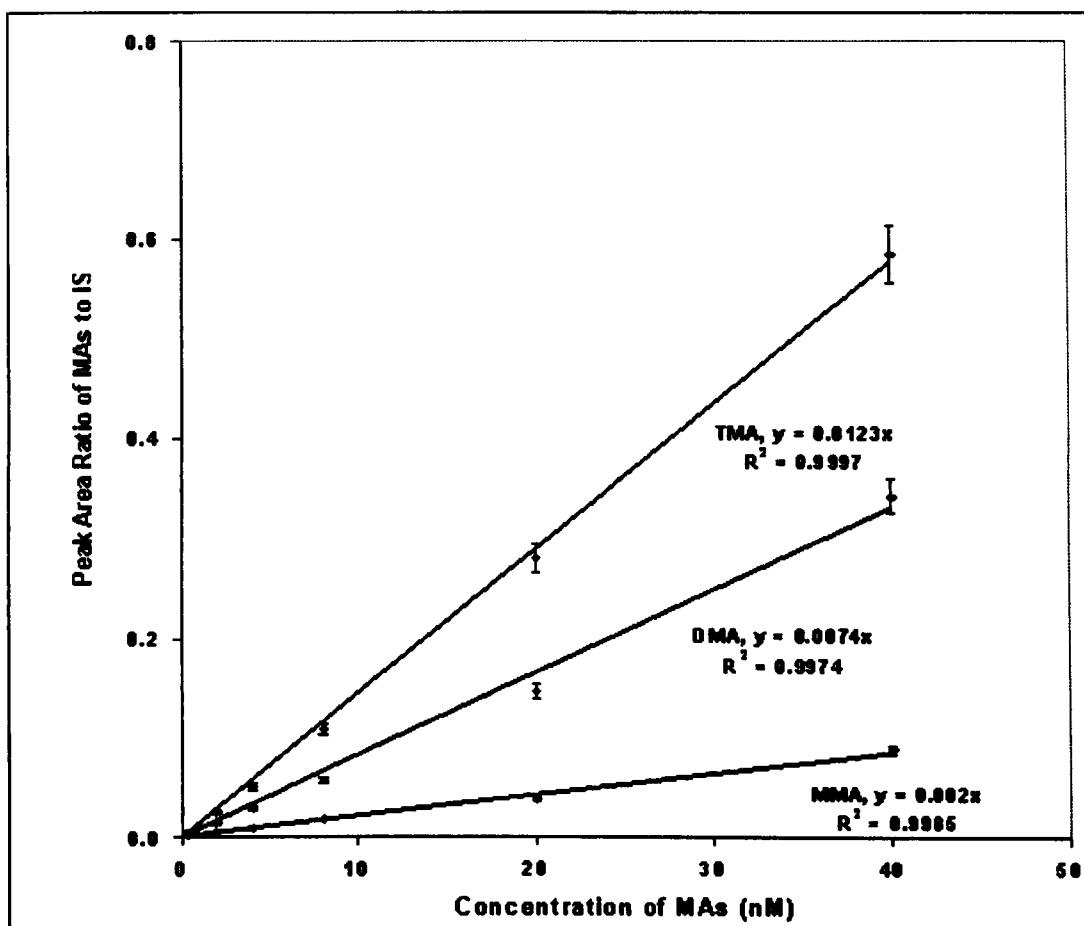


Figure 2-6. Calibration graphs for the three MAs determined by direct injection.

b) Calibration of the micro-diffusion method.

Mixed standard sample concentrations of the MAs were prepared from a 0.4 μM solution using the volumes shown in Table 2-8. The resulting concentrations corresponded to the concentrations of standards used in the direct injection technique, assuming a pre-concentration factor of 250. Standard solutions of MAs were made up as follows. A mixed standard solution of MAs (0.4 μM , for volumes see Table 2-8) and CPA (0.5 μM , 2 mL) were diluted with synthetic seawater (25 mL) and NaOH

(6 M, 2 mL). The solution was mixed thoroughly and made up to volume (50 mL) with synthetic seawater. Following immediate transfer to the micro-diffusion flask, the procedure explained in Section 2.3.3.7 was followed. Duplicate GC analysis was carried out for each concentration (see Section 2.3.3.8) and the results were normalised to the volume of HCl remaining in the cup at the end of the micro-diffusion process. Figure 2-7 shows typical calibration graphs after micro-diffusion in which peak area ratios of MA to CPA are plotted against concentration of MA.

The R^2 values for each of the 3 MAs for the calibration graphs indicate a good linear fit of the peak ratio values with concentrations. This was in good agreement with the calibration by the direct injection method, which also had a strong linear relationship. Replicate mixed standard solutions (8 nM, n = 6) of MAs were pre-concentrated in order to determine the reproducibility of the micro-diffusion method at 2 μ M. The coefficients of variation were 2.1, 1.4, and 0.5% for MMA, DMA and TMA, respectively.

Table 2-8. Concentration and volume of mixed MA standard solutions for calibration using micro-diffusion.

Mixed standards Concentration (nM)	Corresponding concentration by direct injection (μM)	Volume of 0.4 μM Mixed standard solution (mL)	Volume of synthetic seawater (mL)
0.4	0.1	0.05	45.95
2	0.5	0.25	45.75
4	1	0.5	45.5
8	2	1	45
20	5	2.5	43.5
40	10	5	41

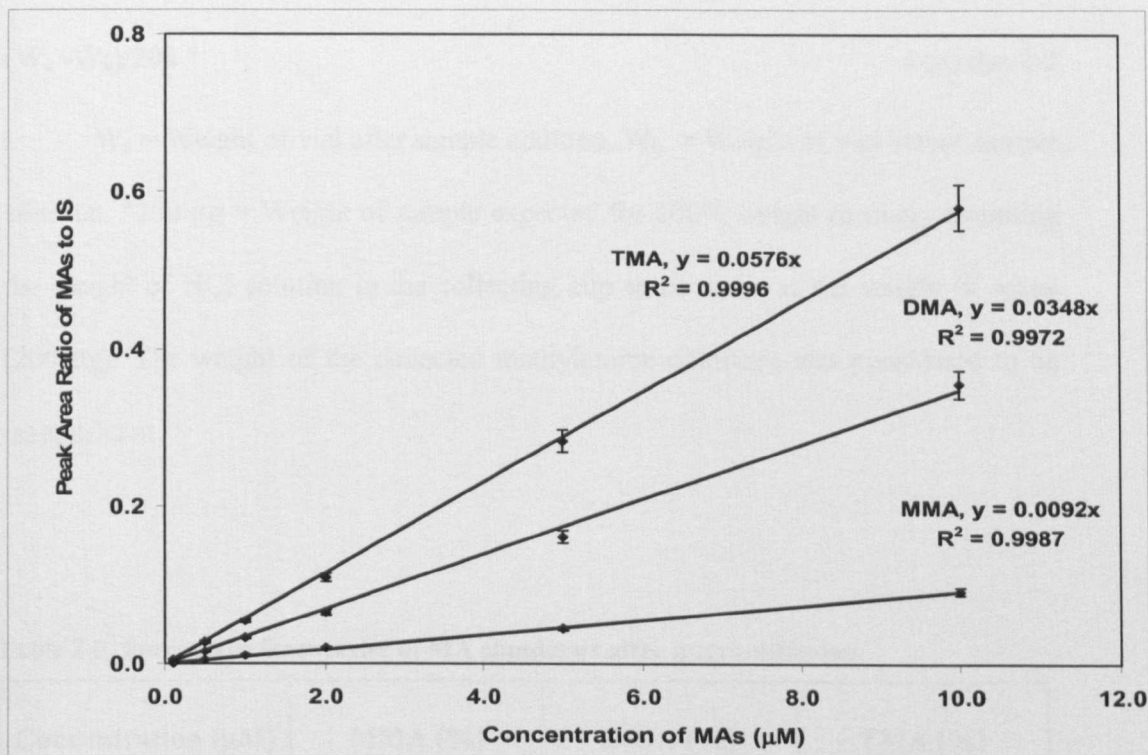


Figure 2-7 Calibration graphs for the three MAs determined by micro-diffusion.

2.3.2.9 Calculation of analyte recovery through micro-diffusion.

MA recoveries were determined at different concentrations (see Table 2-9). Sample recoveries after micro-diffusion were calculated as percentages using Equation 2-1.

$$\text{Percentage Recovery} = \frac{\text{PAR (micro-diffusion)}}{\text{PAR (direct injection)}} \times 1.25 \quad \text{Equation 2-1}$$

Weight recovery factor

Where PAR is the peak area ratio, 1.25 is the correction factor of preconcentration as a result of adding 50 μL of NaOH to the preconcentrated MAs. The weight recovery factor is a normalisation factor for discrepancy in weight of the collecting cup after micro-diffusion, calculated using Equation 2-2.

$$(W_a - W_b)/200 *$$

Equation 2-2

W_a = Weight of vial after sample addition, W_b = Weight of vial before sample addition. *200 μ g = Weight of sample expected for 100% weight recovery assuming the weight of HCl solution in the collecting cup to be same as the weight of water (200 μ g). The weight of the collected methylamine chlorides was considered to be insignificant.

Table 2-9. Percentage Recoveries of MA standards after micro-diffusion.

Concentration (μ M)	MMA (%)	DMA (%)	TMA (%)
0.1	83.4 \pm 3.2	86.4 \pm 4.1	86.9 \pm 3.5
0.5	87.0 \pm 3.4	87.4 \pm 3.4	91.0 \pm 3.7
1.0	90.4 \pm 2.8	88.6 \pm 2.7	93.4 \pm 3.2
2.0	88.1 \pm 2.9	88.8 \pm 2.2	100.1 \pm 1.2
5.0	85.9 \pm 1.2	90.8 \pm 1.8	99.2 \pm 1.4
10.0	95.9 \pm 0.4	96.1 \pm 0.5	100.8 \pm 1.1

Generally, the recoveries of MAs after micro-diffusion increased with increasing concentration (Table 2-9). Recoveries were above 80% for all MAs (83.4 - 100.8%), with highest recoveries for the 2, 5 and 10 μ M TMA standard solutions. The precisions of the recovery method were all below 5%. These data confirm that the micro-diffusion method used in this investigation was reliable for analysis of MAs at previously reported environmental concentrations.

2.3.2.10 Application of the micro-diffusion process.

The following is the general procedure used for environmental samples analyses, where modification to this was needed (for e.g. Ria Formosa Site 2 samples; Section 2.3.4) this is shown in separate sections below.

a) Pore-water Samples.

Pore-water samples were pre-concentrated using micro-diffusion by treating the collected samples with NaOH (6 M, 2 mL) in a 50 mL volumetric flask. CPA (10^{-4} M, 2.5 mL) was then added as an internal standard and the solution made up to volume (50 mL) with synthetic seawater. The solution was thoroughly mixed and transferred to the micro-diffusion flask. HCl (0.02 M, 200 μ L) was added to the collecting cup and the stopper secured with stainless steel springs.

Optimum recovery of the analytes was achieved through incubation of the flask in a fan-assisted oven (60 °C, 24 h). When this time had elapsed, the contents of the collecting cup were quantitatively transferred by micropipette to a glass vial (0.8 mL) and weighed. The percentage recoveries of MAs were calculated using Equation 2-2. Samples were stored in a freezer (-20 °C), if necessary, and were analysed by GC as soon as possible.

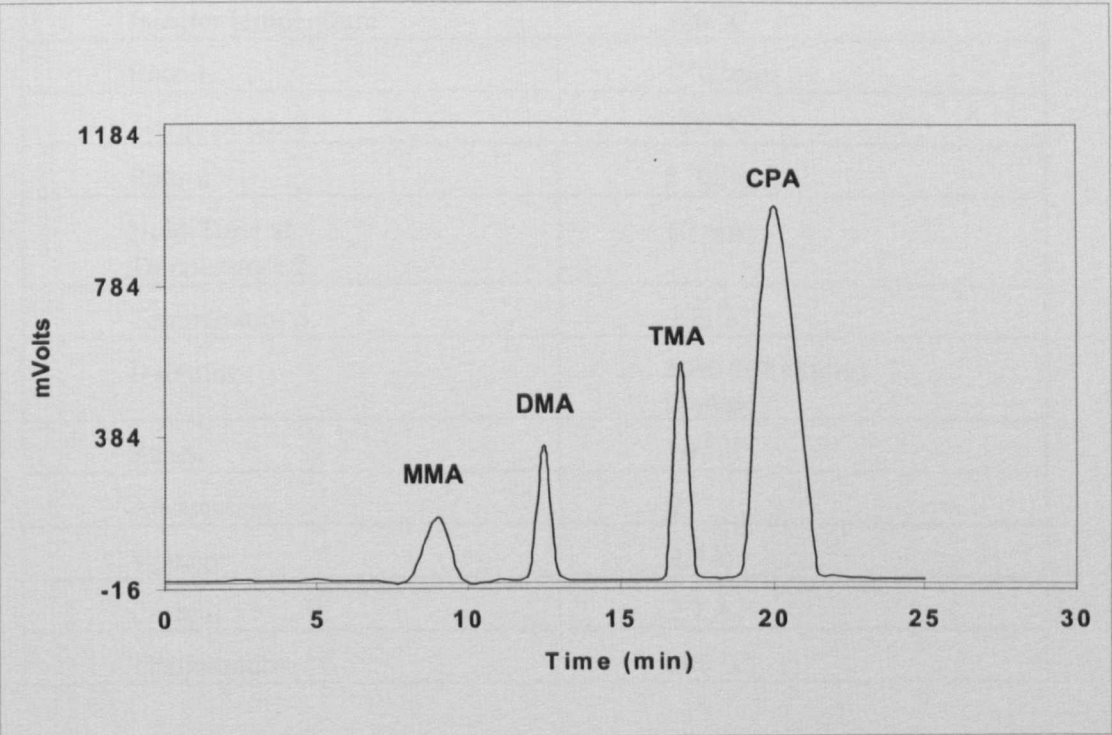
b) Solid-phase sediment samples.

Freeze-dried sediment samples (0.5 g) were accurately weighed, transferred to a volumetric flask, and thoroughly mixed with NaOH (6 M, 2 mL) and CPA (10^{-4} M, 2.5 mL). The solution was made up to 50 mL with synthetic seawater and immediately transferred to the micro-diffusion flask. HCl (0.02 M, 200 μ L) was added to the collecting cup, and the stopper secured with stainless steel springs before

the flask was placed in the oven (60 °C, 24 h). When the incubation was complete, the contents of the collecting cup were treated in the same way as described above.

2.3.2.11 Gas Chromatography.

MA_s were resolved and detected (see Table 2-10 for detection limits) on a Fisons 8000 Series packed column GC equipped with a nitrogen-phosphorus detector (NPD). The GC column (2 m) was packed with Carbo-pack B (60-80 mesh) coated with Carbowax 20 M (4%) and KOH (0.8%). Data were recorded using a PC equipped with Chrom-Card for windows software (Fisons Instruments). The GC operating conditions, listed in Table 2-11, were found to be optimal for analytical run time of 25 minutes, and the chromatograms indicated good resolution and reproducibility of MA_s. A representative chromatogram of a mixed MA standard solution, containing CPA, obtained using these GC conditions, is shown in Fig. 2-8.



*S.D = 4σ

Figure 2-8. Representative chromatogram of MA standards and CPA obtained by direct injection of a 1 μM mixed standard solution.

Table 2-10. Method detection limit of the three MAs by GC-NPD.

MA	Method Detection Limit (nM)*
MMA	8.7
DMA	11.6
TMA	21.6

Table 2-11. GC operating conditions for the determination of MAs.

Carrier gas	N₂
Pressure	50 kPa
Air pressure	80 kPa
Hydrogen pressure	30 kPa
Temperature Gradient	
Temperature-1	100 °C
Injector temperature	200 °C
Rate-1	5 °C/min
Temperature-2	120 °C
Rate-2	8 °C/min
Hold Time at Temperature 2	10 min
Temperature-3	200 °C
Detector	NPD 800 control module
Range	10⁽⁰⁻³⁾
Attenuation	0
Voltage	3.5 V
Current	2.7 A
Temperature	200 °C

2.3.2.12 Reproducibility of environmental samples.

a) Burnham Overy Staithe

Replicate aliquots of pore-water and sediment were analysed ($n = 4$) from each core (at various depths) to determine the intra-sample reproducibility for the analytical technique. The average variations were determined to be 1.4, 0.9 and 0.8% (pore-water) and 7.5, 2.3 and 5.4% (solid-phase) for MMA, DMA and TMA, respectively. The solid-phase and pore-water samples analysed in the first batch of samples were re-analysed after completion of the analyses to determine the effect of storage on MA concentrations. The comparison showed average differences of 3.9, 10.3 and 1.8% in the pore-waters and 13.7, 0.1 and 3.7% in solid-phase for MMA, DMA and TMA, respectively. This result seemed to indicate that solid-phase MMA and pore-water DMA were more labile than the other MAs, suggesting that these samples needed to be analysed as soon as possible after pre-treatment to avoid underestimation of their concentration after a long period of storage.

b) Ria Formosa

The reproducibility of MA analysis of Ria Formosa samples (core sections) was obtained by analysing duplicate samples of each core section and then determining the percentage difference to the mean according to Equation 2-3. Replicate samples ($n = 4$) were also analysed for clam tissue, mantle cavity water and sediment from the clam beds, and the reproducibility was determined as the percentage relative standard deviation to the mean. Table 2-12 shows the reproducibility of the Ria Formosa samples.

Table 2-12. Reproducibility of MA analysis for pore-water, sediment and clam tissue samples from Sites 1 and 2 of the Ria Formosa.

MA	*Solid-phase	*Pore-water	**Clam tissue	**Clam mantle cavity water	**Clam surrounding sediment
MMA	1.08	3.34	4.02	1.09	2.11
DMA	4.2	3.36	3.76	2.87	2.34
TMA	1.91	2.21	2.44	2.06	2.41

* Percentage difference to the mean
 **Percentage Relative Standard Deviation, which was used for clam samples (tissue, mantle cavity water and surrounding sediment) as there were more than two separate analyses enabling the calculation of standard deviation, whereas there were only two separate analyses for sediment samples.

c) Thames Estuary samples

The reproducibility of MA concentrations in samples from the Thames Estuary was expressed in terms of the percentage difference relative to the mean of two separate analyses, calculated using Equation 2-3 (Tables 2-13 to 2-16).

R = 100 x (difference of 1st Analysis and 2nd Analysis)/Mean of the two analyses. Equation 2-3.

Table 2-13. Reproducibility of Thames Estuary MA analysis (Solid-Phase, July samples).

Core/Depth (mm)	1st Analysis			2nd Analysis			(%) Difference to the Mean		
	MMA	DMA	TMA	MMA	DMA	TMA	MMA	DMA	TMA
TE1/0-5	2.5	2.0	2.5	2.4	2.1	2.6	4.1	3.9	3.9
TE1/80-100	2.3	2.0	5.0	2.4	2.1	5.3	4.3	4.9	5.8
TE2/30-40	5.0	2.6	1.9	5.1	2.6	1.8	2.0	1.9	5.4
TE3/40-50	4.6	2.3	4.4	4.5	2.4	4.3	2.2	4.3	2.3
TE4/60-80	2.6	2.2	2.1	2.6	2.1	2.2	0.0	4.6	4.6

Table 2-14. Reproducibility of Thames Estuary MA analysis (Pore-Water, July samples).

Core/Depth (mm)	MA concentration (μM)			MA concentration (μM)			% Difference to the Mean		
	1st Analysis			2nd Analysis					
	MMA	DMA	TMA	MMA	DMA	TMA	MMA	DMA	TMA
TE1/80-100	0.4	0.1	0.0	0.4	0.1	0.00	0.0	6.9	0.0
TE2/30-40	0.3	0.3	0.07	0.3	0.3	0.07	3.5	3.8	4.2
TE3/40-50	0.1	1.2	0.04	0.1	1.2	0.04	0.0	4.4	5.4
TE4/60-80	0.2	0.1	1.0	0.2	0.1	0.09	5.7	0.0	7.5

Table 2-15. Reproducibility of Thames Estuary MA analysis (Solid-Phase, November samples).

Core/Depth (mm)	MA concentration (μmolg^{-1})			MA concentration (μmolg^{-1})			% Difference to the Mean		
	1st Analysis			2nd Analysis					
	MMA	DMA	TMA	MMA	DMA	TMA	MMA	DMA	TMA
TE1/0-5	0.9	1.2	2.1	0.9	1.2	2.1	3.3	3.4	1.9
TE1/80-100	0.7	0.9	1.0	0.7	0.9	1.0	4.3	2.3	2.1
TE2/30-40	1.4	1.4	2.5	1.4	1.4	2.6	1.4	0.0	1.2
TE3/40-50	0.8	1.9	1.6	0.8	2.0	1.7	3.7	4.6	2.4
TE4/60-80	1.5	1.9	2.3	1.5	1.9	2.4	2.0	1.6	3.8

Table 2-16. Reproducibility of Thames Estuary MA analysis (Pore-Water, November samples).

Core/Depth (mm)	MA concentration (μM)			MA concentration (μM)			% Difference to the Mean		
	1 st Analysis			2 nd Analysis					
	MMA	DMA	TMA	MMA	DMA	TMA	MMA	DMA	TMA
TE1/0-5	1.0	1.2	1.4	1.0	1.2	1.3	2.1	3.3	4.4
TE1/80-100	0.5	0.5	0.3	0.5	0.5	0.3	4.0	3.7	3.0
TE2/30-40	0.9	1.1	1.2	0.9	1.2	1.2	3.4	4.4	1.6
TE3/40-50	0.9	0.8	1.2	0.9	0.9	1.3	1.1	3.5	4.0
TE4/60-80	0.5	0.4	0.7	0.6	0.5	0.6	5.3	2.2	4.5

The percentage difference to the mean is a crude measure of the difference of two analyses in the absence of a large number of different analyses of the same sample, where the reproducibility can be determined in terms of percentage relative standard deviation (%RSD). The values in Tables 2-13 to 2-16 provide a guide to the precision of 2 separate analyses of the same sample. Most reproducibilities were within the range of $\pm 5\%$, indicating good precision. Values outside this range were all within $\pm 10\%$, suggesting that a reasonable reproducibility was achieved for the MA analyses of both solid-phase and pore-water samples taken from the Thames Estuary in July and November 2001.

2.3.3 MA determination of Ria Formosa Site 2 samples.

MA concentrations were determined in homogenised clam tissue, mantle cavity water and sediment from the clam beds at Site 2 in the Ria Formosa. Samples were taken before and after tidal inundation in order to assess the potential flux of MAs from the clam tissue to mantle cavity water, and then from mantle cavity water to the surrounding sediment.

2.3.3.1 Mantle cavity water.

One mL mantle cavity water (defined as water drained from the clam on opening the shell) was added to a solution containing LiCl (25 mL, 2 M), NaOH (6 M, 2 mL) and CPA (10^{-4} M, 2.5 mL). The solution was then made up to volume (50 mL) with 2M LiCl and mixed thoroughly before transfer to the micro-diffusion flask. After micro-diffusion, the contents of the collecting cup were quantitatively transferred by micropipette to a glass vial (0.8 mL) and weighed. Samples were stored in a freezer (-20°C), if necessary, and analysed as soon as possible. The GC analysis was carried out according to Section 2.3.3.8.

2.3.3.2 Surrounding sediment and clam tissue.

Moist sediment and tissue samples were also analysed by micro-diffusion. The solid sample (1 g of filtered sediment or 4 to 5 g of clam tissue) was placed in a micro-diffusion flask and 48 ml of 2 M LiCl solution containing CPA was added to desorb exchangeable MAs (Wang and Lee, 1994). The sample was gently mixed and the solution adjusted to pH 12 by addition of 2 ml of 6 M NaOH. The flask was immediately sealed and the micro-diffusion carried out as detailed above. A separate analysis of clam tissue samples was carried out using SSW instead of 2M LiCl. The GC analysis was carried out according to Section 2.3.3.8.

2.3.4 Calculations of potential exchangeable MA concentrations in clam samples.

The potential exchangeable MA concentrations (net MA concentration before and after inundation) from clam tissue to mantle cavity water and from mantle cavity water to surrounding sediment were calculated as described below;

1) From clam tissue to mantle cavity water.

The potential exchangeable MA concentration from or into clam tissue samples after tidal inundation was calculated using Equation 2-4. A positive net concentration indicated accumulation of MAs in the tissue after inundation while a negative net concentration indicated release of MAs to the mantle cavity water and possibly, into the surrounding sediment, or their conversion into another compound.

$$\text{Exchangeable MA concentration} = [\text{MA}]_{\text{CT (A)}} - [\text{MA}]_{\text{CT (B)}} \quad \text{Equation 2-4}$$

$[\text{MA}]_{\text{CT (A)}}$ = Concentration of MAs (mmol kg^{-1}) in clam tissue (after inundation).

$[\text{MA}]_{\text{CT (B)}}$ = Concentration of MAs (mmol kg^{-1}) in clam tissue (before inundation).

2) From mantle cavity water to clam tissue/surrounding sediment.

Mantle cavity water is defined as water drained from the clam on opening the shell. The potential flux of MAs from or into clam mantle cavity water was calculated using Equation 2-5.

$$\text{Exchangeable MA concentration} = [\text{MA}]_{\text{MCW (A)}} - [\text{MA}]_{\text{MCW (B)}} \quad \text{Equation 2-5}$$

$[\text{MA}]_{\text{MCW (A)}}$ = (Concentration of MAs in mantle cavity water $\text{mmol} \cdot \text{kg}^{-1}$) after inundation.
 $[\text{MA}]_{\text{MCW (B)}}$ = (Concentration of MAs in mantle cavity water ($\text{mmol} \cdot \text{kg}^{-1}$) before inundation.
 *per bulk sediment (1mL of mantle cavity water was assumed to weigh 1g).

3) From surrounding sediment to mantle cavity water (assuming the clam was surrounded by same amount of sediment and it remained stationary during inundation). This was calculated using Equation 2-6.

$$\text{Exchangeable MA concentration} = [\text{MA}]_{\text{SS(A)}} - [\text{MA}]_{\text{SS(B)}} \quad \text{Equation 2-6}$$

$[\text{MA}]_{\text{SS (A)}}$ = (Concentration of MAs in surrounding sediment $\text{mmol} \cdot \text{kg}^{-1}$, after inundation).
 $[\text{MA}]_{\text{SS (B)}}$ = (Concentration of MAs in surrounding sediment $\text{mmol} \cdot \text{kg}^{-1}$, before inundation).

2.3.5 Calculation of adsorption coefficients for NH_4^+ and MAs.

The relative affinities of NH_4^+ and MAs for the dissolved and particulate phases of sediment were determined through calculation of their porosity dependent and independent adsorption coefficients (K^* and K). Porosity dependent adsorption coefficients were calculated according to Fitzsimons *et al.* (1997). K was calculated using Equation 2-7.

$$K (\text{mLg}^{-1}) = C_s / C_w \quad \text{Equation 2-7}$$

C_s = $[\text{NH}_4^+, \text{MA}] \text{ mol g}^{-1}$ (solid-phase), C_w = $[\text{NH}_4^+, \text{MA}] \text{ mol mL}^{-1}$ (pore-water).

2.4 Determination of sedimentary total organic carbon (TOC) and total nitrogen (TN) content.

The total organic carbon and nitrogen content of BOS sediment samples were determined using the following technique. Aliquots of freeze-dried sediment samples (~5 mg) were accurately weighed into silver capsules (pre-extracted in a 1:1 mixture of acetone and hexane) and heated in a muffle furnace (250 °C; 14 h). At the same time aliquots (~2 mg) of CaCO₃ (standard) were weighed into separate cups in order to measure the removal of inorganic carbon from the samples. One drop of Milli-Q water (18M Ω cm⁻¹ resistivity) was added to the samples, which were placed in a desiccator containing concentrated HCl (~ 250 ml) until the CaCO₃ disappeared i.e. ~3-4 h (Yamamuro and Kayanne, 1995). The decarbonated sediments were then dried (~ 600 °C; 4-6 h), in order to drive off the water and excess acid, and analysed for TN using a Carlo Erba NC2500 analyser. The analyses were carried out in duplicate and the reproducibility was better than 10%.

2.5 Determination of selected physico-chemical parameters.

The following physico-chemical parameters were determined for all samples except where otherwise indicated.

2.5.1 Measurement of pore-water content.

The pore-water content of each sediment section was determined as follows. Wet sediment (~1g) was accurately weighed and then placed in a clean, dry glass vial. The vials were then placed in an oven (80 °C, 48 h) and the weight of the vial and dry sediment was recorded. Pore-water content was determined as the difference in weight between the wet and dry sediments.

2.5.2 Porosity measurement.

Porosity was defined according to Equation 2-8.

$$\text{Porosity } (\phi) = \frac{V_w}{V_w + M_s/\rho_s} \quad \text{Equation 2-8}$$

V_w = the volume occupied by pore-water, M_s = the weight of solid matter, ρ_s = the density of dry sediment (assumed to be 2.65 g mL⁻¹).

The volume of water was determined by measuring the loss in weight of 1g of wet sediment as a result of overnight drying in an oven at 105 °C. The volume of pore-water was calculated from the weight loss using a water density of 1g mL⁻¹.

2.5.3 Grain Size analysis.

Grain size (particle size) measurements were performed on sediment samples using a Malvern Long-bed Mastersizer-X, with wet sample unit MS17. Samples were presented to the system as wet samples, after removal of organics through wet oxidation using hydrogen peroxide (6%). Data were recorded on Mastersizer-X software, Version 2.18.

2.5.4 Salinity measurement.

Salinity of pore-waters was measured by ion chromatography following dilution of a sample of pore-water with deionised water (1:10 000) to bring the sample concentration within the linear range of the instrument. The chloride ion content (Cl⁻) of the diluted sample was measured on a Dionex DX-120 ion chromatograph, which was externally calibrated on a daily basis using standard chloride solutions. The salinity (S) of the sample was then calculated according to Equation 2-9.

$$S = 1.80655\text{Cl}^- \quad \text{Equation 2-9}$$

2.5.5 Laboratory simulated tidal action experiment.

The effect of tidal-induced resuspension on the distribution of dissolved and exchangeable NH_4^+ and MAs in surface sediments (0-5 mm) from the Thames Estuary was investigated using laboratory simulation experiments designed to mimic sediment resuspension by tidal action. Wet (i.e. unfiltered) sediment samples (1g) were mixed with 1L overlying water (OLW) spiked with 0.1% /v NaN_3 , as a biocide, in an acid-washed Nalgene bottle. The biocide, sodium azide (NaN_3), was added to each OLW sample at a concentration of 0.1% w/v (Morin and Morse, 1999). NaN_3 is used to synthesise amines (Clayden *et al.*, 2001) but only under non-aqueous conditions. Therefore, under these experimental conditions amine formation was not predicted. The natural, unfiltered sediments were added to the respective OLW from each site to create a SPM concentration approximately in the range 0.4 to 0.6 g L^{-1} . This was a higher SPM concentration range than that measured in tidal cycle samples but was similar to that used in previous experiments of this type (Morin and Morse, 1999). A water sub-sample (10 mL) was taken prior to addition of the sediment for the determination of the background dissolved concentrations of the analytes at $t = 0$. The reactors were then sealed and gently agitated on a mechanical shaker held at 25 °C.

Aliquots of the suspension (10 mL) were taken at selected time intervals up to 48 hours (Table 2-17) and filtered through 0.45 μm pore-size filters. The filtrates were analysed for $[\text{NH}_4^+]_D$ and $[\text{MA}]_D$ according to the methods described above. The measurement precision was 4% or less for NH_4^+ and below 10% for the MAs with one exception (12%). The contributions of $[\text{NH}_4^+]_D$ and $[\text{MA}]_D$ from the pore-waters of the unfiltered sediments were calculated to be < 1% of the final concentration in all of the experimental runs. All experiments were carried out in duplicate.

Table 2-17. Time intervals of sampling for tidal action experiment.

Sample	Time sampled (minutes)
1	0
2	10
3	20
4	30
5	60
6	120
7	1020
8	1440
9	2460
10	2880

2.5.6 Extraction of sediments.

To determine the size of the adsorbed exchangeable pools of NH_4^+ and MAs, two different extraction experiments, known as single volume and multi-volume extraction were carried out in duplicate. Multi-volume extractions of sediments were performed as previous work on NH_4^+ suggested that single volume extraction may underestimate sediment-exchangeable NH_4^+ (Laima, 1992; Morin and Morse, 1999).

Wet sediment from the Thames Estuary (1g) was initially centrifuged (3000 rpm, 1 h) to remove pore-water. A solution of KCl (20 mL, 2 M), spiked with biocide NaN_3 (0.1% w/v), was added to the sediment and the resulting slurry shaken (150 rpm, 25°C, 24 h). The agitation was carried out in the same centrifuge tube to avoid sample loss. The solution was then centrifuged (1h, 3000 rpm) and the supernatant passed through a 0.45 μm filter. All subsequent extractions were carried out in the same centrifuge tube. The filter paper was always washed several times with a small volume of the next volume of extractant to ensure that any sediment decanted onto the filter was washed back into the centrifuge tube. Sediment samples were weighed

before and after each extraction to check for possible sediment loss. In the few instances when differences were significant ($> 0.05\text{g}$), concentrations were normalised for that weight. The filtrate from each extraction was analysed for NH_4^+ and MAs as described in Section 2.3.

Optimum recovery for extraction of NH_4^+ and the MAs was determined after extraction of sediment samples from different depth ranges for different lengths of time (12h, 24h, 36h, 48h) which indicated that six sequential steps, each carried out for 24 hours, were sufficient enough to extract 99.8% and 99.6% of NH_4^+ respectively (assuming 48 hours extraction recovered all NH_4^+ and MAs).

Surfacial wet sediment samples ($\sim 1\text{g}$) collected from the Thames Estuary sites were extracted during the July 2001 sampling programme with six volumes of 2 M KCl ($3 \times 20\text{ mL}$; then $3 \times 40\text{ mL}$) using the same procedures as above, and the filtered supernatant analysed for NH_4^+ and MAs. A modified experiment was conducted for the different core sections of the Thames Estuary samples (November, 2001) using $\sim 1\text{g}$ dry sediment. The agitation times were reduced to two hours and constant volumes of the extractant solutions (20 mL) were used for all six extraction steps. All experiments were carried out in duplicate.

2.5.6.1 Calculation of extraction efficiencies of single volume extractions.

The extraction efficiency (%) of each single volume extraction was calculated using Equation 2-10.

$$\text{Extraction Efficiency} = \frac{\text{Concentration of } (\text{NH}_4^+ \text{ and MAs) single step } (\times 100)}{\text{Cumulative concentration of all extractions } (\text{NH}_4^+ \text{ and MAs})} \quad \text{Equation 2-10}$$

3 BURNHAM OVERY STAITHE

3.1 Introduction

One of the most important physical phenomena affecting inter-tidal ecosystems is the tidal cycle. This can lead to changes in pore-water salinity, resuspension of sediments and flushing of pore-waters. Strong tidal currents (mean tidal range > 2m) also mix the water column and reduce the residence time of algae in the photic zone (Dennison and Abal, 1999). Consequently, nutrient concentrations have the potential to build up in the water column in these systems. The effect of tidal dynamics on NH_4^+ , NO_3^- and NO_2^- distributions has been studied extensively (e.g. Usui *et al.*, 1998; 2001).

Although ON constitutes a large amount of both dissolved and particulate N in estuarine ecosystems, its contribution to the total N budget has received little attention, thus far. Fitzsimons *et al.* (1997) measured MAs in a salt marsh (Oglet Bay, Mersey Estuary, UK) over a two weeks spring/neap tidal cycle and found that their concentrations varied significantly between the neap and spring tides; namely that MAs were significantly depleted within pore-waters and sediments during tidal inundation, while enrichments were evident soon after the peak of neap tide. While the depletion of the MAs during tidal inundation could be attributed to pore-water flushing, their enrichment during periods of sediment exposure indicated a sedimentary source. However, interpretation of the data was complicated by the fact that three distinctly different sites on the marsh were sampled, each being of different maturity. The Mersey Estuary was also receiving pulses of untreated sewage at the time, which may have provided an alternative source of MAs (Scully *et al.*, 1988).

This chapter discusses MA concentrations measured in a series of sediment cores taken from a pristine mudflat at the seaward boundary of Burnham Overy Staithe, Norfolk, England. Although this study focuses on diurnal tidal cycles instead of spring/neap cycles as in the case of Fitzsimons *et al.* (1997), the results can be compared in broad terms. It was hoped that the results obtained in this study would help identify the effect of diurnal tidal inundation on the MAs in a mudflat-salt marsh ecosystem.

3.2 Aims of the study

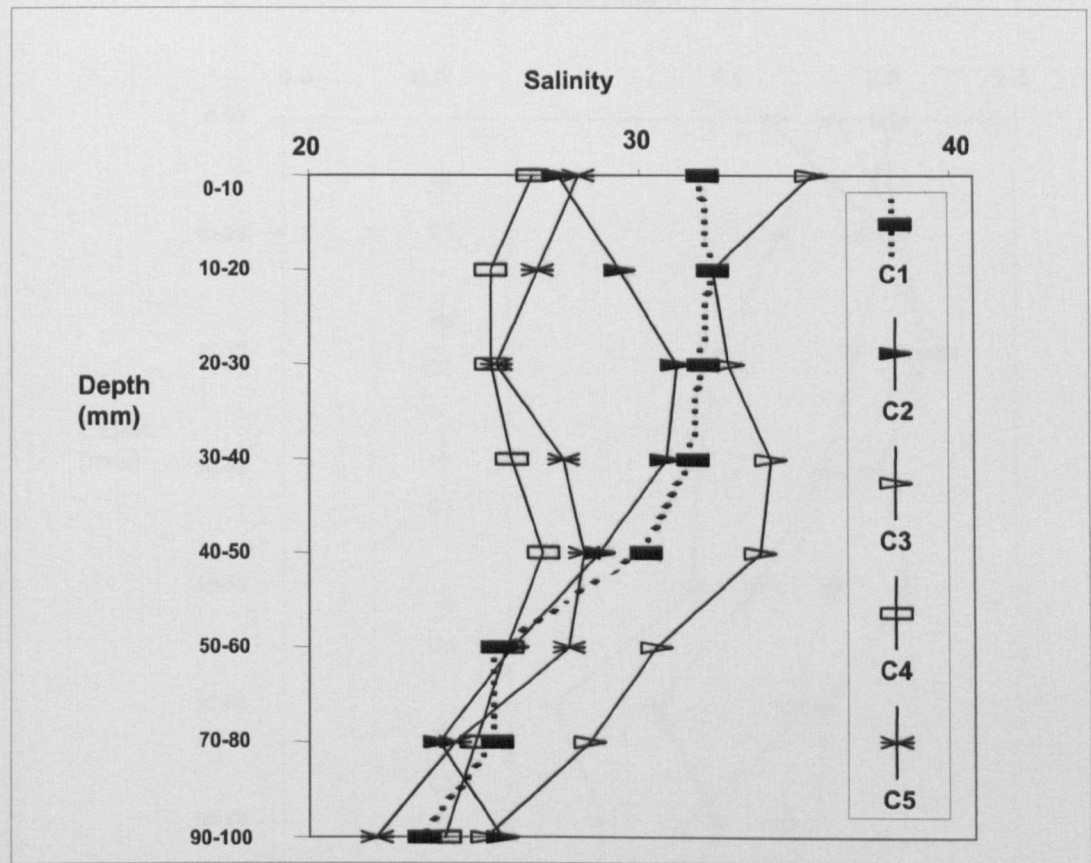
The main objective of this study was to identify the variation in distributions of the NH_4^+ and MAs in a pristine estuarine mudflat (BOS) through sampling at different stages of diurnal tidal cycles, including their abundance and speciation.

3.3 Results

3.3.1 Salinity

Salinity varied with depth within the pore-waters of Cores 1-5, but was generally higher at the core surface (26-34), decreasing to 22-26 at 100 mm depth (Fig. 3-1). Cores 1 and 3 (low tide) showed a similar trend but slightly different values. The two core samples were expected to show similar salinity profiles as they were both collected at low tide. In general pore-water collected in the two cores collected close to high tide (Cores 4 and 5) had lower salinities than the low tide cores, whereas Core 2 (taken at mid-point between high tide and low tide) showed generally intermediate salinity values. These results indicate that salinity may not only be affected by tidal inundation but also by other factors including daily variations in weather conditions, most probably precipitation, which can dilute the surface salinity

to some extent. There is more discussion on the effect of salinity on the abundance of NH_4^+ and the MAs in Section 3.4.



The last two depth ranges are not linear. C1 and C3 were collected at low tide; C4 and C5 close to high tide; C2 at intermediate tide (It is important to note that the cores were from different tidal cycles). For sampling dates refer to Table 2-1.

Figure 3-1. Depth profiles for salinity in Cores 1-5 (C1 = Core 1), BOS.

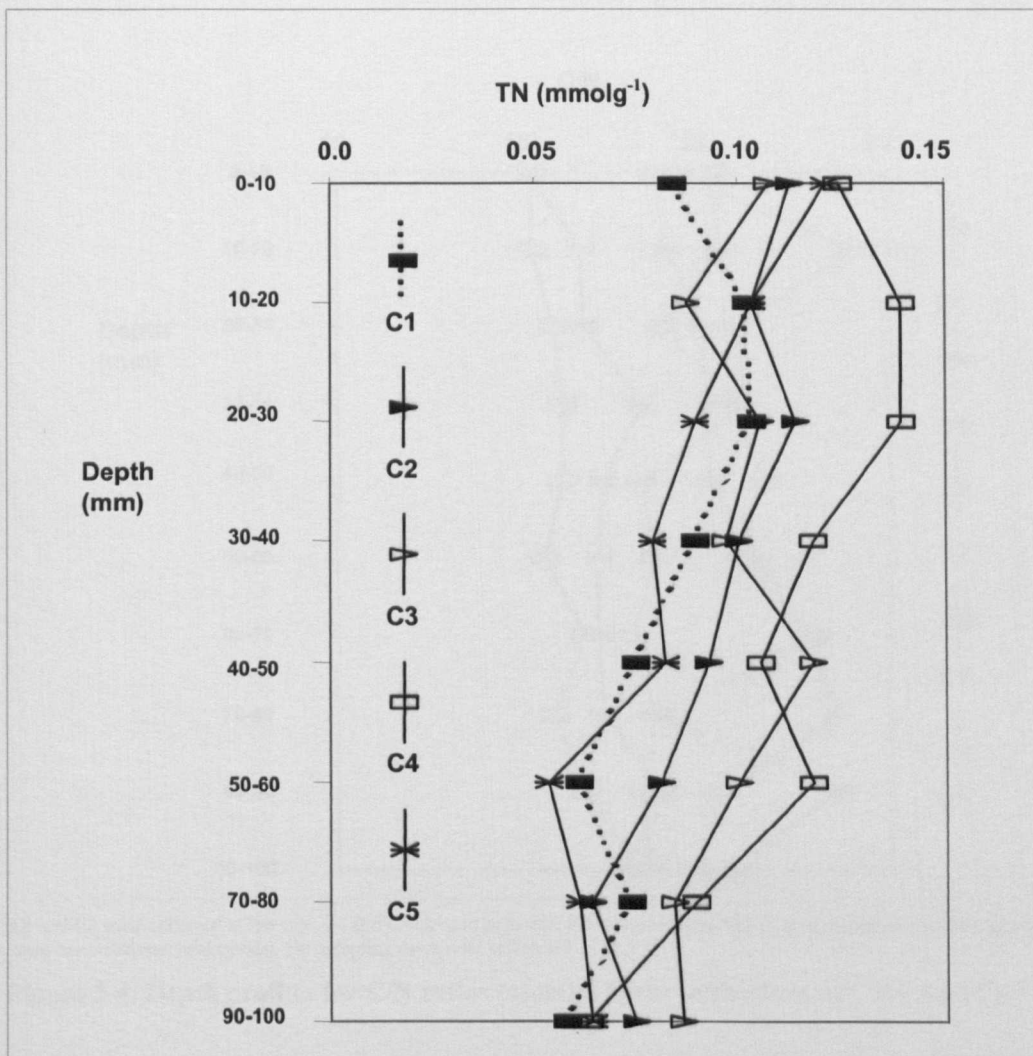
3.3.2 Total organic carbon content, total nitrogen and C/N ratio

The TOC content of the sediments varied from 0.97 mmol g^{-1} (Core 5; 50-60 mm) to 2.34 mmol g^{-1} (Core 2; 20-30 mm). Generally, TOC decreased with depth after 50 mm (Fig. 3-2; see the Appendix, Table A-1 for individual data). TN ranged from $0.05 - 0.14 \text{ mmol g}^{-1}$ (Fig. 3-3).



C1 and C3 were collected at low tide; C4 and C5 close to high tide; C2 at intermediate tide (It is important to note that the cores were from different tidal cycles). For sampling dates refer to Table 2-1.

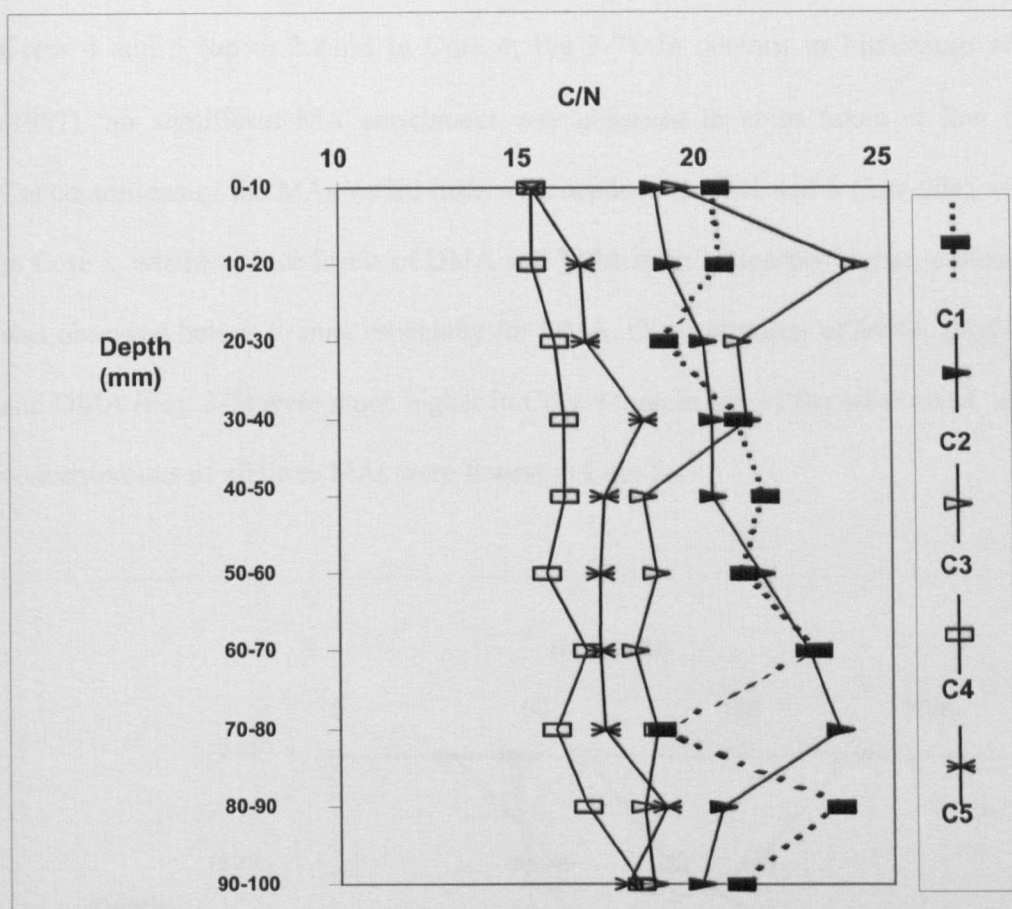
Figure 3-2. Depth profiles of average TOC content of Cores 1-5 (C1 = Core 1) BOS.



The last two depth ranges are not linear. C1 and C3 were collected at low tide; C4 and C5 close to high tide; C2 at intermediate tide (It is important to note that the cores were from different tidal cycles). For sampling dates refer to Table 2-1.

Figure 3-0. Depth profiles of TN in the solid-phase of Cores 1-5 (C1 = Core 1), BOS.

The average atomic TOC to TN ratios (C_{org}/N_{tot} or C/N) for Cores 1-5 are shown in Fig. 3-4. The C/N ratios were always greater than 14, with the highest ratio (24) occurring at 10-20 mm in Core 3. The profiles for Cores 4 and 5 (taken 2 hours before and 2 hours after high tide, respectively) were most similar. There was no consistent trend with depth.



C1 and C3 were collected at low tide; C4 and C5 close to high tide; C2 at intermediate tide (It is important to note that the cores were from different tidal cycles). For sampling dates refer to Table 2-1.

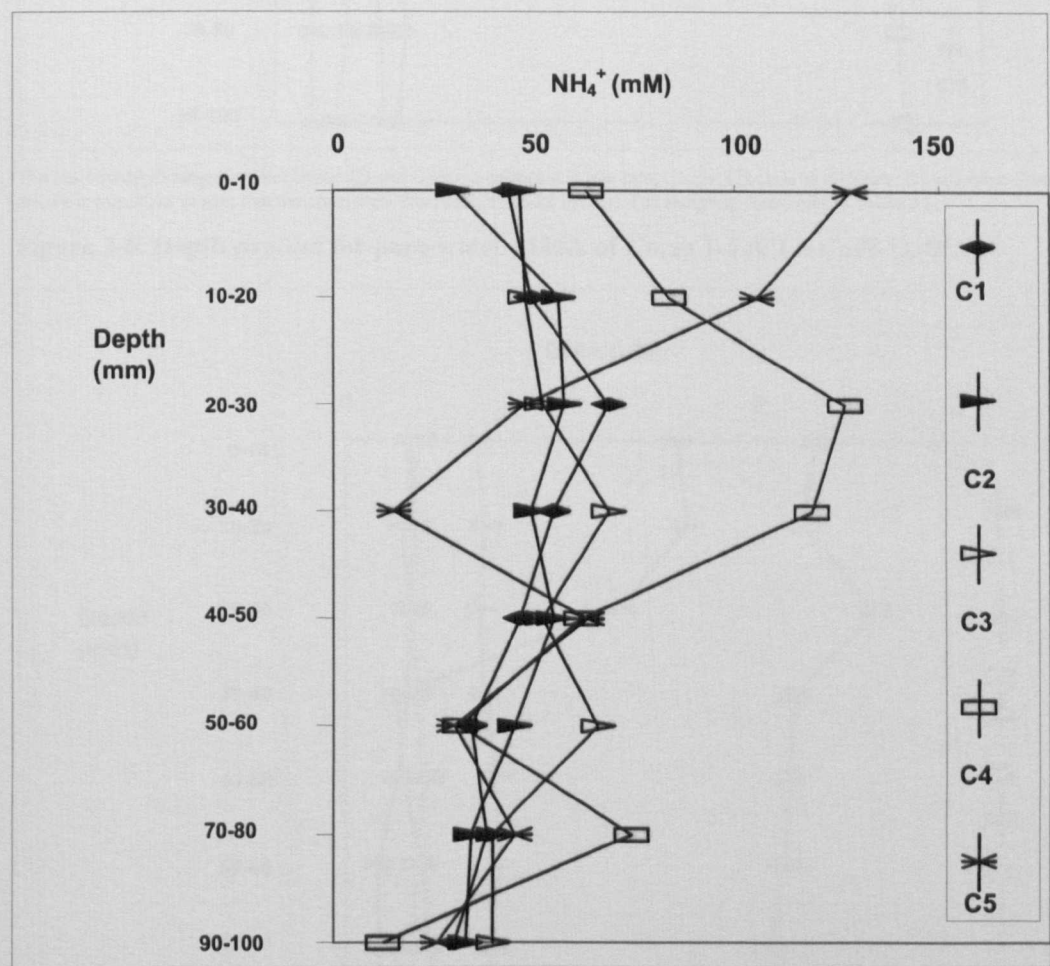
Figure 3-4. Depth profiles for C/N ratios (atomic) in the solid-phase of Core 1-5 (C1 = Core 1).

3.3.3 Depth profiles of NH_4^+ and the MAs

3.3.3.1 Pore-waters

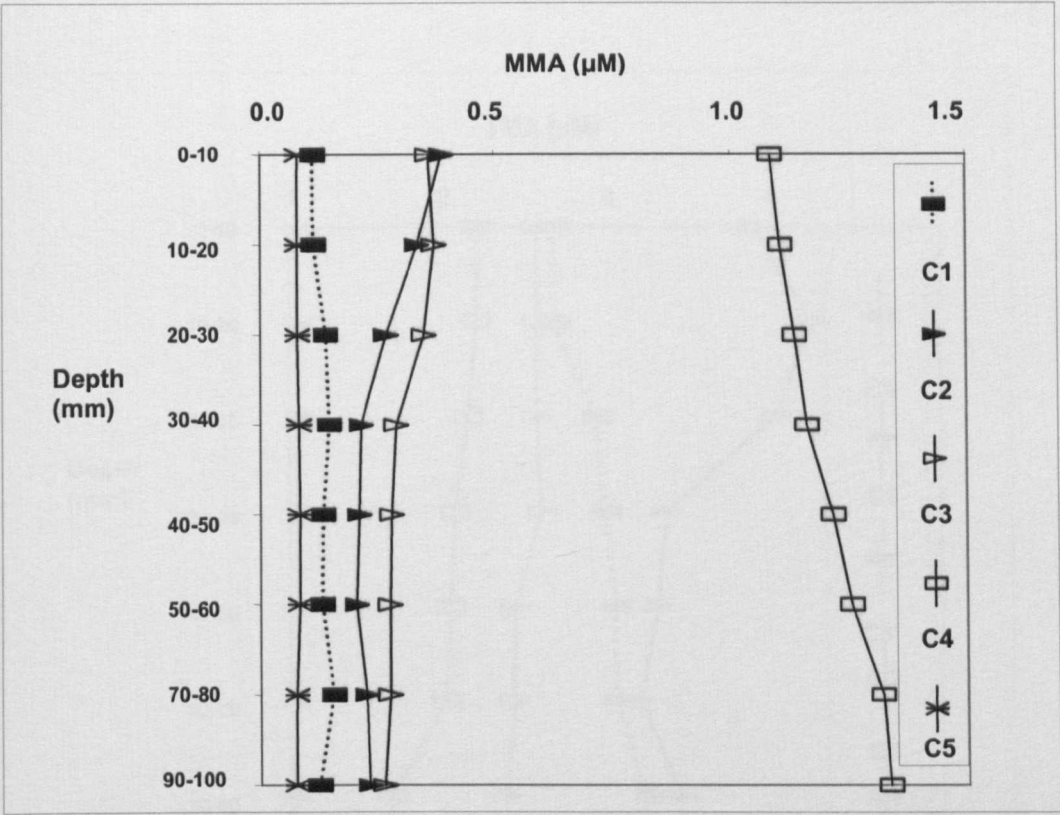
NH_4^+ was present in the pore-waters of all cores and at concentrations that were always at least an order of magnitude higher than those for the MAs. NH_4^+ concentrations decreased with depth (Fig. 3-5), excepting Cores 2 and 4, while for Core 2, NH_4^+ concentrations remained constant at around 50 mM. Concentrations increased down to 20 – 30 mm in Core 4 and decreased below this depth. Pore-water depth profiles for MMA, DMA and TMA are shown in Figs. 3-6, 3-7 and 3-8, respectively. TMA was the most abundant MA in the pore-waters of Cores 1, 2 and 3

(up to 4.68 μM in Core 2; Fig 3-8), while DMA was more abundant than the others in Cores 4 and 5 (up to 2.8 μM in Core 4; Fig 3-7). In contrast to Fitzsimons *et al.* (1997), no significant MA enrichment was observed in cores taken at low tide. Concentrations of the MAs varied little with depth in Cores 1 and 3 (low tide), while in Core 2, where surface levels of DMA and TMA were noticeably higher, a decrease was observed below 30 mm, especially for DMA. Concentrations of MMA (Fig. 3-6) and DMA (Fig. 3-7) were much higher in Core 4 than in any of the other cores, while concentrations of all three MAs were lowest in Core 5.



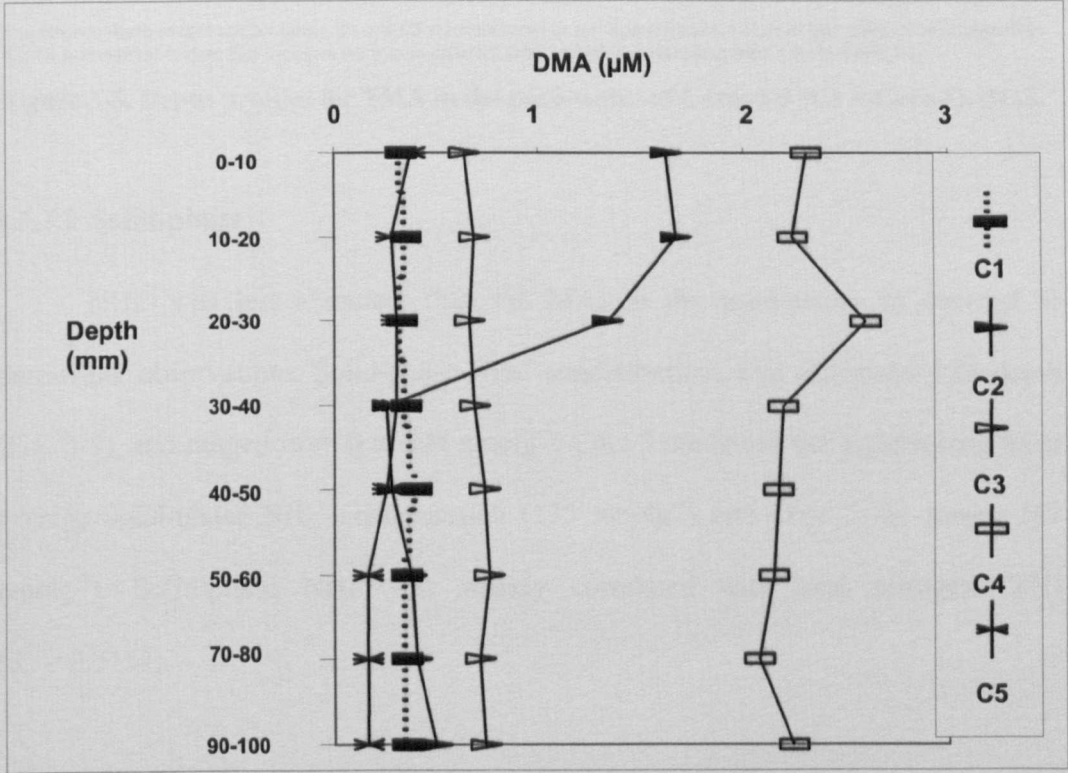
The last two depth ranges are not linear. C1 and C3 were collected at low tide; C4 and C5 close to high tide; C2 at intermediate tide (It is important to note that the cores were from different tidal cycles). For sampling dates refer to Table 2-1.

Figure 3-5. Depth profiles for NH_4^+ concentrations in the pore-water of Cores 1-5 (C1 = Core 1), BOS.



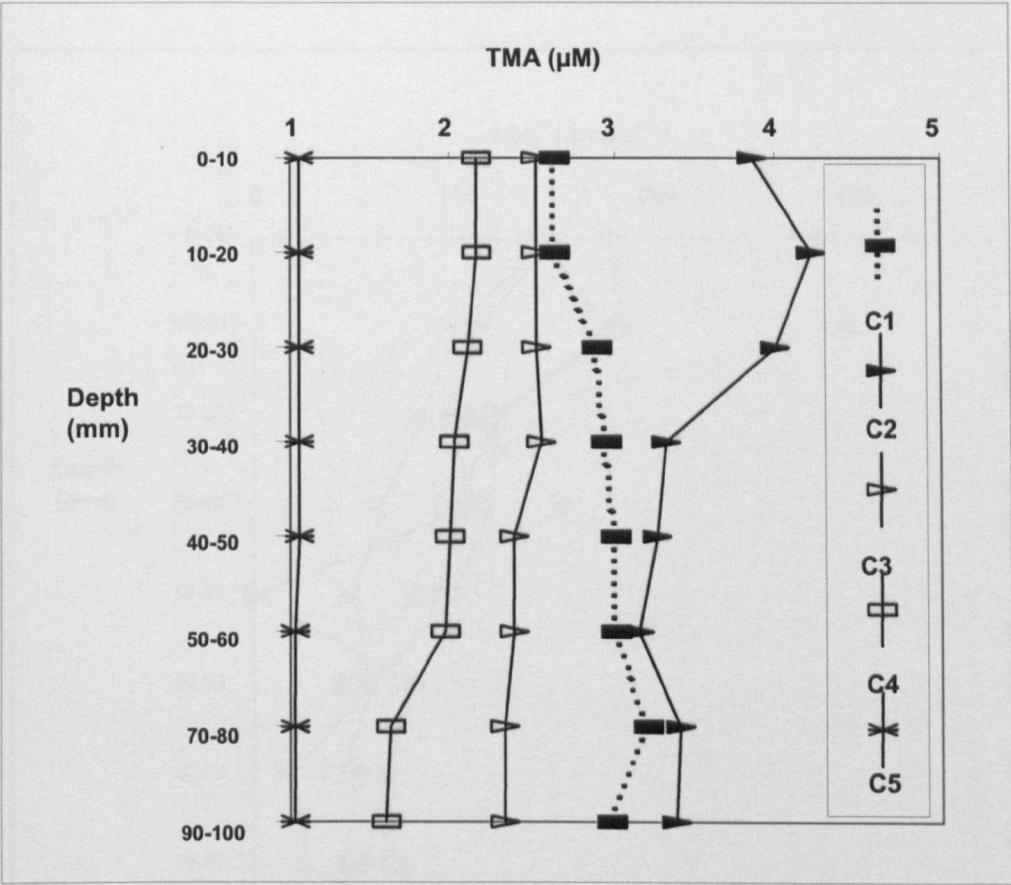
The last two depth ranges are not linear. C1 and C3 were collected at low tide; C4 and C5 close to high tide; C2 at intermediate tide (It is important to note that the cores were from different tidal cycles). For sampling dates refer to Table 2-1.

Figure 3-6. Depth profiles for pore-water MMA of Cores 1-5 (C1 = Core 1), BOS.



The last two depth ranges are not linear. C1 and C3 were collected at low tide; C4 and C5 close to high tide; C2 at intermediate tide (It is important to note that the cores were from different tidal cycles). For sampling dates refer to Table 2-1.

Figure 3-7. Depth profiles for DMA in the pore-water of Cores 1-5 (C1 = Core 1), BOS.

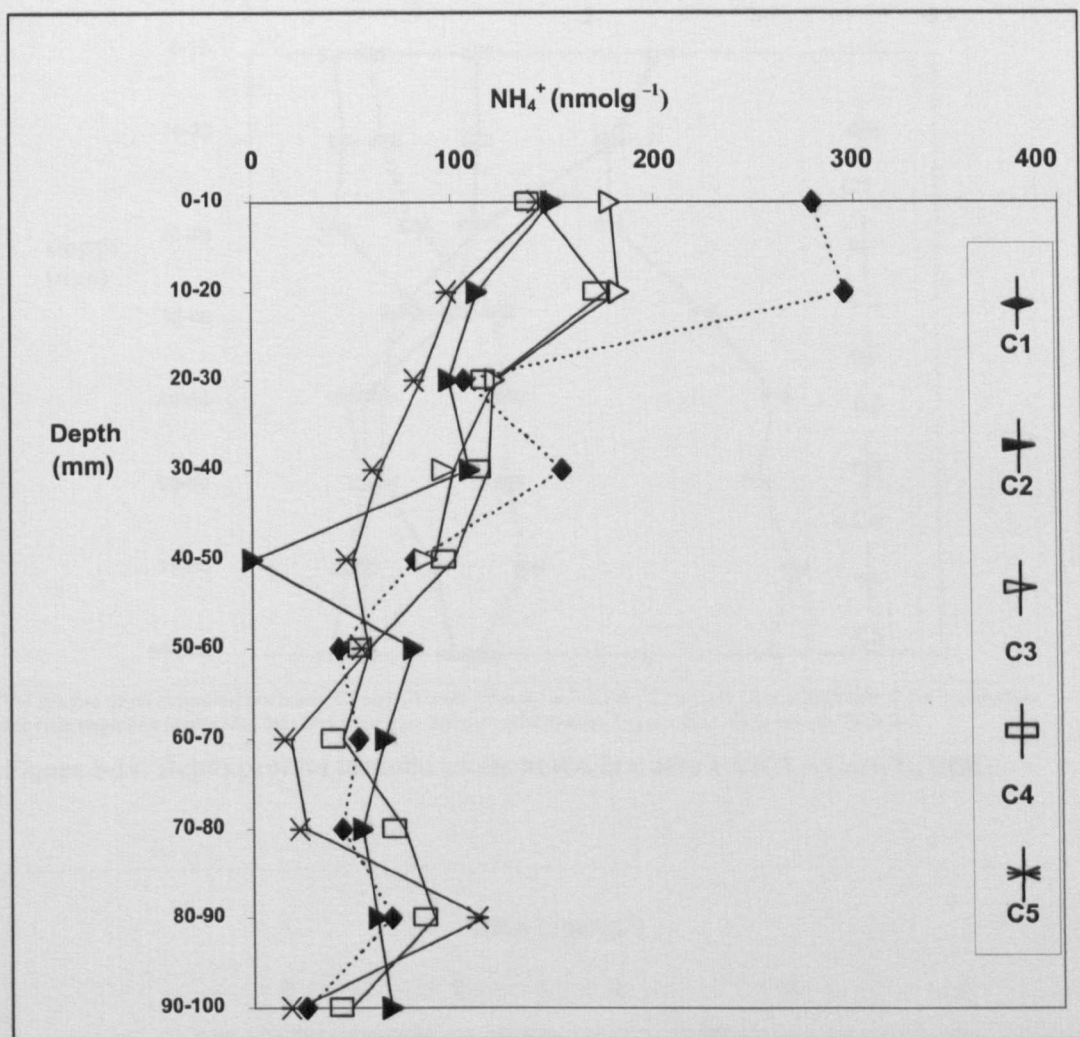


The last two depth ranges are not linear. C1 and C3 were collected at low tide; C4 and C5 close to high tide; C2 at intermediate tide (It is important to note that the cores were from different tidal cycles). For sampling dates refer to Table 2-1.

Figure 3-8. Depth profiles for TMA in the pore-water of Cores 1-5 (C1 = Core 1), BOS.

3.3.3.2 Solid-phase

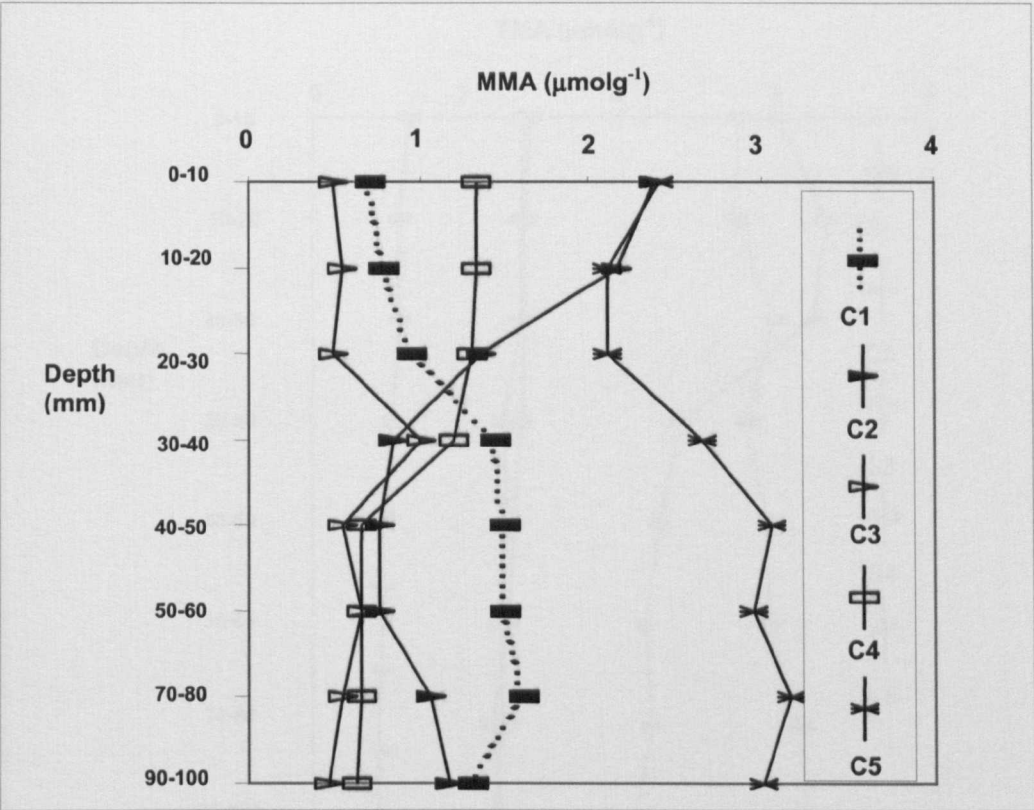
NH_4^+ was less abundant than the MAs in the solid-phase, in contrast to pore-water observations. Solid-phase NH_4^+ concentrations also decreased with depth (Fig. 3-9), and ranged from 0 to 294 nmol g^{-1} . Core 3 contained the highest core-wide average solid-phase NH_4^+ concentration (135 nmol g^{-1}) and Core 5 the lowest (69 nmol g^{-1}). Solid-phase NH_4^+ was weakly correlated with total nitrogen (TN) ($R^2 = 0.5154$).



C1 and C3 were collected at low tide; C4 and C5 close to high tide; C2 at intermediate tide (It is important to note that the cores were from different tidal cycles). For sampling dates refer to Table 2-1.

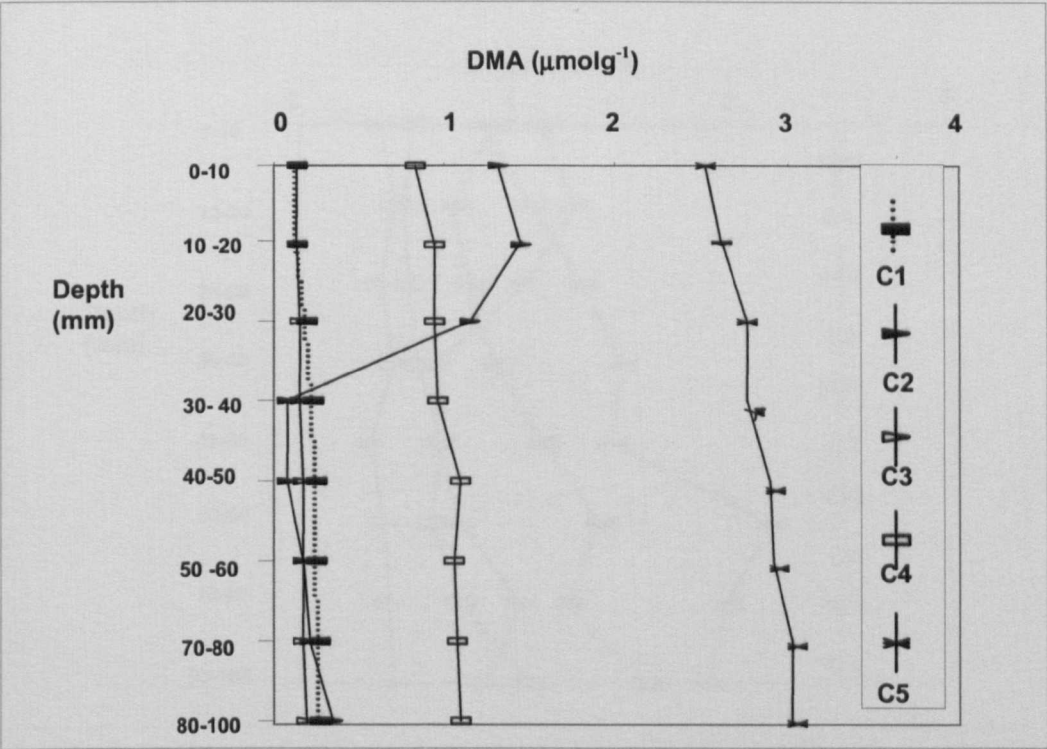
Figure 3-9. Depth profiles of solid-phase NH_4^+ concentrations of Cores 1-5 (C1 = Core 1), BOS.

TMA was again the most abundant MA in the sediments (up to $3.61 \mu\text{mol g}^{-1}$ in Core 2, 10-20 mm) (Fig. 3-12), with DMA concentrations higher only in Core 5 (Fig. 3-11) and MMA again being the least abundant analyte (Fig. 3-10). The contribution of solid-phase MAs to TN was generally below 2% except at 50-60 mm depth in Core 5 where the MAs contributed, on average, about 2.2% towards the total nitrogen (TN). The depth profile of total MA contribution to TN is shown in Fig. 3-13.



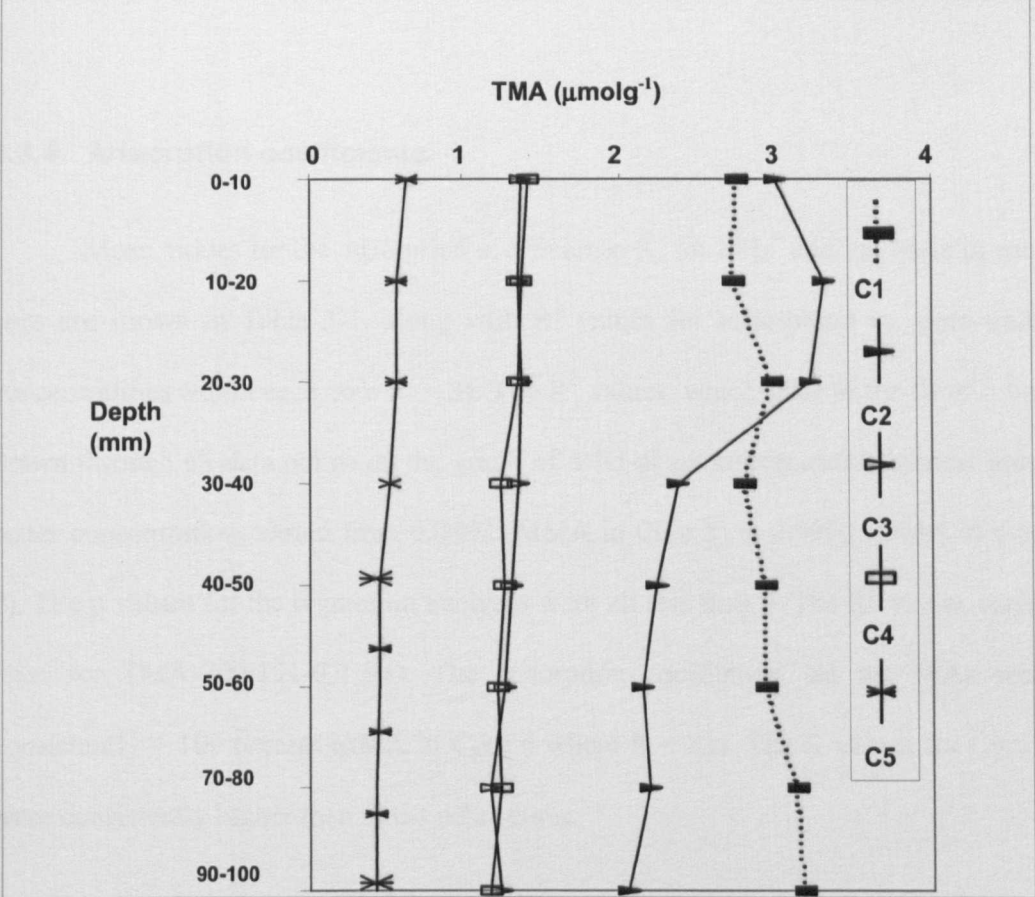
The last two depth ranges are not linear. C1 and C3 were collected at low tide; C4 and C5 close to high tide; C2 at intermediate tide (It is important to note that the cores were from different tidal cycles). For sampling dates refer to Table 2-1.

Figure 3-10. Depth profiles for solid-phase MMA in Cores 1-5 (C1 = Core 1), BOS.



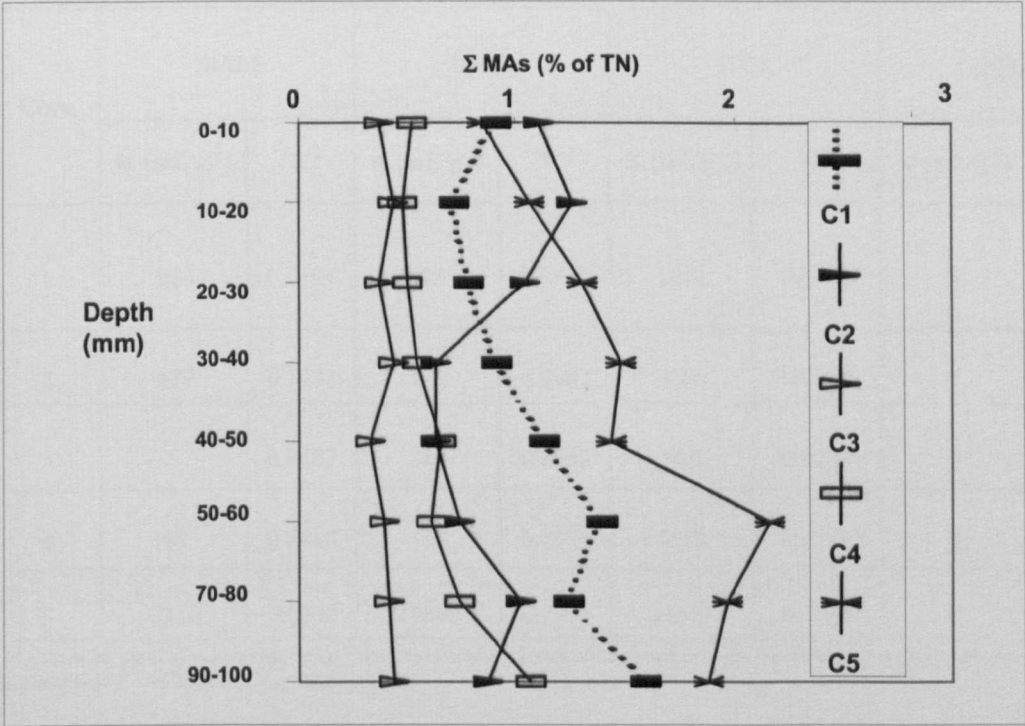
The last two depth ranges are not linear. C1 and C3 were collected at low tide; C4 and C5 close to high tide; C2 at intermediate tide (It is important to note that the cores were from different tidal cycles). For sampling dates refer to Table 2-1.

Figure 3-11. Depth profiles for solid-phase DMA in Cores 1-5 (C1 = Core 1), BOS.



The last two depth ranges are not linear. C1 and C3 were collected at low tide; C4 and C5 close to high tide; C2 at intermediate tide (It is important to note that the cores were from different tidal cycles). For sampling dates refer to Table 2-1.

Figure 3-12. Depth profiles for solid-phase TMA in Core 1-5 (C1 = Core 1), BOS.



The last two depth ranges are not linear. C1 and C3 were collected at low tide; C4 and C5 close to high tide; C2 at intermediate tide (It is important to note that the cores were from different tidal cycles). For sampling dates refer to Table 2-1.

Figure 3-13. Depth profiles of the contribution of MAs (%) to TN content of solid-phase samples of Cores 1-5 (C1 = Core 1), BOS.

3.3.4 Adsorption coefficients

Mean values for the adsorption coefficients, K, for NH₄⁺ and the MAs in each core are shown in Table 3-1, along with R² values for solid-phase vs. pore-water concentrations within each core (n = 8). The R² values, which refer to the fit of a line drawn through all data points on the graph of solid-phase concentration against pore-water concentration, varied from 0.0302 (MMA in Core 5) to 0.9962 (DMA in Core 2). The p values for the regression analyses were all less than 0. The R² values varied least for TMA (0.6191-0.9194). The adsorption coefficients for the MAs were consistently > 100 (except MMA in Core 4 where K = 83). The K values for Core 5 were consistently higher than in the other cores.

Table 3-1. Mean adsorption coefficients (K) for the MAs and NH₄⁺ in Cores 1-5, BOS.

Core	MMA		DMA		TMA		NH ₄ ⁺	
	K (mL g ⁻¹)	[†] R ²	K (mL g ⁻¹)	[†] R ²	K (mL g ⁻¹)	[†] R ²	K (mL g ⁻¹)	[†] R ²
1	920	0.5494	593	0.2929	1542	0.6191	3	0.5409
2	479	0.9773	579	0.9962	994	0.9194	2	0.0304
3	197	0.0487	218	0.6597	905	0.8224	3	0.4465
4	83	0.8440	447	0.2675	1419	0.6414	2	0.4149
5	3350	0.0302	12660	0.7995	11657	0.7869	8	0.3362

[†]R² values for plots of pore-water versus solid-phase concentrations are included to show the variability within each core. For details of how K was calculated, see Section 2.3.6.

Regression analyses were carried out to find out if solid-phase concentrations of NH_4^+ and MAs were having any significant effect on TN. It was concluded that the MAs were having no effect ($p = 0.156$, $R^2 = 0.1411$) at 95% confidence level, since p was greater than 0.05 indicating that the probability of getting a relationship with the stated R^2 , randomly by chance is high ($> 5\%$). However, the solid-phase particulate NH_4^+ did have some effect on TN ($p = 0$, $R^2 = 0.5154$). The result indicates about half of the TN can be predicted by solid-phase NH_4^+ . This was not unexpected, since NH_4^+ is a terminal product of ON degradation in anoxic sediments (Fig. 3-14).

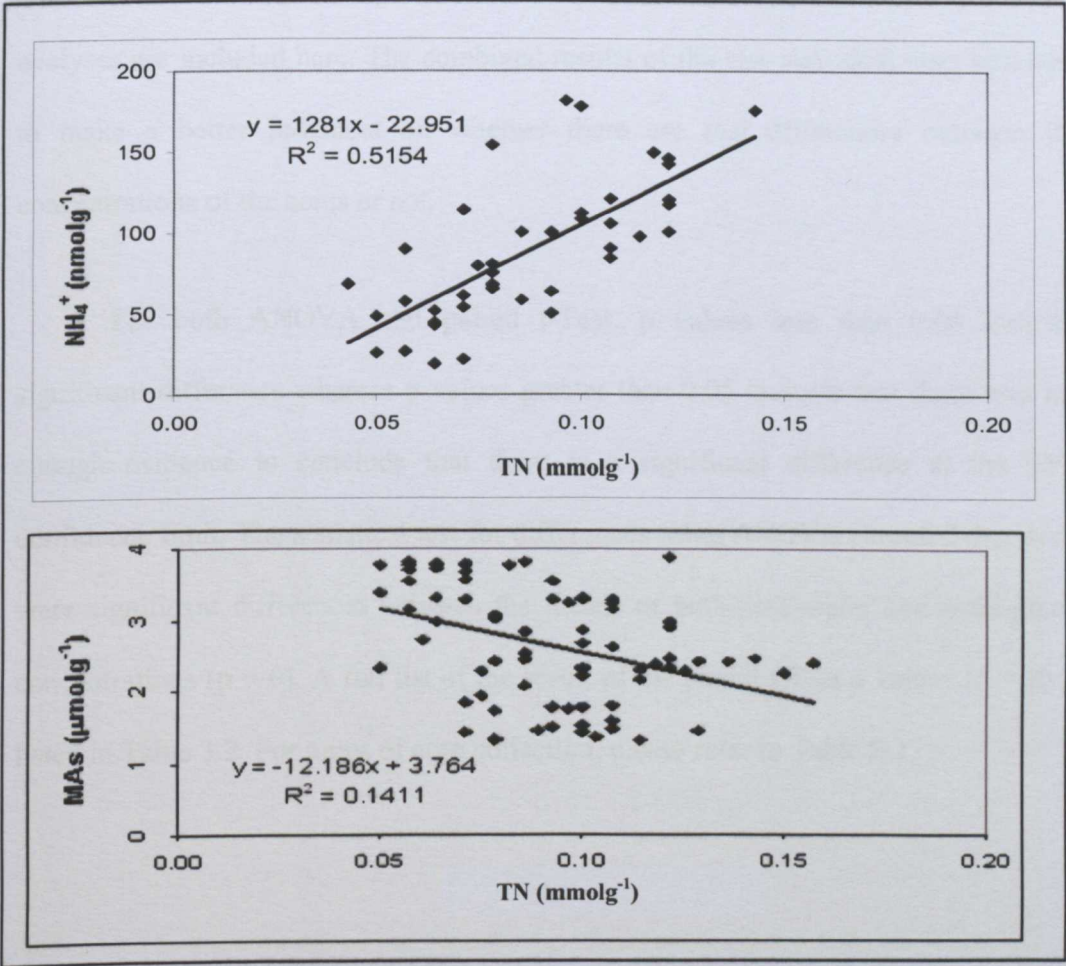


Figure 3-14. Plots of total solid-phase NH_4^+ and MAs versus TN, BOS.

3.4 Statistical analysis for differences in concentrations of NH_4^+ and MAs as a result of tidal action.

Statistical analysis was performed to determine whether concentrations of MAs differed significantly at different stages of the tidal cycle using Student's paired t-Test and ANOVA (One way, Unstacked). The paired Student's t-Test determines if there is a significant difference between two or more paired samples (depth profile of concentrations, in this case). However, as there were more than two sets of samples (i.e., five cores, each with eight core sections) there was a risk of getting a difference just by chance for such a large data set. For this reason, ANOVA was also used as it only tests differences between the mean concentrations of the five cores. All data were tested for normality before the tests were carried out. The results of both analyses are included here. The combined results of the two statistical tests will help to make a better judgment on whether there are real differences between the concentrations of the cores or not.

For both ANOVA and paired t-Test, p values less than 0.05 indicate significant difference whereas p values greater than 0.05 indicate that there was not enough evidence to conclude that there is a significant difference at the 95% confidence limit. The statistical test for differences using ANOVA revealed that there were significant differences between the means of both pore-water and solid-phase concentrations ($p = 0$). A full list of the result of the paired t-Test p values ($n = 8$) is listed in Table 3.2. For times of core collection, please refer to Table 2-1.

Table 3-2. p values for paired Student’s t-Test on NH₄⁺ and MA concentrations (C1/C2 = Comparison of Cores 1 and 2; p values are highlighted in bold where there is a significant difference).

NH ₄ ⁺	C1/C2	C1/C3	C1/C4	C1/C5	C2/C3	C2/C4	C2/C5	C3/C4	C3/C5	C4/C5
Solid-phase	0.124	0.195	0.315	0.034	0.031	0.153	0.168	0.398	0.002	0.003
Pore-water	0.765	0.289	0.036	0.442	0.147	0.059	0.426	0.169	0.719	0.491
MMA	C1/C2	C1/C3	C1/C4	C1/C5	C2/C3	C2/C4	C2/C5	C3/C4	C3/C5	C4/C5
Solid-phase	0.903	0.001	0.270	0.000	0.028	0.069	0.005	0.034	0.000	0.000
Pore-water	0.002	0.000	0.000	0.000	0.007	0.000	0.000	0.000	0.000	0.000
DMA	C1/C2	C1/C3	C1/C4	C1/C5	C2/C3	C2/C4	C2/C5	C3/C4	C3/C5	C4/C5
Solid-phase	0.141	0.003	0.000	0.000	0.082	0.130	0.000	0.000	0.002	0.000
Pore-water	0.086	0.000	0.000	0.014	0.676	0.000	0.000	0.000	0.000	0.000
TMA	C1/C2	C1/C3	C1/C4	C1/C5	C2/C3	C2/C4	C2/C5	C3/C4	C3/C5	C4/C5
Solid-phase	0.154	0.000	0.000	0.000	0.000	0.000	0.000	0.307	0.000	0.018
Pore-water	0.012	0.002	0.000	0.000	0.000	0.000	0.000	0.000	0.000	0.000

For the solid phase NH₄⁺, there was a significant difference (p < 0.05) between Cores 1 and 5 (p = 0.034), Cores 2 and 3 (p = 0.031), Cores 3 and 5 (p = 0.002) and Cores 4 and 5 (p = 0.003). For the pore-waters, there was a significant difference only between Cores 1 and 4 (p = 0.036). Statistical analysis of the data showed that solid-phase NH₄⁺ concentrations were similar for cores taken at low tide (Cores 1 and 3) but for comparison of cores sampled at low tide (Core 1), 2 hours before (Core 4) and 2 hours after (Core 5) there was a significant difference. However for Core 3 (another core sampled at low tide) there was no significant difference with Core 4 (sampled 2 hours before low tide) but there was a significant difference with Core 5 (sampled 2 hours after low tide). This analysis suggests that solid-phase concentrations of NH₄⁺ start to change significantly after low tide but probably return to similar

concentrations after 3 hours (there was no significant difference between Core 1 (low tide) and Core 2 (3 hours after low tide)).

Pore-water concentrations of NH_4^+ in cores sampled at different times of the tidal cycle were similar except for Core 1 (sampled at low tide) and Core 4 (sampled 2 hours before high tide). But there was no significant difference between Core 3 and Core 4. There was no significant difference between Cores 1 and 2, Cores 1 and 4, and Cores 2 and 4, with respect to solid-phase MMA concentrations. In contrast, there was a significant difference between the two cores sampled at low tides (Core 1 and 3). Although similar concentrations were expected for these two cores, the statistical test indicated a significant difference.

There was no significant difference between Cores 1 and 2, Cores 2 and 3, Cores 2 and 4 for solid-phase DMA concentrations. There was no significant difference between Cores 1 and 2 and Cores 2 and 3 for DMA pore-water concentrations. There was a significant difference between both pore-water and solid-phase concentrations of Cores 1 and 3. No significant difference between Cores 1 and 2 and between Cores 3 and 4 was observed for pore-water concentrations. There was significant difference between pore-water concentrations of all cores. There was also a significant difference between the concentrations of TMA both in pore-waters and solid-phases of the two core samples taken at low tide (Cores 1 and 3).

3.5 Discussion

3.5.1 General observations

NH_4^+ was the dominant pore-water analyte with concentrations that were typically an order of magnitude higher than the most abundant MA, whereas the opposite trend was observed for the sediment solid-phase. The MA concentrations were similar to those reported for inter-tidal sediments by other researchers (e.g. Sørensen and Glob, 1987; Wang and Lee, 1994; Fitzsimons *et al.*, 1997). Variation in MA concentration within each core was not large as was the case for mature salt marsh sediments, such as Oglet Bay (Fitzsimons *et al.*, 1997). Wang and Lee (1990) suggested that marsh grass can affect MA distributions by supplying MAs directly to the sediments and through addition of organic detritus, leading to increased adsorption and greater heterogeneity within the sediment.

TOC concentrations, at $< 2.34 \text{ mmol g}^{-1}$, were significantly lower than those determined for Oglet Bay salt marsh (Fitzsimons *et al.*, 1997). Differences in the respective faunal populations were also observed. For example, *Tubifex tubificoides*, an invertebrate species associated with organically enriched sediments was absent from the BOS sampling site. Plant detritus was not observed within the BOS cores and C/N ratios suggested that the OM present was degraded material of marine origin (Bender *et al.*, 1989).

In the water column, ON compounds are preferentially removed by bacteria, relative to organic carbon species. This characteristic is reflected in an increase in the C/N ratio of particulate material with depth (Gordon, 1971; Lee and Cronin, 1982; Wakeham *et al.*, 1984). In sediments, however, organic carbon decreases faster than N, which was thought to be a consequence of the production of low molecular weight

N compounds, which are persistent with depth (Lee and Olsen, 1984). In this study, given the lower TOC concentrations compared to other studies such as Oglet Bay (Fitzsimons, *et al.*, 1997), a significant decrease in C/N ratio with depth was expected but C/N ratios slightly increased with depth in Cores 4 and 5 while there was no consistent or noticeable trend with depth in Cores 1 and 2. The latter may have been due to increased mineralisation or flux of ON compounds through bioturbation by burrowing animals (Burdige and Zheng, 1998).

3.5.2 Sources and controls of the MAs

Fitzsimons *et al.* (1997) found greater MA variation in cores containing plant detritus, which may explain the lower variation in the samples collected for this study. Benthic fauna, which was the dominant biomass in all five cores (Fitzsimons *et al.*, 2001) has previously been quantitatively linked with TMA levels in inter-tidal sediments (Sørensen and Glob, 1987) (The effect of benthic fauna on the distribution of MAs will be discussed in Chapter 4).

Dissolved MA concentrations were plotted against salinity to determine the existence of any interdependence but no correlation was observed (Fig. 3-15). Furthermore, no significant MA enrichment was observed in cores taken at low tide (i.e. as a result of release from animals), suggesting that salinity was not affecting MA pore-water concentrations. However, it may be that other processes, such as preferential bacterial uptake, had obscured any correlation. Bacterial uptake or an adsorption effect is quite plausible since Jorgensen *et al.* (1993) have measured rapid bacterial uptake of MAs in laboratory incubations of inter-tidal sediments, while Wang and Lee (1990) demonstrated rapid adsorption of MAs to sediments.

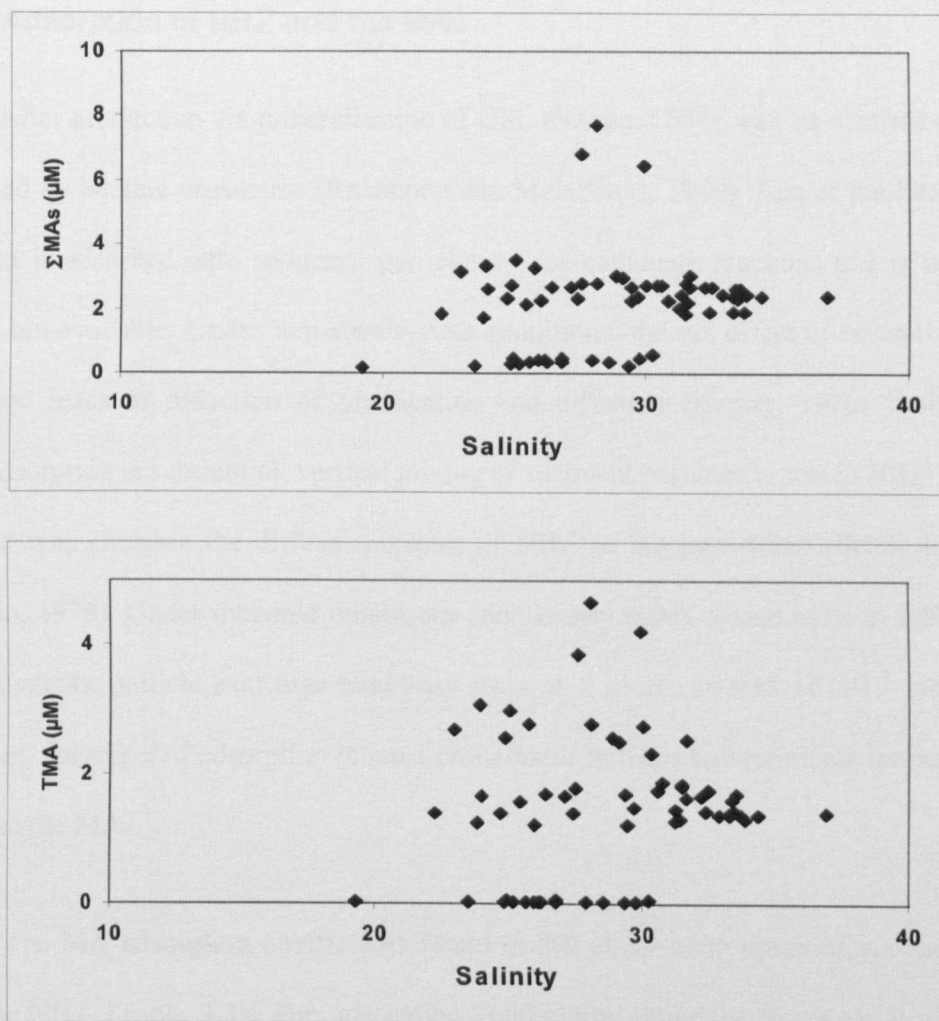


Figure 3-15. Plots of total pore-water MAs and pore-water TMA versus salinity in cores taken from Burnham Overy Staithe.

Lee and Olsen (1984) observed that exchangeable (extracted by 1 M LiCl) and fixed (extracted with HCl) DMA and TMA accounted for less than 0.5% of total N in Buzzard Bay sediments. However, Lee (1988) later found that HF-HCl extraction of these same sediments recovered up to an order of magnitude greater concentration of MAs. This suggests that the contribution of MAs to the total N budget of inter-tidal sediments may be underestimated. It is also possible that there could be interchange of the MA pools, which are at different stages of adsorption in the particulate phase.

3.5.3 Adsorption of NH_4^+ and the MAs

After production via mineralisation of OM, dissolved NH_4^+ can be nitrified or consumed by benthic organisms (Raaphorst and Malschaert, 1996). Part of the NH_4^+ produced is adsorbed onto sediment particles by ion-exchange reactions and is not directly bio-available. Under non-steady state conditions, the net effect of reversible adsorption leads to reduction of nitrification and diffusion (Berner, 1976; 1980). When adsorption is substantial, vertical mixing of sediment particles to which NH_4^+ is adsorbed may increase the diffuse transport of NH_4^+ to the pore-water (Scink and Guinasso, 1978). Under dynamic conditions (non-steady state), which exist in inter-tidal sediments, particle exchange sites may serve as a source or sink of NH_4^+ ions. Therefore, the effect of adsorption is most pronounced in these environments for both NH_4^+ and the MAs.

The MA adsorption coefficients found in this study were much higher than those for NH_4^+ (Table 3-1). The adsorption coefficients generally decreased in the following order: TMA > DMA > MMA > NH_4^+ , which was consistent with previously reported results (Wang and Lee, 1990; 1993). However, this order was not consistent with pK_b values for aqueous MAs (Fessenden and Fessenden, 1982), which indicate that DMA, which is more basic than TMA in aqueous solution (TMA is the most basic MA in the gas phase), should be more strongly adsorbed than TMA. The greater number of methyl substituents should also have a hindering effect to further bond formation (Huheey, 1983). However, the hydrogen bonding of ammonium ions in aqueous solution provides a more satisfactory explanation for the observed trend. The NH_4^+ , MMA and DMA cations contain four, three and two hydrogens bonded with nitrogen, respectively, which greatly increases both their solvation in water and

retention in solution through hydrogen bonding (Solomons, 1996). The protonated TMA ion has only one hydrogen available, resulting in weaker hydrogen bonding and making it more readily available for adsorption with particulate matter. The greater organic character of TMA could also cause an increased affinity for organic-coated particle surfaces. Thus, the TMA ion may adsorb onto particulates more readily than DMA, MMA or NH_4^+ , resulting in a higher adsorption coefficient. K for DMA was only higher than for TMA in Core 5, where DMA concentrations in both the pore-waters and sediments were much higher than for TMA. This behaviour would suggest that MMA and DMA, being less strongly adsorbed, are more bioavailable than TMA though their adsorption coefficients were still much higher than those for NH_4^+ .

The other factor that could influence NH_4^+ and MA adsorption is considered to be Van der Waals forces between molecules (Wang and Lee, 1993). Van der Waals forces are weak forces and could only account for the loosely held MAs, which are easily desorbed by the extraction method used in this study. These forces increase with molecular weight. This means that the effect of Van der Waals forces is weakest for NH_4^+ compared to the three MAs. Of these, TMA will be more affected than the other two MAs. This is also in agreement with the order of the adsorption coefficient values obtained in this study.

Operational K measurements made by Wang and Lee (1990, 1993) revealed the same pattern of adsorption, but the adsorption coefficients were at least an order of magnitude higher than the laboratory values. They attributed this to bacterial uptake of pore-water MAs (the laboratory samples were poisoned). Jorgensen *et al.* (1993) have also shown that MAs can be taken up rapidly by heterotrophic bacteria,

while Fitzsimons (unpublished results) found much higher levels of MAs in water samples from algal cultures treated with antibiotics. Bacterial uptake may also explain the high K values observed in BOS samples, as bacteria also play an important role in controlling the MA pool in sediments (Oremland *et al.*, 1982; King *et al.*, 1983; Giani *et al.*, 1984; King, 1988).

Blackburn and Herinksen (1983) reported that fresh inputs of OM to sediments altered NH_4^+ partitioning between the dissolved and particulate phases. Wang (1989) and Wang and Lee (1990, 1993) reported a strong relationship between the degree of adsorption of MAs to sediments and OM content. They suggested that this occurred because MA adsorption to OM was less reversible than adsorption to clay minerals and that the MAs were more likely to be present as a component of organic detritus rather than being truly 'fixed' within a clay lattice. In this study, no significant correlation between OM content (TOC) and adsorbed MAs was observed ($p > 0.05$, Table 3-3). In fact, highest K values were obtained for NH_4^+ and the MAs in Core 5, which had the lowest TOC content. Therefore, the results obtained from this study suggest that salinity and OM content may not be the major factors influencing the adsorption of NH_4^+ and MAs in pristine inter-tidal sediments, such as those taken from BOS, and that their effects may have been masked by other stronger factors.

Table 3-2. TOC content and mean adsorption coefficients of Cores 1-5 (C1 = Core 1), BOS.

Core	TOC	NH ₄ ⁺	MMA	DMA	TMA
1	1.66	3	920	593	1542
2	1.31	2	479	579	994
3	1.86	3	197	218	905
4	1.66	2	83	447	1419
5	1.31	8	3350	12660	11657
*R ² , p	N/A	0.205, 0.444	0.369, 0.277	0.352, 0.290	0.327, 0.312

*R² and p for concentration vs. TOC content.

3.5.4 Effects of tidal fluctuations on the distributions of MAs.

Total pore-water MAs were the lowest at 2 hours after high tide (Fig. 3-15). The low tide concentrations (6 hours) were averages of Cores 1 and 3 (samples collected at two different low tides). Total solid-phase MAs, like total pore-water concentrations, were lowest at 2 hours after high tide (Fig. 3-16). The highest ranges of concentrations were found for samples collected 3 hours after high tide. Generally, total solid-phase concentrations followed the same trend as the total pore-water concentrations indicating that the tidal cycle seems to affect both in the same way. This was in contrast to what was found by Fitzsimons *et al.* (1997) for samples collected during spring and neap tides where enrichment of MAs was observed just after neap tide.

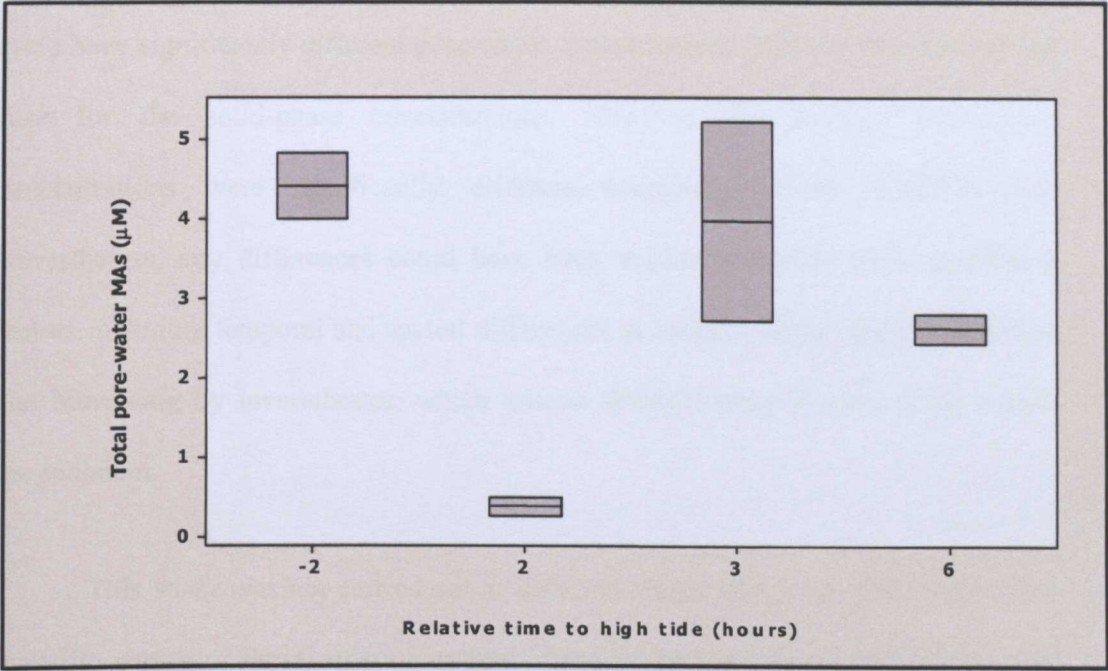


Fig. 3-16. Total pore-water MA concentration ranges of BOS samples at different stages of the tidal cycle (For sampling times refer to Table 2-1; time axis not to scale).

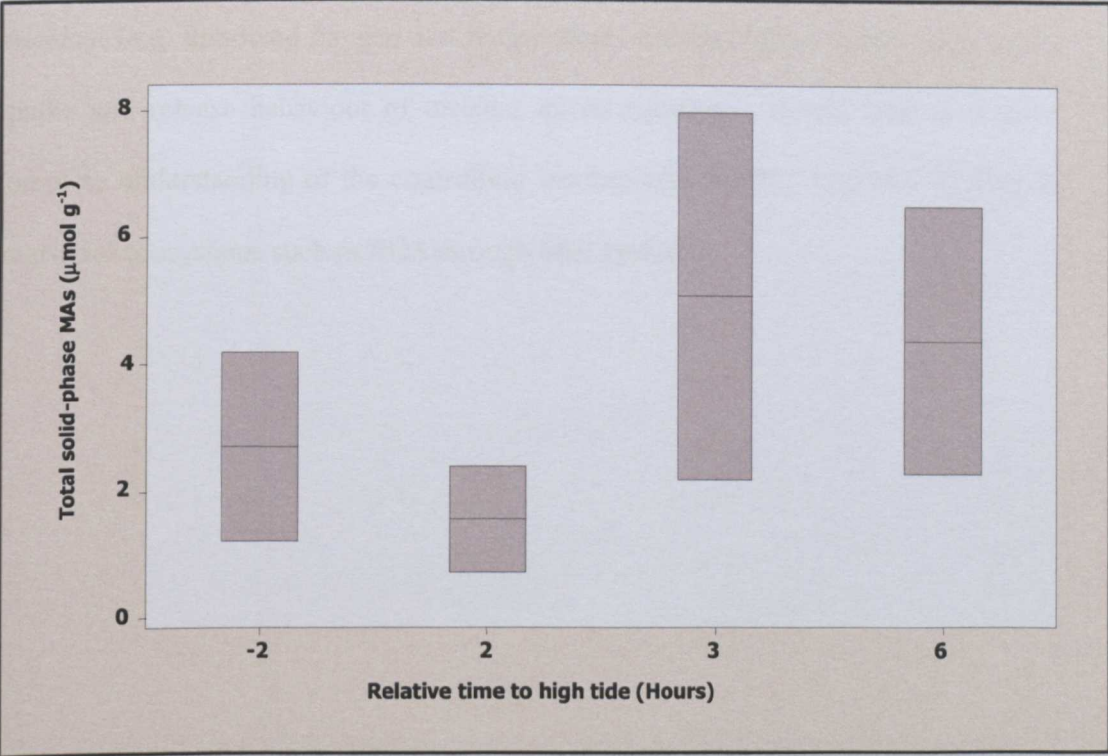


Fig. 3-17. Total solid-phase MA concentration ranges of BOS samples at different stages of the tidal cycle (For sampling times refer to Table 2-1; time drawn not to scale).

The paired t-Test showed that samples taken at different stages of the tidal cycle have significantly different pore-water concentrations, whereas this was not the case for the solid-phase concentrations. However, the average solid-phase concentrations were significantly different according to the ANOVA test. Nevertheless, any differences could have been masked by other more significant factors including temporal and spatial differences in resident fauna, uptake behaviour and burrowing by invertebrates, which creates different micro-environments within the sediment.

This study was not carried out at different stages of a single tidal cycle. The dynamic nature of these ecosystems may mean no two stages of tidal cycles have similar effects on NH_4^+ and MA distributions. In Chapter 4, a study carried out over part of a single tidal cycle is discussed. Further studies using additional physico-chemical (e.g. dissolved oxygen and temperature) and biological factors (e.g. types, uptake and release behaviour of resident micro-organisms) should lead to a more complete understanding of the controlling mechanisms of NH_4^+ and MA cycling in inter-tidal ecosystems such as BOS through tidal cycles.

3.6 Summary.

- The MAs were abundant in a pristine mudflat at concentrations exceeding $\mu\text{mol g}^{-1}$, which further demonstrates their ubiquity in the marine environment.
- There was less variation in MA profiles with depth in BOS core samples in comparison to cores taken from a mature salt marsh in previous studies, which may reflect the absence of plant detritus. Plant detritus creates a micro-environment different from the surrounding sediment leading to variations in adsorption behaviour of ON compounds such as the MAs.
- MA distributions at different stages of the tidal cycle at BOS were determined to investigate their correlation with salinity, which was thought to be an important control on the cycling of these compounds. No correlation was observed, so the possibility of MA inputs to sediments by invertebrates, though plausible, remains unproven.
- The adsorption coefficients determined for the MAs were in the following order: $\text{TMA} > \text{DMA} > \text{MMA} > \text{NH}_4^+$, which can be explained by the basicity of the free compounds, solvation of their protonated analogues, hydrogen bonding, Van der Waals forces and perhaps complex formation with other organic compounds and irreversible chemical reactions with mineral surfaces.
- The particulate MAs contributed up to 2% to TN at depth in one core, which is enough to alter the C/N ratio by one unit, demonstrating the potential importance of these compounds in the sedimentary N budget.

- The main biogeochemical parameters controlling MA cycling in pristine salt marsh sediments like BOS have not been identified from this preliminary study. It seems that the effect of salinity and TOC may not be the dominant factors compared to, for example, uptake or production of MAs by resident fauna and bacteria. Therefore, further investigations are required to explore this possibility.

4 RIA FORMOSA

4.1 Introduction

Sediments are important source of nutrients in the Ria Formosa, but their contribution to potential eutrophic conditions is unknown (Newton *et al.*, 2003). A quantitative knowledge of fluxes of ON species in inter-tidal sediments of the Ria Formosa could considerably enhance our understanding of nutrient cycles in this important ecosystem. Dissolved organic nitrogen (DON) is of special interest due to its abundance and potential bioavailability (Seitzinger *et al.*, 2002). The relative influence of physico-chemical and biological factors on fluxes of dissolved N species in coastal sediments depends on the spatial scale considered (Asmus *et al.*, 1998). At the smallest scale, bacteria, microalgae and meiofauna, combined with chemical processes and solute diffusion, play a significant role (Blackburn and Sørensen, 1998). At the intermediate level, benthic macrofauna and macroflora may affect both the activity of microbial communities and transport processes in the sediment (Aller, 1982; Kristensen, 1984, 1985; Kriesten *et al.*, 1991; Duarte, 1995). On the largest scale, horizontal transport between land and sea and within the marine environment becomes significant (Riedl *et al.*, 1972).

The focus of this study is MA cycling in inter-tidal sediments, which can be categorised as the ‘intermediate’ level on the spatial scale mentioned above. At this level, macrofauna are expected to play a significant role in the biogeochemistry of the MAs. Benthic organisms influence sediment chemistry through bioturbation of the sediments by both deposit and filter-feeding invertebrates (Raffaelli and Hawkins, 1999), or by direct release of chemical species into the sediments (e.g. Sørensen and Glob 1987; Wang and Lee, 1994).

The regular covering and uncovering of sediment by the tide induces a non-equilibrium condition (e.g. Harvey and Odum, 1990; Kerner and Wallman, 1992; Rocha, 1998; Rocha and Cabral, 1998). In Chapter 3 the effect of tidal action on MA cycling in sediment from a pristine temperate inter-tidal system over a three day period was discussed. The impact of sediment exposure and early tidal inundation on MA cycling in inter-tidal sediments involving a study of part of an individual tidal cycle at high temporal resolution will be discussed in this chapter.

Sediment core samples were collected from a single site (Site 1) in the Ria Formosa at different stages of a diurnal tidal cycle during the latter stages of sediment exposure and the early stages of tidal inundation (for timings of sample collections, see Table 2-2). The clam *R. decussates* (L.) and sediment samples were collected from a second site (Site 2), both before and shortly after inundation, to determine the potential contribution of *R. decussates* (L.) to MA cycling.

Specific aims of the work described in this chapter were;

- 1) To determine the effect of sediment exposure and early tidal inundation on the abundance and speciation of MAs.
- 2) To measure MA concentrations in the sand flat-dwelling clam *R. decussatus* (L.) before and after sediment inundation.
- 3) To identify the direction of any MA fluxes relating to clam activity from the sample measurements.

4.2 Results of MA analysis of Site 1 samples.

Water content and particle size were determined for each core-section of the core samples collected at different stages of the tidal cycle at Site 1. Concentrations of MAs in the pore-waters and sediment solid-phase were determined according to the methods described in Chapter 2.

4.2.1 Water content.

The water content of the sediments varied from 46 to 77% (Table 4-1). Water content increased with depth for sediment samples taken before inundation (RF1 and RF2) but there was no distinct trend for RF3 and RF4. Mean water content values increased from RF1 (53%) to RF4 (75%). The water content of surfacial sediment samples in RF1 and RF2 were consistent with sediment dewatering during exposure (Rocha, 1998).

Table 4-1. Depth profile of water content (%) for Ria Formosa sediment samples at Site 1.

Depth (mm)	RF1 *(- 2h)	RF2 *(- 1h)	RF3 *(0h)	RF4 *(+ 0.5h)	Depth average
0-10	47	46	69	76	59.5
10-20	51	53	68	77	62.3
20-30	53	64	53	75	61.3
30-40	52	59	50	73	58.5
40-50	61	63	46	75	61.3
Core average	53	57	57	75	60.5

***Relative time to high tide. Please also refer to Table 2-2 for sampling times.**

4.2.2 Particle size analysis

Particle size of sediments was determined for the four core samples collected from Site 1. The sediment core sections generally contained $\leq 50\%$ sand. The most notable exception was RF4 (0-10 mm), where sand content accounted for 73.3% of particles. RF3 had the lowest proportion of particles classified as sand, the highest of which was only 29.4% (30-40 mm). No trend was observed between grain-size and depth suggesting well mixed, bioturbed sediments.

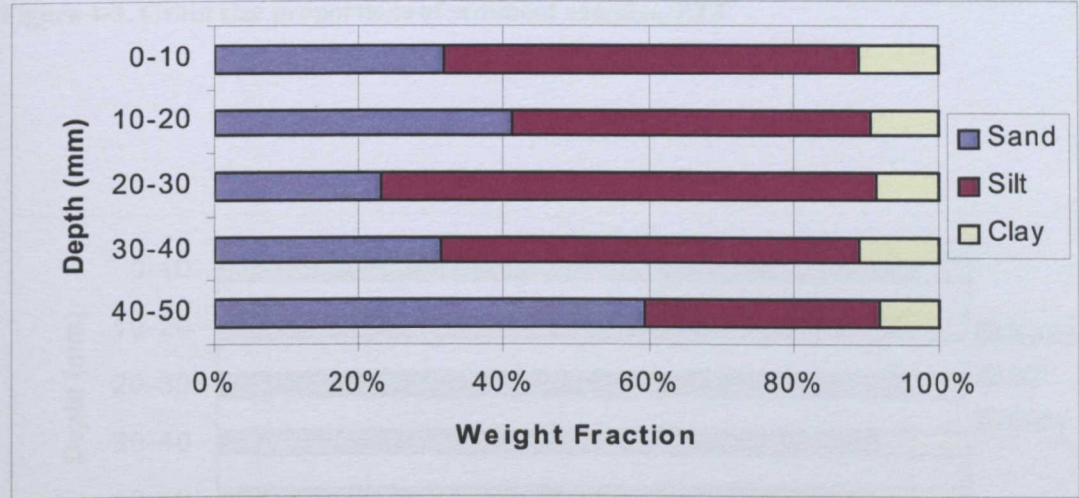


Figure 4-1. Grain size proportions of sediment samples, RF1.

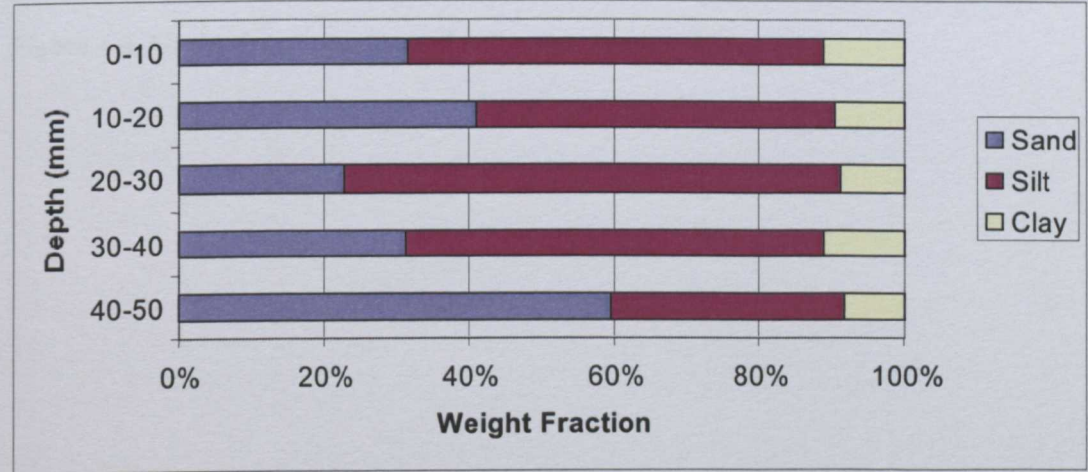


Figure 4-2. Grain size proportions of sediment samples, RF2.

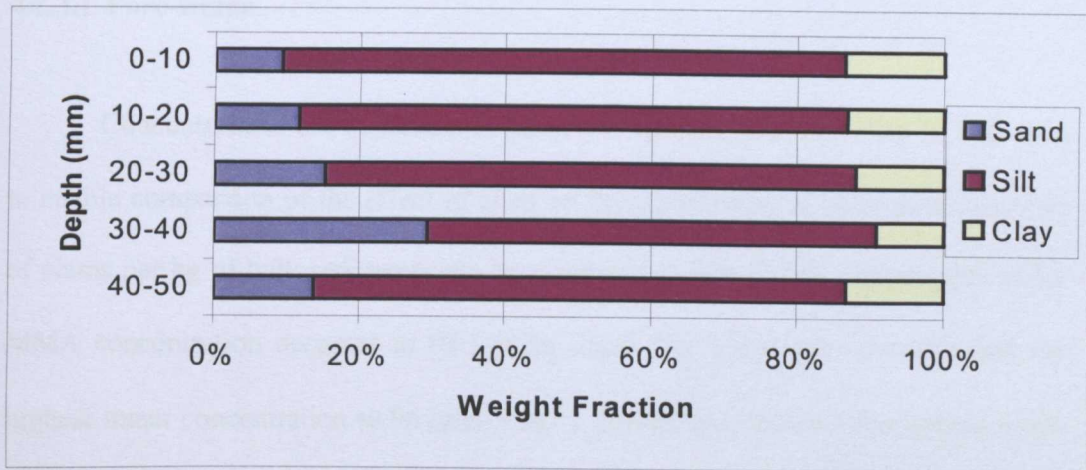


Figure 4-3. Grain size proportions of sediment samples, RF3.

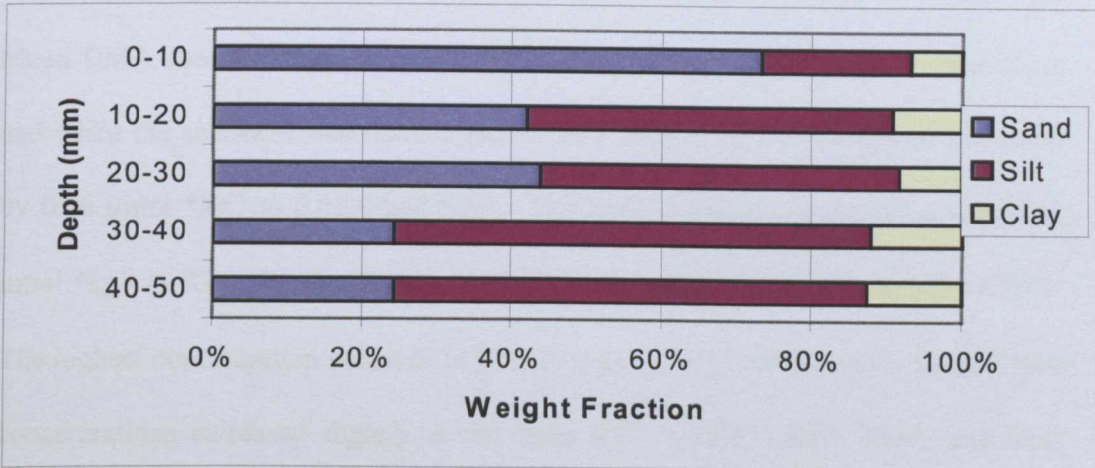


Figure 4-4. Grain size proportions of sediment samples, RF4.

4.2.3 Abundance of MAs

4.2.3.1 Pore-water

Concentrations are expressed in μmol per kg bulk sediment (*kg^{-1}). This was to enable comparison of the effect of clam on the distribution of MAs as the number of clams per kg of bulk sediments can be estimated in Site 2. The highest pore-water MMA concentration occurred in RF3 ($8.26 \mu\text{mol *kg}^{-1}$) and this core also had the highest mean concentration ($6.96 \mu\text{mol *kg}^{-1}$). MMA was depleted throughout cores RF1 and RF2 but increased slightly with depth in RF4, while RF3 showed no noticeable change in MMA concentrations below 20 mm depth.

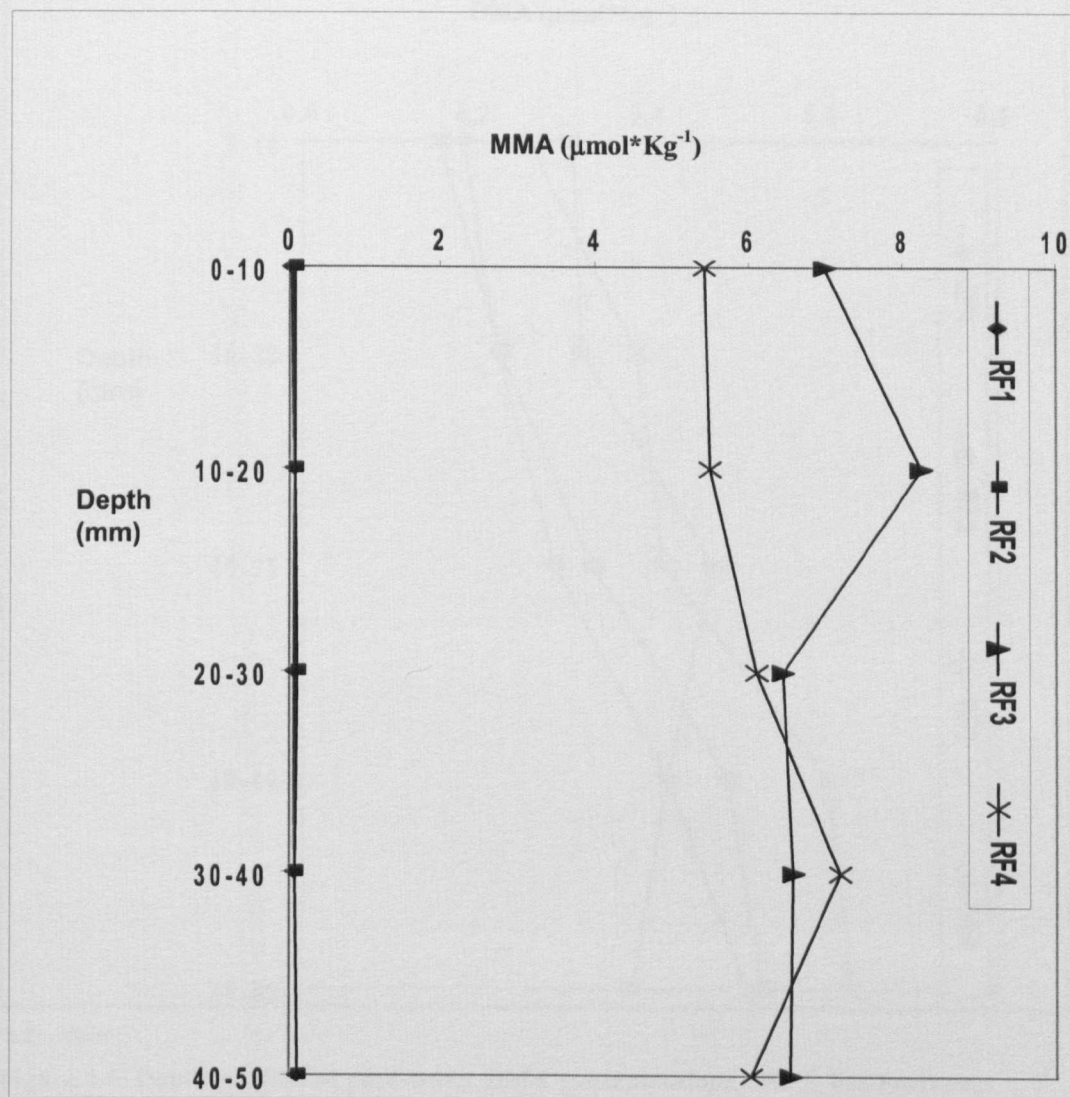
DMA concentrations increased with depth in all cores except RF3 (Fig. 4-6). Mean DMA concentrations increased by $0.03 \mu\text{mol *kg}^{-1}$ at the onset of inundation and when the sediment was flooded (RF4), the mean DMA concentration increased by $0.06 \mu\text{mol *kg}^{-1}$ to $0.46 \mu\text{mol *kg}^{-1}$. The highest DMA concentration was $0.63 \mu\text{mol *kg}^{-1}$ in RF4 (40-50 mm, Fig. 4-7). TMA was depleted in the top half of RF4. The highest concentration occurred in RF2 ($1.5 \mu\text{mol *kg}^{-1}$, 40-50 mm). Mean TMA concentrations increased slightly in the order $\text{RF1} < \text{RF2} < \text{RF3}$. TMA was least abundant in RF4, with a mean concentration of $0.07 \mu\text{mol *kg}^{-1}$.

Statistical analysis was performed to determine whether concentrations of MAs differed significantly at different stages of the tidal cycle using Student's paired T-test and ANOVA (One way, Unstacked). The ANOVA test showed that there was significant difference between the means of the concentrations of the five cores for MMA and TMA ($p = 0$) but there was no sufficient evidence to conclude that there was a significant difference between the means of DMA concentrations ($p = 0.451$).

However the paired T-test indicated different trends; for example, there were significant differences between the depth profiles of all cores for MMA, except RF1 and RF2, RF3 and RF4 ($p > 0.05$) (Table 4-2). DMA showed the least variation in concentration throughout the sampling series. There were significant differences between RF2 and RF4 pore-water depth profiles for all MA concentrations.

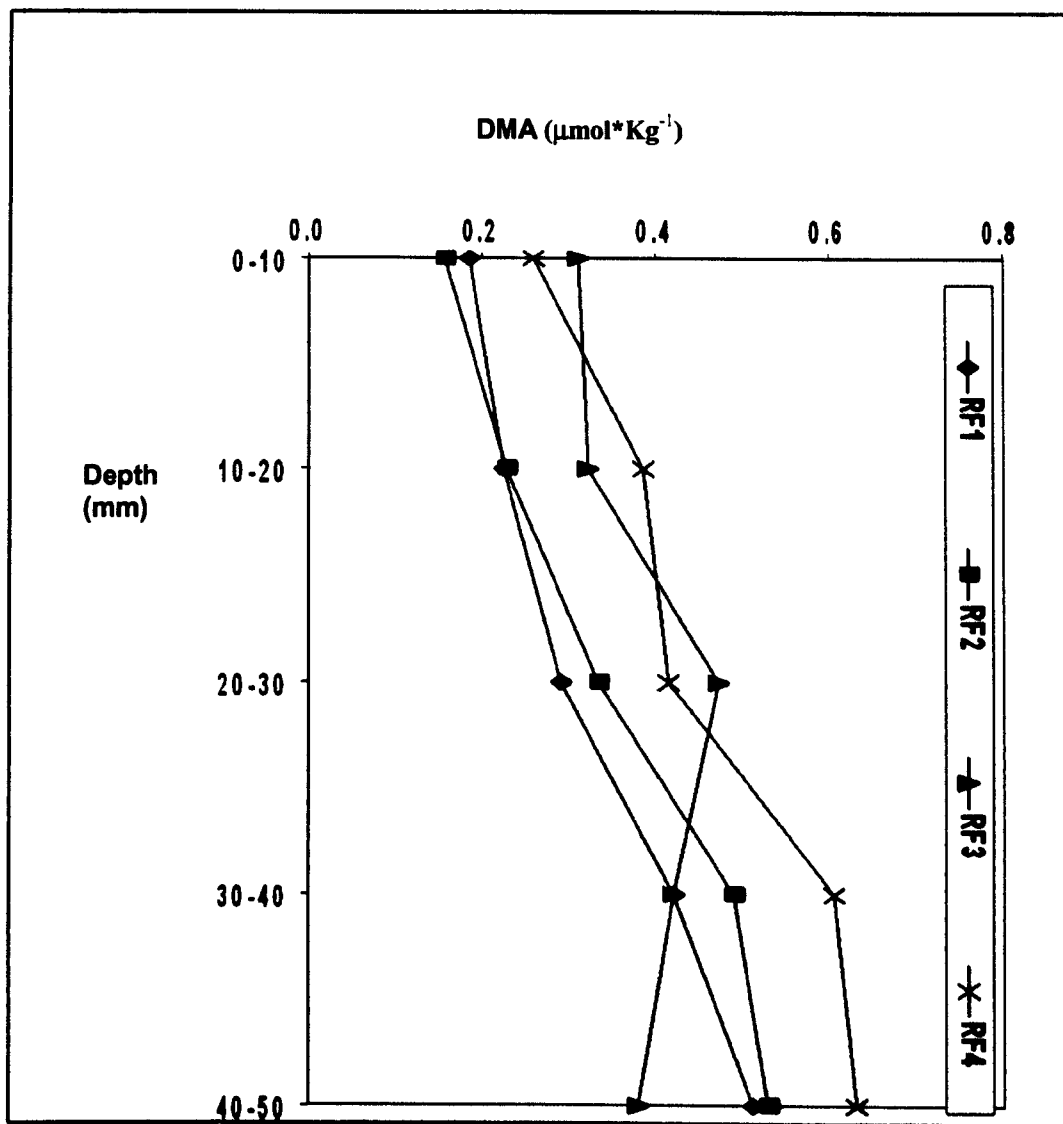
Table 4-2. p values of paired T-test of pore-water and solid-phase concentrations of Ria Formosa samples, Site 1. (RF1/RF2 = Comparison of RF1 and RF2).

MMA	RF1/RF2	RF1/RF3	RF1/RF4	RF2/RF3	RF2/RF4	RF3/RF4
Solid-phase	0.001	0.082	0.001	0.003	0.002	0.002
Pore-water	0.07	0.000	0.000	0.000	0.000	0.185
DMA	RF1/RF2	RF1/RF3	RF1/RF4	RF2/RF3	RF2/RF4	RF3/RF4
Solid-phase	0.003	0.145	0.689	0.006	0.004	0.049
Pore-water	0.305	0.390	0.003	0.623	0.001	0.268
TMA	RF1/RF2	RF1/RF3	RF1/RF4	RF2/RF3	RF2/RF4	RF3/RF4
Solid-phase	0.000	0.000	0.000	0.229	0.000	0.003
Pore-water	0.154	0.169	0.001	0.418	0.001	0.000



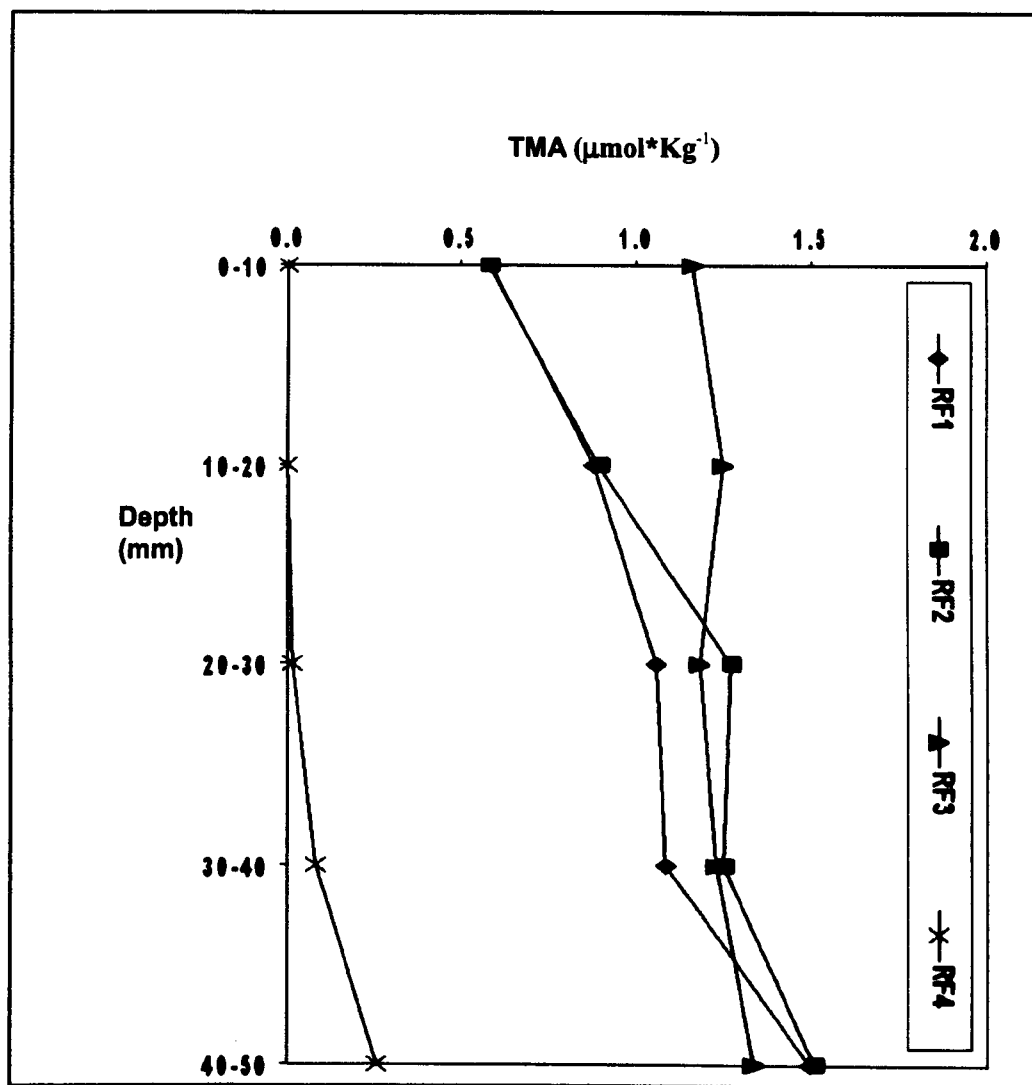
*Bulk sediment

Figure 4-5. Depth profiles of pore-water MMA concentrations, Site 1, Ria Formosa. Relative time to high tide; RF1= -2h, RF2 = -1h, RF3 - 0h, RF4 = 05 h, see also Table 2-2 for sampling times.



*Bulk sediment

Figure 4-6. Depth profiles of pore-water DMA concentrations, Site 1, Ria Formosa. Relative time to high tide; RF1= -2h, RF2 = -1h, RF3- 0h, RF4 = 0.5h, see also Table 2-2 for sampling times.

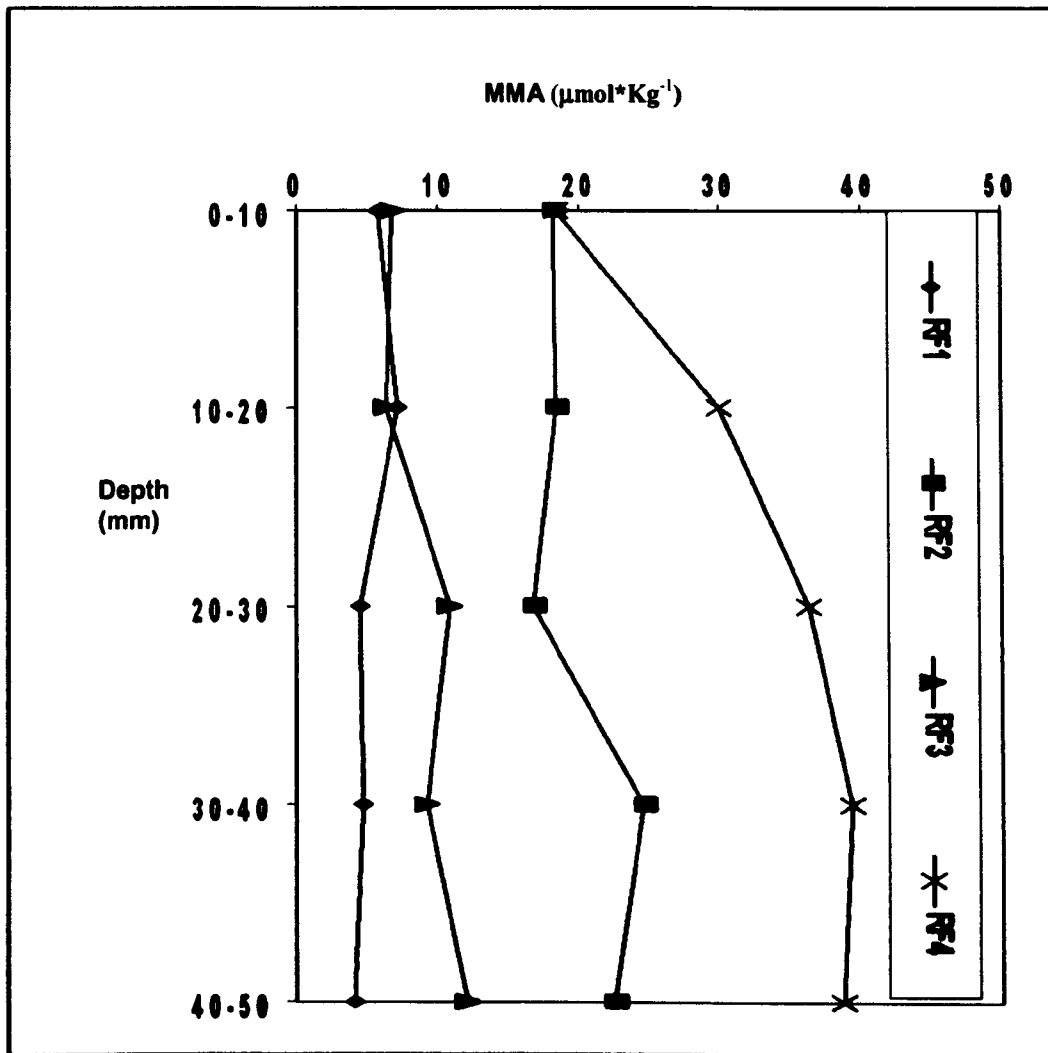


*Bulk sediment

Figure 4-7. Depth profiles of pore-water TMA concentrations, Site 1, Ria Formosa. Relative time to high tide; RF1= -2h, RF2 = -1h, RF3 - 0h, RF4 = 0.5h, see also Table 2-2 for sampling times.

4.2.3.2 Solid-phase

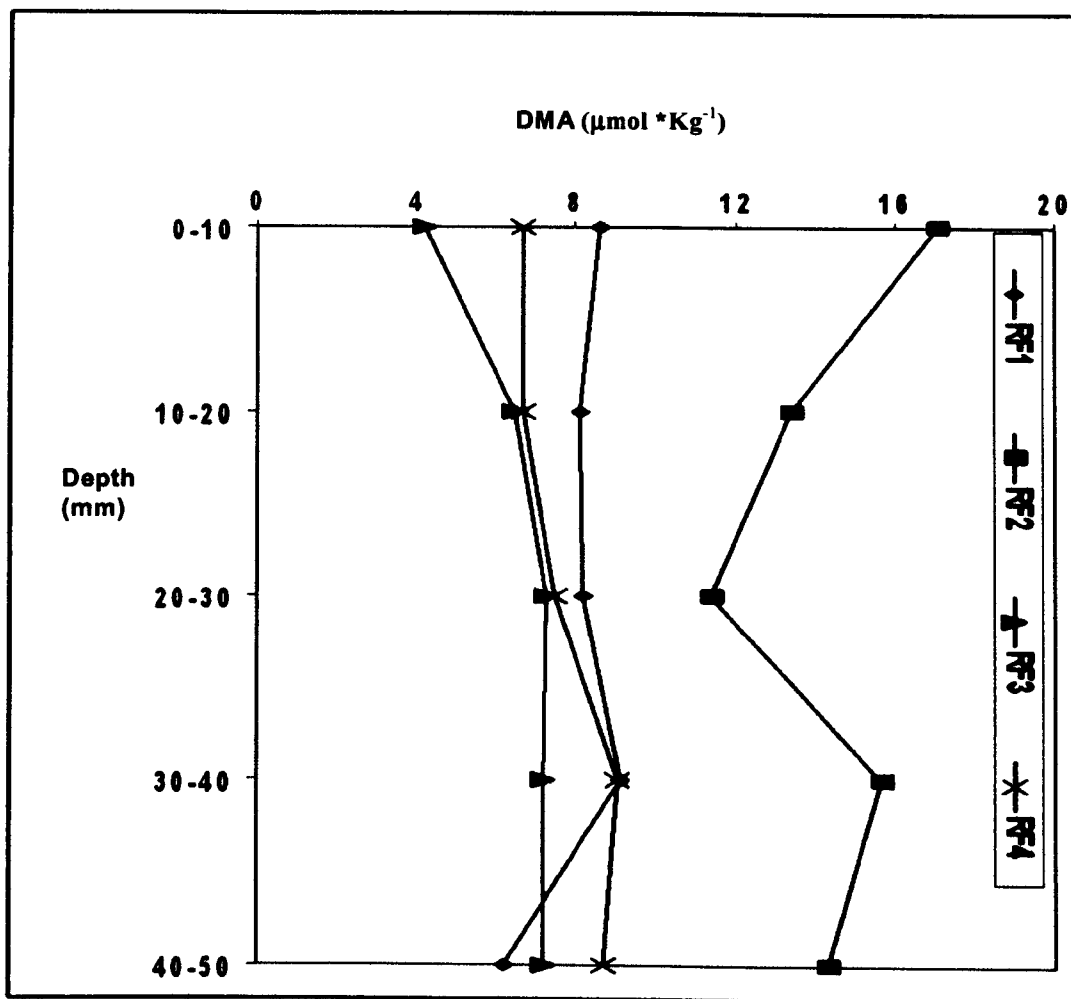
RF2 and RF4 had higher MMA concentrations than RF1 and RF3 (Fig. 4-8). The highest MMA concentration occurred in RF4 ($38.8 \mu\text{mol} \cdot \text{kg}^{-1}$) and the lowest in RF1 ($4.15 \mu\text{mol} \cdot \text{kg}^{-1}$). MMA was the most abundant MA in all cores except RF1 TMA (Fig. 4-10). In this core, TMA was 13 times more abundant than MMA. MMA concentrations increased with depth in RF4 but this trend was not observed in the other cores.



*Bulk sediment

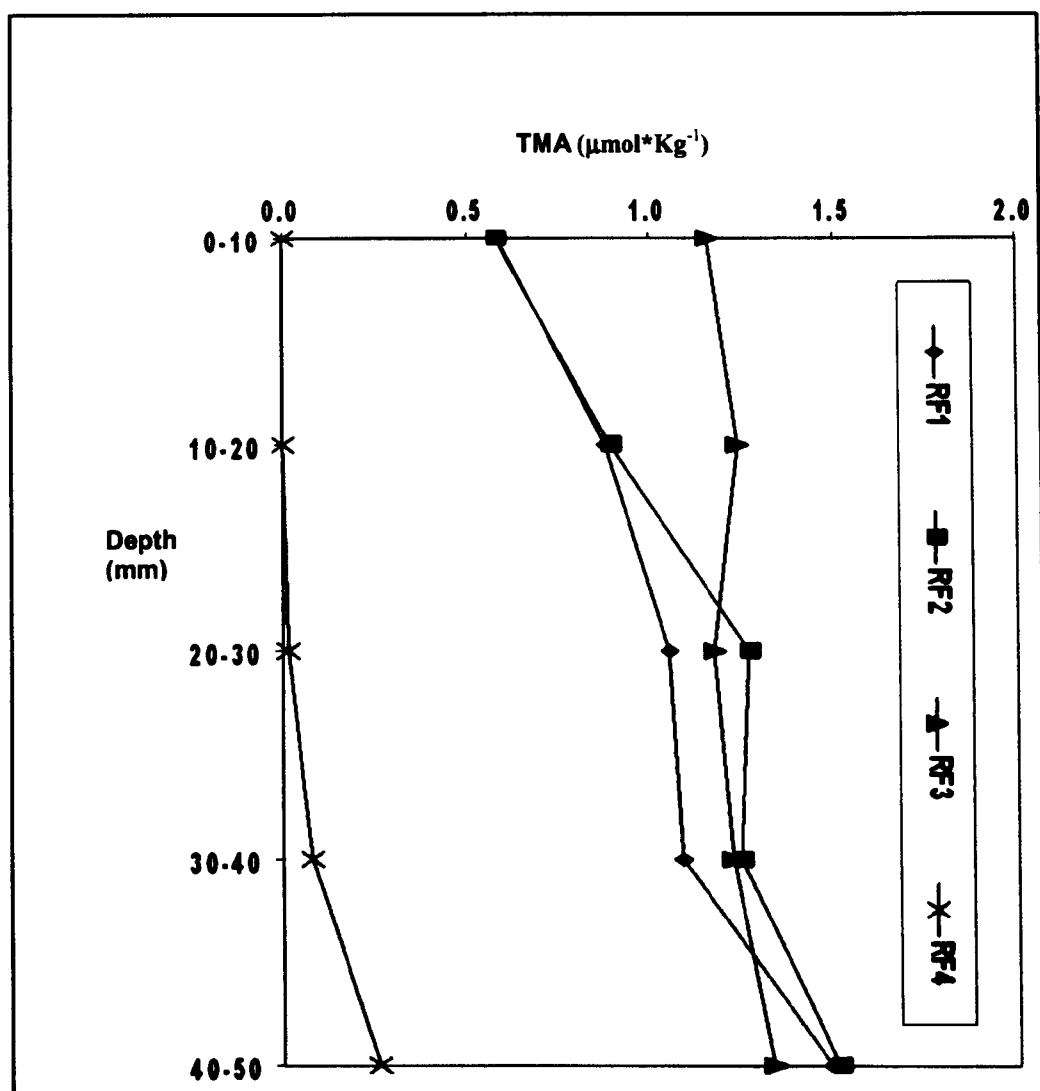
Figure 4-8. Depth profiles of solid-phase MMA concentrations, Site 1, Ria Formosa. Relative time to high tide; RF1= -2h, RF2 = -1h, RF3 - 0h, RF4 = 05 h, see also Table 2-2 for sampling times.

Overall, DMA concentrations varied little with depth. RF2 had the highest DMA concentrations (Fig. 4-9) and RF3 the lowest, though only RF2 was significantly different from the rest (Student's T-test, $p < 0.05$). However, the ANOVA results indicated that there were significant differences between the means of all MAs ($p = 0$). TMA was depleted in RF4 (Fig. 4-10) and most abundant in RF1 (mean concentration of $67.35 \mu\text{mol} \cdot \text{kg}^{-1}$). RF2 and RF3 had similar TMA profiles.



*Bulk sediment

Figure 4-9. Depth profiles of solid-phase DMA concentrations Site 1, Ria Formosa. Relative time to high tide; RF1= -2h, RF2 = -1h, RF3 - 0h, RF4 = 05 h, see also Table 2-2 for sampling times.



*Bulk sediment

Figure 4-10. Depth profiles of solid-phase TMA concentrations, Site 1, Ria Formosa. Relative time to high tide; RF1= -2h, RF2 = -1h, RF3- 0h, RF4 = 0.5h, see also Table 2-2 for sampling times.

4.2.4 Adsorption Coefficients

The dimensionless adsorption coefficients, K^* were used in this study to enable comparison of equivalent pool sizes of MAs in the dissolved and solid-phases. K^* for MMA was highest in RF1 and RF2, while K^* in RF3 and RF4 was less variable. The highest K^* value for MMA (338) was found at 0-10 mm depth in RF2 (Table 4-3). The lowest K^* value (1) was found at 0-20 mm depth and 30-40 mm depth in RF3. R^2 values for regression plots of pore-water concentrations against solid-phase concentrations showed that there was little correlation between these pools within individual cores, the highest value being only 0.6121 for RF3, where the two pools had similar concentration ranges.

The highest K^* value for DMA (109) occurred at 0-10 mm depth in RF2 (Table 4-4) and the lowest (12) at 40-50 mm depth in RF1. Average K^* values for RF1 and RF2 were higher than for RF3 and RF4, which had similar mean K^* values (17 and 18, respectively). R^2 values for regression plots of pore-water against solid-phase concentrations indicated no correlation between these two pools except for RF4 ($R^2 = 0.898$). The highest K^* value (118) for TMA was found at 0-10 mm depth in RF1 (Table 4-5), while the K^* value declined to zero in RF4 at 0-30 mm depth. This decrease in K^* was concurrent with a decrease in solid-phase TMA concentrations with time and also with an increase of water content in the surface layers (0-20 mm) after inundation. K^* decreased with depth in RF1 and RF2. RF1 had much higher K^* values than the other cores. A significant correlation between pore-water and solid-phase concentrations was only observed for RF3 ($R^2 = 0.895$).

Table 4-3. Adsorption coefficients (K*) of MMA Ria Formosa.

Depth (mm)	RF1 (-2h*)	RF2 (-1h*)	RF3 (0h*)	RF4 (+ 0.5h*)
0-10	114	338	1	3
10-20	125	286	1	5
20-30	57	181	2	6
30-40	64	288	1	5
40-50	40	209	2	6
Core average	80	261	1.2	5.2
*R ²	0.5214	0.1895	0.6121	0.5276

R² values for plots of pore-water versus solid-phase concentrations are also included to show degree of correlation within each core.

*Relative time to high tide. Please also refer to Table 2-2 for sampling time.

Table 4-4. Adsorption coefficients (K*) of DMA Ria Formosa.

Depth (mm)	RF1 (-2h*)	RF2 (-1h*)	RF3 (0h*)	RF4 (+0.5h*)
0-10	46	109	13	26
10-20	36	58	20	17
20-30	28	34	16	18
30-40	22	32	17	15
40-50	12	27	19	14
Core average	29	52	17	18
*R ²	0.3031	0.0192	0.5441	0.898

R² values for plots of pore-water versus solid-phase concentrations are also included to show degree of correlation within each core.

*Relative time to high tide. Please also refer to Table 2-2 for sampling time.

Table 4-5. Adsorption coefficients (K*) of TMA Ria Formosa.

Depth (mm)	RF1 (-2h*)	RF2 (-1h*)	RF3 (0h*)	RF4 (+ 0.5h*)
0-10	118	14	3	0.0
10-20	78	6	3	0.0
20-30	63	5	4	0.0
30-40	67	7	6	6.7
40-50	40	5	6	2.0
Core average	73	7	5	3
*R ²	0.4193	0.0	0.895	0.7064

R² values for plots of pore-water versus solid-phase concentrations are also included to show degree of correlation within each core.

*Relative time to high tide. Please also refer to Table 2-2 for sampling time.

4.3 **Results of MA analysis of Site 2 samples.**

4.3.1 **Clam tissue**

Clam tissue samples from Site 2 were analysed as described in Chapter 2, Section 2.3.4.1. Those collected during sediment exposure contained all three MAs. Samples extracted with 2M LiCl showed higher recoveries of MAs than those extracted with SSW (Table 4-6). TMA was more abundant than both MMA and DMA before and after inundation. Average TMA concentrations in clam tissue decreased by a factor of between four and five after inundation (Table 4-6), while MMA concentrations decreased two to three fold. DMA concentrations did not show any noticeable change during inundation for tissue samples extracted with 2M LiCl but increased by 37.1 % for samples extracted with SSW.

Table 4-6. Comparison of average MA concentrations in clam tissues for the two extraction methods.

MA (mmol *kg ⁻¹), LiCl ext ^{''} .			MA (mmol *kg ⁻¹) SSW ext ^{''} .		Change in MA concentrations after inundation, mmol *kg ⁻¹	
	Before inundation	After inundation	Before inundation	After inundation	LiCl ext	SSW ext
MMA	0.52	0.18	0.16	0.08	-0.33	-0.08
DMA	0.48	0.45	0.35	0.48	-0.03	0.13
TMA	191.47	36.10	17.58	4.26	-155.37	-13.32

^{''}ext = extraction

* Bulk sediment

The changes in MA concentrations for samples collected from Site 2 before and after inundation were calculated according to Equations 2-5 to 2-7 (Table 4-7). A negative sign indicates movement out of tissue, mantle cavity-water or surrounding sediment, whereas a positive sign signifies accumulation in clam tissue, mantle cavity-water or surrounding sediment.

Table 4-7. Concentrations of the MAs in samples of *R. decussates* (L.) and sediment taken from Site 2 before and after tidal inundation.

Sample	MMA	DMA	TMA
Clam tissue	mmol kg ⁻¹	mmol kg ⁻¹	mmol kg ⁻¹
Before inundation	0.52	0.48	191.47
After inundation	0.18	0.45	36.10
Change	- 0.33	- 0.03	- 155.38
Mantle cavity water	mmol kg ⁻¹	mmol kg ⁻¹	mmol kg ⁻¹
Before inundation	0.003	0.001	0.013
After inundation	0.003	nd	0.107
Change	0	- 0.001	0.094
Sediment (40% water content)*	mmol *kg ⁻¹	mmol *kg ⁻¹	mmol *kg ⁻¹
Before inundation	0.032	0.010	0.073
After inundation	0.017	0.001	0.909
Change	0.015	- 0.009	0.836

(nd = not detected). Mantle cavity water concentrations are expressed in mmol kg⁻¹ since 1 ml of sample weighed 1 g.
 *Concentrations calculated by assuming pore-water content to be 40% (Rocha *et al.*, 2001) see Section 4.3.2. *Bulk sediment.

4.3.2 Clam mantle cavity-water.

TMA was the most abundant MA in the mantle cavity water of the clams ($0.013 \text{ mmol } * \text{kg}^{-1}$ and $0.107 \text{ mol } * \text{kg}^{-1}$ before and after inundation, respectively) (Table 4-7). DMA was the least abundant MA ($0.001 \text{ mmol } * \text{kg}^{-1}$ and not detectable before and after inundation, respectively). Both MMA and DMA concentrations decreased after inundation while TMA increased more than 8-fold (Table 4-7).

4.3.3 Clam bed sediments.

Sediment at Site 2 consisted almost entirely of quartz sand, with over 40% composed of very coarse to medium sand and a finer fraction (60% by weight) constituting very fine sand. It was not possible to retain enough pore-water from Site 2 sediments during sampling. Which meant it was not possible to determine neither water content nor dissolved analyte concentrations. Moist sediment samples were analysed and solid-phase MA concentrations were determined by assuming the water content of sediments to be 40% (Rocha *et al.*, 2 001). The results are shown in Table 4-6.

The solid-phase MMA concentration before inundation was $32 \text{ } \mu\text{mol } * \text{kg}^{-1}$, which decreased by nearly 50% to $17 \text{ } \mu\text{mol } * \text{kg}^{-1}$ after inundation. The DMA concentration before inundation was $10 \text{ } \mu\text{mol } * \text{kg}^{-1}$, which decreased to $1 \text{ } \mu\text{mol } * \text{kg}^{-1}$ after inundation. TMA was the most abundant MA before and after inundation and, unlike MMA and DMA, its concentrations increased more than 12 times after the onset of inundation (73 to $909 \text{ } \mu\text{mol } * \text{kg}^{-1}$).

4.4 Discussion

4.4.1 General observations (Site 1).

The water content of the Ria Formosa samples correlated to some extent with sand content and to a greater extent with tidal inundation. The MA concentrations at Site 1 were similar to the other sites studied in this work, while the K^* values indicate that most MAs were associated with the solid-phase (before inundation), as observed in previous studies (e.g. Wang and Lee, 1990; Fitzsimons *et al.*, 2001). The water content of the top 20 mm of sediment in RF3 increased significantly compared to cores RF1 and RF2. An increase in the liquid to solid ratio may have contributed to increased desorption of MAs at the onset of tidal inundation, when sediment resuspension is expected to peak (this is discussed in more detail in Chapter 5). This is supported by the K^* values, which generally decreased after inundation.

Pore-water concentrations of the MAs were virtually unchanged in the 2 cores taken before inundation (Figs. 4-5 to 4-7), while solid-phase TMA was consumed; its concentration decreasing by $60 \mu\text{mol kg}^{-1}\text{h}^{-1}$ bulk sediment in the first hour of sampling (i.e. between RF1 and RF2) (Fig. 4-10). The corresponding increase in solid-phase MMA and DMA did not balance all of the TMA consumed and it was presumed that production of NH_4^+ could account for this, a scenario which has been reported for coastal marine sediments by Kim *et al.* (2003). TMA was still present in the pore-water and solid-phase at the onset of inundation (RF3), but was virtually absent in core RF4 (Fig. 4-10).

Although MAs adsorb to sediments readily, their adsorption is reversible (Wang and Lee, 1995). This explains the consumption of TMA in the solid-phase. The calculated rate of TMA consumption in the solid-phase ($60 \mu\text{mol kg}^{-1}\text{h}^{-1}$ between

RF1 and RF2) was comparable to the degradation rate of TMA by halo-tolerant bacteria for a laboratory study conducted by Kim *et al.*, (2003) using coastal sediment slurries.

The largest change in K^* for MMA was observed during inundation (RF3 and RF4, Table 4-3). Since sediment dewatering during exposure favours adsorption, it is likely that hydration of the surface sediment caused repartitioning of MMA in the sediment. Such a process has been described for NH_4^+ (e.g. Rocha *et al.*, 1998; Morin and Morse, 1999). There was no correlation between clay mineral content and adsorption coefficients like BOS samples as observed by Wang and Lee, 1990. A negative correlation between DMA adsorption and clay mineral content found in RF4 indicates that clay mineral content may not be one of the dominant controlling factors of MA adsorption in the Ria Formosa sediments.

Although the adsorption coefficients of MAs (expressed as mL g^{-1} , not shown) in this study were comparable to BOS (Chapter 3), they were many times higher than other studies (e.g. Wang and Lee, 1990; 1995). These adsorption coefficients did not follow the order observed for BOS and other studies (i.e., $\text{TMA} > \text{DMA} > \text{MMA}$). The four cores at Site 1 showed different trends, e.g. $\text{MMA} > \text{TMA} > \text{DMA}$ for RF1 but $\text{MMA} > \text{DMA} > \text{TMA}$ for RF2. However, the change in the order of MA adsorption coefficients and the large variations obtained during the different stages of the diurnal tidal cycle as well as variations in the degree of correlation between solid-phase and pore-water concentrations suggest that the MAs were never in equilibrium during the period of the tidal cycle in which sampling was carried out.

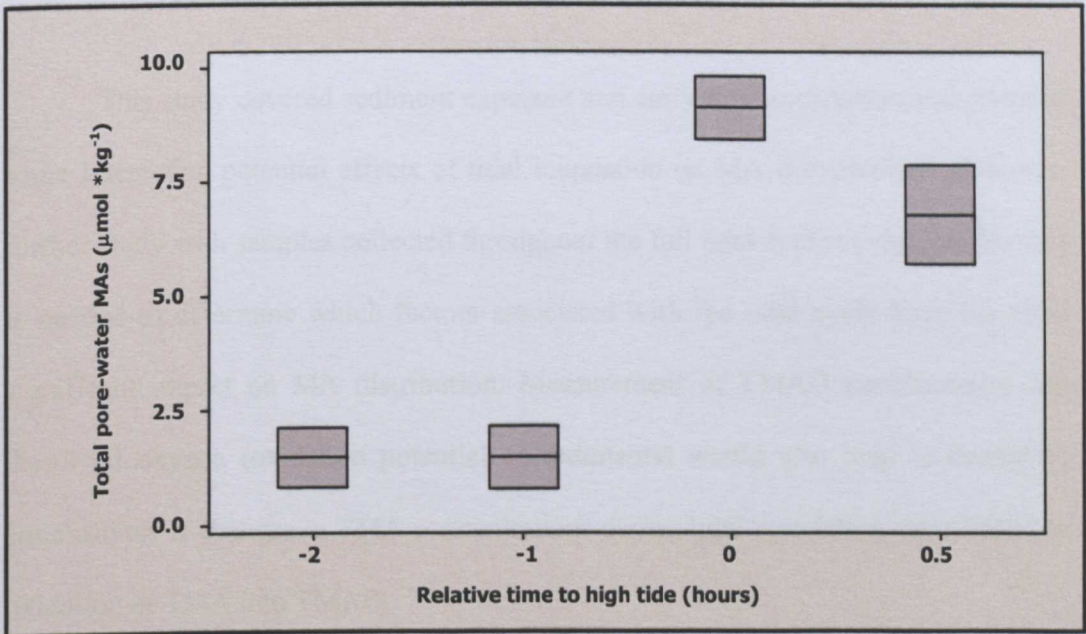
4.4.2 Effect of tidal cycle on MA distribution.

Although a mathematical/statistical model was not developed in this study to determine the significance of the different factors associated with the tidal cycle on MA cycling, the differences in depth profiles of solid-phase and pore-water concentrations of Site 1 samples (significant differences based on statistical analysis, Table A-1) can be partly explained by the following factors. Tidal flushing has been shown to play a significant role in the export of NH_4^+ from sediment to the overlying water in the Ria Formosa (Falcao and Vale, 1995). In fact, Falcao and Vale (1995) found that the daily amount of NH_4^+ exported through pore-water flushing was two orders of magnitude higher than the transport resulting from molecular diffusion in the Ria Formosa.

In this study, MA concentrations were not depleted in the pore-waters at the onset of tidal inundation, possibly as a result of desorption from the solid-phase. However, TMA concentrations were generally lower during inundation (RF4). The introduction of oxygenated seawater when the sediment is flooded may have enabled oxidation of TMA to TMAO to proceed (Kim *et al.* 2003). However, this needs to be further investigated. When sediments with high sand content are exposed, they heat up and are considerably warmer than the incoming seawater at inundation, resulting in a buoyancy effect and rapid turnover of pore-water (Rocha, 1998; 2000). This could result in depletion of pore-water MAs at inundation (i.e. RF3). However, in this study MMA concentrations increased at the start of inundation while DMA concentrations did not change significantly. TMA concentrations in RF3 were the highest and RF4 concentrations were the lowest. This may be due to the compensatory effect of a substantial amount of TMA being released by invertebrates at the onset of tidal

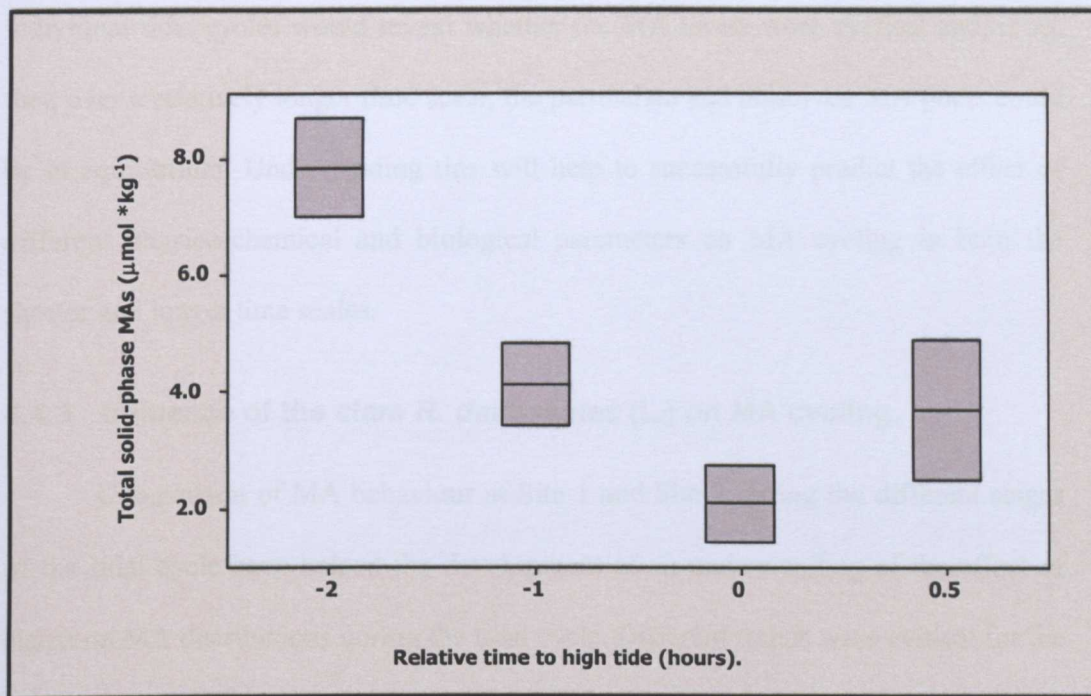
inundation as evidenced by the high outflux of TMA from clam tissue samples during early inundation. This is discussed in more detail in Section 4.4.3.

Total pore-water concentration ranges did not change in the samples collected before inundation while there was a rapid increase in pore-water MAs at the beginning of tidal inundation, which subsequently decreased after a further 0.5 hours (Fig. 4-11). This trend is expected as tidal inundation enhances desorption of particulate MAs as a result of decrease in solid to solution ratio and increased competition for binding sites by seawater cations. Total solid-phase MA concentrations decreased as flooding started. An increase in total MA concentration was observed for samples taken 0.5 hours after inundation had started (Fig. 4-12).



*Bulk sediment

Figure 4 -11. Total pore-water MA concentration ranges of Ria Formosa Site 1 samples at different stages of a tidal cycle (time axis not to scale).



*Bulk sediment

Figure 4-12. Total solid-phase MA concentration ranges of Ria Formosa Site 1 samples at different stages of a tidal cycle (time axis not to scale).

This study covered sediment exposure and early tidal inundation and revealed some interesting potential effects of tidal inundation on MA distributions. However, further study with samples collected throughout the full tidal cycle at regular intervals is needed to determine which factors associated with the tidal cycle have the most significant impact on MA distribution. Measurement of TMAO concentration and dissolved oxygen (oxidation potential of sediments) would also help to determine conclusively if changes in TMA concentrations during tidal inundation were linked to oxidation of TMA into TMAO.

Different micro-environments created for a short period of time through bioturbation by invertebrates or rapid microbial uptake may have resulted in variations in MA distribution throughout the tidal cycle. Comparison of several

individual tidal cycles would reveal whether the MA levels were cyclical and, if so, then over a relatively longer time scale, the particulate and dissolved MA pools could be in equilibrium. Understanding this will help to successfully predict the effect of different physico-chemical and biological parameters on MA cycling in both the shorter and longer time scales.

4.4.3 Influence of the clam *R. decussates* (L.) on MA cycling.

Comparison of MA behaviour at Site 1 and Site 2 during the different stages of the tidal cycle have helped the development of an understanding of the effect of clams on MA distributions during the tidal cycle. Different trends were evident for the three MAs during tidal inundation. There was a $0.33 \text{ mmol } * \text{kg}^{-1}$ decrease in MMA in clam tissue after inundation, no decrease in mantle-cavity water and a decrease of $0.015 \text{ mmol } * \text{kg}^{-1}$ for sediment. DMA decreased by $0.03 \text{ mmol } * \text{kg}^{-1}$ in clam tissue after inundation by $0.001 \text{ mmol } * \text{kg}^{-1}$ in mantle cavity water, and by $0.009 \text{ mmol } * \text{kg}^{-1}$ in sediment. TMA was much more abundant than DMA and MMA at Site 2. Its concentration decreased by $155.38 \text{ mmol } * \text{kg}^{-1}$ in clam tissue after inundation. The mantle-cavity water TMA concentrations increased by $0.094 \text{ mmol } * \text{kg}^{-1}$ in the mantle-cavity water compared to an increase of $0.836 \text{ mmol } * \text{kg}^{-1}$ in the surrounding sediment.

The increased TMA concentrations in mantle cavity water and solid-phase of Site 2 sediments indicate that TMA was released from the clam tissue into mantle-cavity water and the surrounding sediment after tidal inundation. It is appropriate to mention here that no mass balance experiments were carried out; hence the changes in MA concentrations in Site 2 samples can only be used as an estimate of the magnitude of the MA pool exchanged between clam tissues, mantle cavity water and surrounding

sediment during tidal inundation. The results suggest that clams can supply relatively large concentrations of ON to sediments, since the MAs (especially, TMA) appear to be directly released to the surrounding sediments.

R. decussates (L.) excretes NH_4^+ at a rate of $30 \text{ mmol clam}^{-1}\text{h}^{-1}$ (Sobral and Widdows, 1997). This, coupled with the potential to release MAs to surrounding sediments highlights the significance of benthic invertebrates in the cycling of N in inter-tidal sediments. The idea that benthic invertebrates could be a direct source of MAs has been suggested (Sørensen and Glob, 1987; Wang and Lee, 1994). Invertebrates isolated from sediments also respond to immersion in low salinity water with direct release of TMA from their body fluids (Sørensen and Glob, 1987). This implies that direct release or diffusion of TMA from the intracellular solutions of marine organisms does occur. This is supported by the result of this study, which clearly indicated a significant amount of TMA being released by the clam *R. decussates* (L.) during tidal inundation. However, whether TMA is released as a result of changes in salinity cannot be confirmed, as pore-water salinity was not measured because of the difficulty in obtaining an adequate volume from sediments. The change in TMA concentration in clam tissue may be related to changes in salinity or passive accumulation by the clams directly from their food (de Vooy, 2002).

A comparison of sediment core samples from Sites 1 and 2 infers that the increased numbers of the clam *R. decussatus* (L.) in Site 2 sediment samples enhanced the MA pool. Natural macrofaunal density in the sandy sediments of the Ria Formosa is 40 to 200 individuals m^{-2} (Sprung, 1994), *R. decussatus* is seeded at Site 2 (i.e. juvenile clams are introduced into a semi-controlled environment, named the clam rearing plot) to a maximum density of 600 individuals m^{-2} in sandy sediments

(Fitzsimons *et al.*, 2005). The following example illustrates the effect of increased numbers of invertebrates on MA cycling at Site 2. TMA was the dominant MA in the sediment samples collected before tidal inundation at Site 1 (RF1 and 2) but was depleted after inundation (RF4), while MMA became the most dominant MA after inundation. In Site 2 sediment samples, TMA was the most abundant MA before and after inundation.

Higher number of clams at Site 2 may also have led to greater oxygenation of sediments as result of increased bioturbation. Uptake of MAs by micro-organisms occurs faster in oxic seawater than in anoxic sediments (Lee, 1992). Tidal inundation introduces oxygen deeper into sediments possibly, enhancing the depletion of MAs by microbial uptake. The decrease in TMA concentrations was followed by an increase in MMA and DMA in Site 1 sediments, suggesting that the concentrations were enhanced through degradation of TMA. The decrease in both MMA and DMA concentrations at Site 2 after inundation confirms that they are unlikely to be released in high quantities by the clams. Although the higher concentration of clams in Site 2 sediments was expected to create more oxic conditions than at Site 1, as a result of animal burrowing, the release of a considerable amount of TMA by the clams during sediment inundation seems to have compensated for any loss of TMA through oxidation of TMA or rapid uptake by microorganisms.

TMA concentrations in some parts of Site 2 sediments may have been higher, but homogenisation of the sediments would have masked any concentration gradients. Solid-phase TMA concentrations before inundation were similar to RF1. Site 2 samples were composed almost entirely of quartz sand, which is less efficient at adsorbing cations than silt or clay. The larger particle size would also facilitate pore-

water flushing during tidal inundation. Thus, while mariculture may introduce a greater density of clams in the sediment, this may also increase the export of labile ON to the water column, a substantial fraction of which may be in the form of TMA or its degradation products.

TMA is toxic (Anthoni *et al.*, 1991; Marzo and Curti, 1997) and is generally converted to TMAO within living animals for use in osmoregulation (Seibel and Walsh, 2002). Therefore, it is unclear why *R. decussatus* (L.) should contain high concentrations of TMA over the period of sediment exposure. TMAO is derived from dietary choline via its conversion to TMA by bacteria in the gut of marine animals (Seibel and Walsh, 2002), so some of the TMA measured may have originated from choline. Its conversion to TMAO requires oxygen. Enough oxygen for conversion of TMA into TMAO will only be available at inundation. Therefore, it seems that the clam may have been forced to retain TMA until the onset of inundation when it can excrete or oxidise TMA into TMAO as oxygen-enriched water starts to pass through the siphons during feeding. Excretion of TMA could arguably be the simpler physiological solution (Fitzsimons *et al.*, 2005). The slight increase in DMA concentrations in the clam tissues after tidal inundation can be attributed to accumulation of DMA from food sources (directly or indirectly) and then excretion.

The mean weights of tissue and mantle cavity water per clam were 2.36 and 1.25 g, respectively ($n = 20$), which equated to 451 μmol TMA per clam before inundation and 86 μmol per clam after inundation. The clam density at Site 2 was 10 ind. kg^{-1} bulk sediment, so if each clam excreted 365 μmol of TMA (the concentration difference between samples), then, assuming a pore-water content of 40% (Rocha *et al.*, 2001) and $K^* = 1$, the resulting solid-phase TMA concentration

would be $3.13 \text{ mmol kg}^{-1}$ bulk sediment. The TMA solid-phase concentration increased by $0.84 \text{ mmol kg}^{-1}$ bulk sediment after inundation, which was a substantial increase but less than the predicted amount. Therefore, $2.29 \text{ mmol kg}^{-1}$ bulk sediment TMA is unaccounted for (the increase in mantle cavity water was ignored as it was less than $1.2 \text{ } \mu\text{mol kg}^{-1}$ bulk sediment).

Sediment resuspension is common in the Ria Formosa (Sobral and Widdows, 2000). This makes the desorption of a substantial amount of TMA from solid-phase likely during the early stages of tidal inundation as observed for Thames Estuary sediments (Chapter 5). The fact that the clams excrete waste near the surface (Sobral and Widdows, 2000) increases the possibility of TMA being flushed from the sediment. If each clam excretes 365 mmol then each clam exports $281 \text{ } \mu\text{mol}$ to the water column then, the total number of clams m^{-2} (approx. 600) will result in a total 'burst flux' of $169 \text{ mmol TMA m}^{-2}$. However, this is only a rough estimate, as the rate of TMA consumption during early inundation is not known. Nonetheless, flushing of pore-water TMA, desorption of TMA from solid-phase and consumption of TMA in both solid-phase and pore-water account for the 'missing' TMA. Determination of TMA in overlying water would have given a more accurate estimate of the TMA flux during early tidal inundation.

The environmental impact of the physical disturbance of sediments as a result of clam mariculture is beyond the scope of this study. However, it is perhaps appropriate to mention that in addition to the effect of clams on the concentration of ON species, such as the MAs, in clam bed sediments, the physical activities associated with mariculture may also bring about significant changes to the nutrient dynamics of the sediments. A study by Falcao *et al.* (2003) in the same region of

Portugal found that sediment reworking as a result of dredging for clams did significantly increase the transfer of pore-water DON species to overlying water, immediately after dredging.

4.5 Summary

The main findings of this study of Ria Formosa sediments are summarised below.

- The MAs were abundant at Site 1, a cohesive sediment and Site 2, a sand flat used for mariculture of the clam *R. decussatus* (L.).
- Substantial amounts of MAs were found in the solid-phase. The adsorption coefficients were much greater than those determined in previous studies and are comparable to the adsorption coefficient values measured for Burnham Overy Staithe samples. Particle size did not seem to be a significant factor affecting MA adsorption in the Ria Formosa sediments. Tidal inundation led to changes in MA distributions at Site 1, possibly Site 2.
- The clam *R. decussatus* (L.) seemed to influence the distribution of MAs (especially TMA) in marine sediments. This species appeared to release a substantial amount of TMA into the surrounding sediment, possibly as a response to tidal inundation (i.e. excretion). The large numbers of *R. decussatus* (L.) in clam bed sediments has the potential to significantly increase the flux of N to the water column, which may have implications for water quality in the Ria Formosa.

5 THAMES ESTUARY

5.1 Introduction

Estuarine sediments typically contain large amounts of organic carbon. These sediments create a natural buffer zone for nearby coastal waters by trapping nitrates and other N species (Spiro and Stigliani, 1996). In general, estuarine sediments are considered as sinks for ON and sources of NH_4^+ , which can diffuse across the sediment-water interface (Rocha, 1998), while the flux of sedimentary ON is thought to be moderated by adsorption (e.g. Henrichs and Sugai, 1993; Keil *et al.*, 1994; Fitzsimons *et al.*, 2001).

Basic ON compounds adsorb to particles. For example, in the Amazon River, basic amino acids were found to dominate the amino acid component of ON within the fine ($< 63 \mu\text{m}$) particle fraction (Hedges *et al.*, 1994). Adsorption of bulk organic matter (OM) to particles appears to be reversible as adsorbed riverine OM is extensively ($> 60\%$) lost in estuaries and deltas (Hedges and Kiel, 1994). Henrichs (1995) suggested that this might be caused by the decreased particle to solution ratio in seawater compared to that in the environment where the OM was preserved, which results in increased competition for adsorption sites from marine OM, such that it would replace the terrestrial OM if present in large enough concentrations, regardless of its adsorption strength. Studies on the adsorption strength of ON compounds, such as amino acids (AAs) and MAs, have shown that they adsorb strongly onto marine sediments (sometimes irreversibly), particularly those with a high organic content. However, competition with seawater cations and OM content restricts their affinity for sediment exchange sites in saline environments (Wang and Lee, 1990; Henrichs and Sugai, 1993; Montuçon and Lee, 2001).

Estuarine sediments form part of a dynamic system, where sediment resuspension can occur diurnally through tidal influence or during extreme events such as storms. Anthropogenic activities, such as dredging, also lead to sediment resuspension (e.g. Morin and Morse, 1999). Resuspension of sediments can release NH_4^+ into the water column (Morin and Morse, 1999), with the flux dominated by desorbed NH_4^+ . The decrease in the particle to water ratio brought about by sediment resuspension may alter any established equilibrium and force desorption of ON molecules both through disturbance of equilibrium and increased competition with seawater cations (Shideler, 1984).

Reactions at particle surfaces strongly influence the distributions and concentrations of the ON fraction in sediments. For example, AAs and MAs can form reversible ionic bonds with negatively charged surface exchange sites on particles due to the protonation of the amino groups at seawater pH (Henrichs and Sugai, 1993; Wang and Lee, 1993). The size of this 'exchangeable' pool is usually determined through a single extraction of dry sediment with a concentrated salt solution, at a weight to volume ratio of 1:10 or 1:20. Any compound not extracted is then considered as 'fixed' within the particle (Wang and Lee, 1990). However, the existence of sediment NH_4^+ pools with different exchange capacities has been reported by Laima (1992), with the more 'tightly bound' ions being released through multi-volume extraction with 2M KCl solution. This sequential release of NH_4^+ was also observed by Morin and Morse (1999). The NH_4^+ ion is highly soluble in water but can also adsorb to sediments and it is possible that the behaviour of sorbed ON species will also be partly dependent on the solubility of the molecule and the ionic strength of the solution.

There is some evidence that ON compounds may be preferred substrates for bacteria in estuarine waters (Jørgensen *et al.*, 1999; Middleburg and Nieuwenhuize, 2000). Middleburg and Nieuwenhuize (2000) measured biological uptake of N substrates in the outer Thames Estuary, UK (NO_3^- , NH_4^+ , and AAs) and found that AAs accounted for 50% of the N taken up, while they were the main N substrate in the adjacent North Sea waters. Thus, an understanding of the conditions under which ON can be released from sediments is necessary for the accurate determination of N fluxes to the water column and for the management of activities such as dredging, which cause sediment resuspension. Adsorption coefficients of ON species have been measured by spiking ^{14}C -labelled compounds into aqueous slurries (e.g. Wang and Lee, 1990; Henrichs and Sugai, 1993; Montluçon and Lee, 2001). However, the degrees of binding of the molecules to particles may not be properly accounted for under these conditions (Laima, 1992), making environmental extrapolation uncertain.

In this part of the study, an attempt was made to study the kinetics of ON desorption from estuarine sediments, using the MAs as proxies for ON, and with reference to NH_4^+ , which was studied in tandem. Sediment samples were collected from the outer Thames Estuary during July and November 2001 (see Chapter 2, Sections 2.1.3 and 2.2.3). Analyte concentrations were determined in the dissolved and particulate phases. Single and multi-volume sediment extractions were performed for each analyte, using 2M KCl, to measure recoveries using each method. Finally, natural sediment samples were resuspended in overlying water ($0.4\text{--}0.6\text{ g L}^{-1}$) for 48 hours and the change in dissolved concentrations of each analyte with time was determined under conditions designed to simulate natural sediment resuspension. The results were compared to dissolved concentrations measured through part of a tidal cycle at one of the sampling sites (TE3).

5.2 Results

The results for the different physico-chemical parameters measured and experiments carried out on the sediment samples collected from the Thames Estuary in July and November 2001 are presented in this section. The cores are labelled as TE1J, TE1N...etc. to indicate the month of collection (i.e. July or November) with the numbers indicating the point on the transect where the core was collected.

5.2.1 Seasonal NH_4^+ and MA distributions in Thames Estuary sediment samples.

5.2.1.1 Particle size analysis.

Sediment particle sizes of July samples were determined and the results are shown in the Appendix (Figs. A-1 to A-4). TE1J and TE2J were similar in their particle make up, with sand and silt being the major components. TE3J and TE4J contained higher amounts of silt than clay and sand. Sand was much less abundant in TE3J and TE4J samples (excepting 0-5 mm for TE4J), while the clay content of the sediments increased from less than 10% in cores TE1J and TE2J to 15-17% in TE3J and TE4J.

5.2.1.2 Pore-water NH_4^+ .

Pore-water NH_4^+ was much more abundant than the MAs in July. Concentrations of NH_4^+ generally decreased with depth in each core (Fig. 5-1). The highest concentrations of NH_4^+ for individual cores occurred at 5-10 mm in TE1J (65 μM) and TE4J (27 μM). In TE2J and TE3J, the maximum concentrations occurred at 0-5 mm depth (39 and 54 μM , respectively). The lowest pore-water NH_4^+ concentration (1 μM) occurred in TE4J at 80-100 mm.

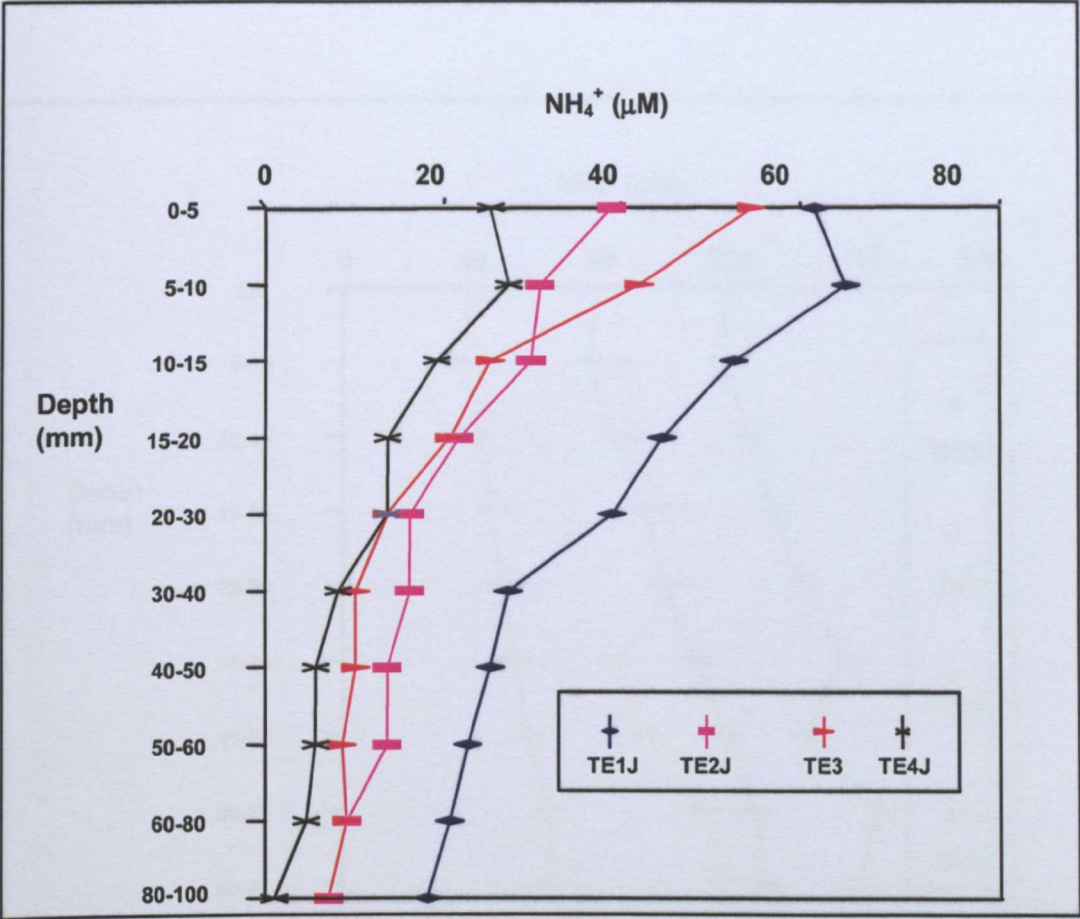


Figure 5-1. Depth profiles of Thames Estuary pore-water NH_4^+ concentrations in July 2001 (TE1J = Core 1).

Pore-water NH_4^+ concentrations in November ranged from 39 μM (TE3N, 0-5 mm) to 170 μM (TE4N, 80-100 mm). Generally, concentrations increased with depth (Fig. 5-2). Average concentrations through the depth profiles were in the following order; TE4N (153 μM) > TE1N (103 μM) > TE2N (95 μM) > TE3N (51 μM). TE1N and TE2N exhibited subsurface minima whereas the minimum concentrations occurred in the surface core sections for TE3N and TE4N.

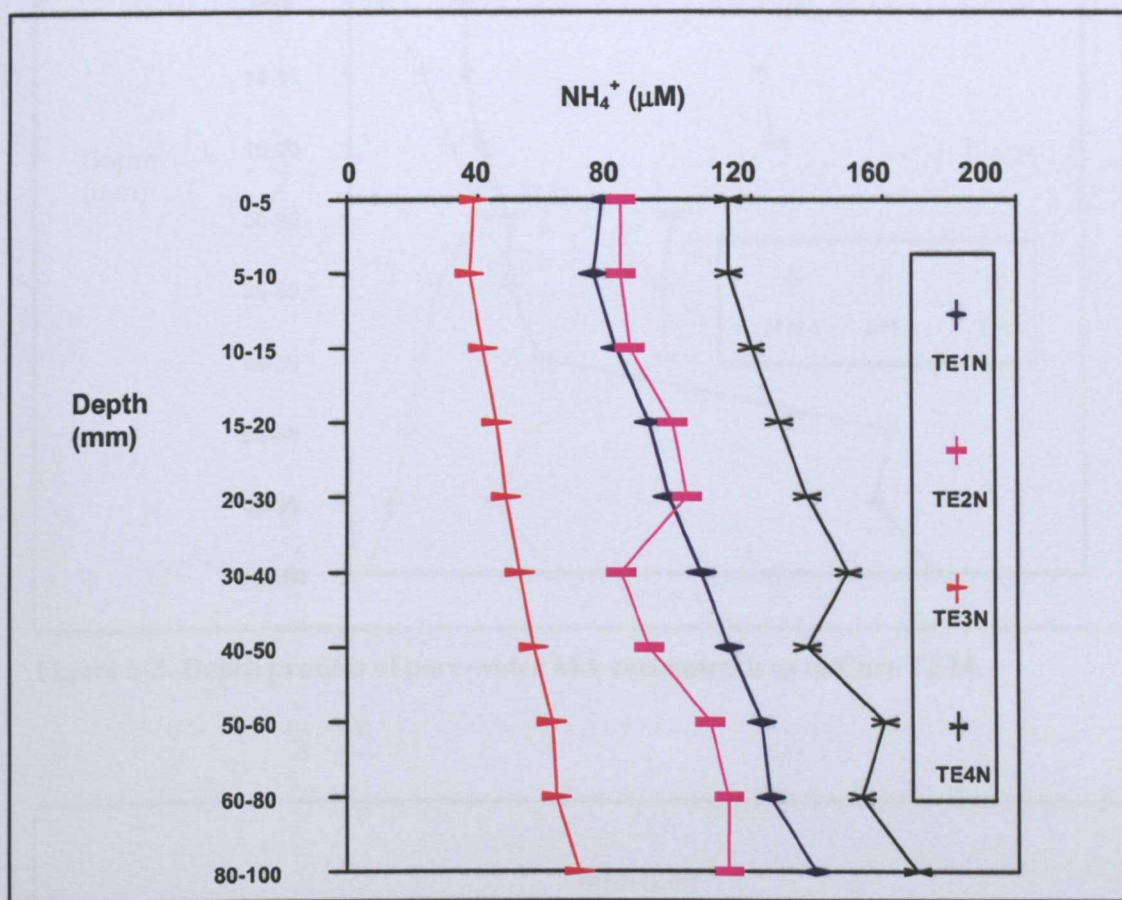


Figure 5-2. Depth profiles of pore-water NH_4^+ concentrations of Thames Estuary samples in November 2001 (TE1N = Core 1).

5.2.1.3 Pore-water MAs

The three MAs were detected in all of the cores that were analysed. Pore-water DMA was the most abundant pore-water MA above 50 mm in July, while MMA became more abundant at depth except for TE3J (Figs. 5-3 to 5-6). TMA was the least abundant MA in all cores. TE3J had the highest total average pore-water MA concentration ($1.17 \mu\text{M}$) (Fig. 5-5) whereas the lowest was found in TE1J ($0.45 \mu\text{M}$) (Fig. 5-3). A decrease in DMA in TE1J was matched by an increase in MMA between 40 and 100 mm. The same pattern was repeated in TE2J and TE4J whereas there was no evidence of such a relationship in TE3J.

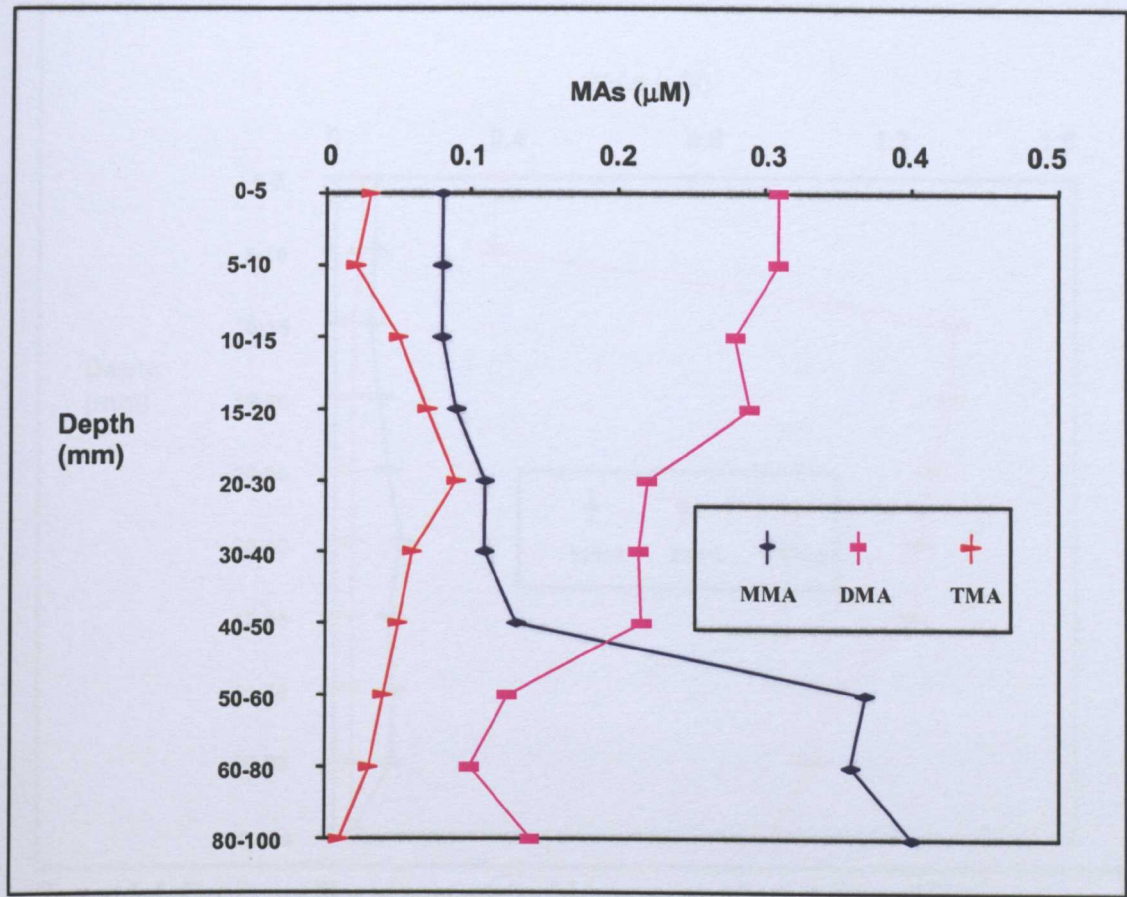


Figure 5-3. Depth profiles of pore-water MA concentrations in Core TE1J.

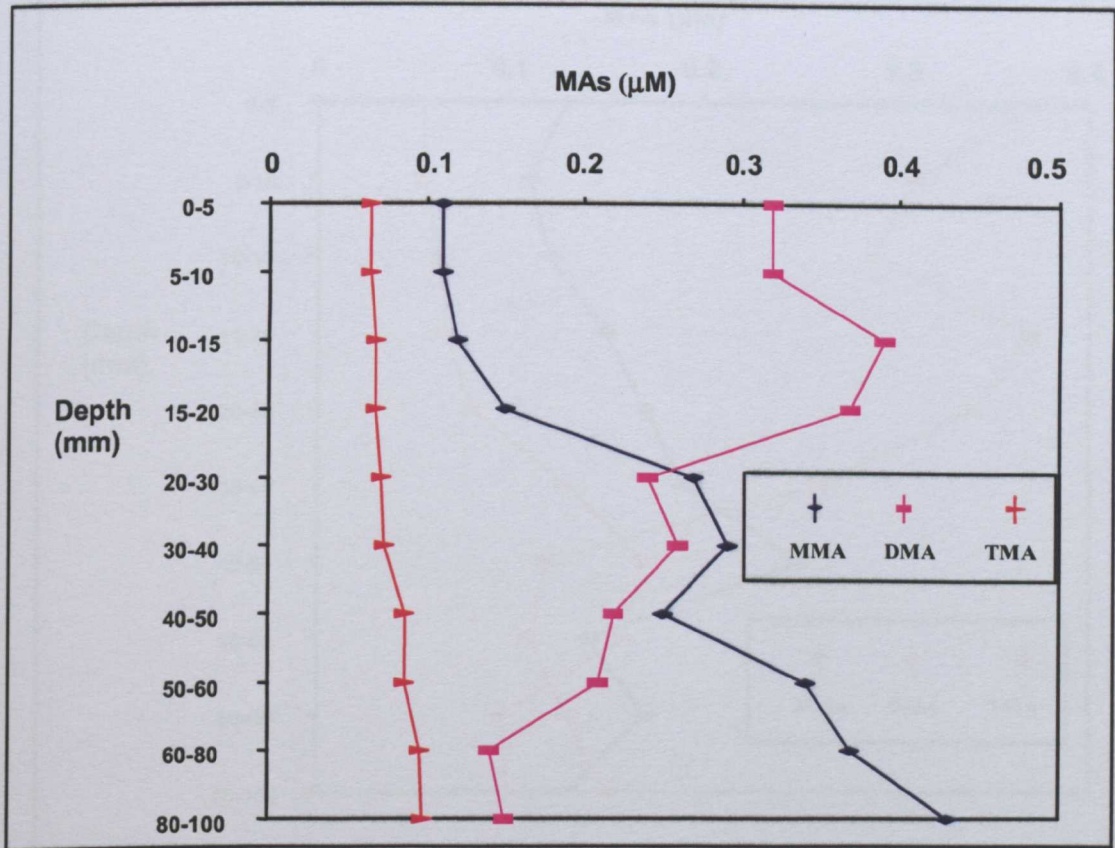


Figure 5-4. Depth profiles of pore-water MA concentrations in Core TE2J.

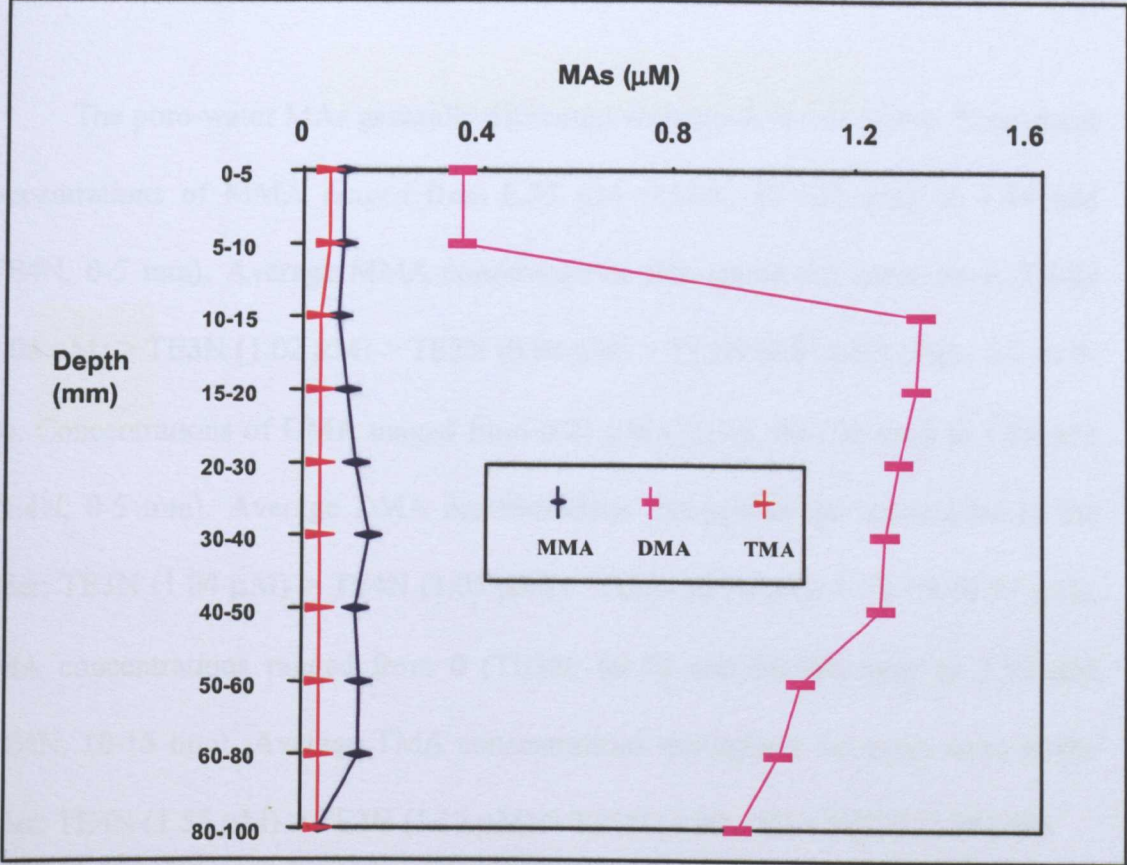


Figure 5-5. Depth profiles of pore-water MA concentrations in Core TE3J.

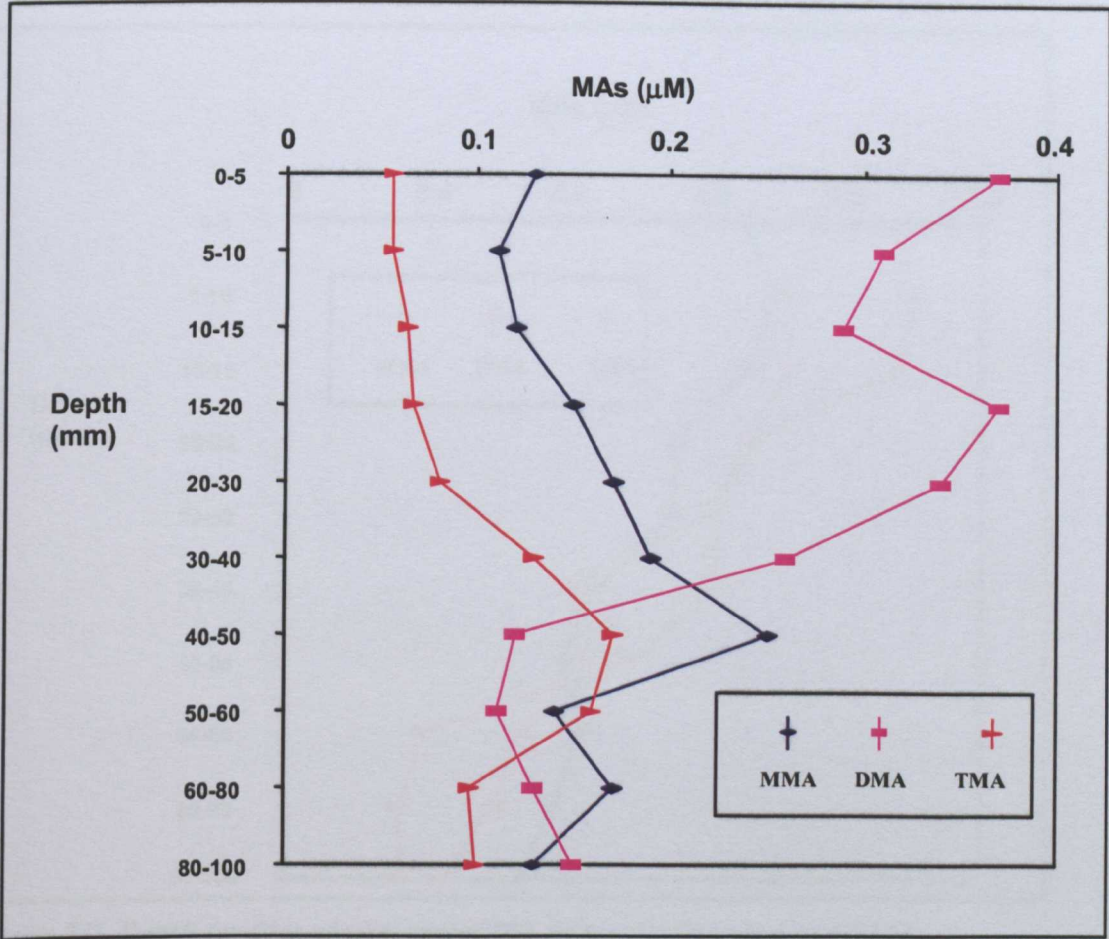


Figure 5-6. Depth profiles of pore-water MA concentrations in Core TE4J.

The pore-water MAs generally decreased with depth in November. Pore-water concentrations of MMA ranged from 0.33 μM (TE3N, 80-100 mm) to 1.44 μM (TE4N, 0-5 mm). Average MMA concentrations throughout the cores were; TE4N (1.08 μM) > TE3N (1.02 μM) > TE2N (0.94 μM) > TE1N (0.81 μM) (Figs. 5-7 to 5-10). Concentrations of DMA ranged from 0.22 μM (TE3N, 80-100 mm) to 1.85 μM (TE4N, 0-5 mm). Average DMA concentrations throughout the cores were in the order; TE3N (1.04 μM) > TE4N (1.03 μM) > TE2N (0.94 μM) > TE1N (0.87 μM). TMA concentrations ranged from 0 (TE3N; 60-80 and 80-100 mm) to 2.33 μM (TE4N, 10-15 mm). Average TMA concentrations throughout the cores were in the order; TE4N (1.55 μM) > TE3N (1.12 μM) > TE1N (0.99 μM) > TE2N (0.80 μM).

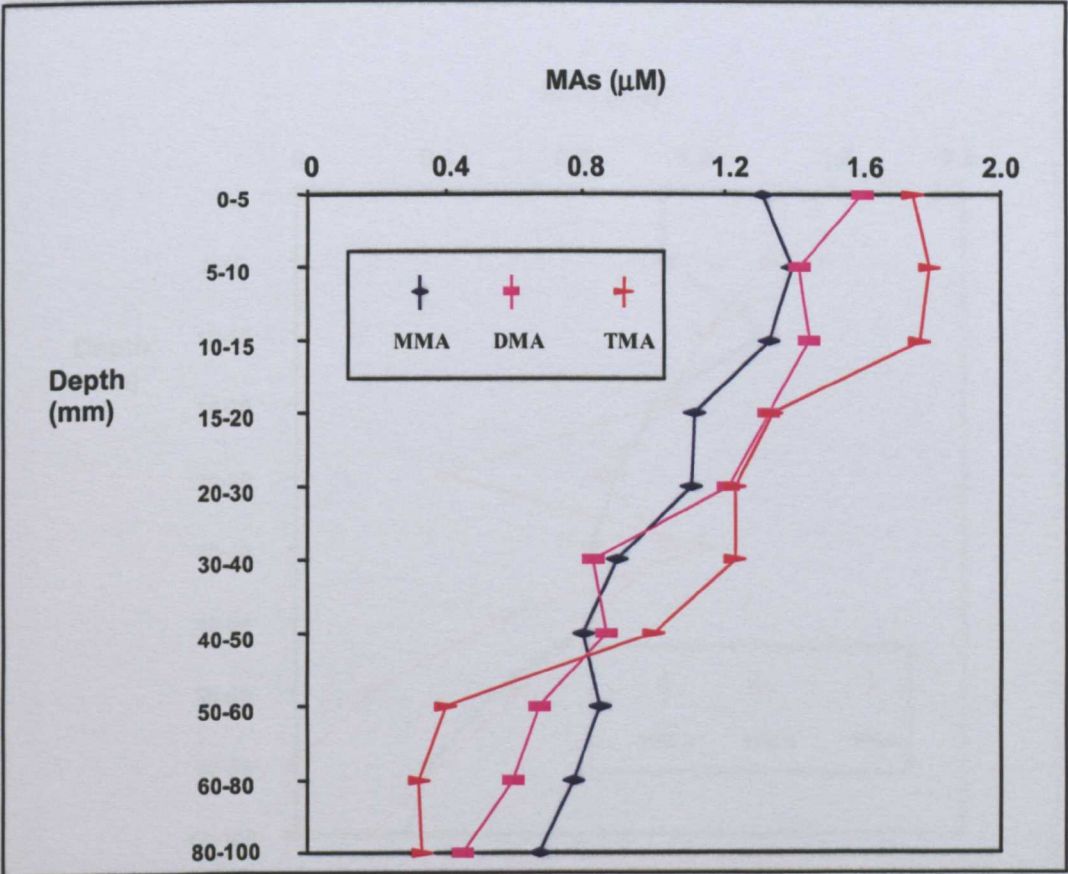


Figure 5-7. Depth profiles of pore-water MA concentrations in Core TE1N.

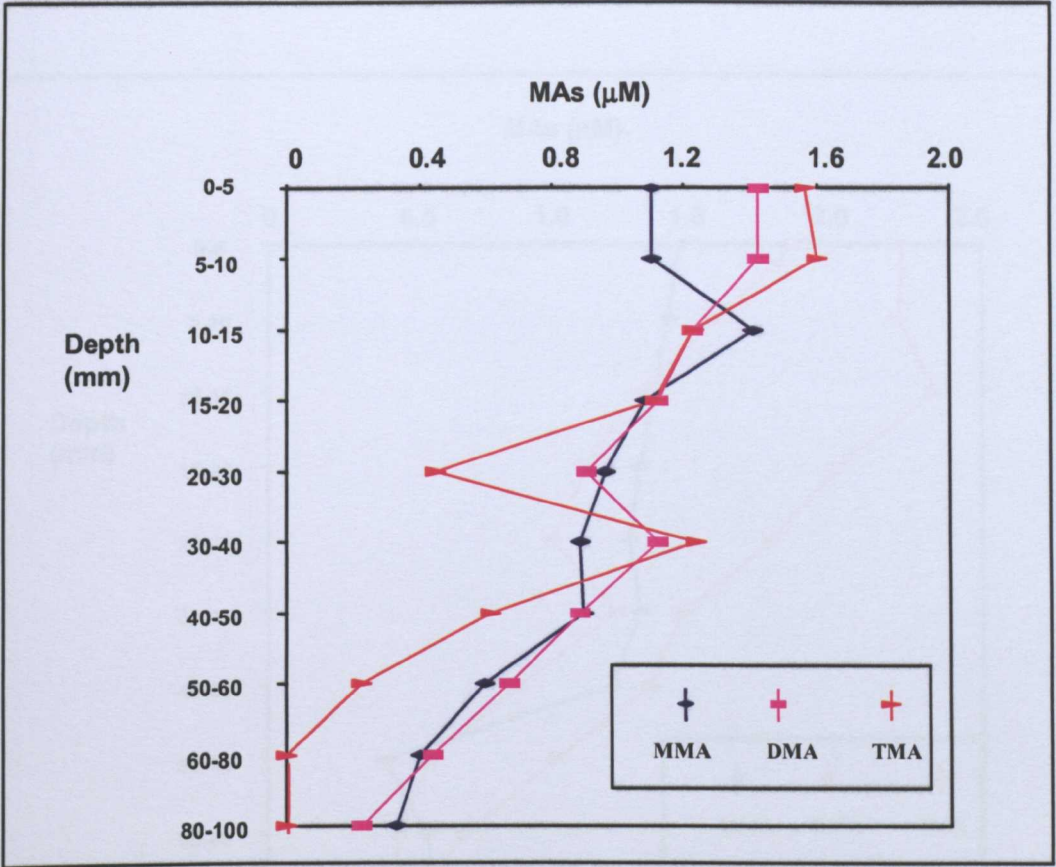


Figure 5-8. Depth profiles of pore-water MA concentrations in Core TE2N.

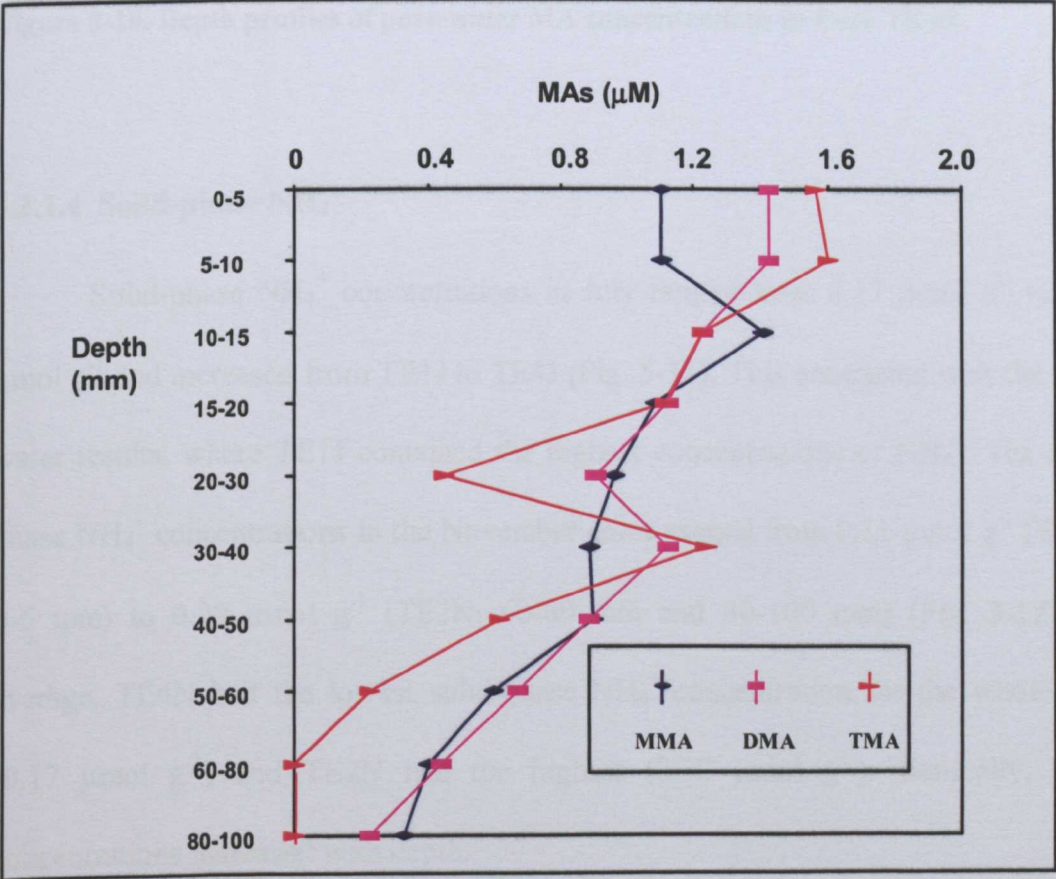


Figure 5-9. Depth profiles of pore-water MA concentrations in Core TE3N.

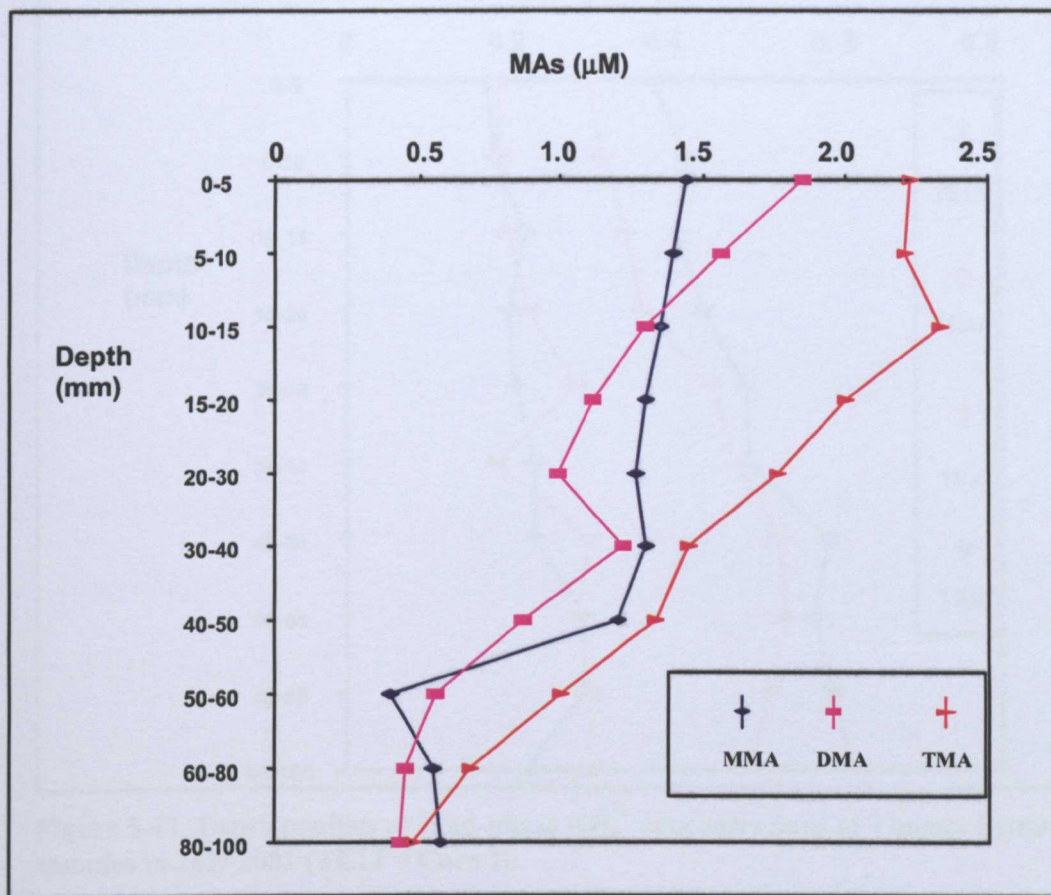


Figure 5-10. Depth profiles of pore-water MA concentrations in Core TE4N.

5.2.1.4 Solid-phase NH_4^+

Solid-phase NH_4^+ concentrations in July ranged from $0.17 \mu\text{mol g}^{-1}$ to $0.62 \mu\text{mol g}^{-1}$ and increased from TE1J to TE4J (Fig. 5-11). This contrasted with the pore-water results, where TE1J contained the highest concentrations of NH_4^+ . The solid-phase NH_4^+ concentrations in the November cores ranged from $0.11 \mu\text{mol g}^{-1}$ (TE4N, 0-5 mm) to $0.30 \mu\text{mol g}^{-1}$ (TE2N, 60-80 mm and 80-100 mm) (Fig. 5-12). On average, TE4N had the lowest solid-phase NH_4^+ concentration for the whole core ($0.17 \mu\text{mol g}^{-1}$) and TE2N had the highest ($0.30 \mu\text{mol g}^{-1}$). Generally, NH_4^+ concentrations increased with depth.

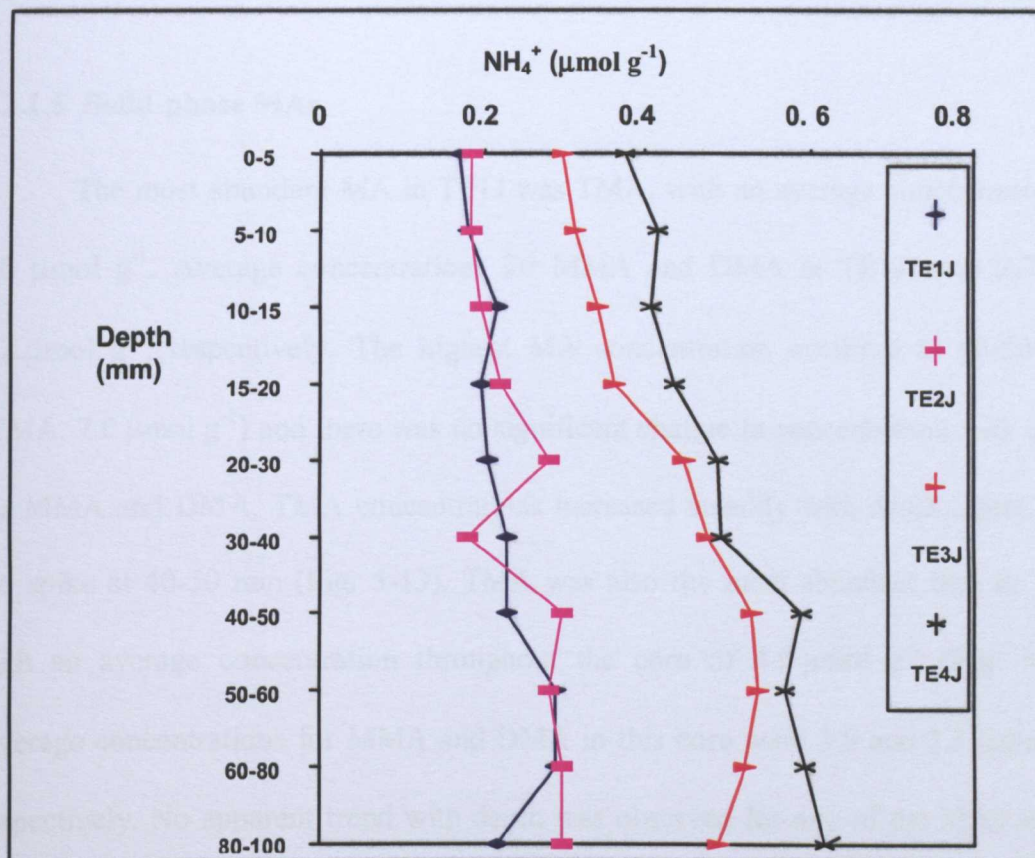


Figure 5-11. Depth profiles of solid-phase NH_4^+ concentrations of Thames Estuary samples in July 2001 (TE1J = Core 1).

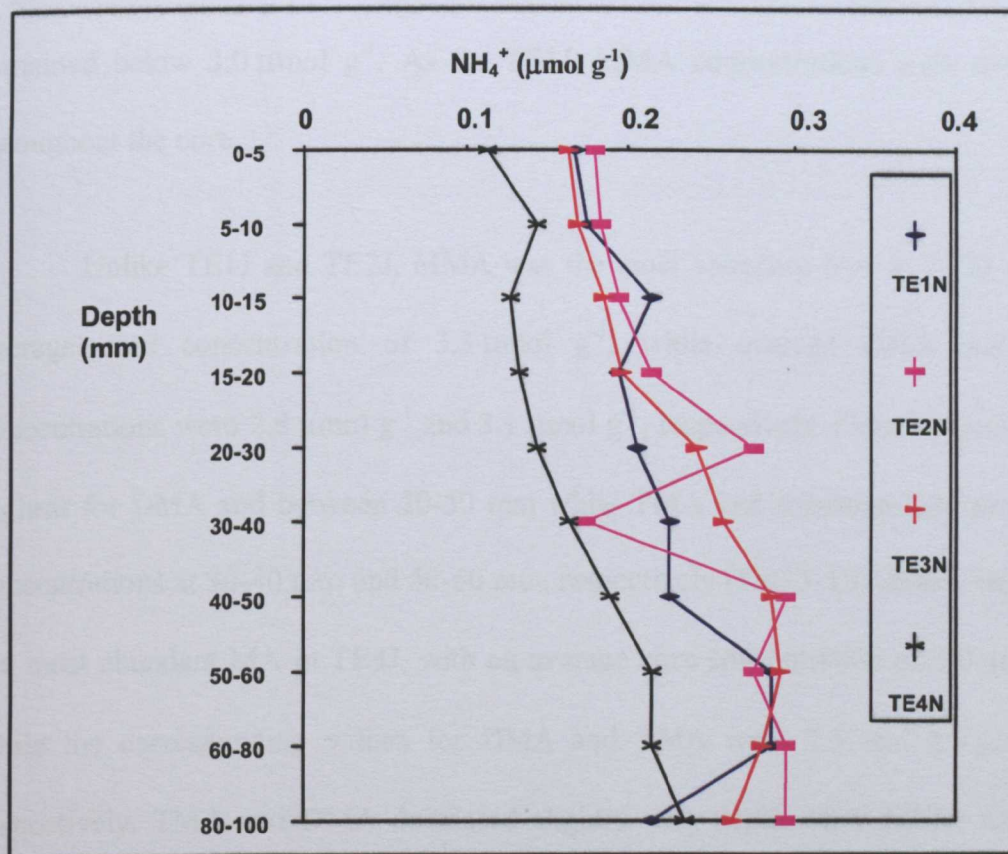


Figure 5-12. Depth profiles of solid-phase NH_4^+ concentration of Thames Estuary samples in November 2001 (TE1N = Core 1).

5.2.1.5 Solid-phase MAs

The most abundant MA in TE1J was TMA, with an average concentration of $4.0 \mu\text{mol g}^{-1}$. Average concentrations for MMA and DMA in TE1J were 2.7 and $2.2 \mu\text{mol g}^{-1}$, respectively. The highest MA concentration occurred at 40-50 mm (TMA, $7.0 \mu\text{mol g}^{-1}$) and there was no significant change in concentration with depth for MMA and DMA. TMA concentrations increased steadily with depth, apart from the spike at 40-50 mm (Fig. 5-13). TMA was also the most abundant MA in TE2J with an average concentration throughout the core of $4.0 \mu\text{mol g}^{-1}$ (Fig. 5-14). Average concentrations for MMA and DMA in this core were 3.0 and $2.3 \mu\text{mol g}^{-1}$, respectively. No apparent trend with depth was observed for any of the MAs except that TMA concentrations increased above $4.0 \mu\text{mol g}^{-1}$ below 50 mm depth while MMA concentrations increased to $5.1 \mu\text{mol g}^{-1}$ between 20-40 mm depth and then remained below $3.0 \mu\text{mol g}^{-1}$. As for TE1J, MMA concentrations were consistent throughout the core.

Unlike TE1J and TE2J, MMA was the most abundant MA in TE3J with an average core concentration of $3.3 \mu\text{mol g}^{-1}$, while average DMA and TMA concentrations were $2.8 \mu\text{mol g}^{-1}$ and $3.1 \mu\text{mol g}^{-1}$, respectively. Concentrations were highest for DMA and between 20-50 mm while TMA had minimum and maximum concentrations at 30-40 mm and 40-50 mm, respectively (Fig. 5-15). MMA was again the most abundant MA in TE4J, with an average core concentration of $3.6 \mu\text{mol g}^{-1}$, while the corresponding values for DMA and TMA were 2.5 and $2.8 \mu\text{mol g}^{-1}$, respectively. TMA and DMA decreased slightly with depth while MMA increased with depth to a maximum at 40-50 mm and then decreased to concentrations observed at the surface (Fig. 5-16).

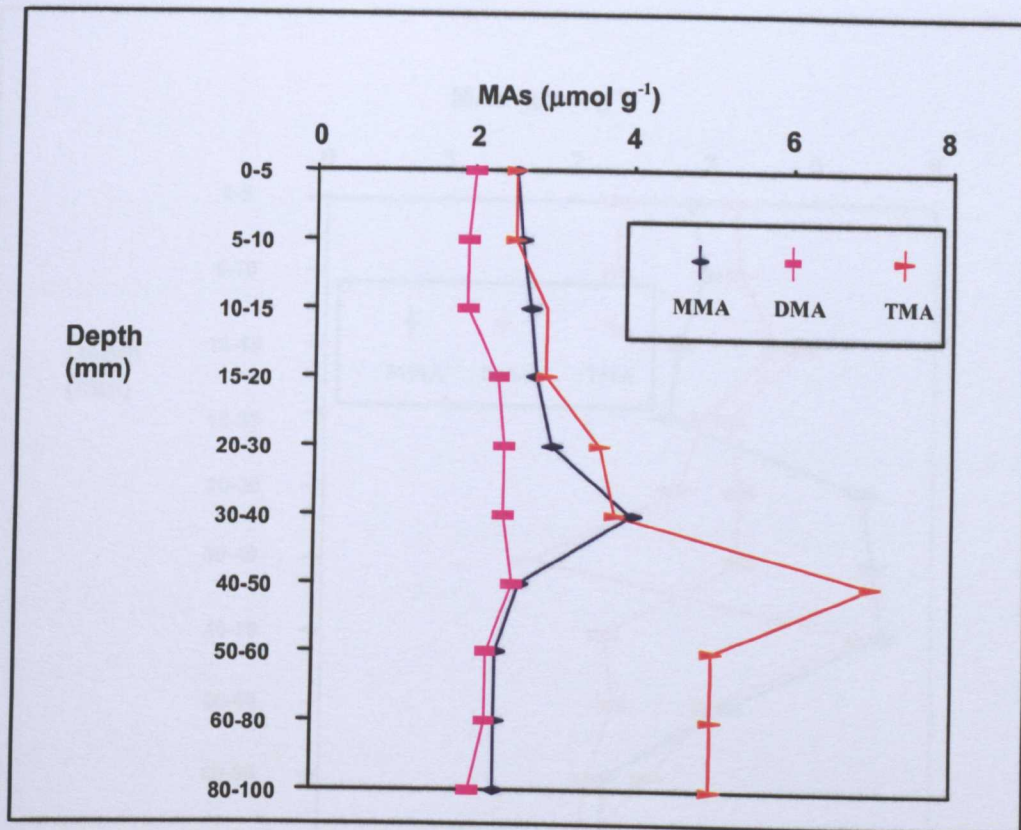


Figure 5-13. Depth profiles of solid-phase MA concentrations in Core TE1J.

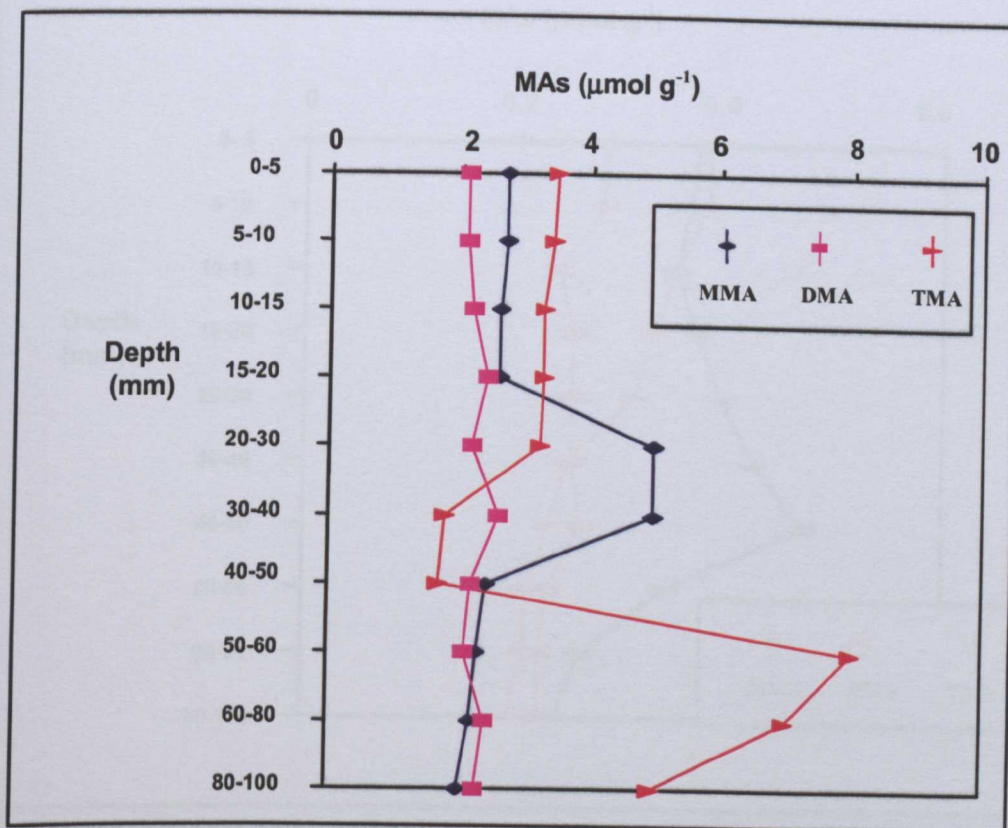


Figure 5-14. Depth profiles of solid-phase MA concentrations in Core TE2J.

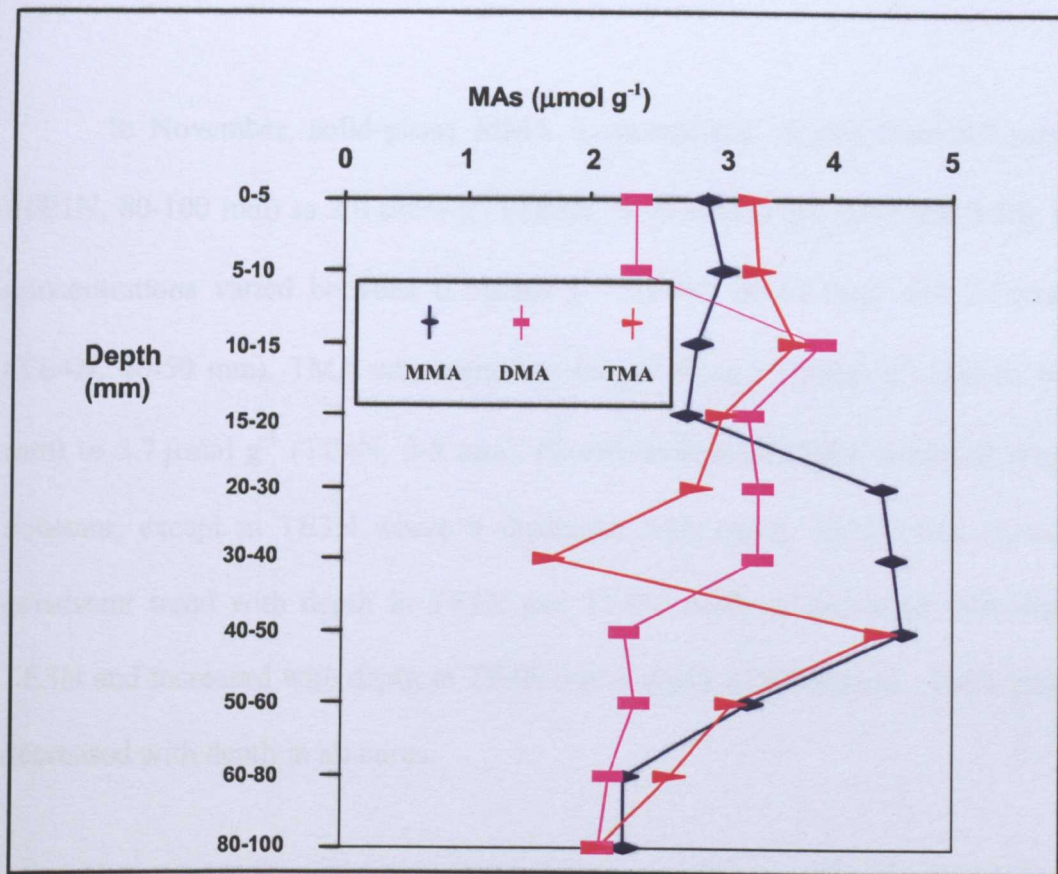


Figure 5-15. Depth profiles of solid-phase MA concentrations in Core TE3J.

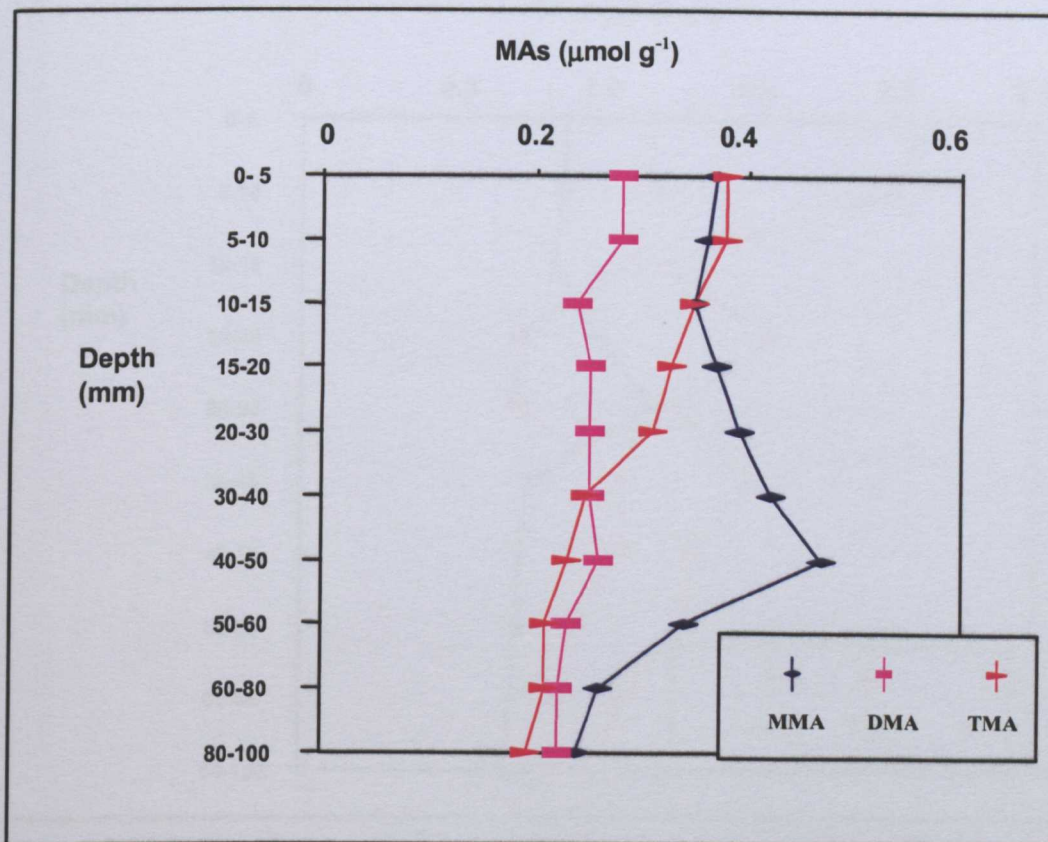


Figure 5-16. Depth profiles of solid-phase MA concentrations in Core TE4J.

In November, solid-phase MMA concentrations ranged from 0.7 $\mu\text{mol g}^{-1}$ (TE1N, 80-100 mm) to 2.0 $\mu\text{mol g}^{-1}$ (TE3N, 5-10 mm) (Figs. 5-17 and 5-20). DMA concentrations varied between 0.7 $\mu\text{mol g}^{-1}$ (TE1N, 20-30 mm) and 2.7 $\mu\text{mol g}^{-1}$ (TE4N, 40-50 mm). TMA concentrations ranged from 1.1 $\mu\text{mol g}^{-1}$ (TE1N, 80-100 mm) to 3.7 $\mu\text{mol g}^{-1}$ (TE4N, 0-5 mm). Concentrations of MMA remained relatively constant, except in TE3N where it decreased with depth while DMA showed no consistent trend with depth in TE1N and TE2N, while it decreased with depth in TE3N and increased with depth in TE4N (up to depth of 40-50mm). TMA generally decreased with depth in all cores.

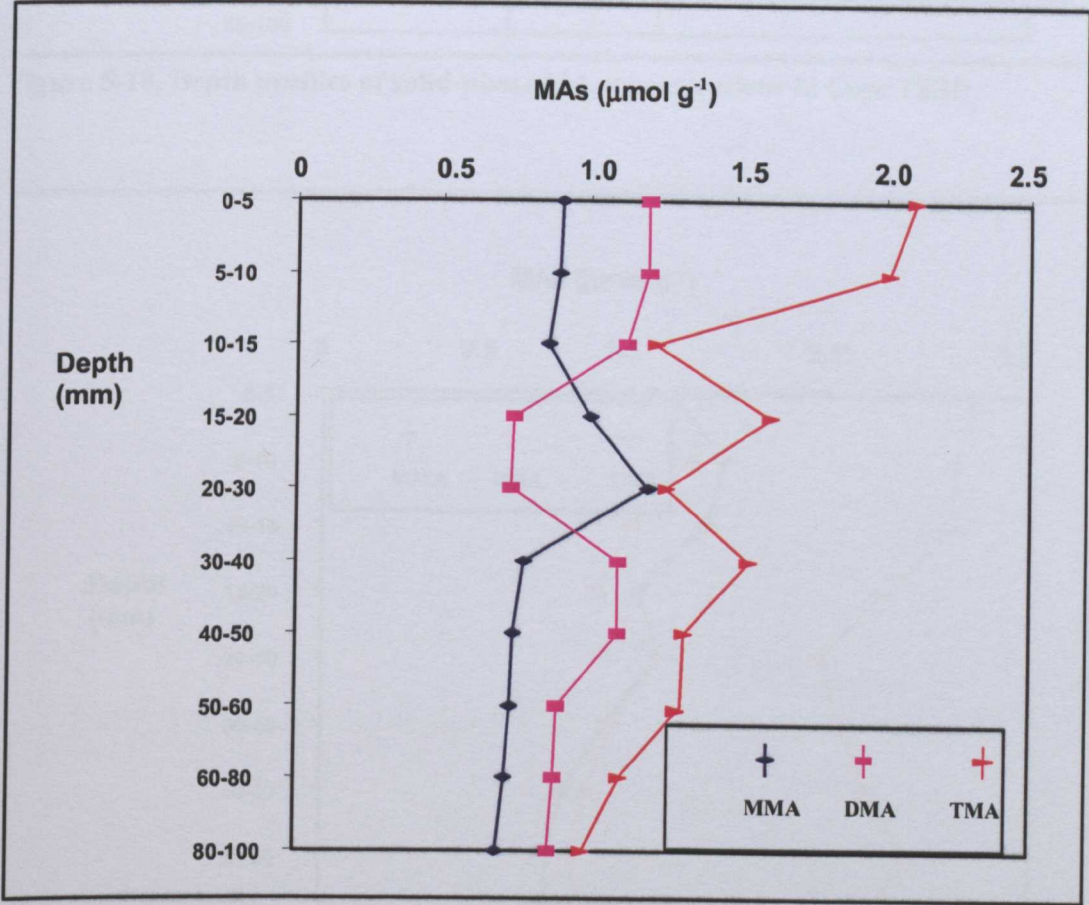


Figure 5-17 Depth profiles of solid-phase MA concentrations in Core TE1N.

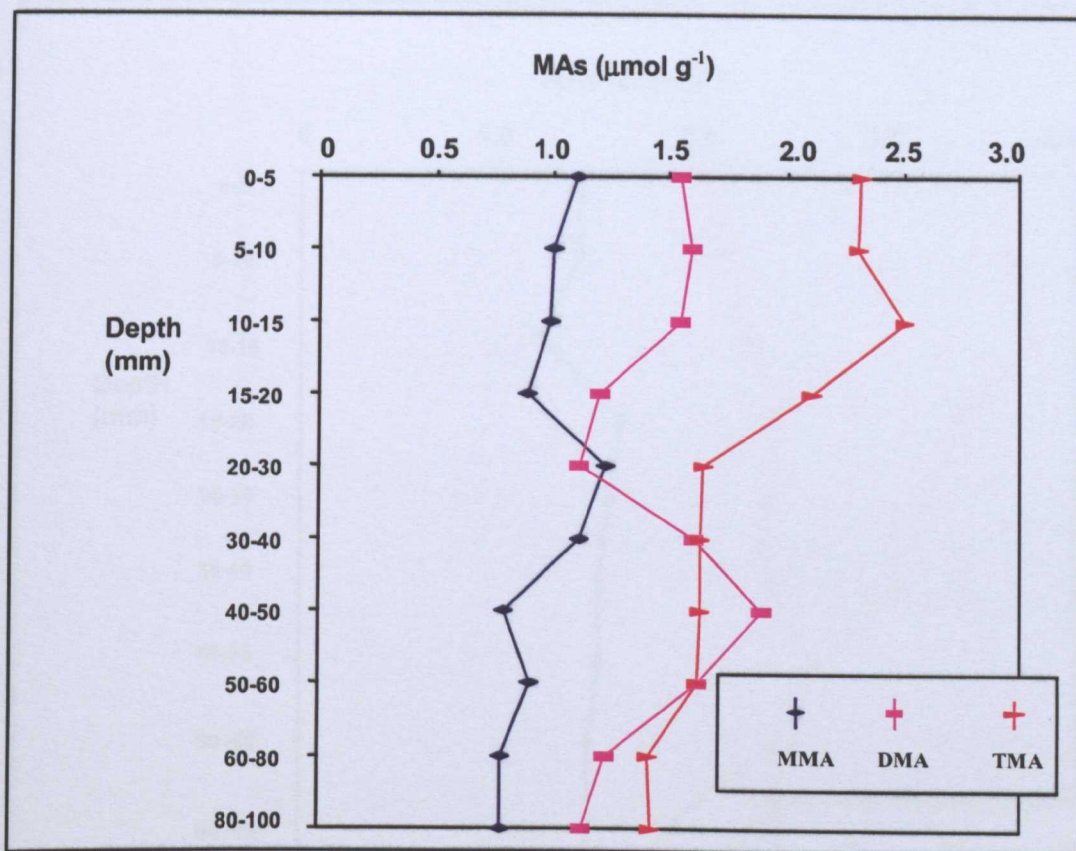


Figure 5-18. Depth profiles of solid-phase MA concentrations in Core TE2N.

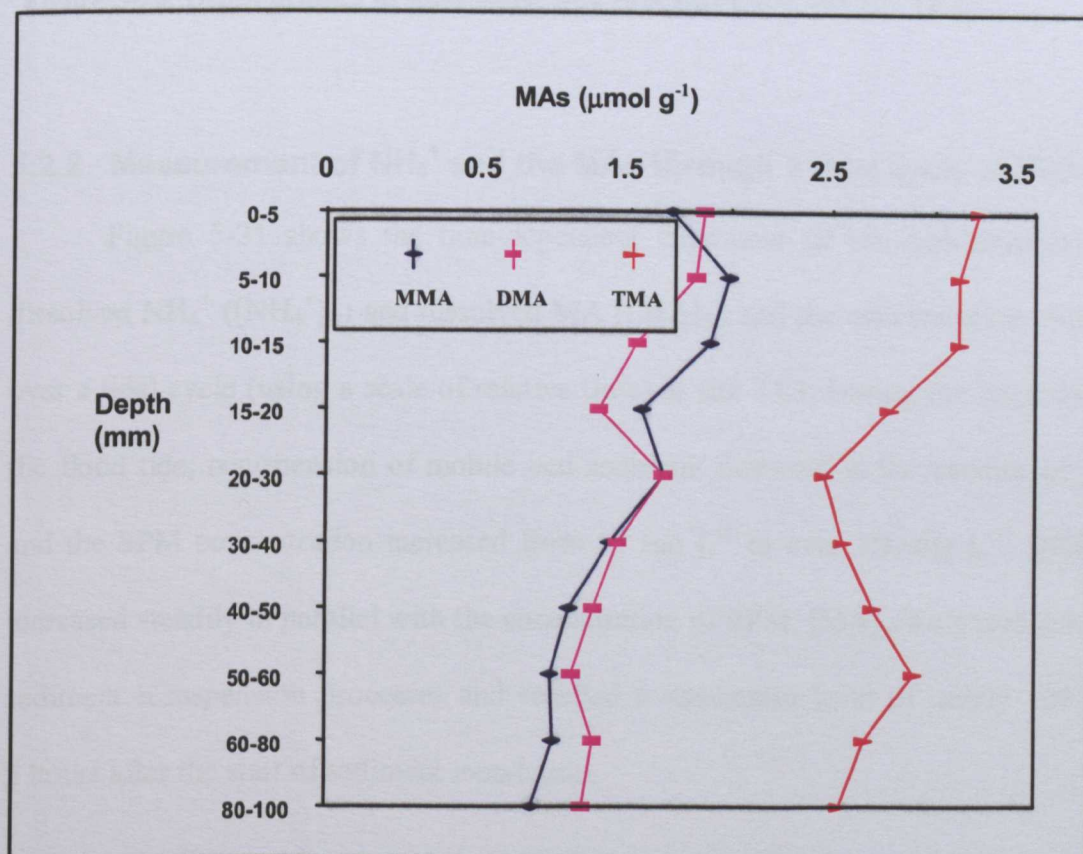


Figure 5-19. Depth profiles of solid-phase MA concentrations in Core TE3N.

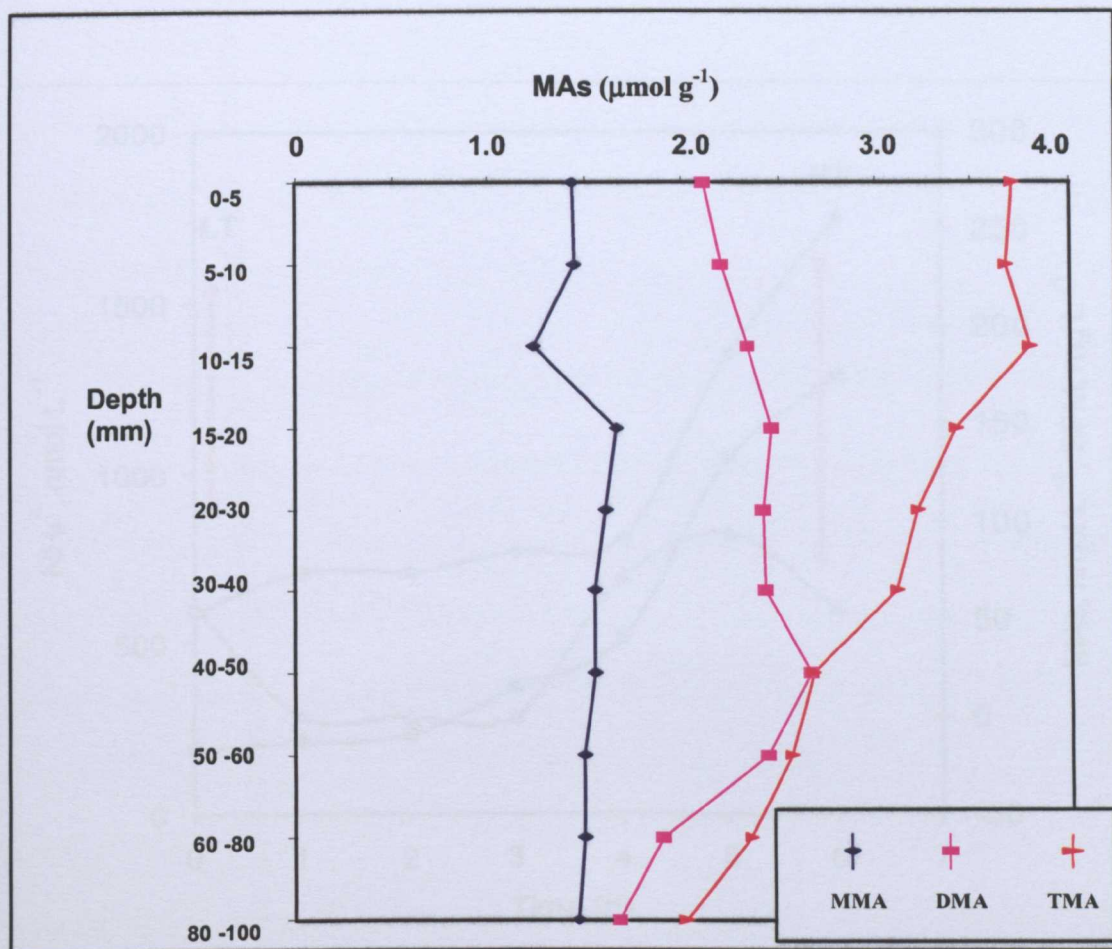
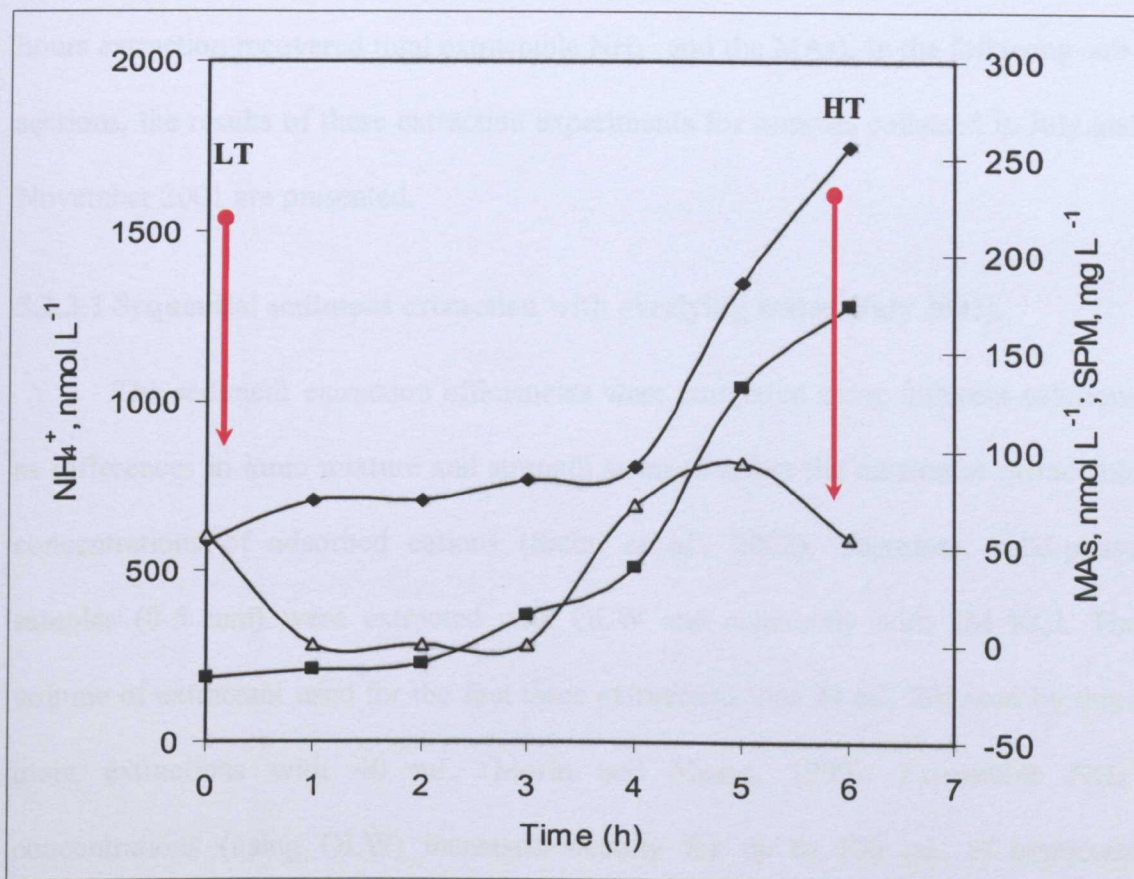


Figure 5-20. Depth profiles of solid-phase MA concentrations in Core TE4N.

5.2.2 Measurement of NH_4^+ and the MAs through a tidal cycle at TE3.

Figure 5-21 shows the time-dependent behaviour of the concentrations of dissolved NH_4^+ ($[\text{NH}_4^+]_D$) and dissolved MA ($[\text{MA}]_D$) and the concentration of SPM over a tidal cycle (using a scale of relative time) at site TE3. During the incursion of the flood tide, resuspension of mobile bed sediment occurred in the vicinity of TE3 and the SPM concentration increased from 55 mg L^{-1} to over 250 mg L^{-1} . $[\text{NH}_4^+]_D$ increased steadily in parallel with the concentration of SPM. $[\text{MA}]_D$ increased prior to sediment resuspension processes and reached a maximum level of nearly 100 nM 5 hours after the start of sediment inundation.



◆-SPM, ■-NH₄⁺, △-total MAs

Figure 5-21. Concentrations of SPM, dissolved NH₄⁺ and total dissolved MAs over part of a tidal cycle at site TE3 in March 2002 (LT = Low Tide, HT = High Tide).

5.2.3 Measurements of exchangeable NH₄⁺ and the MAs.

Several methods have been used previously to determine potential fluxes of N species, such as NH₄⁺, from the particulate phase. The commonly used method to estimate the solid-phase NH₄⁺ fraction in sediments is a single step extraction at 1:20 (w/v) using 2M KCl. However, this method has been found to underestimate the total extractable NH₄⁺ (Liama, 1992; Morin and Morse, 1999). Therefore, in this study, sequential extraction experiments were carried out to achieve maximum extractable concentrations of analytes. Extraction of NH₄⁺ and the MAs from different sediment depth ranges for different lengths of time indicated that six sequential steps, each carried out for 24 hours, were sufficient to extract 99.8% and 99.6% of the NH₄⁺ and

MAAs, respectively from the Thames Estuary sediment samples (Assuming the 48 hours extraction recovered total extractable NH_4^+ and the MAAs). In the following subsections, the results of these extraction experiments for samples collected in July and November 2001 are presented.

5.2.3.1 Sequential sediment extraction with overlying water (July 2001).

The sediment extraction efficiencies were compared using different solutions as differences in ionic mixture and strength seem to affect the maximum extractable concentrations of adsorbed cations (Salbu *et al.*, 2002). Therefore, solid-phase samples (0-5 mm) were extracted with OLW and separately with 2M KCl. The volume of extractant used for the first three extractions was 20 mL followed by three more extractions with 40 mL (Morin and Mores, 1999). Extractable NH_4^+ concentrations (using OLW) increased steadily for up to 100 mL of extractant followed by small increases up to 140 mL with analyte concentrations changing little from 140-180 mL (Fig. 5-22). Cumulative NH_4^+ concentrations were lowest for TE4J ($3.07 \mu\text{mol g}^{-1}$) and highest for TE2J ($4.14 \mu\text{mol g}^{-1}$). Most of the MAAs (> 50%) were released into solution during the first three extractions (Fig. 5-23). Cumulative extractable concentrations of MAAs in TE1J rapidly increased during the first two extractions and remained unchanged for the last three extractions. TMA and DMA had very similar maximum extractable concentrations (9.13 and $9.26 \mu\text{mol g}^{-1}$), which were larger than MMA ($8.03 \mu\text{mol g}^{-1}$).

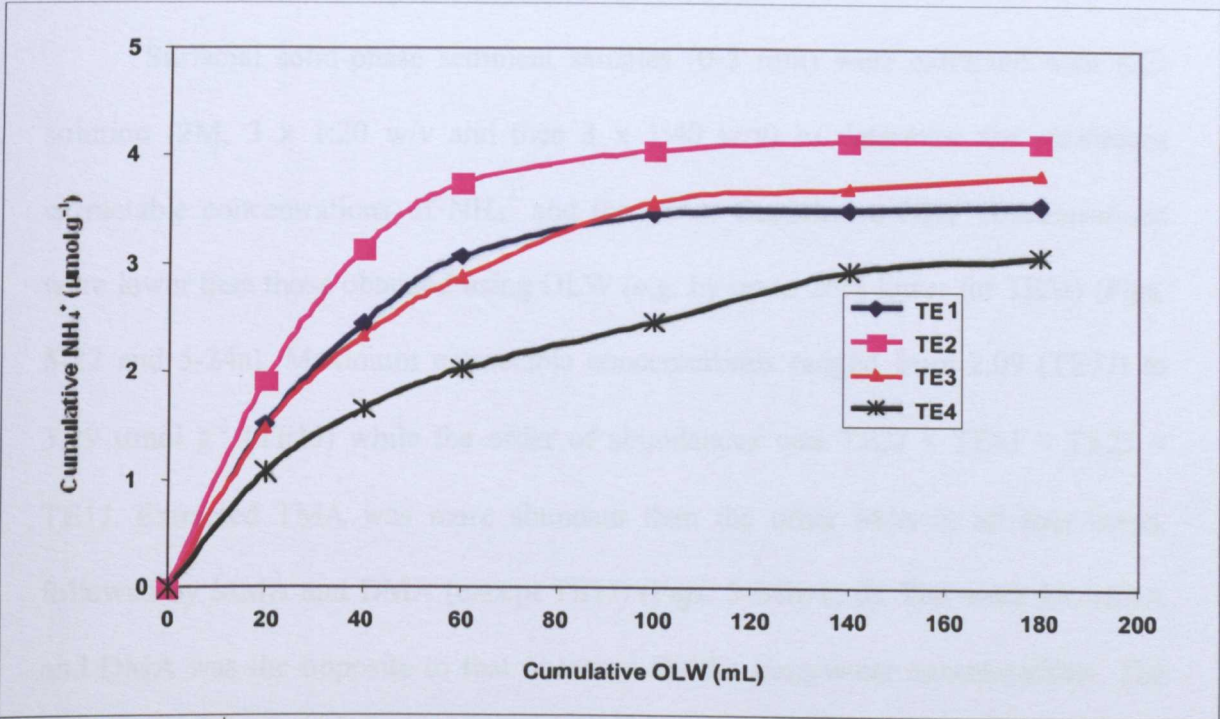


Figure 5-22. NH_4^+ concentrations in Thames Estuary sediments at 0-5 mm depth extracted with multiple volumes of OLW (July 2001).

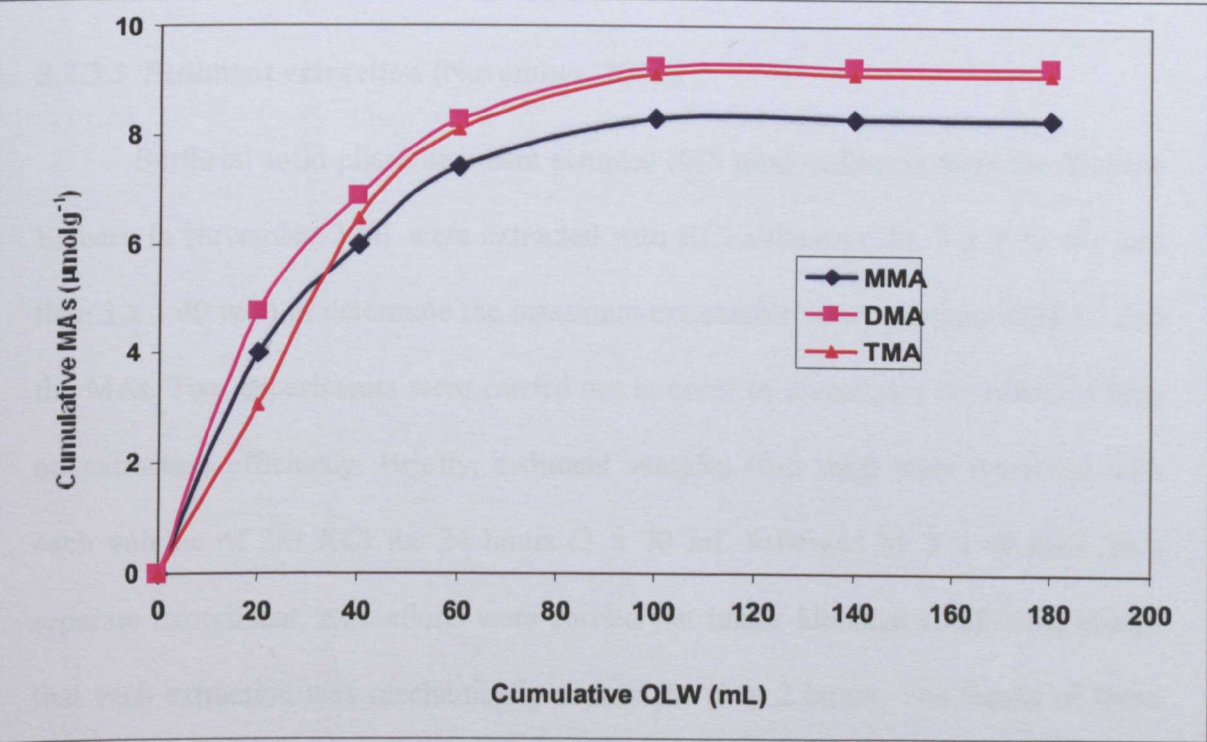


Figure 5-23. MA concentrations in Thames Estuary sediments at 0-5 mm depth extracted with multiple volumes of OLW (TE1J).

5.2.3.2 Sediment extraction with 2M KCl (July 2001).

Surfacial solid-phase sediment samples (0-5 mm) were extracted with KCl solution (2M, 3 x 1:20 w/v and then 3 x 1:40 w/v) to determine the maximum extractable concentrations of NH_4^+ and the MAs. Cumulative NH_4^+ concentrations were lower than those obtained using OLW (e.g. by up to 26% lower for TE3J) (Figs. 5-22 and 5-24a). Maximum extractable concentrations ranged from 2.09 (TE3J) to 3.29 $\mu\text{mol g}^{-1}$ (TE1J) while the order of abundances was TE3J < TE4J < TE2J < TE1J. Extracted TMA was more abundant than the other MAs in all four cores, followed by MMA and DMA (except TE1J) (Figs. 5-24b, c, d). The order for MMA and DMA was the opposite to that observed for the pore-water concentrations. The highest total extractable MAs were found in TE4J (26.5 $\mu\text{mol g}^{-1}$) and the lowest in TE3J (11.8 $\mu\text{mol g}^{-1}$).

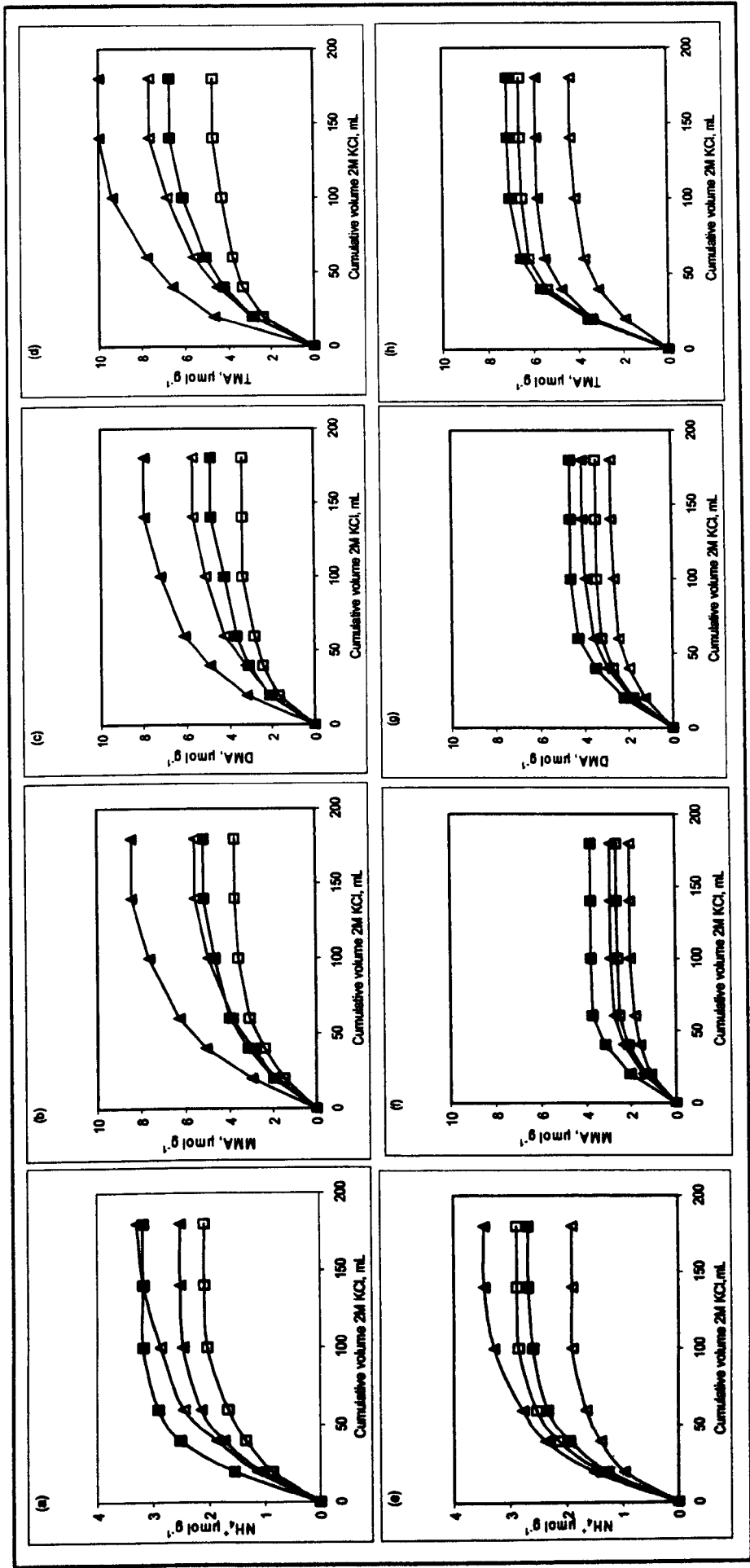
5.2.3.3 Sediment extraction (November, 2001).

Surfacial solid-phase sediment samples (0-5 mm) collected from the Thames Estuary in November 2001 were extracted with KCl solution (2M, 3 x 1:20 w/v and then 3 x 1:40 w/v) to determine the maximum extractable concentrations of NH_4^+ and the MAs. Two experiments were carried out in order to investigate the effect of time on extraction efficiency. Briefly, sediment samples (0-5 mm) were extracted with each volume of 2M KCl for 24 hours (3 x 20 mL followed by 3 x 40 mL). In a separate experiment, extractions were carried out under identical conditions, except that each extraction was mechanically shaken for only 2 hours. The results of these experiments are presented below.

a) Surfacial sediments (24 hours extraction).

Cumulative extractable NH_4^+ concentrations increased with extractant volume in all four cores up to 100 mL cumulative volume of extractant (Fig. 5-24e). For TE1N and TE3N, cumulative NH_4^+ did not increase in subsequent extractions while for TE2N and TE4N small increases were observed up to 140 mL. The highest extractable NH_4^+ concentration was found in TE4N ($3.48 \mu\text{mol g}^{-1}$) and the lowest in TE1N ($1.91 \mu\text{mol g}^{-1}$). Maximum extractable NH_4^+ concentrations for TE2N and TE3N were $2.69 \mu\text{mol g}^{-1}$, and $2.89 \mu\text{mol g}^{-1}$, respectively.

Cumulative extractable MAs showed a slightly different pattern to NH_4^+ (Figs. 5-24; f, g, h). Concentrations increased for all cores up to 60 mL cumulative volume of extractant. For TE1N and TE2N, maximum cumulative concentrations for MMA were reached by the 4th extraction (i.e. 100 mL); $2.05 \mu\text{mol g}^{-1}$ and $3.81 \mu\text{mol g}^{-1}$, respectively. For TE3N and TE4N, the maximum cumulative MMA concentrations occurred at 140 mL ($2.65 \mu\text{mol g}^{-1}$ and $2.93 \mu\text{mol g}^{-1}$, respectively). For all cores maximum cumulative DMA and TMA concentrations were reached after the 5th extraction (140 mL). The highest extractable DMA concentration was found in TE2N ($4.66 \mu\text{mol g}^{-1}$) and the lowest in TE1N ($2.81 \mu\text{mol g}^{-1}$). The highest extractable TMA concentration was in TE2N ($7.15 \mu\text{mol g}^{-1}$) and the lowest was in TE1N ($4.37 \mu\text{mol g}^{-1}$).



▲ - TE1; ■ - TE2; □ - TE3; ▲ - TE4

Figure 5-24. Concentrations of NH_4^+ and MAs in Thames Estuary sediments at 0-5 mm depth using multiple volumes of 2M KCl; July 2001 (a) NH_4^+ , (b) MMA, (c) DMA and (d) TMA and November 2001 (e) NH_4^+ , (f) MMA, (g) DMA and (h) TMA.

b) All core sections (2 hours agitation).

Understanding the behaviour of total MA concentrations with depth reveals whether the total available MA pool in deeper sediments is controlled by different physico-chemical parameters compared to the oxic top layer. To estimate the total available MA pool, the subsurface core sections needed to be extracted in the same way as the surfacial sediments. However, due to the time consuming processes of sequential extraction and the number of samples involved it was desirable to minimise the experimental time without compromising the outcome of the experiment. Therefore, it was decided to extract each core section for 2 hours instead of 24 hours. However, using the surfacial sediments extracted for 24 hours and 2 hours, a relative recovery factor was calculated for different time periods for NH_4^+ and the MAs using Equation 5-1 to compensate for the shorter period of extraction time.

$$R = [\text{Cumulative extractable } \text{NH}_4^+, \text{MA}]_{24 \text{ h}} / [\text{Cumulative extractable } \text{NH}_4^+, \text{MA}]_{2 \text{ h}}.$$

Equation 5-1.

Where, R = recovery factor.

All surfacial sections of the November sediment samples (0-5 mm) were extracted using 2M KCl (2 hours) and NH_4^+ and MA concentrations determined. The maximum extractable NH_4^+ concentration was reached after the 5th extraction (140 mL) for all cores. The highest concentration was found in TE4N ($2.85 \mu\text{mol g}^{-1}$) and the lowest in TE1N ($1.87 \mu\text{mol g}^{-1}$). The maximum extractable NH_4^+ concentrations in TE2N and TE3N were $2.22 \mu\text{mol g}^{-1}$ and $2.54 \mu\text{mol g}^{-1}$, respectively (Fig. 5-25). The results show that time did affect the maximum extractable concentrations as all extractions using a 2 hours agitation period resulted in reduced amounts of total extractable NH_4^+ and MA concentrations compared to 24 hour extractions.

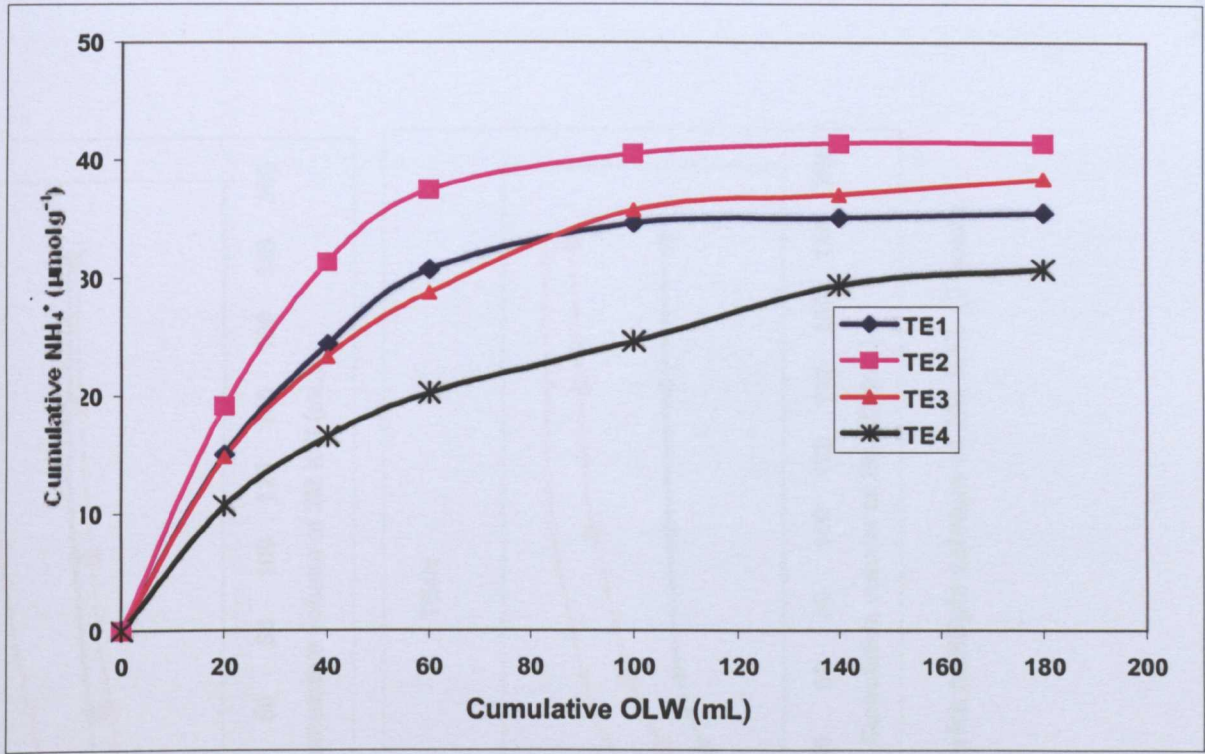


Figure 5-25. NH_4^+ concentrations in Thames Estuary sediments at 0-5 mm depth using multiple volumes of 2M KCl (2 hours).

For TE1N, the maximum extractable MMA ($3.02 \mu\text{mol g}^{-1}$) and DMA ($3.66 \mu\text{mol g}^{-1}$) concentrations were reached after the 5th extraction (140 mL) and TMA reached its peak concentration after the 6th extractions ($6.95 \mu\text{mol g}^{-1}$ Fig. 5-26). For TE2N, MMA reached its peak concentration after 5 extractions ($2.73 \mu\text{mol g}^{-1}$) and DMA and TMA after 6 extractions ($2.73 \mu\text{mol g}^{-1}$ and $4.13 \mu\text{mol g}^{-1}$, respectively, Fig. 5-26). For TE3N, DMA reached its peak concentration after 5 extractions ($3.32 \mu\text{mol g}^{-1}$, Fig. 5-26). MMA and TMA concentrations were levelling off after 4 extractions and reached $2.82 \mu\text{mol g}^{-1}$ and $6.32 \mu\text{mol g}^{-1}$, respectively after 6 extractions. For TE4N, MMA reached its peak concentration after 5 extractions ($3.36 \mu\text{mol g}^{-1}$). DMA and TMA concentrations were levelling off after 4 extractions and reached $6.02 \mu\text{mol g}^{-1}$ and $6.75 \mu\text{mol g}^{-1}$, respectively after 6 extractions (Fig. 5-26).

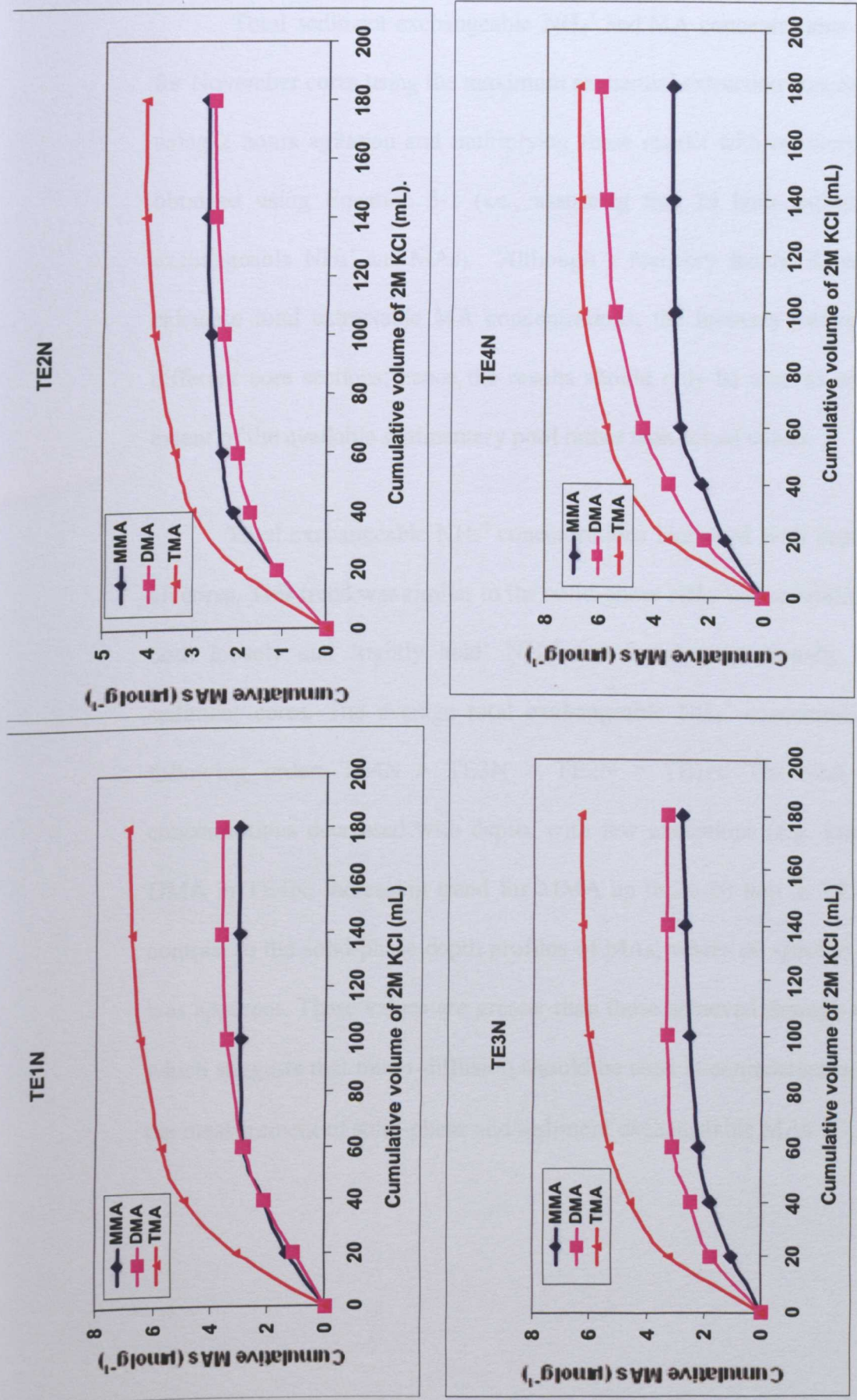


Figure 5-26. MA concentrations in Thames Estuary sediments at 0-5 mm depth extracted with multiple volumes of 2M KCl (2 hours, November 2001).

5.2.3.4 Total sediment-exchangeable NH_4^+ and MA concentrations (November, 2001).

Total sediment-exchangeable NH_4^+ and MA concentrations were determined for November cores using the maximum sequential extraction concentrations obtained using 2 hours agitation and multiplying these results with recovery coefficients (R) obtained using Equation 5-1 (i.e., assuming that 24 hour extraction removes all exchangeable NH_4^+ and MAs). Although a recovery factor, R, was introduced to calculate total extractable MA concentrations, the recovery values might vary for different core sections; hence the results should only be used as an indicator of the extent of the available sedimentary pool rather than actual values.

Total exchangeable NH_4^+ concentrations increased with depth (Table 5-1) in all cores. This trend was similar to the solid-phase NH_4^+ concentrations indicating that both loosely and 'tightly held' NH_4^+ are found proportionally through out the sediment cores. The average total exchangeable NH_4^+ concentrations were in the following order; TE4N > TE3N > TE2N > TE1N. The total extractable MA concentrations decreased with depth, with few exceptions (e.g. increasing trend for DMA in TE4N; increasing trend for MMA up to 20-30 mm in TE1N). This was in contrast to the solid-phase depth profiles of MAs, where no specific trend with depth was apparent. These values are greater than those achieved through micro-diffusion, which suggests that micro-diffusion should be used in conjunction with extraction for the measurement of solid-phase and sediment exchangeable MAs.

Table 5-1. Depth profile of total extractable* NH_4^+ and MAs (μmolg^{-1}) in Thames Estuary sediments (November, 2001).

Depth (mm)	TE1N				TE2N			
	NH_4^+	MMA	DMA	TMA	NH_4^+	MMA	DMA	TMA
0-5	1.91	2.05	2.81	4.37	2.69	3.81	4.66	7.15
5-10	1.99	2.03	2.81	4.18	2.79	3.54	2.81	6.18
10-15	2.46	2.08	2.64	3.56	2.83	3.31	2.64	4.56
15-20	2.23	2.28	2.73	3.37	2.96	3.16	2.73	3.37
20-30	2.34	2.74	2.71	3.32	3.16	3.18	2.71	3.21
30-40	2.58	1.78	2.57	3.20	3.19	3.19	2.57	3.20
40-50	2.88	1.69	2.57	2.77	3.40	2.74	2.57	2.77
50-60	3.28	1.66	2.08	2.75	3.46	2.51	2.08	2.75
60-80	3.28	1.62	2.06	2.31	3.60	2.53	2.06	2.31
80-100	3.46	1.57	2.04	2.04	3.64	2.30	2.04	2.04
Depth (mm)	TE3N				TE4N			
	NH_4^+	MMA	DMA	TMA	NH_4^+	MMA	DMA	TMA
0-5	2.89	2.65	3.51	6.63	3.46	2.93	4.14	5.90
5-10	2.92	2.28	3.26	6.49	3.23	3.28	4.15	5.63
10-15	3.12	2.23	3.28	6.51	3.12	2.80	4.45	4.90
15-20	3.24	2.01	3.14	5.78	3.14	3.78	4.33	4.81
20-30	3.26	1.78	3.18	5.12	3.36	3.65	4.39	4.70
30-40	3.19	1.53	3.15	5.30	3.35	3.53	4.66	4.45
40-50	3.27	1.80	3.07	5.32	3.17	3.53	5.22	4.55
50-60	3.33	1.05	3.08	5.32	3.43	3.40	5.29	4.32
60-80	3.58	1.06	3.07	5.53	3.41	3.40	5.42	3.87
80-100	3.61	1.06	2.95	5.28	3.45	3.33	5.91	3.81

*Total extractable concentrations were obtained by multiplying maximum sequential extraction (2hours) concentrations with R.

5.2.4 Desorption of NH_4^+ and the MAs during simulated sediment resuspension.

Simulated sediment resuspension experiments were carried out using unfiltered sediment (0-5 mm) prepared as detailed in Section 2.5.5. Water samples were removed at timed intervals over a 48 hour period to measure the change in dissolved concentrations of NH_4^+ and the MAs occurring as a result of sediment resuspension. The results of these experiments are presented in the following subsections.

Representative results for the time-dependent desorption experiments are shown in Figures 5-27 and 5-28 for TE1 in July and November and TE3 in July and November, respectively. A summary of physico-chemical data for both July and November samples (0-5 mm) are shown in Table 5-2. Equilibrium concentrations of NH_4^+ and the MAs for both July and November samples are also shown in Tables 5-3 and 5-4, respectively.

The reaction profiles for the resuspension experiments show that there was an initial fast rise in concentration, particularly for NH_4^+ , followed by a slower approach to equilibrium. Most of the NH_4^+ reaction profiles were characterised by a small, short-term enhanced concentration increase after about 30 minutes, in which NH_4^+ initially released from the SPM was followed by re-adsorption, a phenomena also observed by Morin and Morse (1999). Typically, the plateaux in dissolved NH_4^+ concentrations ($[\text{NH}_4^+]_D$) for the July samples were obtained within 1 hour. The $[\text{NH}_4^+]_D$ values at equilibrium were highest in July (Table 5-3) compared to November (Table 5-4).

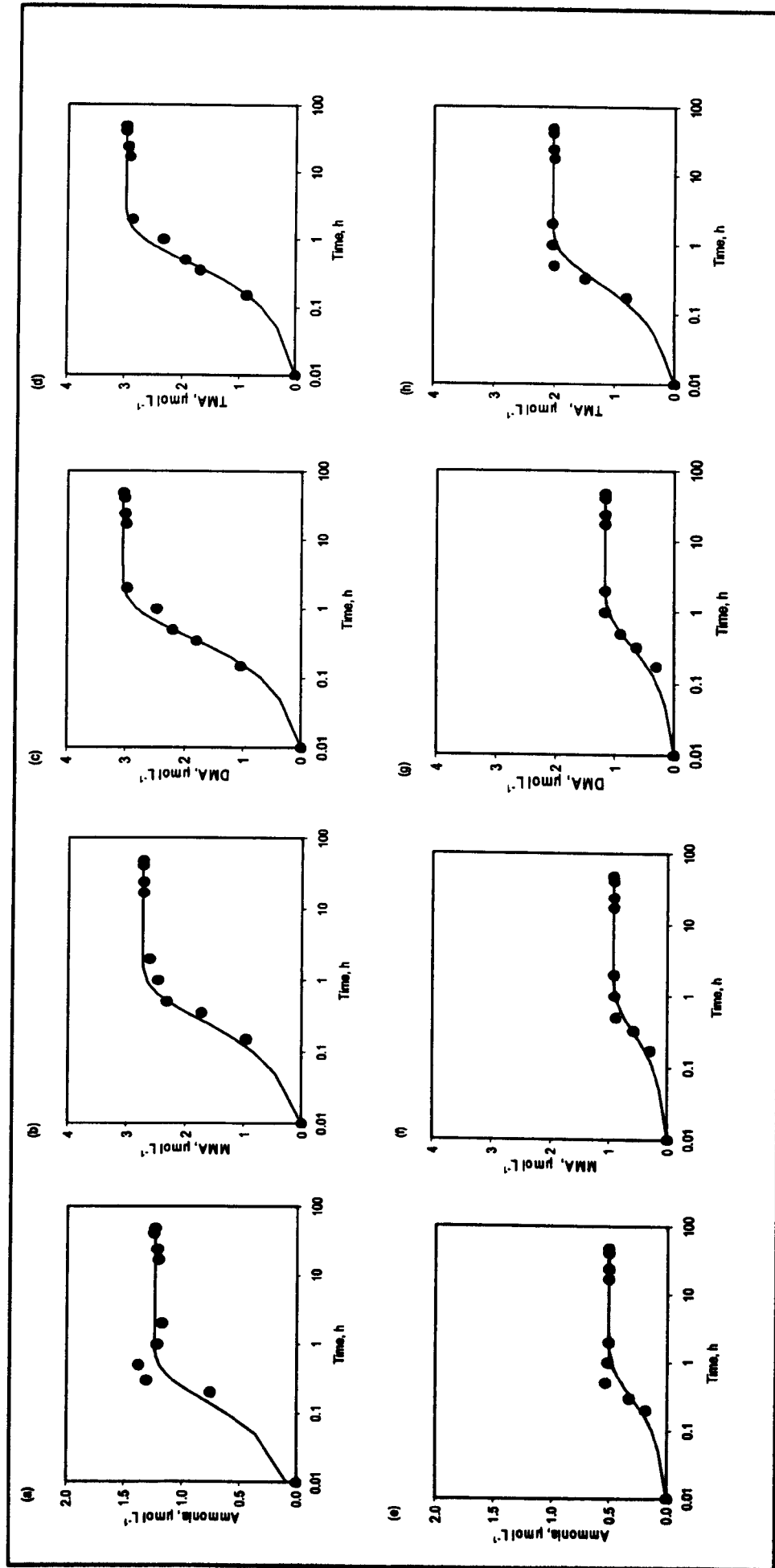


Figure 5-27. Time dependent desorption of NH_4^+ and MAs from Thames Estuary sediments collected at site TE1, July 2001 (a) NH_4^+ , (b) MMA, (c) DMA and (d) TMA and November 2001 (e) NH_4^+ , (f) MMA, (g) DMA and (h) TMA. The filled circles are the observations and the line is the predicted time course derived from a first-order reversible mechanism.

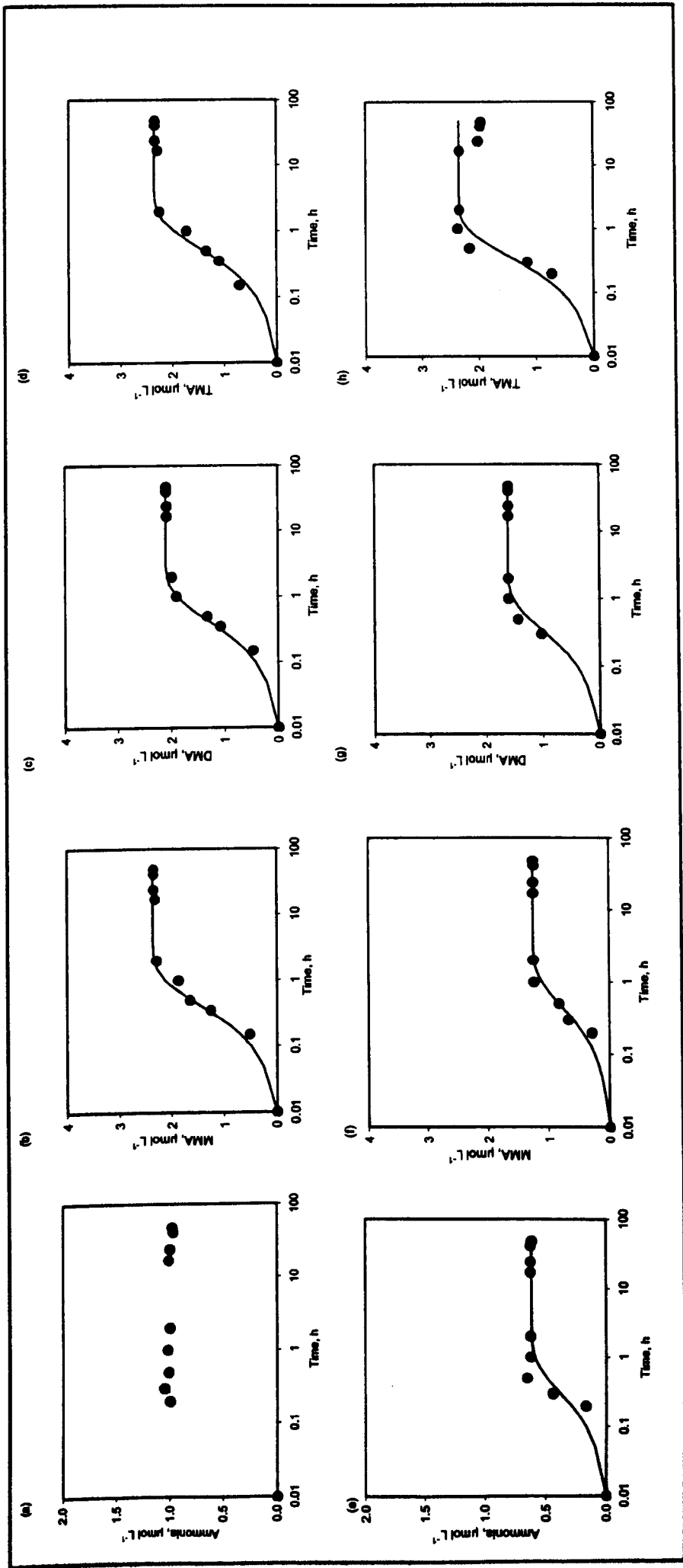


Figure 5-28. Time dependent desorption of NH_4^+ and MAs from Thames Estuary sediments collected at site TE3, July 2001 a) NH_4^+ , (b) MMA, c) DMA and (d) TMA and November 2001 (e) NH_4^+ , (f) MMA, (g) DMA and (h) TMA. The filled circles are the observations and the line is the predicted time course derived from a first-order reversible mechanism.

Table 5-2. Summary of physical and chemical data for surface sediments (0-5 mm depth) sampled in the Thames Estuary.

Sample	Grain Size	% Size Fraction	POC (%)	PN (%)	C/N (atomic)	% Water	Pore-water concentrations, $\mu\text{mol L}^{-1}$				Available Particulate concentrations, $\mu\text{mol g}^{-1}$				MAs as % of PN
							NH_4^+	MMA	DMA	TMA	NH_4^+	MMA	DMA	TMA	
TE1J	Sand Silt Clay	45 45 10	0.54	0.05	14.7	49	61	0.08	0.31	0.03	3.29	5.58	5.72	7.66	59
TE2J	Sand Silt Clay	76 20 4	0.26	0.02	24.8	42	39	0.11	0.32	0.06	3.18	5.17	4.87	6.72	124
TE3J	Sand Silt Clay	6 77 17	2.03	0.20	12.1	37	54	0.09	0.35	0.06	2.09	3.76	3.40	4.72	9
TE4J	Sand Silt Clay	40 48 12	2.06	0.19	12.7	51	25	0.13	0.37	0.06	2.52	8.44	7.96	10.0	11
TE1N	Sand Silt Clay	49 43 8	0.46	0.05	12.4	32	77	0.98	1.20	1.40	1.91	2.05	2.81	4.37	30
TE2N	Sand Silt Clay	61 32 7	0.24	0.03	14.6	33	82	1.10	1.42	1.56	2.69	3.81	4.66	7.15	51
TE3N	Sand Silt Clay	19 67 14	1.71	0.18	11.3	55	92	1.31	1.60	1.75	2.89	2.65	3.51	6.63	9
TEN4	Sand Silt Clay	64 29 7	0.65	0.04	18.7	57	113	1.44	1.85	2.23	3.46	2.93	4.14	5.90	64

Table 5-3. Reaction constants for desorption experiments on Thames Estuary samples collected in July 2001, where $(k_1 + k_{-1})$ = the sum of the forward and reverse rate constants; n = number of points used in kinetic analysis; R^2 = regression coefficients for points in the kinetic analysis.

Sample/ N compound	* Particulate NH_4^+ or MA available for desorption, $\mu\text{mol } \text{g}^{-1}$	Equilibrium concentration, $\mu\text{mol L}^{-1}$	K_D , L kg^{-1}	$(k_1 + k_{-1})$, h^{-1}	n	R^2	τ_{resp} , h
TE1J							
NH_4^+	1.7	1.4	410	ND			
MMA	2.9	2.9	--	2.8	5	0.88	0.36
DMA	3.0	3.4	--	2.1	4	0.87	0.48
TMA	3.9	3.6	180	2.0	4	0.75	0.50
TE2J							
NH_4^+	1.9	1.3	650	ND			
MMA	3.0	2.8	130	2.5	5	0.83	0.40
DMA	2.8	3.2	--	2.2	5	0.98	0.46
TMA	3.9	3.5	200	2.0	5	0.97	0.49
TE3J							
NH_4^+	1.3	1.1	400	ND			
MMA	2.4	2.5	--	2.4	5	0.89	0.42
DMA	2.1	2.5	--	2.5	5	0.99	0.40
TMA	3.0	2.8	100	2.3	4	0.85	0.44
TE4J							
NH_4^+	1.2	0.84	920	ND			
MMA	4.1	2.0	2040	2.4	5	0.91	0.41
DMA	3.9	2.1	1640	1.9	5	0.87	0.53
TMA	4.9	2.4	2000	1.7	5	0.96	0.57

*Total NH_4^+ or MA per gram of wet sediment available to multiple extractions using 2M KCl. ND = Not determined. -- Experiments where the equilibrium concentration exceeds the maximum extracted by 2M KCl, determination of K_D is not possible.

Table 5-4. Reaction constants for desorption experiments collected in November 2001, where $(k_1 + k_{-1})$ = the sum of the forward and reverse rate constants; n = number of points used in kinetic analysis; R^2 = regression coefficients for points in the kinetic analysis.

Sample	*Particulate NH_4^+ or MA available for desorption, $\mu\text{mol g}^{-1}$	Equilibrium concentration, $\mu\text{mol L}^{-1}$	K_D , L kg^{-1}	$(k_1 + k_{-1})$, h^{-1}	n	R^2	τ_{resp} , h
TE1N							
NH ₄ ⁺	1.3	0.52	2043	3.1	3	0.99	0.32
MMA	1.4	0.93	--	3.1	3	0.97	0.32
DMA	1.9	1.2	--	2.8	3	0.98	0.36
TMA	3.0	2.0	--	3.4	3	0.91	0.29
TE2N							
NH ₄ ⁺	1.8	0.60	2890	5.2	3	0.98	0.19
MMA	2.5	1.8	550	1.9	3	0.99	0.52
DMA	3.1	1.9	870	1.8	3	0.99	0.55
TMA	4.7	3.4	590	2.1	3	0.98	0.48
TE3N							
NH ₄ ⁺	1.3	0.64	2260	3.6	3	0.92	0.28
MMA	1.2	1.3	--	2.2	4	0.98	0.46
DMA	1.6	1.6	--	2.9	3	0.96	0.35
TMA	3.0	2.0	1070	2.7	3	0.99	0.37
TE4N							
NH ₄ ⁺	1.6	0.73	2520	4.2	3	0.94	0.24
MMA	1.3	1.6	--	3.1	3	0.97	0.32
DMA	1.8	2.2	--	2.9	3	0.97	0.35
TMA	2.5	3.7	--	3.6	3	0.88	0.28

*Total NH_4^+ or MA per gram of wet sediment available to multiple extractions using 2M KCl. -- Experiments where the equilibrium concentration exceeds the maximum extracted by 2M KCl, determination of K_D is not possible.

5.2.4.1 Kinetics of NH_4^+ and MA desorption during sediment resuspension.

Predicted kinetic behaviour of the constituents was obtained by encoding ModelMaker (Millward and Liu, 2003) with the appropriate, tabulated constants and plotting the time course of the desorption reaction. The kinetic analysis was conducted using the maximum extractable concentrations of NH_4^+ and the MAs from the sequential extraction experiments. In some cases (such as TE1J) the 2M KCl extract removed less MMA and DMA than was released at equilibrium during the resuspension experiment (i.e. the % of maximum was > 100%). In these cases a kinetic analysis was not undertaken.

It was assumed that desorption of NH_4^+ and the MAs is described by a first-order reversible mechanism (Millward and Liu, 2003), with particulate constituents (MA_p) exchanging reversibly with the dissolved phase MA_d . The basic assumptions are summarised below. Desorption is described by a first-order reversible mechanism, with the constituents being loosely bound to the surface. It is assumed that none of the compounds are irreversibly bound in the particle matrix. This is described by Equation 5-2, using MMA as an example;



1. The reaction has a forward rate constant, designated k_1 , and a reverse rate constant, designated k_{-1} .
2. The concentration of a constituent at equilibrium, $[\text{MMA}]_E$, is obtained from the laboratory experiments observing the time-dependent behaviour of the desorption. Normally the 48 hour determination was taken as the equilibrium value.

3. The total concentration of desorbable constituent, $[MMA]_T$, was obtained from the sequential extraction experiments involving 2M KCl and OLW. The $[MMA]_T$ value was taken after extraction by 180 mL of the extractant solution. Solving the differential equation for Equation 5.2 gives an integrated rate equation of the form: -

$$[MMA]_t = [MMA]_E * (1 - e^{-(k_1 + k_{-1}) * t}) \quad \text{Equation 5-3.}$$

Where $[MMA]_t$ is the concentration of the constituent at time t. The system response time, τ_{resp} , (i.e. the time to achieve 63% of the new equilibrium) is given by: -

$$\tau_{resp} = \frac{1}{(k_1 + k_{-1})} \quad \text{Equation 5-4.}$$

The values for the sum of the rate constants, $(k_1 + k_{-1})$, can be obtained from the slope of the line obtained by re-arranging Equation 5-3 and plotting $\ln([MMA]_E / ([MMA]_E - [MMA]_t))$ versus time. The values for the individual rate constants are then obtained from the equilibrium condition and the mass balance, such that k_{-1} can be estimated from: -

$$k_{-1} = \frac{[MMA]_E (k_1 + k_{-1})}{[MMA]_T} \quad \text{Equation 5-5.}$$

Once values for k_1 and k_{-1} were estimated, they were used, together with a value for $[MMA]_T$ from the 2M KCl extracts in ModelMaker software code, to predict the evolution of the desorption process as a function of time.

The partition coefficients, K_D s, calculated during the desorption experiments were derived from:-

$$K_D = \frac{([MMA]_P^e - [MMA]_D^e)}{[MMA]_D^e * [SPM]} \quad \text{Equation 5-6.}$$

Where, $[MMA]_D^e$ is the equilibrium concentration of dissolved MA (or NH_4^+), $[MMA]_P^e$ is the equilibrium concentration of particulate MA (or NH_4^+). $[SPM]$ is the SPM concentration in $kg\ L^{-1}$.

The predicted K_D values for NH_4^+ were in a range from 400 to 920 $L\ kg^{-1}$ for the July samples, whereas in November the K_D values were significantly higher at each site and in a range from 2043 to 2890 $L\ kg^{-1}$. The K_D values for the MAs were site dependent in July such that at sites TE1J, TE2J and TE3J they did not exceed 600 $L\ kg^{-1}$, whereas at site TE4J they varied from 1640 to 2040 $L\ kg^{-1}$. For the November samples, it was only possible to determine K_D values for TE2N (all MAs) and TE3N (TMA), where the values were in the range 550 to 1070 $L\ kg^{-1}$.

The rate parameters for the kinetic analyses are given in Tables 5-3 and 4, where it is evident that the maximum concentrations of ammonium, $[NH_4]_T$, available to a 2M KCl extract did not vary significantly between the two surveys. Generally, the maximum concentrations of NH_4^+ in the sediments (available to a 2M KCl extract) in July (1.2 to 1.9 μM) were similar to November (1.3 to 1.8 μM). It was not possible to determine the NH_4^+ desorption kinetics for July samples as the equilibrium concentrations were higher than the maximum available concentrations but the kinetics (the sum of the rate constants) for the November samples were in a narrow range of 3.1 h^{-1} to 5.2 h^{-1} , giving typical chemical response times from about 12 to

19.2 minutes. The values for the rate constants were encoded into ModelMaker to predict the time course of the reaction, as plotted for the examples in Figure 5-27 for July 2001 and in Figure 5-28 for November 2001. R^2 values for the regression analysis for points in the kinetics analysis were all greater than 0.92 enabling strong confidence in the model prediction.

5.3 Discussion of results

5.3.1 Seasonal NH_4^+ and MA distributions in Thames Estuary sediment samples.

Temperature variation has a pronounced effect on the production rate of NH_4^+ in temperate coastal sediments (Laima, 1992), which could partly explain the greater amount of NH_4^+ observed near the surface of all summer samples in this study. Higher primary production in the summer leads to increased abundance of labile nitrogenous OM, which can be mineralised rapidly. In the summer samples, cores TE1J and TE2J were predominantly grey in colour, indicating anoxic conditions while TE3J and TE4J appeared brown, suggesting oxic conditions. TE3J and TE4J contained lower concentrations of NH_4^+ in the upper 50 mm depth, possibly due to the more oxic conditions and flushing of pore-waters, which may have led to the depletion of NH_4^+ by nitrification. According to classical models of N cycling, nitrification declines with depth as a result of reduced penetration of oxygen, which normally leads to an increase in NH_4^+ concentration at depth in marine sediments (Blackburn and Sørensen, 1988). Thus, one would expect to see a rise in NH_4^+ concentration with depth but the reverse was true in all summer core samples.

Thamdrup and Dalsgaard (2002) reported that anaerobic oxidation of NH_4^+ was coupled to nitrate reduction in sediment samples collected from the Baltic-North Sea transition (Skagerrak and Aarhus Bay), revealing a novel metabolism that could short circuit the N cycle, by passing what was previously thought to be a purely aerobic process and providing an alternative pathway for N_2 gas formation in the environment (Trimmer *et al.*, 2003). By shunting N directly from NH_4^+ to N_2 , anaerobic NH_4^+ oxidation promotes the removal of fixed N in marine sediments. Trimmer *et al.* (2000) found that although organically-enriched sediments in the

Thames Estuary represented only 18% of the total sediment area in one study, they were responsible for 34% of the total mineralisation of organic material. In a later study, Trimmer *et al.* (2003) found that maximum anaerobic NH_4^+ oxidation to N_2 in the Thames Estuary occurred within organically enriched sediments. This process may partially explain the NH_4^+ deficiencies observed in the deeper anoxic parts of the Thames Estuary sediments in this study.

Bioturbation, which may have introduced oxygen into greater depths of the cores, could also have led to nitrification, which might have depleted the NH_4^+ concentration to a greater extent than expected. This is not surprising, particularly in TE1J and TE2J as many invertebrates were found in the core samples during core sectioning and although the predominant colour of the two cores was grey, they also contained significant patches of brown sediments suggesting localised oxic conditions. Future studies of N cycling in the Thames Estuary need to include measurement of the sediment organic content (see Table 5.2 for POC and PN at 0-5 mm depth) and levels of NO_3^- and dissolved O_2 to clearly understand the role of anaerobic oxidation of NH_4^+ . Unlike the summer samples, pore-water NH_4^+ concentrations increased with depth in TE1N and TE3N cores, while the trend with depth was not well defined in TE2N and TE4N. Solid-phase concentrations generally increased with depth perhaps due to the limited oxidation occurring lower in the cores.

There have been few seasonal studies of MA cycling in inter-tidal sediments. Wang and Lee (1994) observed strong seasonal variations in the abundance and biological uptake of MAs, and also demonstrated that diagenesis and adsorption of MAs in marine sediments were dependent on the quality and rate of input of fresh

OM. Higher production of MAs in summer was observed by Wang and Lee (1994) but in this study the concentrations of pore-water MAs were lower in summer. On average, solid-phase MAs were more abundant in July samples (Table 5-5). This may be due to higher production being offset by a number of factors, including increased adsorption correlating with increased POM in the sediments and enhanced uptake of bioavailable (i.e. pore-water) MAs.

Table 5-5. Total average pore-water and solid-phase MA concentrations in Thames Estuary samples.

Cores	Pore-water MAs (μM)		Solid-phase MAs (μmol g ⁻¹)	
	July	November	July	November
TE1	0.45	2.66	8.91	3.28
TE2	0.58	2.62	9.23	5.74
TE3	1.17	3.18	9.16	4.25
TE4	0.5	3.66	8.89	6.8

5.3.2 Measurement of NH₄⁺ and the MAs at TE3.

Data on suspended solids in the Thames Estuary are collected frequently by the Environment Agency but data on the composition of particulates is limited and will depend on the state of the tide when the sample was taken (see the Appendix, Tables A-2 to A-7, for various environmental data collected for Benfleet Sewage Treatment Plant (STW) by the Environment Agency). In fact, large changes can occur at a specific location within a few hours. Surveys over a tidal cycle are required to

gain a better understanding of the amount of suspended particles as this will affect turbidity. Turbidity is an important factor affecting primary production as it limits light penetration to the overlying seawater. The Thames Estuary is a turbid estuary but the amount of particulate matter resuspended which affects turbidity at a particular time can vary, as observed in this study (Fig. 5-21).

Estuarine suspended solids are influenced by tidal movement, but can settle and resuspend in a cyclical manner (Kinniburgh, 1998). Spring tides will resuspend greater quantities of solids than neap tides because of the greater velocities. This means reduced primary production, but the associated reduced input of N can be compensated for as organic material deposited on the bed is bioavailable, when suspended, leading to oxygen depletion within the water column and, in the case of ON-rich particulates, the potential for nutrient regeneration leading to eutrophication.

The time-dependent behaviour of the concentrations of $[MA]_D$ and the concentration of SPM over a tidal cycle at TE3 (Fig. 5-21) reflect release to, and removal from, the dissolved phase (e.g. Wang and Lee, 1993). However, since $[NH_4^+]_D$ and $[MA]_D$ were added to the water column at similar times, they may have a common source, which is linked to the resuspension process. Thus, if there are significant pore-water concentrations of the analytes they could be introduced into the water column during resuspension or the analytes could be desorbed from the resuspended particles, or a combination of both processes occurs.

Estimates of the potential injection of $[\text{NH}_4^+]_D$ and $[\text{MA}]_D$ into the water column from the sediments can be made assuming; (a) a uniform texture in the sediment column (b) the tidal shear mixes the sediments to a depth of 0.1 m and (c) the water column is well mixed during the tidal incursion. Taking a mean water content of 45% for the sediments, a mean $[\text{NH}_4^+]_D$ in pore-waters of $68 \mu\text{mol L}^{-1}$ and a mean $[\text{MA}]_D$ in pore-waters of $0.82 \mu\text{mol L}^{-1}$ then, to a first approximation, the total amounts of $[\text{NH}_4^+]_D$ and $[\text{MA}]_D$ available for injection into the water column are 3 mmol m^{-2} and $37 \mu\text{mol m}^{-2}$, respectively. Since the average depth of water at the sites is about 5 m, the $[\text{NH}_4^+]_D$ and the $[\text{MA}]_D$ will increase by $\sim 700 \text{ nmol L}^{-1}$ and $\sim 7 \text{ nmol L}^{-1}$, respectively, as a result of the remobilisation of sediment pore-waters into the water column.

On this basis approximately 50% of the observed $[\text{NH}_4^+]_D$ increase is predicted to originate from sediment pore-waters. This is a similar conclusion to that observed by Morin and Morse (1999) in the Laguna Madre. On the other hand, the predicted pore-water contribution for MAs is $< 10\%$ of the peak concentration in Figure 5-21, suggesting another prominent MA source, such as desorption. Whether the sediment pore-waters are a continuous source of $[\text{NH}_4^+]_D$ and $[\text{MA}]_D$ is questionable. However, the period of time between neap and spring tides may be sufficient for benthic anoxia to become established and replenish the pore-water concentrations of NH_4^+ and MAs (e.g. Rocha, 1998).

5.3.3 Measurement of exchangeable NH_4^+ and MAs.

For both July and November surfacial sediment samples, more NH_4^+ and MAs were extracted after 6 extractions using 2M KCl than with one, indicating that a single extraction will underestimate the total extractable concentrations of these analytes. Multi-volume extraction of surfacial sediments of July samples with OLW also resulted in higher amounts of both extractable NH_4^+ and MAs compared to single volume extraction. Previously, this has only been observed for NH_4^+ (Laima, 1992; Morin and Morse, 1999). Therefore, a good estimate of particle exchangeable NH_4^+ and MAs can only be made using multi-volume extractions of sediments.

The MAs remaining associated with the sediment solid-phase after extraction with 1M LiCl (2h, 1 volume sediment; 20 volume water) have been categorised as 'fixed' within the sediment matrix (Wang and Lee, 1990; 1994). However, the equilibrium concentrations of all MAs released during the sediment resuspension experiments involving OLW were greater than the amount released by a single-volume extraction with 2M KCl and in some cases, by multi-volume extraction (Tables 5-3 and 5-4). These findings suggest that 2M KCl may not be an appropriate reagent for the determination of total $[\text{NH}_4^+]_p$ and $[\text{MA}]_p$ and, by extrapolation, for the estimation of bioavailable sedimentary organic N. Nevertheless, 2M KCl is in common use and it has been used in this study as a basis for estimating the total $[\text{NH}_4^+]_p$ and $[\text{MA}]_p$ available for desorption.

More NH_4^+ was extracted with OLW compared to 2M KCl indicating that cations such as Ca^{2+} may release adsorbed N cations into overlying seawater more effectively during resuspension of sediments. Depletion of total extractable MAs with depth in the November samples could either be due to incorporation of MAs into the

sediment matrix or degradation by microbial processes. The increasing order of average total extractable MA concentrations (i.e. MMA < DMA < TMA) is very likely a result of their adsorption coefficients and probably preferential degradation of MAs that require fewer demethylations steps. The increase in NH_4^+ concentrations with depth also supports this assumption, as NH_4^+ is a terminal product of OM mineralisation.

OM is mineralised with depth and NH_4^+ accumulates as nitrification does not occur through lack of available oxygen in the absence of bioturbation and frequent resuspension (Maksymowska-Brossard and Piekarek-Jankowska, 2001). Due to the reduced input of fresh OM in late autumn, anaerobic oxidation of NH_4^+ may also be reduced to some extent. However, seasonal variations in anaerobic NH_4^+ oxidation need to be further investigated. The depth profiles of total extractable NH_4^+ and MA concentrations suggest that in late autumn, when the supply of fresh OM starts to diminish microorganisms may use 'strongly' adsorbed MAs, even if this requires more energy. MMA is degraded faster than the other MAs because of its lower adsorption coefficient and because it is relatively easier to degrade due to the lower number of methyl groups.

5.3.4 Desorption of NH_4^+ and the MAs during simulated sediment resuspension.

Most studies on sediment resuspension have focused on the effects of particulate organic matter (POM) degradation as it is transferred into the overlying water (Chrost and Riemann, 1994), or its transport (Abril and Leon, 1994). There have been few investigations on the effect of sediment resuspension on the release of nutrients to the overlying water. Storm-induced resuspension has been associated with increased N concentrations in bottom waters (Fanning *et al.*, 1982), and release of

pore-water nutrients to overlying water was observed in a mixed mesocosm (Sloth *et al.*, 1996). Morin and Morse (1999) observed that dredging of sediments released a significant amount of NH_4^+ into the overlying water. However, to date there has been no attempt to investigate the release of ON into overlying water as a result of sediment resuspension by both natural and man-made activities.

A significant amount of MAs desorbed from the solid-phase during the simulated resuspension experiments of Thames Estuary sediments. MAs are very soluble in natural waters due to protonation and hydrogen bonding. The MA adsorption coefficients for different sediment types are typically higher than for NH_4^+ and can be explained in terms of the successive replacement of hydrogen atoms with methyl groups, resulting in less hydrogen bonding. However, adsorption did not appear to restrict their release from the sediments, which occurred in the same proportion as their relative abundances in the solid-phase. Thus, TMA, which was more abundant than MMA and DMA in the solid-phase, was also released in greatest amounts into solution during resuspension.

The effect of wave action on the resuspension of sediments has been documented in marine, estuarine and lacustrine systems (Krone, 1966; Schuble, 1968; Anderson, 1972; Lam and Jaquet, 1976; Roman and Tenore, 1978; Ullman and Sandstorm, 1987; Simon, 1988). One of the effects of sediment resuspension is a large decrease in the particle to solution ratio (Shideler, 1984). Morin and Morse (1999) performed a laboratory resuspension experiment on coastal sediments and found that more NH_4^+ was released when the particle to solution ratio of the suspended sediments was decreased. Bordas and Bourg (2001) studied the behaviour of Cu, Zn, Pb and Cd during sediment resuspension and found that as the particle concentration

decreased from 50 to 0.1 g L⁻¹, the percentage of metal mobilised from sediment increased substantially.

In natural aquatic systems, sediments act as temporary and permanent sinks of ON compounds. Because of the reversibility of N immobilisation, sediments can buffer water column concentrations of DON. When sediments are resuspended, there is a decrease in the particle to solution ratio, shifting the equilibrium towards the dissolved phase. This may increase the remobilisation of ON cations such as the MAs. As dilution increases, the cations attached to the particle surface will have more contact with dissolved, competing ions and water molecules, increasing the probability of their release into solution (Calvet and Msaky, 1990; Dzombak and Morel, 1990). Therefore, a change in the particle to solution ratio is one of the main factors governing the release of adsorbed NH₄⁺ and MAs in this study.

A similar desorption study found that NH₄⁺ released from the solid-phase accounted for most of the NH₄⁺ released during sediment resuspension (Morin and Morse, 1999). This has an important implication for estuarine ecosystems as alterations in the NH₄⁺ concentration, specifically the ratio of available NH₄⁺ to available NO₃⁻, was found to have an impact on algal communities in the overlying seawater (Morin and Morse, 1999). The results of this study suggest that compounds from the ON fraction may be similarly desorbed. The release of bound ON may have environmental consequences. Increased nutrient levels during prolonged and recurrent resuspension could lead to eutrophication even if other nutrient inputs have been controlled. Hence, effective coastal management needs to account for release of N from all possible sources if accurate fluxes are to be determined.

5.3.4.1 Kinetics of NH_4^+ and MA desorption during sediment resuspension.

The kinetics of NH_4^+ and MA desorption during simulated sediment resuspension indicated that the maximum MA concentrations available for desorption were similar for July and November samples (Tables 5-3 and 5-4). The reaction curves for the MAs demonstrated a smooth, slow approach to equilibrium and, in contrast to NH_4^+ , there was no overshoot. This is due to the release of MAs being a slower process than for NH_4^+ , which means equilibrium could have been reached before the concentrations peaked. This is expected, since K values for MAs are generally much higher (Chapters 3 and 4) than for NH_4^+ and they are likely to be released at a slower rate than NH_4^+ under similar conditions. This is supported by the results of the resuspension experiments, where the τ_{resp} for the MAs were consistently higher than for NH_4^+ (Table 5-3).

Although τ_{resp} for the MAs is longer than for NH_4^+ , 63% of the new equilibrium was achieved between 21.6 and 34.2 minutes in July and between 16.8 and 33 minutes in November. MMA seemed to desorb slightly faster than DMA and TMA in July samples. The reverse was true for the November samples (except TE2N). This indicated seasonal and temporal differences in MA reactivity in the Thames Estuary sediments.

This study has shown that resuspension of sediments can lead to desorption of substantial amounts of NH_4^+ and the MAs into overlying seawater. Estuaries such as the Thames need sustainable management plans to minimise the potential release of 'fixed' nutrients as a result of both man-made activities (e.g. dredging) and natural events (e.g. storm events). Understanding the kinetics of the mobilisation of particulate NH_4^+ and ON species, such as the MAs, can help underpin this effort.

5.4 Summary

- Spatial and seasonal variability in NH_4^+ and MA abundances was observed within core samples collected from the Thames Estuary. Depth profiles of NH_4^+ and MAs suggest that redox conditions may help control their distribution in inter-tidal sediments. However, sometimes clear trends with depth were not observed, suggesting that bioturbationrdp52iq
- by invertebrates could be responsible by introducing oxic conditions into deeper sediments as well as releasing MAs to surrounding sediment during tidal fluctuations. However, the role of redox conditions on the distribution of ON compounds in inter-tidal sediments needs to be further investigated.
- A clear seasonal variation in concentrations of MAs in Thames Estuary sediments was observed. This was assumed to be related to differences in OM content at different times of the year, with OM acting as a direct source, or indirectly providing additional exchange capacity for adsorption.
- During sediment resuspension, release of NH_4^+ and the MAs into the overlying water occurred predominantly through desorption. Release of MAs from resuspended sediments was rapid but generally slower than desorption of NH_4^+ with maximum concentrations typically observed after 2 hours. The fact that ON substrates are preferred by bacteria in the outer Thames Estuary may mean that sediment release of MAs could be disproportionately more important than NH_4^+ .

- The results of this study suggest that, as for NH_4^+ , single-volume extraction of MAs at a 20:1 ratio of solution (OLW, 2M KCl) to sediment can considerably underestimate the exchangeable MA pool in sediments because it rarely released more than 50% of total exchangeable NH_4^+ and MAs.
- Resuspension of sediments in 1L of seawater sometimes released more NH_4^+ and MAs than was predicted by sequential extraction with 2M KCl, indicating that the particle to solution ratio plays a significant role in the dissolution of adsorbed NH_4^+ and MAs in the Thames Estuary.
- Dredging of estuarine sediments releases bound NH_4^+ into the water column. The results of this study suggest that some of the ON fraction may be similarly desorbed. Thus, an assessment of the impact of activities such as dredging on water quality must include the mobility of the ON fraction if accurate fluxes are to be determined.

6. CONCLUSIONS AND RECOMMENDATIONS FOR FUTURE WORK.

6.1 Conclusions

Inter-tidal sediments occupy a unique position between land and sea giving them an important role in the movement of materials from terrestrial to oceanic environments. Most studies on N cycling in estuarine ecosystems have concentrated on inorganic forms of N and much less is known about the distribution and cycling of ON compounds. This study has attempted to elucidate the role of the MAs in pathways and mechanisms of N cycling in estuarine environments. The study focussed on inter-tidal mudflats to investigate the role of certain physico-chemical factors in the cycling of the MAs. Three separate inter-tidal ecosystems were studied: Burnham Overy Staithe, the Thames Estuary (both UK) and the Ria Formosa (Portugal). Some conclusions drawn from these specific studies are summarised below.

The MAs are ubiquitous in marine systems at concentrations ranging from nanomolar in the open ocean to micromolar in estuarine sediments (see Table 6-1). However, their cycling in the marine environment and their role within organisms is not fully understood. The summary of MA concentrations determined in this study and previously reported marine MA data are shown in Table 6-1.

**PAGE
MISSING
IN
ORIGINAL**

Table 6-1. Summary of MA concentrations determined in this study collated with previously reported MA data in the marine environment.

Authors (Yr)	Location	MMA			DMA			TMA		
		PW (μ M)	EX (μ mol g ⁻¹)	F (μ mol g ⁻¹)	PW (μ M)	EX (μ mol g ⁻¹)	F (μ mol g ⁻¹)	PW (μ M)	EX (μ mol g ⁻¹)	F (μ mol g ⁻¹)
This study	BOS	0.08 – 1.34	0.05 – 0.32	nd	0.16 – 2.61	0.16 – 2.61	nd	0.04 – 3.22	0.42 – 3.24	nd
	Ria Formosa	0.11 – 14.21	0.19 – 3.10	nd	0.34 – 0.84	0.22 – 0.77	nd	0 – 2.89	0 – 3.06	nd
	Thames Estuary	0.04 – 1.44	0.7 – 5	*2.35	0.1 – 1.85	0.7 – 4.0	*2.52	0 – 2.33	0.01 – 8	*3.6
Lee and Olson (1984)	Coastal	bd	bd	nd	0.048	†0.07	nd	0.029	†0.02	nd
	Open ocean	bd	bd	nd	0.5	†0.02	nd	0.1	†0.002	nd
Van Neele <i>et al.</i> (1987)	Pacific- Hawaii (coastal, average)	*0.052 ± 0.02	nd	nd	*0.0015 ± 0.0002	nd	nd	*0.012 ± 0.0003	nd	nd
	Atlantic- Massachusetts (coastal)	*0.2 ± 0.058	nd	nd	*0.0089 ± 0.0044	nd	nd	*0.041 ± 0.027	nd	nd
Abdul-Rashid (1990)	Liverpool Bay (sea water)	0.2	nd	nd	bd	nd	nd	0.5	nd	nd
	Hale Salt marsh Mersey Estuary, UK	2.5	nd	nd	1	nd	nd	10	nd	nd
Wang and Lee (1990)	Long Island Sound	0.12	4.9	0.3	870	13.6	0.9	nd	nd	nd
	Flax Pond New York	0.19	2.9	1.5	10	6.1	3.4	nd	nd	nd
Abdul-Rashid (1991)	Irish sea	* (0 – 0.619)	nd	nd	* (0 – 0.1)	nd	nd	* (0 – 0.004)	nd	nd
Gibb <i>et al.</i> (1994)	Mediterranean sea (offshore; average)	*0.0075 ± 0.0055	nd	nd	*0.0046 ± 0.003	nd	nd	*0.0014 ± 0.0016	nd	nd
	Coastal (Gulf of Lions; average)	*0.018 ± 0.001	nd	nd	*0.012 ± 0.00114	nd	nd	*0.0010 ± 0.0069	nd	nd
Wang and Lee (1994)	Flax pond New York	2	0.06	nd	3.6	0.02	nd	0.06	0.1	nd
Fitzsimons <i>et al.</i> (1997)	Oglet Bay, Mersey Estuary, UK	0 – 0.319	†(0.03 – 2.44)	nd	0 – 9	†(0 – 0.81)	nd	0 – 50	†(0.01 – 0.98)	nd
Gibb <i>et al.</i> (1999)	Arabian sea (average)	*0.0126	nd	nd	*0.0032	nd	nd	*0.0002	nd	nd

*Sea water sea water concentrations, PW = Pore-water, † per g dry weight, EX = Exchangeable, F = Fixed, *Average total MA per gram of wet surficial sediment available to multiple extractions using 2M KCl (see also Section 5.2.4), nd = not determined,

There is a lack of standard methods for the determination of MAs in the marine environment. Seawater, pore-water, exchangeable and fixed MA concentrations have been measured using different analytical methods. Therefore, to make any meaningful comparison the variations in the methods of each study should be taken into account. However, Table 6.1 can be used as an indicative guide to the range of MA concentrations in the marine environment.

NH_4^+ and MAs were present at different concentration ranges in all three sites. However, a close scrutiny of the abundance of both analytes showed that this is influenced by different physico-chemical factors including organic matter content, tidal action and bioturbation. Where NH_4^+ and MA concentrations were compared, the former was more abundant in the pore-waters, while the reverse was observed for the solid-phase. This can be explained by the greater basicity of the MAs. Tidal flushing was linked to the depletion of pore-water MAs, though an increase in TMA concentrations occurred in Ria Formosa when sediments were flooded, possibly through its release by invertebrates. The role of grain-size on the biogeochemistry of the MAs was unclear from this study. In the dynamic environments that exist in inter-tidal sediments, other factors such as preferential rapid uptake of MAs by micro-organisms could mask any relationship.

The clam, *R. decussates* (L.), was found to release a significant amount of TMA during tidal inundation, which may have been exported to overlying waters. Mariculture of *R. decussates* (L.) may therefore, significantly increase the flux of ON to the water column, with implications for water quality in the Ria Formosa. Among these, the declining bivalve harvest is one of the most serious economic consequences (Dinis, 1992). Clam farmers also report an increase in the mortality of their stock,

with mass mortalities in some areas of the Ria Formosa lagoon (Newton, 2003). There is also evidence of increase in incidences of harmful algal blooms and fish kills in the summer months (Newton, 2003).

Previous studies have shown that the OM content of sediments affects the adsorption of NH_4^+ and MAs in marine sediments (Rosenfeld, 1979; Mackin and Aller, 1984; Wang and Lee, 1990). TOC was only determined in BOS samples but no significant correlation between TOC and adsorbed NH_4^+ and MAs was observed. However, since BOS was a pristine site the quality and quantity of OM was expected to be different from an impacted environment. Therefore, although no particular correlation was observed in BOS samples, OM content is suspected to have some impact on the adsorption of NH_4^+ and MAs, and higher adsorption coefficients for Ria Formosa and the Thames Estuary samples support this assumption. However; direct evidence is needed to ascertain this in future studies, with direct measurement of TOC.

The general trend of NH_4^+ and MA adsorption was in the following order; $\text{TMA} > \text{DMA} > \text{MMA} > \text{NH}_4^+$. However, there were some variations to this, especially for sediments collected at different stages of a tidal cycle in the Ria Formosa indicating that dynamic changes associated with tidal inundation of sediments have a significant impact on the adsorption of MAs. Nevertheless, the general trend could be explained by the basicity of the free compounds, solvation of their protonated analogues and hydrogen bonding, Van der Waals forces and perhaps complex formation with other organic compounds and irreversible chemical reactions with mineral surfaces.

Seasonal differences in NH_4^+ and MA abundance were observed in the sediment core samples (0-100 mm) collected from four sites in the Thames Estuary in July and November 2001. NH_4^+ was much more abundant in the pore-waters of July samples than November samples, which was attributed to an increase in temperature and the amount of fresh OM. Solid-phase NH_4^+ concentrations decreased with depth in July samples, in contrast to what was expected. This could be partly due to bioturbation by invertebrates introducing oxygen to deeper sediments and leading to the removal of NH_4^+ by nitrification or anaerobic oxidation of NH_4^+ .

The extraction of NH_4^+ and MAs with a single volume of 2M KCl solution (i.e. the standard method for measuring sediment-exchangeable NH_4^+) considerably underestimated the sediment-exchangeable pool of these analytes. Sediment-exchangeable NH_4^+ and MAs were also determined using multi-volume extraction of sediments with 2M KCl. However, multi-volume extraction of TE sediment samples with OLW recovered even more NH_4^+ than 2M KCl, indicating that cations such as Ca^{2+} may enhance desorption of N cations during sediment resuspension.

Resuspension of unfiltered surficial sediment (0-5 mm depth) samples in OLW released NH_4^+ and MAs predominantly through desorption from the solid-phase. The release of MAs was rapid but generally slower than desorption of NH_4^+ , with maximum concentrations typically observed after 2 hours. The sediments sometimes released more NH_4^+ and MAs than would be expected from the multi-volume extractions with 2M KCl, indicating that the particle to solution ratio and cations present in OLW may have enhanced desorption of the analytes. The results suggest that sediment resuspension is an important mechanism by which sediment-water exchange of solute takes place in inter-tidal mud flats.

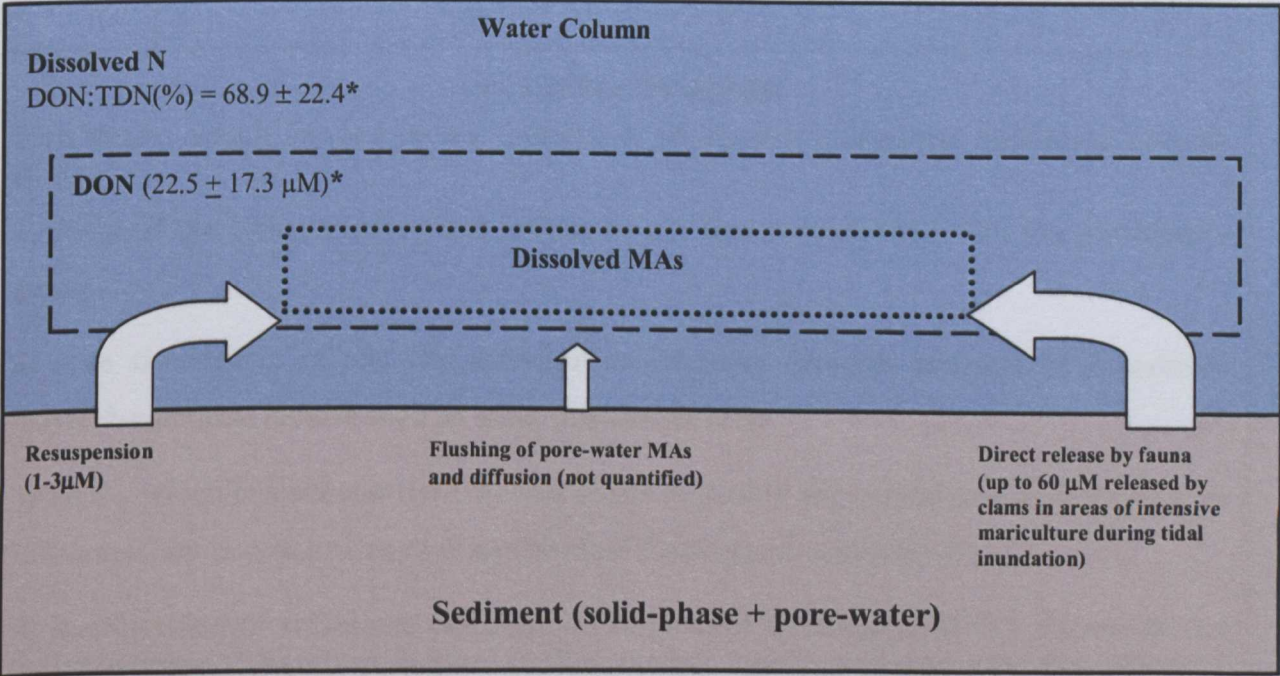
Human activities such as dredging of sediments in coastal areas and maritime traffic are known to cause sediment resuspension. Mobilisation of OM during sediment resuspension could result in benthic fluxes of nutrients to the overlying waters. Therefore, these activities need to be closely monitored in order to curb potential nutrient enrichment. This can only be done through sustainable stewardship that will minimise the perturbation of the delicate balance that exists in most shallow coastal ecosystems.

6.1.1 The impact of MAs on N cycling in inter-tidal sediments.

A semi-quantitative conceptual map of the impact of MAs on the cycling of N in inter-tidal sediments was constructed (Fig. 6-1) by assuming;

1. The existence of an inter-tidal flat, which has invertebrates releasing MAs as documented for *Ruditapes decussates* (L.) by Fitzsimons *et al.* (2005). The faunal density of the sediment is similar to that measured for the Ria Formosa Site (1) (a maximum of 200 individuals m⁻²) by Sprung *et al.* (1994).
2. The presence of a typical sediment resuspension processes resulting in 500 mg L⁻¹ of SPM (Fitzsimons *et al.*, 2006).
3. The overlying waters have an average composition for the N pool which is typical of estuarine waters (DON = 68.9 ± 22.4 (%) TDN; modified from Bronk, 2002).
4. The concentration of dissolved MAs in the water column is similar to that found for TE3 in March 2002 (Chapter 5) at low tide (~ 0.6 µM).

For a typical SPM concentration of 500 mg L^{-1} , $1\text{--}3 \text{ }\mu\text{M}$ of MAs desorbed from the Thames Estuary sediments at equilibrium (Fitzsimons *et al.*, 2006). The extent of MA flux to the water column as a result of tidal flushing and diffusion has not been quantified. Release by the clams could contribute up to $20 \text{ }\mu\text{mol L}^{-1}$ DON in the form of TMA at the onset of tidal inundation (i.e., a third of the burst flux of TMA observed at Ria Formosa Site (2), Fitzsimons *et al.*, 2005). The mean DON concentration for estuaries is $22.5 \pm 17.3 \text{ }\mu\text{M}$ (Bronk, 2002). The release of TMA by clams therefore, contributes significantly to the DON pool in the overlying water at the onset of tidal inundation, especially in areas of intensive mariculture. However, measurement of DON in the water column at different stages of the tidal cycle, along with sediment concentrations, will make similar models more accurate in predicting the impact of MAs on the N flux to overlying waters in inter-tidal sediments.



*(Bronk, *et al.*, 2002)
Fig. 6-1. Semi-quantitative conceptual map showing the impact of MAs on the cycling of N in a hypothetical inter-tidal system. *TDN = DON + NH_4^+ + (NO_3^- + NO_2^-).

6.1.2 Diagrammatic representation of the main conclusions of the study.

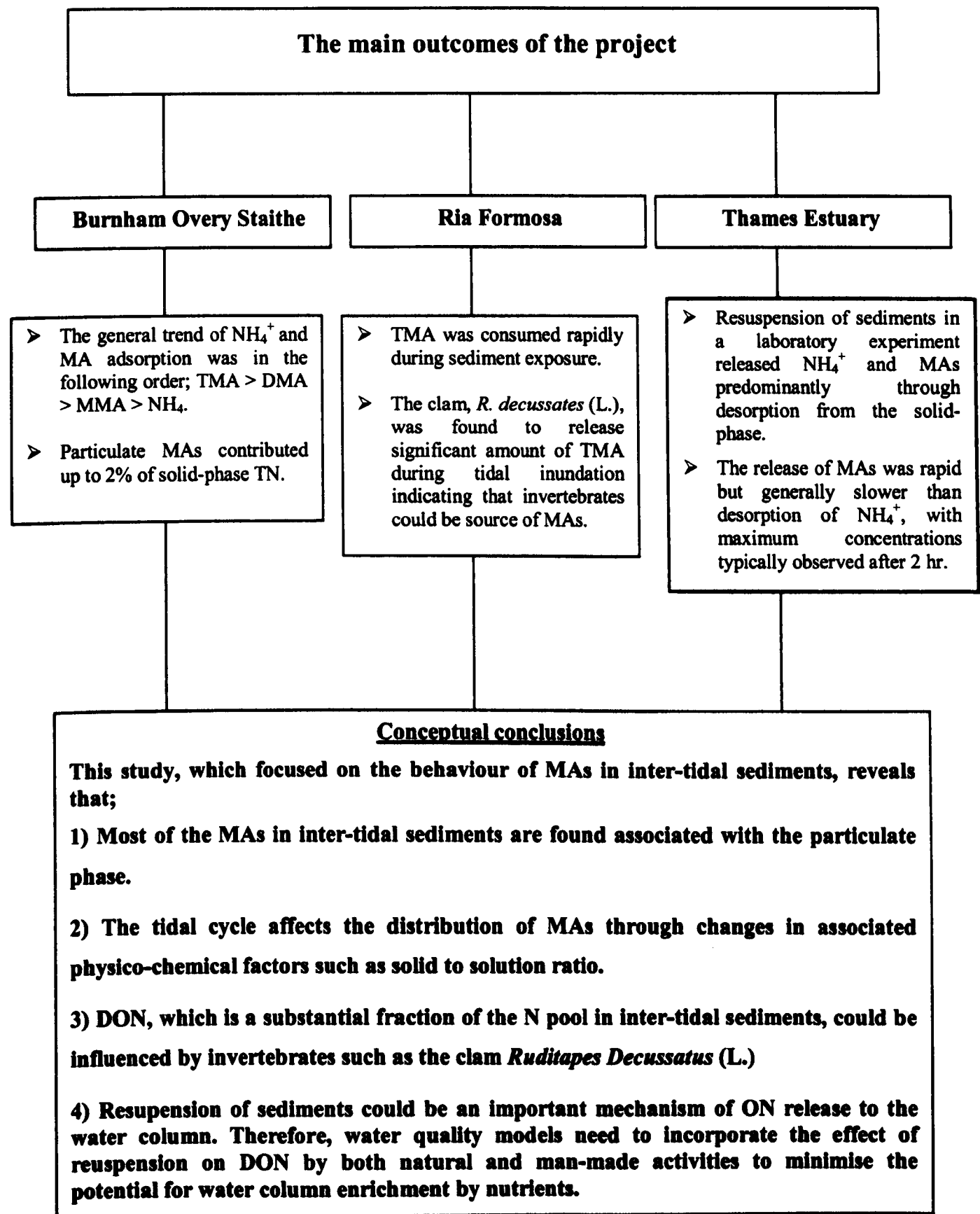


Figure 6-2. Conceptual model of the summary of the study.

6.2 Recommendations for further work.

Unsurprisingly, the study generated a number of questions worthy of further study. Differences in microbial and invertebrate populations need to be taken into account in future studies to, if possible, uncover their role in ON cycling in inter-tidal sediments. Currently, it is not possible to identify all the factors that influence the cycling and reactivity of particulate ON, due to limitations in our understanding of the role of microorganisms and bioturbation. The full picture of ON cycling in inter-tidal sediments can only be understood by collecting a number of highly spatially and temporally resolved data and constructing an ecosystem model. This model can then be tested by analysing environmental data to confirm its reliability and precision in predicting the behaviour of ON compounds in inter-tidal ecosystems under different physico-chemical parameters.

Although it is feasible that tidal flushing may have depleted pore-water MAs, this needs to be further investigated. The determination of MA distributions in living and non-living (poisoned) cores within a flume system at different stages of a simulated tidal cycle could achieve quantification of MA loss through flushing, diffusion and bacterial activity. This would also allow concurrent high resolution measurement of redox, pH, dissolved O₂ and temperature.

In this study, the clam *R. decussates* (L.) was found to release large amounts of TMA. It is not clear how the clam produces TMA although it seems likely that it could be a degradation product of its dietary intake. Quantification of the flux of benthic ON within the Ria Formosa sediments should lead to greater understanding of the impact of human activities, such as mariculture, on the water quality of the lagoon, which is crucial for its sustainable development.

Multi-volume extraction of Thames Estuary November samples revealed that cumulative extractable NH_4^+ increased with depth while cumulative extractable MAs decreased with depth. This is suspected to be the result of strongly adsorbed MAs being degraded by microorganisms during periods of lower fresh OM supply or the adsorbed MAs undergoing irreversible change with depth. ^{15}N -labelled MAs could be used in a laboratory study to identify their fate with depth by simulating seasonal differences in future studies.

References

- Abdul-Rashid, M., Riley, P.J., Fitzsimons, F.M. and Wolff, A.G. (1991). Determination of volatile amines in sediment and water samples, *Anal. Chimi. Acta.*, **252**:223-226.
- Abril, G., Nogueira, M., Etcheber, H., Cabezas, G., Lemaire, E. and Brogueira, M.J. (2002). Behaviour of organic carbon in nine contrasting European estuaries. *Estuar. Coast. Shelf Sci.*, **54**:241-262.
- Abril, J.M. and García-León, M. (1994). Modelling the distribution of suspended matter and the sedimentation process in a marine environment. *Ecological Modelling*, **71**:197-219.
- Adam, P. (1990). *Salt Marsh Ecology*, Cambridge University Press, Cambridge, p461.
- Admiraal, W. (1977). Tolerance of estuarine benthic diatoms to high concentrations of ammonia, nitrite ion, nitrate ion and orthophosphate. *Mar. Biol.*, **43**:307-315.
- Aller, R.C. (1982). The effect of macrobenthos on chemical properties of marine sediments and overlying water in P.L. Mc Call and M.J.S. Tevesz. (eds.). *Animal-Sediment Relations, The Biogenic Alterations of Sediments*, Plenum Press, New York, pp53-102.
- Anderson, F.E. (1972). Resuspension of estuarine sediments by small amplitude waves. *J. Sed. Petr.*, **42**:402-607.
- Anita, N.J., Harrison, P.J. and Oliveira, L. (1991). The role of dissolved organic nitrogen in phytoplankton nutrition, cell biology and ecology. *Phycologia*, **30**:1-89.
- Anthoni, U., Christophersen, C., Hougaard, L. and Neilsen, P.H. (1991). Quaternary ammonium compounds in the biosphere - An example of a versatile adaptive strategy. *Comp. Biochem. Physiol.*, **99B**:1-18.

- Asmus, R.M., Jensen, M.H., Jensen, K.M., Kristensen, E., Asmus, H. and Wille, A. (1998). The role of water movement and spatial scaling for measurement of dissolved inorganic nitrogen fluxes in inter-tidal sediments. *Estuar. Coast. Shelf Sci.*, **46**:221-232.
- Asmus, R. (1986). Nutrient fluxes in short-term enclosures of inter-tidal sand communities. *Ophelia*, **26**:1-18.
- Austin, M.C., Warwick, R.M., Rosado, M.C. and Castro, J.J. (1989). Meiobenthic and macrobenthic community structure along a putative pollution gradient in southern Portugal. *Mar. Poll. Bull.*, **20**:398-405.
- Bebianno, M. J. (1995). Effects of pollutants in the Ria Formosa Lagoon. *Sci. Total Env.*, **171**:107-115.
- Bender, M.L., Jahanke, R., Weiss, R., Martin, W., Heggie, D.T., Ovchado J. and Sower S.T. (1989). Organic carbon oxidation and benthic nitrogen and silica dynamics in San Clementine Basin, a continental borderland site. *Geochim. Cosmochim. Acta.*, **53**:689-697.
- Berner, R.A. (1980). *Early Diagenesis - A theoretical approach*. Princeton University Press, Princeton, N.J. p241.
- Berner, R.A. (1977). Stoichiometric models for nutrient regeneration in anoxic sediments. *Limnol. Oceanogr.* **22**(5):781-786.
- Berner, R.A. (1976). Inclusion of adsorption in the modelling of early diagenesis. *Earth Planet. Sci. Lett.*, **29**:333-340.
- Berounsky, V.M. and Nixon, S.W. (1993). Rates of nitrification along an estuarine gradient in Narragansett Bay. *Estuaries*, **16**:718-730.
- Blackburn, T. H. and Sørensen, J. (1988). Nitrogen Cycling in Coastal Marine Environments. *SCOPE 33*, Wiley & Sons, Chichester, p455.

- Blackburn, T. H. and Henriksen, K. (1983). Nitrogen cycling in different types of sediments from Danish waters. *Limnol. Oceanogr.*, **28**:477-493.
- Blackburn, T.H. (1980). Seasonal variation in the rate of organic N mineralization in anoxic marine sediments. In: *Biogéochimie de la matière organique al'interface eau-sédiment marine*, Edition du CNRS, Paris 173-183.
- Bordas, F. and Bourg, A. (2001). Effect of solid/liquid ratio on the remobilization of Cu, Pb, Cd and Zn from polluted river sediment. *Water, Air and Soil Pollution*, **128**: 391-400.
- Boynton, R. and Kemp, W.M. (1985). Nutrient regeneration and oxygen consumption by sediment along estuarine salinity gradient. *Mar. Ecol. Prog. Ser.*, **23**:45-55.
- Bradley, P.M. and Morris, J.T. (1990). Physical characteristics of salt marsh sediments: ecological implications. *Mar. Ecol. Prog. Ser.*, **61**:245-252.
- Brampton, A.H. (1992). Engineering significance of British salt marshes in J.R.L. Allen and K. Pye (eds.) *salt Marshes: 112-22*, Cambridge University Press, Cambridge, p184.
- Bronk, D. A. (2002). The Dynamics of DON, in D.A. Hansell and C.A. Carlson (eds.) *Biogeochemistry of Marine Dissolved Organic Matter*. Academic Press, New York, pp153-247.
- Bronk, D.A., Glibert, P.M. and Ward, B.B. (1994). Nitrogen uptake, dissolved organic nitrogen release, and new production. *Science*, **265**:1843–1846.
- Burdige, D.J. and Gardner, K.G. (1998). Molecular weight distribution of dissolved organic carbon in marine sediment pore-waters. *Mar. Chem.*, **62**:45-64.
- Burdige, D. and Zheng, S. (1998). The biogeochemical cycling of dissolved organic nitrogen in estuarine sediments. *Limnol. Oceanogr.*, **43**:1796–1813.

- Calvet, R., Bourgeois, S. and Msaky J.J. (1990). Some experiments on extraction of heavy-metals present in soil. *Int. J. Anal. Chem.*, **39**(1):31-45.
- Carpenter, E. J. and Capone, D. G. (1983). In *Nitrogen in the Marine Environment* (eds.), Plenum Press, New York, pp649-678.
- Carpenter, E.J. and Dunham, S. (1985). Nitrogenous nutrient uptake, primary production, and species composition of phytoplankton in the Carmans River Estuary, Long Island, New York. *Limnol. Oceanogr.*, **30**:513-526.
- Chorst, R.J. and Riemann, B. (1994). Storm-simulated enzymatic decomposition of organic matter in benthic/pelagic coastal mesocosms. *Mar. Ecol. Prog. Ser.*, **108**:185-192.
- Christensen, D. and Blackburn, T.H. (1982). Turnover of ^{14}C -labelled acetate in marine sediments. *Mar. Biol.*, **71**:113-119.
- Christensen, D. and Blackburn, T.H. (1980). Turnover of ^{14}C -labelled alanine in marine sediments. *Mar. Biol.*, **58**:97-103.
- Clayden, J., Greeves, N., Warren, S., Wothers, P. (2001). *Organic Chemistry*. Oxford University Press. p1512.
- Cloern, J.E. (2001). Our evolving conceptual model of the coastal eutrophication problem. *Mar. Ecol. Prog. Ser.*, **201**:223-253.
- da Costa, K.A., Vrbanc, J.J. and Zeisel, S.H. (1990). The measurement of dimethylamine, trimethylamine and trimethylamine N-oxide using capillary gas chromatography-mass spectrometry. *Anal. Biochem.*, **187**(2):234-239.
- dal Pont, G., Hogan, M. and Newll, B. (1974). Laboratory techniques in marine chemistry II. Determination of ammonia in seawater and the preservation of samples for nitrate analysis. *Commonwealth scientific and Industrial Research organisation, Division of Fisheries and Oceanography, Report 55*, p8.

- Darley, W.M., Montague, C.L., Plumley, F.G., Sage, W.W. and Psalidas, A.T. (1981). Factors limiting edaphic algal biomass and productivity in a Georgia salt marsh. *J. Phycol.*, **17**:122-128.
- Davis, J. A. (1982). Adsorption of natural dissolved organic matter at the oxide/water interface. *Geochim. Cosmochim. Acta*, **46**:2381-2394.
- Dennison, W.C. and Abal, E.G. (1999). *Moreton Bay Study: A Scientific Basis for the Healthy Waterways Campaign, South East Queensland Water Quality Management Strategy*, p245.
- de Vooy, C.G.N. (2002). Occurrence and role of a Quaternary base, trimethylamine oxide, in two cockle species, *Cerastoderma edule* and *Cerastoderma lamarcki*. *J. Sea Res.*, **47**:69-73.
- Dinis, M.T. (1992). Situacao da aquacultura no Algarve: perspectivas e condicionantes. In: *Mesas redondas, Ponte International do Guadiana, Fev., 1992*.
- Dzombak, D.A. and Morel, F.M.M. (1990). *Surface complexation modelling: Hydrous Ferric Oxide*, Wiley, New York.
- Ertel, J.R., Hedges, J.I., Devol, A.H., Richey, J.E. and Ribeiro, M. (1986). Dissolved humic substances of the Amazon River system. *Limnol. Oceanogr.*, **31**:739-754.
- Falcão, M., Gaspar, M.B., Caetano, M., Santosb, M.N. and Vale, C. (2003). Short-term environmental impact of clam dredging in coastal waters (south of Portugal): Chemical disturbance and subsequent recovery of seabed. *Mar. Environ. Res.* **56**:649-664.
- Falcão, M. and Vale, C. (1995). Tidal flushing of ammonium from inter-tidal sediments of Ria Formosa, Portugal. *Netherlands J. Aqua. Ecol.*, **29**:239-244.
- Fanning, K.A., Carter, K.L. and Betzer, P.R. (1992). Sediment re-suspension by coastal waters: A potential mechanism for nutrient re-cycling on the ocean's margins. *Deep Sea Res.*, **8**:953-965.

- Fessenden, R. J. and Fessenden, J.S. (1982). *Organic Chemistry*, Second ed. Willard Grant Press, Boston.
- Fisher, T. R., J. D. Hagy, and E. J. Rochelle-Newall (1998). Dissolved and particulate organic carbon in Chesapeake Bay. *Estuaries*, **21**:215-229.
- Fitzsimons M.F., Millward G.E., Revitt D.M. and Dawit M.D. (2006). Desorption kinetics of ammonium and methylamines from estuarine sediments: Consequences for the cycling of nitrogen. *Mar. Chem.*, **101**:12-26.
- Fitzsimons, M.F., Dawit, M., Revitt, D.M. and Rocha, C. (2005). Effects of early tidal inundation on the cycling of methylamines in inter-tidal sediments. *Mar. Ecol. Prog. Ser.*, **294**:51-61.
- Fitzsimons, M.F., Kamhi-Danon, B. and Dawit, M. (2001). Tidal control on distributions of the methylamines in an East-Anglian estuary: a potential role for benthic invertebrates? *Environ. Experim. Bot.*, **46**:225-236.
- Fitzsimons, M.F., Jemmett, A.W. and Wolff, G.A. (1997). Distributions of the methylamines in a heterogeneous salt marsh through a tidal cycle. *Org. Geochem.*, **27**(1):15-24.
- Froelich, P.N., Klinckhamer, G.P, Bender, L.A., Luedke, N.A., Heath, G.R., Cullen, D., Dauphin, P., Hammond, D., Hartman, B. and Maynard, V. (1979). Early oxidation of organic matter in pelagic sediments of the eastern equatorial Atlantic: suboxic diagenesis. *Geochimica. Cosmochimica. Acta.*, **43**:1075-1090.
- Gardner, W.S., McCarthy, M.J., An, S., Sobolev, D., Sell, K.S., Brock, D. (2006). Nitrogen fixation and dissimilatory nitrate reduction to ammonium (DNRA) support nitrogen dynamics in Texas estuaries. *Limnol. Oceanogr.*, **51**:558-568.
- Giani, D., Giani, L., Cohen, Y. and Krumbein, W. (1984). *FEMS, Microbiol. Lett.*, **24**: 219-224. *Biogeo. Cyc.*, **13**:161-178.

- Gibb, S.W., Fauzi, R., Mantoura, C. and Liss, P.S. (1999). Ocean-atmosphere exchange and atmospheric speciation of ammonia and methylamines in the region of the NW Arabian Sea. *Global Biogeochem. Cycles*, **13**:161-178.
- Glibert, P.M., Dennett, M.R. and Caron, D.A. (1988). Nitrogen uptake and NH_4^+ regeneration by pelagic microplankton and marine snow from the North Atlantic, J., *Mar. Res.*, **46**:837-852.
- Gordon, D. (1971). Distribution of particulate organic carbon and nitrogen at and oceanic station in the central Pacific. *Deep Sea Res.*, **18**:1127– 1134.
- Harvey, J.W. and Odum W.E. (1990). The influence of tidal marshes on upland groundwater discharge to estuaries. *Biogeochem.*, **10**:217-236.
- Hedges, J.I. (1988). Polymerisation of humic substances in natural environments, in F.H. Frimmel and R.F. Christman (eds.) *Humic substances and their role in the environment*. John Wiley & Sons, New York, pp45–58.
- Hedges, J.I. and Kiel, R.G. (1999). Organic geochemical perspectives on estuarine processes: Sorption reactions and consequences. *Mar. Chem.*, **65**:55-65.
- Hedges, J.I., Cowie, G.L., Richey, J.E., Quay, P.D., Benner, R., Strom, M. and Forsberg, B.R. (1994). Origins and processing of organic matter in the Amazon River as indicated by carbohydrates and amino acids. *Limnol. Oceanogr.*, **39**:743-761.
- Heggie, D., Maris, C., Hudson, A., Dymond, J., Beach, R., and Cullen, J. (1987). Organic carbon oxidation and preservation in NW Atlantic continental margin sediments, in P. P. E. Weaver and J. Thomson *Geology and Geochemistry of Abyssal Plains* (eds.), Blackwell Science, pp215–236.
- Hemminga, M.A., Koutstaal, B.P., van Soelen, J. and Merks, A.G.A. (1994). The nitrogen supply to inter-tidal eelgrass (*Zostera marina*). *Mar. Biol.*, **118**(2): 223-228.
- Henrichs, S. M. (1995). Sedimentary organic matter preservation: an assessment and speculative synthesis - a comment. *Mar. Chem.*, **49**:127-136.

- Henrichs, S.M. and Sugai, S.F. (1993). Adsorption of amino acids and glucose by sediments of Resurrection Bay, Alaska, USA: functional group effects. *Geochim. Cosmochim. Acta.*, **57**:823-835.
- Herbert, R.A. (1999). Nitrogen cycling in coastal marine ecosystems. *FEMS: Microbiol Rev.*, **23**:563-590.
- Huheey, J.E., (1983). *Inorganic Chemistry, Third ed.* Harper and Row, New York.
- Jackson, G.A. and Williams, P.M. (1985). Importance of dissolved organic nitrogen and phosphorus to biological nutrient cycling. *Deep Sea Res.*, **32**:223-235.
- Jørgensen, N.O.G., Kroer, N., Coffin, R.B. and Hock, M.B. (1999). Relations between bacterial nitrogen metabolism and growth efficiency in an estuarine and an open ecosystem. *Mar. Ecol. Prog. Ser.*, **98**:135 -148.
- Jørgensen, B.B. (1983). Processes at the sediment-water interface: The Major Biogeochemical cycles and Their Interaction, in B. Bolin and R.B. Cook (eds.), *SCOPE*, pp477-515.
- Jørgensen, B.B. (1982). Mineralization of organic matter in the sea bed - The role of sulphate reduction. *Nature*, **296**:643-645.
- Keil, R.G., Montluçon, D.B., Prahl, F.G. and Hedges, J. (1994). Sorptive preservation of labile organic matter in marine sediments. *Nature*, **370**: 549-552.
- Kerner, M. and Wallman, K. (1992). Remobilisation events involving Cd and Zn from inter-tidal flat sediments in the Elbe Estuary during the tidal cycle. *Estua. Coast Shelf Sci.*, **35**:371-393.
- Kim, S.G., Bae, H.S., Oh H.M., Lee, S.T. (2003). Isolation and characterisation of novel halotolerant and/or halophilic denitrifying bacteria with versatile metabolic pathways for the degradation of trimethylamine. *FEMS, Microbiol Lett.*, **225**:263-269.

- Kimmerer, W.J., Smith, S.V. and Hollibaugh, J.T. (1993). A simple heuristic model of nutrient cycling in an estuary. *Estuar. Coast. Shelf Sci.*, **37**:145-159.
- King, G.M., Klug M.J., and Lovely, D.R. (1983). Metabolism of acetate, methanol, and methylated amines in inter-tidal sediments of Lowes Cove, *Marine. Appl. Environ. Microbiol.*, **45**:1848-1853.
- King, G.M. (1988). Distribution and metabolism of quaternary amines in marine sediments, in Blackburn, T.H. and Sorensen, J. (eds.). Nitrogen Cycling in Coastal Marine Environments. *SCOPE*, Wiley, New York, pp143-173.
- Kinniburgh, J. (1998). Physical and chemical characteristics of the Thames Estuary, in M.J. Attrill (ed.). *A Rehabilitated Estuarine Ecosystem*, Kluwer Academic Publishers pp27-48.
- Kristensen, E., Jensen, M.H., Aller, R.C. (1991). Direct measurement of dissolved inorganic nitrogen exchange and denitrification in individual polychaete (*Nereis virens*) burrows. *J. Mar. Res.*, **49**:355-377.
- Kristensen, E. (1985). Oxygen and Inorganic Nitrogen Exchange in a *Nereis virens* (Polychaeta) bioturbated sediment-water system *J. Coastal Res.*, **1/2**:109-116.
- Kristensen, E. (1984). Effect of natural concentrations on nutrient exchange between a polychaete burrow in estuarine sediment and the overlying water. *JEMBE*, **75**:171-190.
- Klump, J.V. and Martens, C.S. (1989). The seasonality of nutrient regeneration in organic rich coastal sediment: Kinetic modeling of changing pore-water nutrient and sulfur distributions. *Limnol. Oceanogr.*, **34**:559-77.
- Krone, R.B. (1966). *Predicted suspended sediment inflows to the San Francisco Bay system*. Report prepared for the Central Pacific River Basins Comprehensive Water Pollution Project, Federal Water Pollution Control Administration Southwest Region, p133.

- Kuwata, K., Akyima, E., Yamazaki, Y., Yamasaki, H. and Kuge, Y. (1983). Trace determination of Low Molecular Weight Aliphatic Amines in Air by Gas Chromatography. *Anal. Chem.*, **55**:2199-2201.
- Laima, M.J.C. (1992). Extraction and seasonal variation of NH_4^+ pools in different types of coastal marine sediments. *Mar. Ecol. Prog. Ser.*, **82**:75-84.
- Lam, D.C.L. and Jaquet, J.M. (1976). Computations of physical transport and regeneration of phosphorus in Lake Erie, Fall 1970. *Journal of Fisheries Resources Board, Canada*, **33**:550.
- Lee, C. (1992). Controls on organic carbon preservation: The use of stratified water bodies to compare intrinsic rates of decomposition in oxic and anoxic systems *Geochim. Cosmochim. Acta.*, **56**:3323-3335.
- Lee, C. (1988). Nitrogen Cycling in Coastal Marine Environment, in Blackburn and Sorensen (eds.), *SCOPE*, John Wiley and Sons Ltd, p137.
- Lee, C. and Cronin, C. (1982). The vertical flux of particulate organic nitrogen in the sea: decomposition of amino acids in the Peru upwelling area and the equatorial Atlantic. *J. Mar. Res.*, **40**:227-51.
- Lee, C. and Olsen, B.L. (1984). Dissolved exchangeable and bound amines in marine sediments, in Blackburn and Sorensen (eds.), Nitrogen Cycling in Coastal Marine Environment, *SCOPE*, John Wiley and Sons Ltd. pp125-141.
- Lomstein, B.A., Jensen, A.G.U., Hansen, J.W., Andresen, J.B., Hansen, L.S., Berntsen, J. and Kunzendorf, H. (1998). Budgets of sediment nitrogen and carbon cycling in the shallow water of Knebel Vig, Denmark, *Aquat. Microb. Ecol.*, **14**:69–80.
- Mackin, J.E. and Aller, R.C. (1984). Ammonium adsorption in marine sediments. *Limnol. Oceanogr.*, **29**:250-257.

- Maksymowska-Brossard, D. and Piekarek-Jankowska, H. (2001). Seasonal variability of benthic ammonium release in the surface sediments of the Gulf of Gdansk (Southern Baltic Sea). *Oceanologia*, **43**(1):113-136.
- Malcolm, S.J. and Sivy, D.B. (1997). Nutrient cycling in inter-tidal sediments. In *Biogeochemistry of inter-tidal sediments*. pp84-96, Cambridge University Press, Cambridge.
- Marzo, A. and Curti, S. (1997). L-Carnitine moiety assay: An up-to-date reappraisal covering the commonest methods for various applications. *J. Chromatogr.*, **702**:1-20.
- Mayer, L.M. (1993). Organic Matter at the sediment–water interface. In: *Organic Geochemistry: Principles and Applications* in M.H. Engel. and S.A. Macko (eds.), Plenum Press, New York, pp171-184.
- Middleburg, J. J. and Nieuwenhuize, J. (2000). Uptake of dissolved inorganic nitrogen in turbid, tidal estuaries. *Mar. Ecol. Prog. Ser.*, **192**:79-88.
- Millward, G.E. and Liu, Y.P. (2003). Modelling metal desorption kinetics in estuaries. *Sci. Total Environ.*, **314**:613-623.
- Montluçon, D.B. and Lee, C. (2001). Factors affecting lysine sorption in a coastal sediment. *Org. Geochem.*, **32**:933-942.
- Morin, J. and Morse, J.W. (1999). Ammonium release from resuspended sediments in the Laguna Madre Estuary. *Mar. Chem.*, **65**:97-110.
- Mudge, S.M., Bebianno, M.J., East, J.A. and Barreira, L.A. (1999). Sterols in the Ria Formosa lagoon, Portugal, *Wat. Res.*, **33** (4):1038-1048.
- Mudge, S.M. and Seguel, C.G. (1997). Trace organic contaminants and lipid biomarkers in Cocepcion and San Vicente Bays, *Biol. Soc. Chil. Quim.*, **42**:5-15.

- Murrell, M.C., Hollibaugh, J.T. (2000). Distribution and composition of dissolved and particulate organic carbon in northern San Francisco Bay during low flow conditions. *Estu. Coastal and Shelf Sci.*, **51**:75-90.
- Nagata, T. and Kirchman, D.L. (1996). Bacterial degradation of protein adsorbed to model submicron particles in seawater, *Mar. Ecol. Prog. Ser.*, **132**:241-248.
- Neira, C. and Hopner, T. (1993). Fecal pellet production and sediment reworking potential of the polychaete *Heteromastus filiformis* show a tide dependent periodicity. *Ophelia*, **37**:175-185.
- Newton, A., Icelyb, J.D., Falcaoc, M., Nobred, A., Nunesd, J.P., Ferreirad, J.G. and Val, C. (2003). Evaluation of eutrophication in the Ria Formosa coastal lagoon, Portugal. *Continental Shelf Res.*, **23**:1945–1961.
- Nixon, S.W. (1992). Quantifying the relationship between nitrogen input and the productivity of marine ecosystems. *Proceed. Adv. Mar. Tech. conf.*, Tokyo, **5**:57-83.
- Nixon, S.W. (1988). Physical energy inputs and the comparative ecology of lake and marine ecosystems. *Limnol. Oceanogr.*, **33**(4):1005-1025.
- Nixon, S.W. (1986). Nutrient dynamics and the productivity of coastal waters, in Hallway R., Clayton D. and Behbehani M. (Eds.) *Marine Environment and Pollution*, The Alden Press, Oxford, pp97-115.
- Nixon, S.W. (1981). Remineralisation and nutrient cycling in coastal marine ecosystems, in Neilson, B. and L. Cronin (eds.) *Estuaries and Nutrients*, Humana Press, Clifton, New Jersey, pp111-138.
- Nowicki, B.L. (1994). The effect of temperature, oxygen, salinity and nutrient enrichment on estuarine denitrification rates measured with a modified nitrogen gas flux technique. *Estuar. Coast. Shelf Sci.*, **38**:137-556.

- Nowicki, B.L. and Oviatt, T. (1990). Are estuaries trap for anthropogenic nutrients? Evidence from estuarine mesocosms. *Mar. Ecol. Prog. Ser.*, **66**:131-46.
- Oremland, R.S., Marsh, L.M. and Polcin, S. (1982). Methane production and simultaneous sulphate reduction in Anoxic, Salt Marsh Sediments. *Nature*, **296**:143-145.
- Owens, N. J. P., Burkill, P. H., Mantoura, R. F. C., Woodward, E. M. S., Bellan, I. E., Aiken, J., Howland, R. J. M. and Llewellyn, C. A.. (1993). Size-fractionated primary production and nitrogen assimilation in the northwestern Indian Ocean. *Deep Sea Res. Part II: Topical Studies in Oceanography*, **40**(3):697-709.
- Raaphorst, W.V. and Malschaert, J.F.P. (1996). Ammonium adsorption in superficial North Sea sediments. *Cont. Shelf Res.*, **16**:1415-1435.
- Raffaelli, D. and Hawkins, S. (1999). *Inter-tidal Ecology*, Kluwer Academic Publishers, Dordrecht.
- Raffaelli, D. and Cha, D. (1995). Interactions between macroalgal mats and invertebrates. *Oceanography and Marine Biology an Annual Review*.
- Revsbech, L. B. Nielsen, L., Christensen, B., and Scorensn, J. (1988). A combined oxygen and nitrous oxide microsensor for denitrification studies. *Appl. Environ. Microbiol.*, **54**:2245-2249.
- Riedl, R. J. and Machan, E. A. (1972). Hydrodynamic patterns in lotic inter-tidal sands and their bioclimatological implications. *Mar. Biol.*, **13**:179-209.
- Riley, J.P. and Sinhaseni, P. (1957). The determination of ammonia and total inorganic nitrogen in Seawater. *J. Mar. Biol. Assoc. UK.*, **36**:161-168.
- Rocha, C., Mesquita, S., Vidal, S. and Galvão, H. (2001). Impact of Clam harvesting on benthic nitrifiers in sandy inter-tidal sediments of the Ria Formosa Coastal lagoon, Portugal. *J. Coastal Res.*, **SI 34 (ICS 2000 New Zealand)**: 623-632.

- Rocha, C. (2000). Density-driven convection during flooding of warm, permeable inter-tidal sediments: the ecological importance of the convective turnover pump. *J. Sea Res.*, **43**:1–14.
- Rocha, C. (1998). Rhythmic ammonium regeneration and flushing in inter-tidal sediments of the Sado Estuary. *Limnol. Oceanogr.*, **43**: 823-831.
- Rocha, C. and Cabral, A.P. (1998). The influence of tidal action on pore-water nitrate concentration and dynamics in inter-tidal sediments of the Sado Estuary. *Estuaries* **21**: 635–645.
- Roman, R.R. and Tenore, K.R. (1978). Tidal resuspension in Buzzard's Bay, Massachusetts. I. Seasonal changes in the resuspension of organic carbon and chlorophyll. *Estua. Coastal Mar. Sci.*, **6**:37-46.
- Rosenfeld, J.K. (1979). Ammonium adsorption in near shore anoxic sediments. *Limnol. Oceanogr.*, **24**:356-364.
- Schink, D.R., Guinasso, N.L., Jr. (1978). Redistribution of dissolved and adsorbed materials in abyssal marine sediments undergoing biological stirring. *American J. Sci.*, **278**:687-702.
- Schubel, J.R. (1968). Suspended sediment of northern Chesapeake Bay. *Chesapeake Bay Institute Technical Report*, **35**:264 pp.
- Scully, F.E. J.R., Howell, G.D., Penn, H.H., Mazina, K. and Johnson, J.D. (1988). Small molecular weight organic amino nitrogen compounds in treated municipal waste-water. *Environ. Sci. Tech.*, **22**:1186-1190.
- Seibel, B.A. and Walsh, P.J. (2002). Trimethylamine oxide accumulation in marine animals: Relationship to acylglycerol storage. *J. Exp Biol.*, **205**:297-1236.
- Seitzinger, S.P., Sanders, R.W. and Styles, R. (2002). Bioavailability of DON from natural and anthropogenic sources to estuarine plankton. *Limnol. Oceanogr.* **47**:353-366.

- Seitzinger, S.P and Sanders, R.W. (1997). Contribution of dissolved organic nitrogen from rivers to estuarine eutrophication. *Mar. Ecol. Progr. Ser.*, **159**:1-12.
- Seitzinger, S.P., Nixon S.W. and Pilson, M.E. (1984). Denitrification and nitrous oxide production in coastal marine ecosystems. *Limnol. Oceanogr.*, **29**:73-83.
- Shiedler, G.L. (1984). Suspended sediment responses in a wind dominated estuary of the Texas Gulf Coast. *J. Sed. Petr.*, **54**:731-745.
- Sigg, L. and Stumm, W. (1981). The interaction of anions and weak acids with the hydrous goethite (α -FeOOH) surface. *Colloids Surf.*, **2**:101-117.
- Simon, N. S. (1988). Nitrogen cycling between sediment and the shallow-water column in the transition zone of the Potomac river and estuary. I. Nitrate and ammonium fluxes. *Estuar. Coast. Shelf Sci.*, **26**:483-497.
- Simon, N.S. (1988). Nitrogen Cycling between Sediment and the Shallow-Water Column in the Transition Zone of the Potomac River and Estuary. II. The Role of Wind-Driven Resuspension and Adsorbed Ammonium, *Estuar. Coast. Shelf Sci.*, **28**: 531-547.
- Sloth, N.P., Riemann, B., Nielsen, L.P. and Blackburn, T.H. (1996). Resilience of pelagic and benthic microbial communities to sediment resuspension in a coastal ecosystem, Knebel Vig, Denmark. *Estuar. Coast. Shelf Sci.*, **42**:405-415.
- Sobral, P. and Widdows, J. (1997). Influence of hypoxia and anoxia on the physiological responses of the clam *Ruditapes decussatus* from southern Portugal. *Mar. Biol.*, **127**:455-461.
- Solomons, T.W.G. (1996). Organic Chemistry, Sixth ed. Wiley New York.
- Sorensen, J. and Glob, E. (1987). Influence of benthic fauna on trimethylamine concentrations in coastal marine sediments. *Mar. Ecol. Prog. Ser.*, **39**:15-21.

- Spiro, T.G. and Stigliani, W.M. (1996). *Chemistry of the Environment*. Prentice Hall Publishing Company, New Jersey.
- Sprung, M. (1994). Macrobenthic secondary production in the inter-tidal zone of the Ria Formosa, a lagoon in Southern Portugal. *Estuar Coast Shelf Sci.* **38**:539–558.
- Stumm, W. and Morgan, J. (1996). *Aquatic Chemistry*. Third ed. Wiley and sons, New York.
- Sugai, F. and Henrichs, S.M. (1992). Rates of amino acid uptake and mineralization in Resurrection Bay (Alaska) sediment. *Mar. Ecol. Prog. Ser.*, **88**:129-141.
- Sullivan, M. J. and Daiber, F. C. (1975). Light, nitrogen, and phosphorus limitation of edaphicalgae in a Delaware salt marsh. *J. Exp. Mar. Biol. Ecol.*, **18**:79-88.
- Tersashi, A., Handa, Y., Kido, A and Shinohara, R. (1990). Determination of primary and secondary aliphatic amines in the environment as sulphonamide derivatives by GC-MS. *J. Chrom.*, **503**:369-375.
- Thamdrup, B. and Dalsgaard, T. (2002). Production of N₂ through Anaerobic ammonium oxidation coupled to nitrate reduction in marine sediments. *Appl. And Env. Microbiol.*, **68**(3):1312-1318.
- Tinsley, D. (1998). *The Thames Estuary: a history of the impact of humans on the environment and a description of the current approach to environmental management. A Rehabilitated Estuarine Ecosystem: the environment and ecology of the Thames Estuary* (ed. M.J. Attrill), pp5–26, Kluwer Academic Publishers, Dordrecht.
- Tipping, E. (1981). The adsorption of aquatic humic substances by iron oxides. *Geochim. Cosmochim. Acta.*, **55**:191-199.
- Trimmer, M., Gowen, R.J. and Stewart, B.M. (2003). Changes in sediment processes across the western Irish Sea front. *Estuar. Coast Shelf Sci.*, **56**:1011-1019.

- Trimmer, M., Nedwell, D.B., Sivyer, D.B. and Malcolm, S.J. (2000). Seasonal benthic organic matter mineralisation measured by oxygen uptake and denitrification along a transect of the inner and outer River Thames estuary, UK. *Mar. Ecol. Prog. Ser.*, **197**: 103-119.

- Ullman, W.J and Sandstrom, M.W. (1987). Dissolved nutrient fluxes from near shore sediment of Bowling Green Bay, Central Great Barrier Reef Lagoon (Australia). *Estuar. Coast. Shelf Sci.*, **24**:289-303.

- Usui, T., Koike, I. and Ogura, N. (2001). N₂O production, nitrification and denitrification in an estuarine environment. *Estuar. Coast. Shelf Sci.*, **52**:769-781.

- Usui, T., Koike, I. and Ogura, N. (1998). Tidal effect on dynamics of pore-water nitrate in inter-tidal sediment of a eutrophic estuary. *J. Oceanogr.*, **54**:205-216.

- Valiela, I., Teal, J.M., Volkmann, S., Shafer, D. and Carpenter, E.J. (1980). On the measurement of tidal exchanges and groundwater flow in salt marshes. *Limnol. Oceanogr.*, **25**:187-192.

- Valiela, I., Teal, J.M., Volkmann, S., Shafer, D. and Carpenter, E.J. (1978). Nutrient and particulate fluxes in a salt marsh ecosystem: Tidal exchanges and inputs by precipitation and groundwater. *Limnol. Oceanogr.*, **23**:798-812.

- Vörosmary, C.J. and Loder, T.C. (1994). Spring-neap tidal contrasts and nutrient dynamics in a marsh-dominated estuary. *Estuaries*, **17**:537-551

- Wakeham, S.G., Lee, C., Farrington, J.W. and Gagosian, R.B. (1984). *Biogeochemistry of particulate organic matter in the oceans: Results from sediment trap experiments.* **31**:509-528.

- Walsh, T. W. (1989). Total dissolved nitrogen in seawater: A new high temperature combustion method and a comparison with photo-oxidation. *Mar. Chem.*, **26**:295–310.

- Wang, X. C and Lee, C. (1995). Decomposition of aliphatic amines and amino acids in anoxic salt marsh sediment. *Geochim. Cosmochim. Acta.*, **59**:1787-1797.
- Wang, X.C and Lee, C. (1994). Sources and distribution of aliphatic amines in salt marsh sediment. *Org. Geo.* **22**:(6)1005-1021.
- Wang X.C. and Lee C. (1993). Adsorption and desorption of aliphatic amines, amino acids and acetate by clay minerals and marine sediments. *Mar. Chem.*, **44**:1-23.
- Wang, X-C and Lee, C. (1990). The distribution and adsorption behavior of aliphatic amines in marine and lacustrine sediments, *Geochim. Cosmochim. Acta.*, **54**:2759-2774.
- Wilson, T.R.S. (1975). The major constituents of seawater. In: (J.P. Riley and G. Skirrow, eds.). *Chemical Oceanography*. **1**(2):365-413. Academic Press.
- Yamamuro, M. and Kayanne, H. (1995). Rapid determination of organic carbon and nitrogen in carbonate bearing sediments with Yanaco MT-5 CHN analyser. *Limnol. Oceanogr.*, **40**:1001-1005.
- Zhang, J., Liu, S.M., Xu, H., Yu, Z.G., Lai, S.Q., Zhang, H., Geng, G.Y. and Chen, J.F. (1998). Riverine sources and estuarine fates of particulate organic carbon from North China in late summer. *Estuar. Coast. Shelf Sci.*, **46**:439-448.

GLOSSARY

- **Aphotic zone**: deepest and largest zone, which is a region of darkness extending to the seafloor where the only light source is bioluminescence.
- **Benthic environment**: includes the sea floor and those species of plants and animals that live on or within the sea bed form the benthos.
- **Biogeochemical cycle**: closed circuit described by an essential element (e.g. carbon (C), sulphur (S) or nitrogen (N) as it passes from within organisms (biotic phase) into physical, i.e. geochemical, environment (abiotic phase), and back again.
- **Biogeochemistry**: the study of the distribution and movement of chemical elements present in living organisms in relation to their geographical environment, and the movement of elements between living organisms and their non-living environment.
- **Detritus**: A Mass of substance gradually worn off solid bodies; an aggregate of loosened fragments; especially of rock and accumulated debris.
- **Diagenesis**: the sum total of processes that bring about changes in sediment or sedimentary rocks subsequent to its deposition in water. Early diagenesis occurs during the burial of the deposits to a depth of a few hundred metres.
- **Dissolved Organic matter (DOM)**. is operationally defined as the material that passes through a filter paper (0.45µm) when seawater is passed through it.
- **Estuary**: That part of a river where fresh water meets the open sea. Estuaries are semi – enclosed body of water with a free connection to the sea and at least one fresh water inflow.
- **Euphotic zone**: the region where light is sufficient for growth of plants (0-150 m in clear ocean water).

- **Inter-tidal:** occurring between high-tide and low-tide marks: occurring within or forming the area between high and low tide levels in a coastal zone.
- **Limiting nutrients:** such as nitrogen and phosphorous (and silica for diatoms) that can slow photosynthetic rates.
- **Mineralisation:** Decomposition of organic matter into simple molecules.
- **New production:** is defined as that part of primary production sustained by nitrogen inputs from upwelling benthic mineralization or terrestrial run off (mainly; NO_3^-).
- **Particulate organic matter (POM):** is operationally defined as the material retained on a filter paper (0.45 μm) when seawater is passed through it.
- **Nitrogen uptake:** the transformation of nitrogen in soluble substrate form into cellular nitrogen bound in organisms.
- **Osmosis:** is the net movement of solvent molecules across a selectively permeable membrane from an area with high concentration of solvent molecules to an area of lower concentration. In living system the chief solvent is water.
- **Pelagic environment:** that of the water column from the sea surface to the waters immediately above the seafloor.
- **Regenerated:** is defined as that part of nitrogen available to organisms as a result of sediment mineralization from rapidly degradable organic matter and planktonic mineralisation mainly NH_4^+ .
- **Remineralisation:** The decomposition of organic matter to its constituent compounds.

Appendix

A. 1 Additional data for Thames Estuary samples

A. 1.1 Grain size analysis

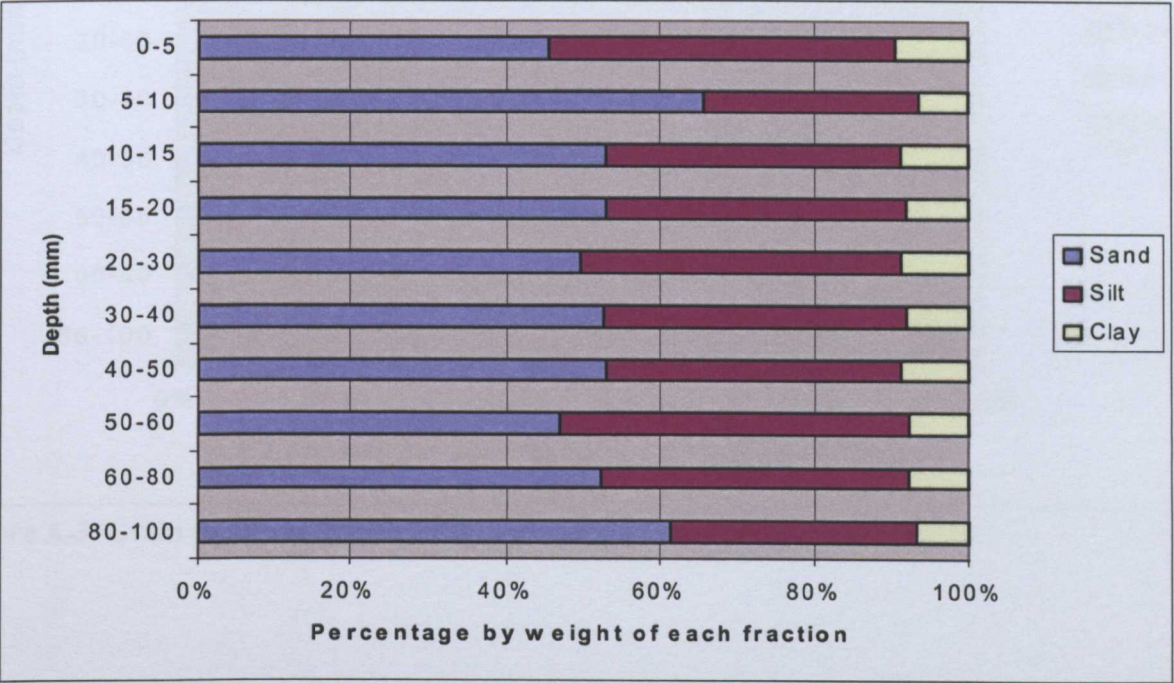


Figure A-1. Grain size proportion of sediment samples, Thames Estuary (TEJ1).

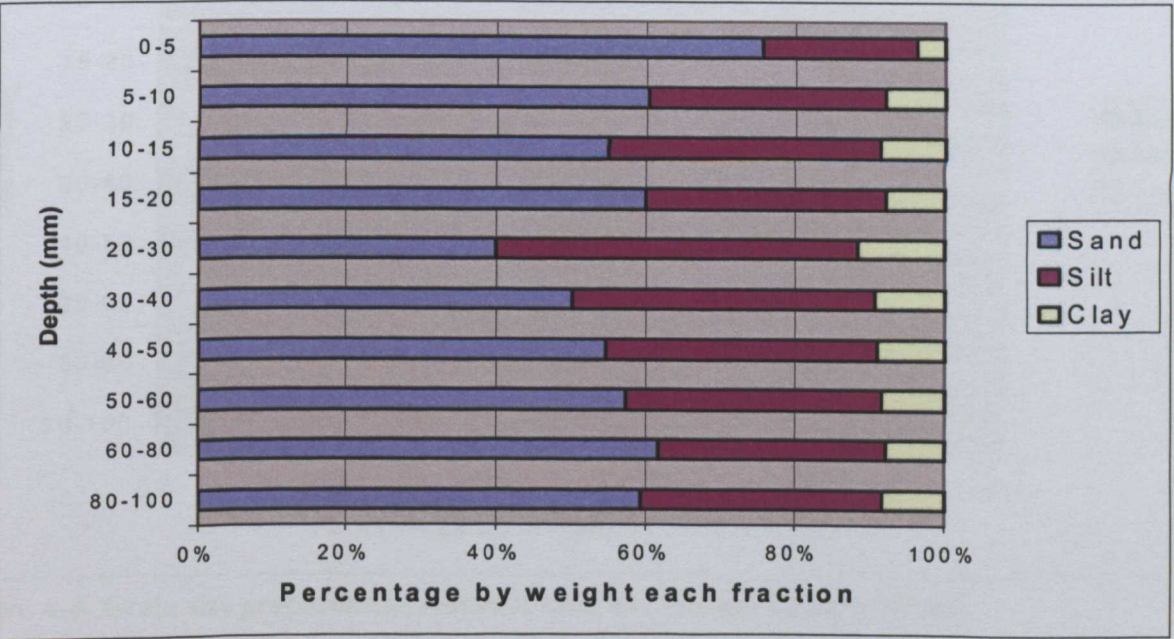


Figure A-2. Grain size proportion of sediment samples, Thames Estuary (TE2J).

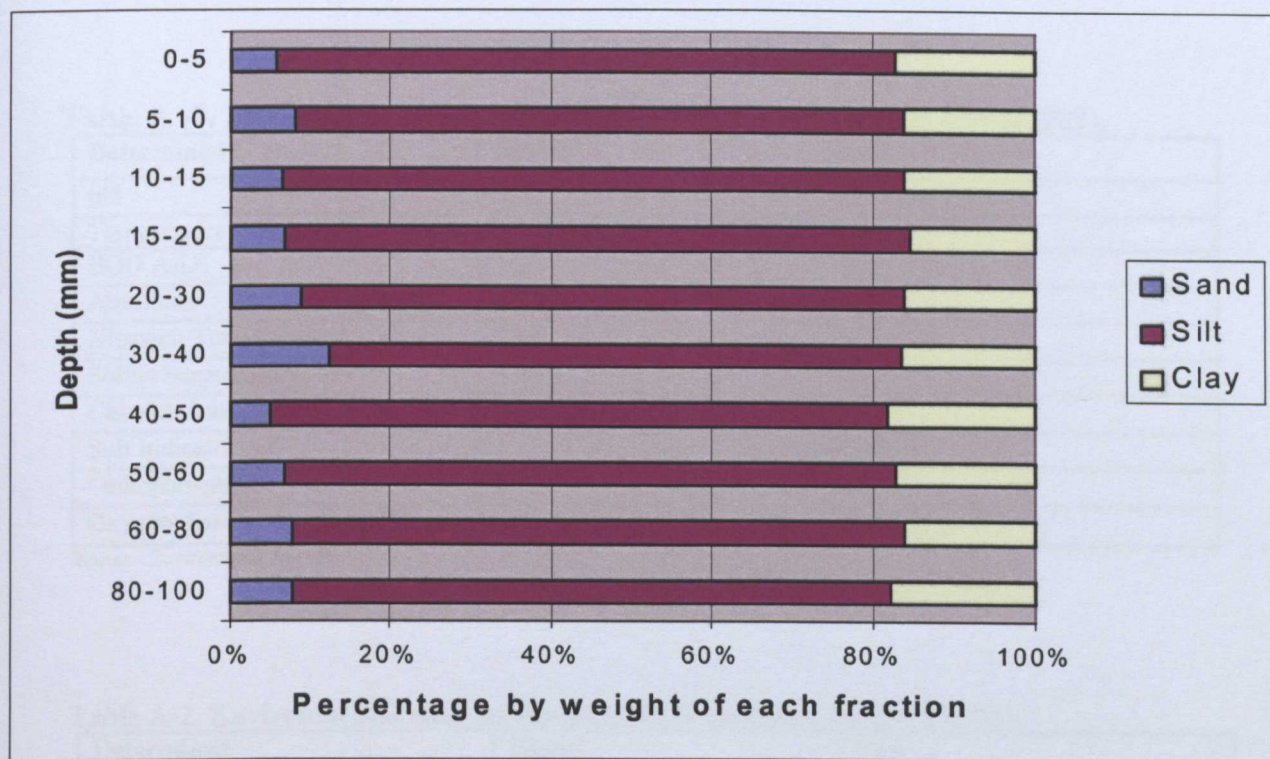


Figure A-3. Grain size proportion of sediment samples, Thames Estuary (TE3J).

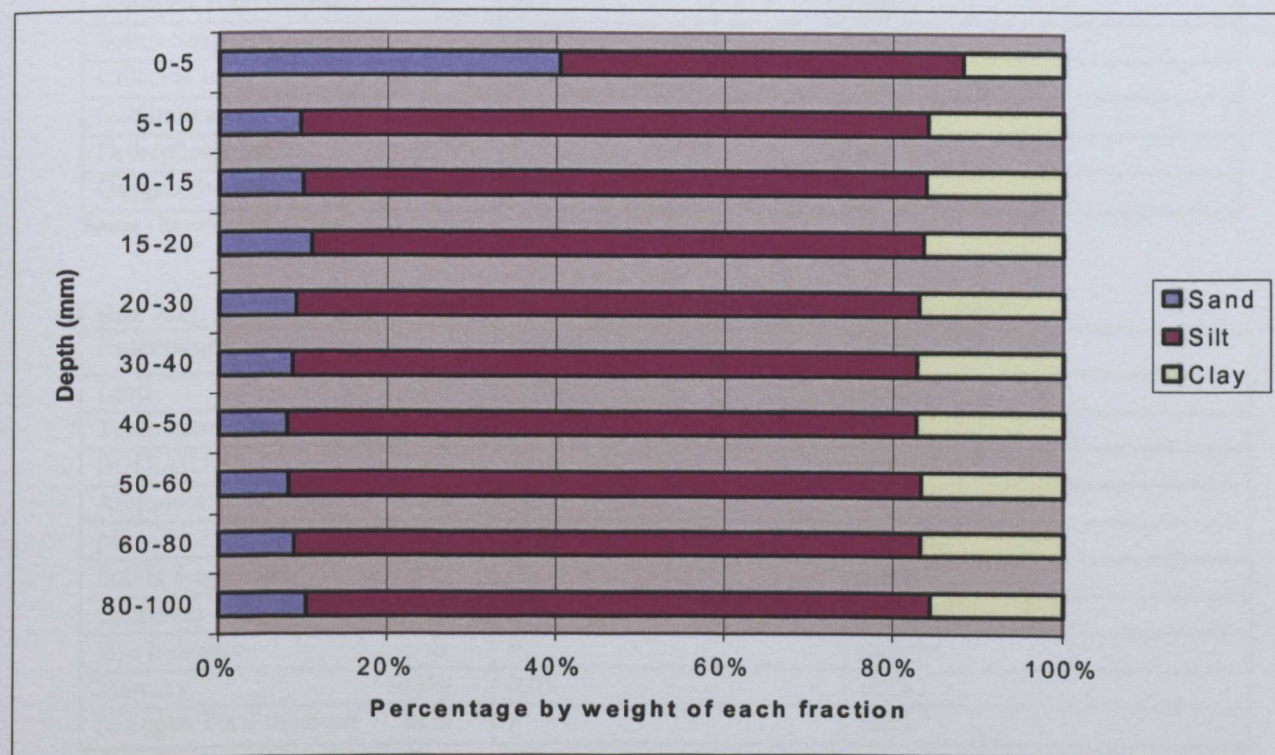


Figure A-4. Grain size proportion of sediment samples, Thames Estuary (TE4J).

A. 1-2 Environmental data for Ben fleet Sewage Treatment Plant (STW) May – (November, 2001).

Table A -1. Environmental data for Benfleet STW (sampled on 15/08/2001).

Determined	Result	Unit
pH	7.53	pH Units
Temperature Water	21.78	°C
BOD AIU	15.7	mg L ⁻¹
Ammonia as N	6.46	mg L ⁻¹
Nitrogen Total oxidised as N	10.2	mg L ⁻¹
Solids Suspended @105°C	17.4	mg L ⁻¹
Chloride Ion- as Cl ⁻	112	mg L ⁻¹
Suit Indicator -E	1	unitless
Orthophosphate as P	9.9	mg L ⁻¹
Oxygen dissolved as %S	47.8	%

Source - Environment Agency

Table A-2. Environmental data for Benfleet STW (sampled on 29/08/2001).

Determined	Result	Unit
pH	7.55	pH Units
Temperature Water	20.62	°C
BOD AIU	24.8	mg L ⁻¹
Ammonia as N	11.5	mg L ⁻¹
Nitrogen Total oxidised as N	8.1	mg L ⁻¹
Solids Suspended @105°C	26.7	mg L ⁻¹
Chloride Ion- as Cl ⁻	117	mg L ⁻¹
Suit Indicator -E	1	unitless
Orthophosphate as P	9.94	mg L ⁻¹
Oxygen dissolved as % S	34.9	%

Source - Environment Agency

Table A-3. Environmental data for Benfleet STW (sampled on 02/09/2001).

Determined	Result	Unit
Lead as Pb	1.15	mg L ⁻¹
Temperature Water	20.21	°C
BOD AIU	21.8	mg L ⁻¹
Ammonia as N	10.5	mg L ⁻¹
pH	7.43	pH units
Solids Suspended @105°C	0.1	mg L ⁻¹
Cadmium as Cd ⁺	0.1	mg L ⁻¹
Suit Indicator -E	9	unitless
Mercury as Hg	0.01	mg L ⁻¹
Nitrogen Total oxidised as N	9	mg L ⁻¹

Source - Environment Agency

Table A-4. Environmental data for Benfleet STW (sampled on 17/09/2001).

Determined	Result	Unit
pH	7.68	pH Units
Temperature Water	17.26	°C
BOD AIU	47.8	mg L ⁻¹
Ammonia as N	14.2	mg L ⁻¹
Nitrogen Total oxidised as N	6.3	mg L ⁻¹
Solids Suspended @105°C	48	mg L ⁻¹
Chloride Ion- as Cl ⁻	127	mg L ⁻¹
Suit Indicator -E	1	unitless
Orthophosphate as P	9.5	mg L ⁻¹
Oxygen dissolved as %S	26.7	%

Source - Environment Agency

Table A-5. Environmental data for Benfleet STW (sampled on 01/10/2001).

Determined	Result	Unit
pH	7.7	pH Units
Temperature Water	17.59	°C
BOD AIU	10.5	mg L ⁻¹
Ammonia as N	2.87	mg L ⁻¹
Nitrogen Total oxidised as N	8.3	mg L ⁻¹
Solids Suspended @105°C	15.3	mg L ⁻¹
Chloride Ion- as Cl ⁻	86	mg L ⁻¹
Suit Indicator -E	1	unitless
Orthophosphate as P	4.44	mg L ⁻¹
Oxygen dissolved as %S	67.6	%

Source - Environment Agency

Table A-6. Environmental data for Benfleet STW (sampled on 26/10/2001).

Determined	Result	Unit
pH	7.8	pH Units
Temperature Water	16.61	°C
BOD AIU	18.2	mg L ⁻¹
Ammonia as N	6.72	mg L ⁻¹
Nitrogen Total oxidised as N	13.7	mg L ⁻¹
Solids Suspended @105°C	23.4	mg L ⁻¹
Chloride Ion- as Cl ⁻	100	mg L ⁻¹
Suit Indicator - E	1	unitless
Orthophosphate as P	6.79	mg L ⁻¹
Oxygen dissolved as % S	65	%

Source - Environment Agency